To my parents with oceans of love

AUTOMATED STATIC PERIMETRY AND DIMENSIONAL CHARACTERISTICS OF THE INTRA- AND PERI-PAPILLARY RETINAL FEATURES IN MYOPIA

A Thesis submitted by

Alicja Regina Rudnicka

for the degree of
DOCTOR OF PHILOSOPHY

Applied Vision Research Centre

City University, London

1994

TABLE OF CONTENTS

LIST OF TABLES

LIST OF ILLUSTRATIONS

Acknowledgements

I gratefully acknowledge my supervisors Mrs Jennifer Birch and Mr David Edgar, both have given me considerable encouragement and counselling throughout this project. A special thank you to David for his unruffled 'Irish charm', which, in combination with my 'Polish temperament', has lead to many hours of pleasant deliberation.

I also wish to thank various members of the academic and technical staff within the Optometry Department of City University. Professor John Barbur for his advice on aspects on physiological optics, Alf Goodbody for his enthusiastic assistance in the optics laboratory, Colin Longhurst and Ernie Caswell for their technical skills, Ali Harlow and Daryl DeCunha for their computer programming expertise, and Professor Geoffrey Woodward for always being helpful particularly with matters concerning finances!

I am indebted to the late Arthur Bennett whose extensive knowledge of physiological and visual optics has been invaluable. It was a great pleasure to have the opportunity to work with such a distinguished scientist in this field.

I would also like to thank Mr Steven Bailey for his assistance in preparation for presentations, and his photographic skills, Dr Fred Fitzke for allowing me to use computer facilities at the Institute of Ophthalmology, and Jörg Weber for his advice on certain aspects of visual field analysis.

I am obliged to thank the following for their financial support, which enabled me to attend conferences, the British College of Optometrist, Allergan Humphrey Instruments, European Glaucoma Society, Keeler Ltd, The Wellcome Trust, Dr G. Zinser and The British Council.

I will always be grateful for the friendship of members of staff and fellow postgraduates within the Optometry Department, especially to Nancy Guttridge with whom I have worked very closely. I am very glad to now have Nancy as one of my closest friends. I am also greatly appreciative of the constant support, encouragement, collection of inter-library loans, and photocopying of papers by Chris Owen. He has in the latter part of this project helped me through the painstaking writing-up stage. No doubt he is as glad as me to see this thesis finally completed.

Finally, I would like to thank my parents for their love and endless support which gave me the impetus to see this project to its end.

Declaration

I grant the powers of discretion to the University Librarian to allow this thesis to be copied in whole or in part without further reference to me. This permission covers only single copies made for study purposes, subject to normal conditions of acknowledgement.

Abstract

The purpose of this project was to investigate the central visual field by automated static perimetry in a group of healthy myopic individuals with peripapillary crescents and tigroid fundus changes only. The appearance of the optic nerve head and surrounding structures were used to classify subjects into groups for the analysis of field data. In addition, the dimensions of features of the optic nerve head and peripapillary crescents were evaluated.

The study population comprised 122 young, healthy volunteers between the ages of 18.5-35.4 years, free from any ocular or systemic condition, with refractive errors ranging from +4.00D to -25.75D. A young subject population was deliberately chosen to avoid confounding the results with age-related changes affecting the visual field, for example crystalline lens opacities.

The central visual field was examined using two different programs of the Humphrey Field Analyzer. A combination of these two programs yields a test point resolution of 4.2° within the central 30° field. Optimum experimental design for this field examination procedure was established following a preliminary study of serial visual fields in normals, with due regard to the effects of learning on the visual field. A customised program was configured on the Humphrey Field Analyzer to examine the blind spot region with a test point resolution of 1.4°.

A ray tracing program was devised to determine the true area of the intra- and peripapillary optic nerve head features from photographic slides of the ocular fundi taken with the Carl Zeiss Jena fundus camera. For this program the magnification of the fundus camera employed and that of the human eye are required. The former was determined experimentally using a model eye. Differing methods for estimating the latter are presented.

Visual field analysis showed a decline in the differential light sensitivity in myopes with peripapillary changes only. These field changes become more pronounced with increases in the degree of myopia, axial length and area of the peripapillary crescent. The field region most affected appeared to be the superior hemifield, particularly the upper-temporal quadrant. Enlargement of the blind spot occurred in subjects with relatively larger peripapillary crescents, who were inclined to have longer axial lengths and more myopia. Results suggest that the sensitivity decline of the central field occurs in subjects with axial lengths above 26mm and more than 5D of myopia, whereas BS enlargement appears to occur in subjects with axial lengths above 28mm and more than 10D of

myopia.

The areas of the optic disc, neuroretinal rim and peripapillary crescent increase with increasing axial length and increasing myopic refraction. A log transformation of the optic disc parameters showed them to increase linearly with axial length and ocular refraction, apart from cup area. Marked inter-individual variations exist for the areas of the intra- and peri-papillary optic disc structures. Significant correlations exist between disc area and neuroretinal rim area, and between peripapillary crescent area and disc area.

Knowledge of typical sensitivity values with automated static perimetry in myopia may help in the differential diagnosis of diseases, including glaucoma, which cause visual field abnormalities. Knowledge of the dimensions of the optic nerve head and peripapillary crescents may aid in the diagnosis of pathologically disturbed optic discs.

KEY OF ABBREVIATIONS/SYMBOLS

ANOVA	Analysis of variance
asb	Apostilb
BS	Blind spot
CPSD	Corrected pattern standard deviation
dB	Decibel
FL	Fixation losses
FN	False negative
FP	False positive
HFA	Humphrey Field Analyzer
IOL	Intra-ocular lens
LF	Long-term fluctuation
LF(HE)	Long-term fluctuation (heterogeneous)
LF(HO)	Long-term fluctuation (homogenous)
MD	Mean deviation
MS	Mean sensitivity
NRA	Neuroretinal rim area
POAG	Primary open angle glaucoma
PSD	Pattern standard deviation
SD	Standard deviation
SF	Short-term fluctuation

CHAPTER 1

Myopia

1.1 INTRODUCTION

There are many reviews of the aetiology and progression of myopia (Donders 1864; Tron 1940; Sorsby *et al* 1957; van Alphen 1961; Duke-Elder 1970; Curtin 1985; Grosvenor 1987). The incidence of myopia in the Western world is about 25% (Sveinsson 1982; Sperduto *et al* 1983). It is well established that the main ocular factor causing myopia is axial length extension, which occurs during postnatal growth and primarily affects the oraequatorial region. However, relatively low grades of myopia can have axial lengths within the expected emmetropic range, but have greater corneal and/or lenticular powers.

The refraction of the eye is determined by four variables: corneal power, anterior chamber depth, lens power and axial diameter of the globe. The sum of the powers of the cornea and the lens, modified by the anterior chamber depth, yield what is referred to as the total refractive power of the eye. Refractive error at birth has been generally believed to be between 2-3D of hyperopia. However, Cook and Glassock (1951) and Goldschmidt (1969) have shown a wide distribution of refractive error at birth, extending to 7D or more in both the myopic and hyperopic directions.

Axial length in new-borns is about 18.7mm, according to Sorsby (1973), who describes two growth phases. The first is a rapid infantile phase, in the first three years of life, when the axial length increases by 4.5mm. This requires a decrease in the power of the cornea and crystalline lens to prevent myopia of the order of 12-13D. Flattening of the cornea reduces its power by about 15D, and the crystalline lens becomes less spherical. In the slower juvenile growth phase the axial length increases by 1mm between the ages of 3 to 14 years. Normally, compensatory changes do not entirely neutralise the axial elongation, thus hypermetropia is reduced by 1.5-2.0D during childhood. Axial length reaches adult proportions usually by the age of 14 years (Sorsby *et al* 1961; Sorsby and Leary 1970), and continued axial elongation beyond this age is usually only found in progressive juvenile myopia. Goss *et al* (1990) showed that the age of cessation of axial elongation in myopes was similar to the age of cessation of increases in height. Previous studies have also shown that the anterior chamber depth normally reaches its maximum depth, and the crystalline lens its maximum thickness, by about 15 years of age (Sorsby *et al* 1961; Sorsby and Leary 1970; Jansson 1963).

Stenstrom (1946) showed that the distribution curve for refraction had the same

disposition as that for axial length, featuring a positive excess at emmetropia and a skewness toward myopia. Sorsby and co-workers (1957) observed an emmetropization process in the distribution curves of refraction as a result of correlation between corneal power and axial length. In ametropias of 4D or more this relationship breaks down. However, it must be stressed that as axial length can only lie within certain limits for a human eye, and the same is true for corneal power, it is almost inevitable that some degree of correlation will exist between these two factors, depending upon the population sample and its size. An extensive review of this aspect of the literature is given by Curtin (1985, Chapter 2). In a recent study (Scott and Grosvenor 1993) of emmetropic and myopic eyes between -5 to -7D, corneal radius and vitreous chamber depth were demonstrated to be the most important components determining refractive state. Longer eyes tended to have flatter corneas, but comparing the two groups, the myopic group were found to have significantly steeper corneas, as found also by Sorsby *et al* (1957). Additionally, the inter-correlation of the various components of refraction were not the same for the emmetropic and myopic eyes (Scott and Grosvenor 1993), suggesting that they come from statistically discrete populations, therefore supporting the concept that myopic and emmetropic eyes develop differently (Hirsch 1950). However, Garner *et al* (1992) found a significant difference in crystalline lens power and not corneal curvature between a group of age-matched emmetropes and myopes. McBrien and Millodot (1987) found the major cause of late onset myopia (onset after 15 years of age) to be vitreous chamber elongation.

Several theories have been suggested as to the cause of axial elongation.

- Van Alphen (1961) proposed that
  - the choroid and ciliary body form an elastic envelope that limits the stretch of the sclera by counteracting a part of the intraocular pressure
  - the macula supplies information regarding focus to the brain, which in turn feeds back information concerning the required degree of stretch. He suggested that this stretch factor ultimately governs the refractive state of the eye. When this system failed, it was due to a loss of sympathetic tone, which allowed the choroid to stretch to its elastic limit and resulted in both a posterior staphyloma and steepening of the cornea.

- It has been hypothesised that retinal image quality regulates the release of growth factors responsible for axial elongation (Raviola and Wiesel 1985; Wallman *et al* 1987; Holden *et al* 1988). They have demonstrated in laboratory studies that defocus or degradation of retinal imagery in animals induces axial myopia, as have Sivak *et al* (1989), and the earlier the insult to the visual system the greater will be the degree of induced myopia.

- Accommodation has been suggested as a causative factor in myopia development (Young 1975; Fledelius 1981).

- Greene (1980) believed that prolonged contraction of the superior oblique muscle caused pressure changes in the posterior part of the eye as well as scleral traction, resulting in axial elongation.

- Clinical and experimental studies have indicated a relationship between the amount of near work and myopia (Young *et al* 1969; Bear *et al* 1981; Young 1961), and that sustained near work can produce shifts in the tonic accommodation, and may be a precursor to induced myopia (Bullimore and Gilmartin 1987; Gilmartin and Bullimore 1987; Ebenholtz 1983).

- Intraocular pressure has also been proposed as one of the factors responsible for myopic progression (Tomlinson and Phillips 1970; Perkins and Phelps 1982; Parssinen 1990; Ziylan *et al* 1993).

There is no general agreement as to the mode of inheritance of myopia nor of the optical components. The genesis of myopia has been described as being both autosomal dominant and recessive, and sex-linked pedigrees have been observed (Sorsby and Benjamin 1973). Taking inheritance in conjunction with environmental factors the development of myopia is clearly complex. Myopia can also occur in association with systemic and ocular disorders (Curtin 1985, Chapter 5).

1.2 FUNDUS CHANGES ASSOCIATED WITH MYOPIA

In low myopia any changes at the posterior pole are minor. The commonest reported is the myopic crescent, which has a predominantly temporal location and may increase in size with the progression of myopia (Donders 1864). With high myopia, in addition to peripapillary crescents, the earliest changes may be localised thinning or chorio-retinal degeneration, particularly around the margin of the crescent, and an area of tessellation and pallor may develop. With time, a variable degree of ectasia of the pale, tessellated fundus area usually ensues, leading to a posterior staphyloma (Curtin 1985; Otsuka 1967; Stenstrom 1946). Atrophy of the retinal photoreceptors, pigment epithelium and choroid may cause significant peripapillary atrophy that eventually encroaches upon the macular area (Brown and Tasman 1983). Discrete regions of retinal degeneration, retinal haemorrhages and lacquer cracks may also occur. Lacquer cracks are seen as yellowish white lines of irregular calibre that traverse the posterior pole. They are associated with posterior staphylomas and choroidal haemorrhages (Klein and Curtin 1975), and are

thought to represent fissures in the retinal pigment epithelium-lamina vitrea-choriocapillaris complex.

If the retinal pigment epithelium, Bruch's membrane, and choroid fall short of the disc margin a scleral crescent will be apparent. This appears as a white halo proximal to the disc margin. A choroidal crescent occurs if only the pigment epithelium fails to reach the disc margin. At its termination point, the pigment epithelium may impart a variable amount of pigmentation giving rise to a pigmented crescent.

The frequency (Huang *et al* 1987; Curtin and Karlin 1971; Jonas *et al* 1988d; Pierro *et al* 1993) and size (Stenstrom 1946; Otsuka 1967) of peripapillary crescents increases with degree of myopia and axial length elongation. Huang *et al* (1987) expressed the crescent area as a percentage of the disc area and found it to increase significantly with myopia ($r = -0.49$) and axial length ($r = 0.51$). Fulk *et al* (1992) found males to be more likely to have crescents than females, and a statistically significant increase in the horizontal diameter of the crescent with increasing myopia ($r = -0.3$), but no significant relationship with axial length. This is unexpected, since higher degrees of myopia are associated with axial elongation. In their study of 224 subjects, the maximum degree of myopia was only 7.25D, with a mean of -0.67D for the sample, suggesting a preponderance of lower degrees of myopia, and the mean axial length for the group with largest crescents was low, being only 24.11mm. It is likely that the range of axial lengths included was insufficient to elicit a relationship between crescent size and axial length. Relatively low grades of myopia can have axial lengths within the expected range for emmetropia. In the same study subjects with larger crescents showed more myopia per millimetre of axial length than those without a myopic crescent, 1.26D/mm as compared with 0.66D/mm. Jonas and co-workers (1988d) believe the area of peripapillary atrophy to increase with increasing size of the optic disc ($r = 0.8$) and with increasing myopia ($r = 0.59$). In their sample of myopes with refractions from -8D to -28D, the mean area of peripapillary chorioretinal atrophy was 33.05 $\pm$23.84mm^2 (0.0 to 60mm^2 or more). In the same study the area of the optic disc was calculated to increase by about 0.77mm^2 for every dioptre increase in myopia. Interindividual variation in disc size increased with increasing myopia, and the optic nerve head form became more oval.

Age, and front surface keratometry do not appear to have any bearing upon the presence/absence of a crescent (Fulk *et al* 1992). A group of myopes ranging from -5 to -19D, with primary open angle glaucoma (POAG), seemed to have a higher frequency of peripapillary atrophy, the width of which was largest temporally and below the horizontal meridian (Chihara and Sawada 1990), than non myopic POAG patients. However, this observation in the myopic POAG group may be the consequence of myopia alone. In congenital myopia it is not uncommon to have a tilted optic disc particularly temporally,

giving rise to a temporal crescent (Curtin 1963). In a few cases the crescent can be inferior, in which case it is usually scleral.

In all the papers quoted in this section, photographic methods have been used to determine the true size of the optic disc and crescents. Calculation of the true size of the optic disc or peripapillary crescent is dependent upon the method used to calculate the magnification of the human eye, and the photographic system. This aspect will be dealt with in more detail in Chapter 8.

A number of causes of the crescent formation have been suggested

- oblique insertion of the optic nerve head may cause traction, usually on the temporal side of the optic disc, which may result in a crescent (Curtin 1985, Chapters 7 and 8)

- myopic crescents may be due to pathological stretching of the globe with a pull on the RPE and choroid. Perhaps an embryonic defect prevented normal growth of the RPE and choroid (Stenstrom 1946; Otsuka 1967; Curtin and Karlin 1971)

- it has been postulated that there may be asymmetric expansion of the sclera in the myopic eye (Ts'o and Friedman 1968). A change of this type would cause a shearing displacement temporally of the retinal pigment epithelium, Bruch's membrane and the choriocapillaris, which would produce a crescent on the temporal side of the optic nerve, and a piling up of the choroid and retina on the nasal side. This apparent dragging of the retinal and choroidal tissues over the nasal surface of the optic nerve head is called supertraction

- myopic crescents have been attributed to atrophy of the peripapillary tissues (Donders 1864).

Fantes and Anderson (1989) studied histological sections of eyes that had been photographed before enucleation. Apart from misalignments of the RPE, choroid and sclera, such as might be caused by continued growth of the sclera in axial myopia, crescents could also result from three other histological features. These are firstly, the presence of a thickened scleral lip at the edge of the optic nerve, secondly, malposition of the embryonic fold, and thirdly, hypopigmentation or hyperpigmentation of the RPE. These crescents are not necessarily associated with myopia. During embryonic development the neuroectoderm forms a double layer, the outer layer becoming the RPE and the inner layer forming the neural retina. The RPE is continuous with the neural retina at the disc border as a fold of neuroectoderm. If the RPE border does not coincide exactly with the fold, one of two things can occur. Either the RPE continues beyond the

fold giving rise to a double layer of RPE and hence a region of intense pigmentation (the same would occur with a single layer of deeply pigmented RPE), or the neuroretina continues beyond the fold and the RPE does not reach the fold. In this case a region devoid of pigmentation occurs exposing the underlying choroid. If the RPE was present but depigmented the same picture would result ophthalmoscopically, and in this instance the edge of the RPE may be marked by a band of hyperpigmentation. It is almost impossible to distinguish ophthalmoscopically between all the various possible misalignments of the retina, RPE and choroid at the disc margin. Even determining the exact borders of the disc and peripapillary changes can often be difficult. But separation between pigmented and non-pigmented peripapillary changes is usually possible.

1.3 CLASSIFICATION OF MYOPIA

There have been many classifications of myopia in an attempt to describe its development and progression. Curtin's classification, described below, was used as a starting point for this research (Curtin 1985). Age of onset of myopia will not be used as a factor in the analysis because often the reliability of such information is questionable. Myopes will be divided into groups according to the fundus appearance, and their central visual field sensitivities compared.

Group 1: Physiological myopia

In this type of myopia postnatal development has rendered the eye myopic. Ocular fundi are normal and devoid of a distinct crescent around the optic disc. The maximum myopia is approximately -3 to -5D and the axial length lies between 22.0mm and 25.5mm.

Groups 2: Intermediate myopia

There is an expansion of the globe that is in excess of normal ocular growth. It may involve the entire posterior segment, with generalised spreading and thinning of the retinal pigment epithelium resulting in a tigroid fundus picture. This type of myopia occurs rarely below -3D, but it is common between -3 to -10D. It shows an increasing prevalence in eyes with axial diameters from 22.0 to 25.5mm. Beyond this it is the most common type up to 32.5mm. Because of the posterior segment growth these eyes show distinctive crescent formation, with or without supertraction, tessellation and pallor of the fundus. The peripheral fundus shows an increasing prevalence of changes associated with increased axial diameter, including white without pressure, lattice, pigmentary and pavingstone degenerations. There is also an increased incidence of retinal detachment and glaucoma in these eyes.

Group 3: Pathological myopia

Pathologic myopia is a potentially sight-threatening disease. The characteristic changes in the posterior fundus are myopic crescents, posterior staphyloma, chorioretinal atrophy, Fuch's spot and lacquer cracks.

1.4 VISUAL FIELD CHANGES IN MYOPIA

1.4.1 Manual perimetric investigations

It is well known that pathological myopia can give a variety of visual field defects (Traquair 1957; Matsuno *et al* 1967). Visual field changes as a result of myopic choroidal atrophy parallel those seen ophthalmoscopically (Harrington 1981). Peripheral degenerations tend to produce general depression and contraction of the isopters. Other typical defects within the visual field described by Harrington (1981) are

- central, paracentral and pericentral defects due to atrophic and degenerative changes, and haemorrhages
- enlargement of the blind spot from peripapillary crescents and haloes
- arcuate defects, which can occur if degenerative or atrophic changes cause damage to the nerve fibre bundle near the optic disc

Both Reed and Drance (1972), and Harrington agree that myopic field defects seem to be more pronounced under conditions of lower illumination.

Sato *et al* (1984) demonstrated a depression of the isopters in a group of myopic subjects, aged 10-75 years, with tigroid fundus changes only. They found that eyes with longer axial lengths or greater degrees of myopia tend to produce more marked visual field defects, particularly if the visual acuity has been affected. Takizawa (1983), using a Goldmann perimeter adapted to allow simultaneous viewing of the fundus, demonstrated a decrease in the retinal sensitivity of the papillomacular area of myopes over -6.25D, as compared with normal non-myopic subjects. The age of his sample was between 10-65 years, and this decline in sensitivity was observed in subjects under and over the age of 40 years. In addition, myopic scleral crescents and chorioretinal atrophic lesions produced corresponding scotomata in visual space. The decrease in sensitivity was slight if the lesion was restricted to the RPE.

Enlargement of the blind spot has been reported in inferior conus, inverted disc or nasally directed scleral canal, temporal crescents of the optic disc (Reed and Drance 1972) and

in myopia (Nakase 1987a). An enlargement of the blind spot may not be expected to occur if one considers the reduced angular subtense of the optic nerve head with increased axial length, and the minification produced by the minus prescription. However, other factors influencing the size of the blind spot are the true size of the optic disc, which is believed to be larger in myopes (Jonas *et al* 1988d), and the presence of any peripapillary crescents. Nakase (1987a), using Goldmann kinetic perimetry found high myopes (-8.25D to -28D), mean age 43 years, to exhibit enlargement of the blind spot, and minimal changes in the paracentral region. Defects in the mid-periphery were rare. Masukagami *et al* (1987), using manual kinetic perimetry in myopes of -6.25D or more (aged 16-60 years, mean 32), found an enlargement of the blind spot. The instrument they used allowed simultaneous viewing of the fundus during perimetry, and they observed that the size of the blind spot extended beyond the margins of the optic disc in both normal and myopic individuals. Reasons given for this discrepancy are as follows

- angioscotomata - particularly at the superior and inferior poles of the optic disc
- a true depression of retinal sensitivity due to a reduced number of photoreceptors or altered properties of the receptive fields in the vicinity of the disc margin. This seemed more pronounced in the inferior nasal region, which may be related to the closure of the inferior-peripapillary area in foetal development
- presence of a myopic crescent.

Spectacle lenses of negative power produce an increase in the extent of the apparent field of view. They also minify the test stimulus size, and in manual kinetic perimetry concentric contraction of the field may be observed (Voronova 1967). Spectacle distortion and the lens rim can produce a wide variety of visual field defects. Tokoro *et al* (1976) found that when the patient was corrected with a spectacle lens as opposed to a contact lens the isopters were constricted, as measured by Goldmann perimetry. Any spectacle lens will absorb and reflect light and therefore reduce the amount of light admitted to the eye, but the contrast thresholds in perimetry remain unaltered.

Bitemporal visual field losses, particularly superiorly, have been reported in the literature in myopic individuals with specific fundus changes (Rucker 1946; Caccamise 1954; Schmidt 1955; Berry 1963; Riise 1966; Odland 1967; Graham and Wakefield 1973; Young *et al* 1976). However, the field depressions did not respect the midline, and in some cases the field loss could only be demonstrated on a tangent screen and not on a perimeter. Ocular fundi of these myopic patients exhibited inferior-nasal fundus ectasia/depigmentation with downward tilting of the optic nerve head together with an inferior or nasal scleral crescent (conus). In some cases the blood vessels turned nasally first before heading off temporally, giving the disc an inverted appearance, referred to as

situs inversus (Brown and Tasman 1983). Situs inversus can be associated with an inferior conus and an inferiorly titled disc, inferior fundus ectasia, myopia, astigmatism and temporal or altitudinal field loss. Several names have been given to this condition including tilted disc syndrome, nasal fundus ectasia and Fuch's coloboma. Because of the association of situs inversus with a tilted disc and its concomitant ectasia of the nasal fundus, temporal visual field defects may co-exist. In bilateral cases the field defect does not respect the midline and should not be confused with field defects resulting from chiasmal lesions (Graham and Wakefield 1973; Brown and Tasman 1983). Therefore, careful fundal examination is necessary in patients presenting with myopia and field loss. Fundus ectasia appears as a paler region, which may be due to hypoplasia of the retina and choroid, and thus fewer photoreceptors. This may give rise to refraction scotomas which disappear (Schmidt 1955) or reduce in size (Odland 1967) when stronger myopic corrections are used. It is well established that retinal/choroidal degenerations will give relative scotomas. In addition to the temporal field loss, Manor (1974) reported arcuate scotomas, concentric contraction and baring of the blind spot in subjects with nasally tilted discs with nasal or inferior-nasal crescents, most of whom were myopic.

1.4.2 Automated perimetric investigations

Chihara and Sawada (1990) investigated the central field using the Octopus automated perimeter in a group of 45 myopes, mean age 46.9 ± 16.6 years. With myopia, from -5 to -19D, they found the field sensitivity (as measured by a global index mean defect, described later) to be abnormal in 11% of subjects, and the defective area was located in the mid peripheral part of the field. High pass resolution perimetry in a group of myopes from -3 to -9D, aged 21- 49 years, showed a slight increase in threshold with increasing myopia, which correlated significantly with the degree of myopia and enlargement of the blind spot (Martin-Boglind 1991). A reduction in the light sensitivity on the Octopus automated perimeter was demonstrated in 71subjects, aged 12-64 years, with more than 8.25D of myopia and tigroid fundus changes only, as compared to a non-myopic control group (Huang and Tokoro 1990). The upper-temporal quadrant was significantly more affected than the other quadrants, in agreement with the manual perimetric investigations described above. This preferential loss in the upper-temporal region may be due to the ectasia and degeneration of the retina which tends to occur in the inferior-nasal fundal area.

Patients with tilted disc syndrome are usually myopic, and abnormal threshold values have been reported using the Octopus perimeter (Brazitikos *et al* 1990). In this group of 12 subjects with a mean age of 44 years (range from 19 to 67 years), the index mean defect increased as the degree of myopia increased. Again the field loss was more pronounced in the upper-temporal quadrant.

1.5 MYOPIA AND GLAUCOMA

1.5.1 Introduction

Glaucoma is more prevalent in myopic than in emmetropic eyes, and myopia is found more often in glaucomatous patients than in the general population (Goldschmidt 1968; Tomlinson and Phillips 1970; Drance *et al* 1973; Leighton and Tomlinson 1973), particularly in subjects with myopia of more than 10D (Mastropasqua *et al* 1992). Perkins (1979), and Perkins and Phelps (1982), revealed approximately 30% of patients with POAG to be myopic. In the latter study, myopia occurred more frequently in ocular hypertensives, and, in agreement with others (Drance *et al* 1973; Huang and Zhou 1990; Geijssen and Greve 1992), in low tension glaucomas, as compared with the normal population. Wilson and co-workers (1987), however, found only a weak association between glaucoma and myopia. This may have resulted from the degree of myopia in their sample, which was not stated. Wilson *et al* (1987) suggested that differences between studies may occur when different methods of statistical analysis are used. Mastropasqua *et al* (1992), examined 1000 POAG patients aged 20 to 80 years, and myopia was present in 32.6% of the glaucomatous patients, of which 18% had myopia of more than 10D. The prevalence of myopia in juvenile POAG (patients under the age of 35 years) was found to be 54% by Goldwyn *et al* (1970), and 73% by Lotufo *et al* (1989). In the latter study 39% had more than 6D of myopia, and they also showed 59% of juvenile ocular hypertensives to be myopic. In addition, the prevalence of myopia in blacks with juvenile open angle glaucoma is higher than in whites (Lotufo *et al* 1989).

Tomlinson and Phillips (1970), and David *et al* (1985) found the average intraocular pressure to be higher in myopes than in emmetropes or hyperopes, and to increase with axial length. Mastropasqua *et al* (1992) demonstrated a significant positive correlation between intraocular pressure and refractive error in a group of myopes with refractive errors greater than 10D. A positive correlation between axial length and POAG has been shown by Curtin (1970). As the axial length in myopes increased from 26.5mm to 33.5mm the incidence of POAG increased from 3% to 28%. No such association was found by Leighton and Tomlinson (1973) in a group of low-tension glaucoma patients, although the average refraction for the sample was clearly myopic (-5D). Daubs and Crick (1981) did not elucidate any relationship between intraocular pressure and refraction, but found that myopia was a significant risk factor for developing POAG. They determined that myopes of more than 5D were 3.1 times more likely, and myopes less than 5D 1.3 times more likely to develop glaucoma than emmetropes.

Tomlinson and Phillips (1969) concluded, in agreement with the general clinical impression, that myopes tend to have larger cups, particularly if the myopia is axial. They

suggested that the absolute area of the optic disc probably varies with the size of the eyeball, whereas the volume of nerve fibres congregating at the optic nerve head is fairly constant. However, the correlation coefficient between cup area/disc area and axial length was only 0.23 in their study. Nakase (1987b) reported that notching of the neuroretinal rim is a diagnostic feature that separates glaucomatous cups from myopic cups, because notching is a rare occurrence in healthy myopic discs. The optic disc in myopia may appear less pink and have an oblique insertion, which hinder the assessment of cupping (Brown and Tasman 1983). This is further complicated by the relative anterior position of the cribriform plate in myopic discs (Donders 1864, Curtin 1985), this limits the amount of excavation of the optic disc associated with glaucomatous damage. Thus, in myopes with glaucoma the cup may appear shallow because of this anatomical variation. Scleral and choroidal crescents, so frequently found in myopes, also tend to be more common, larger and more obvious in glaucoma patients than in normal individuals (Hayreh 1969; Wilensky and Kolker 1976; Anderson 1983; Buus and Anderson 1989), and this further complicates the diagnosis. Peripapillary atrophy, if present, has been reported to correspond with the sector of the disc having greatest cupping/excavation and with the localised field loss, in keeping with the distribution of the nerve fibre bundles (Anderson 1983; Heijl and Samander 1985). It may be that peripapillary atrophy signifies a region of the optic disc and retinal nerve fibre layer more susceptible to damage from an elevated intraocular pressure.

The following reasons have been proposed for the association between myopia and glaucoma

- a raised intraocular pressure may cause axial elongation (Pruett 1988; Parsinen 1990; Jensen 1992), although this is unlikely in the adult eye
- anatomical differences: in general the cup-disc ratio is higher in myopes and this enlarged cup may predispose more nerve fibres to glaucomatous damage at any level of intraocular pressure (Tomlinson and Phillips 1969)
- fluorescein angiographic studies have suggested a reduced choroidal blood flow in myopia (Amalric *et al* 1966; Aetisov and Savitskaya 1977), which may cause the circulation to the optic disc to be more susceptible to increases in the intraocular pressure
- it has been shown that myopes are more likely to be corticosteroid responders than emmetropes or hyperopes (Podos *et al* 1966). This suggests that their regulation of glycosaminoglycans may be abnormal. Glycosaminoglycans is found within the extracellular spaces of the trabecular meshwork and its concentration may influence the outflow of aqeuous .

1.5.2 Manual perimetric investigations

Reed (1960) stated that field loss in myopia may mimic field loss found in glaucoma. Phelps (1982) demonstrated that the presence of myopia did not appear to predispose POAG patients to visual field loss as compared with non-myopic glaucoma patients. However, myopes with ocular hypertension are more likely to develop glaucomatous damage than non-myopic eyes with equal intraocular pressures. It was postulated that once the ocular tension was reduced by treatment, myopia ceased to be a risk factor in developing glaucomatous visual field loss. In contrast, Nakase (1987a) found visual field defects in high myopes with POAG to progress more quickly than in POAG without myopia, and the defects extended into the macular area at a relatively earlier stage.

Greve and Furuno (1980) found, in a group of 216 myopic glaucoma patients, the following visual field defects using manual kinetic and static perimetry

- enlargement of the blind spot (18-40% of subjects)
- superior-temporal refraction defects (2-30% of subjects)
- irregular scotomas which parallel areas of chorioretinal atrophy (percentage not given)
- typical nerve fibre bundle defects (nasal wedge, arcuate and isolated paracentral) (percentage not given)
- atypical nerve fibre bundle defects
    - sector shaped temporal defects extending from the peripheral isopters centrally, either respecting the horizontal meridian or not even bordering the horizontal meridian (5-20% of subjects)
    - centrocaecal defects respecting the horizontal meridian (9-18% of subjects)

The myopes were divided into three groups according to their refractive error, from -1 to -5.75D constituted group 1 (144 eyes), -6D to -11.75D group 2 (62 eyes) and beyond -12D group 3 (10 eyes). As the degree of myopia increased, the incidence of atypical nerve fibre bundle field defects increased, being 17% in group 1, and 30% in groups 2 and 3. Enlargement of the blind spot and superior-temporal refraction defects increased in frequency with the degree of myopia. Oblique or tilted discs and peripapillary atrophy occurred more frequently in eyes with atypical field defects.

These atypical nerve fibre bundle field defects occurred at an earlier stage in the myopic glaucoma group. In non-myopic glaucoma, where typical glaucomatous nerve fibre bundle defects are the nasal wedge, arcuate and paracentral defects, atypical defects occur at a later stage in the disease process. No other subsequent studies have reported on these atypical nerve fibre bundle field defects. However, the atypical temporal nerve

fibre defects may be related to the ectasia in the corresponding fundal area, as described in section 1.4.1. The centrocaecal defect may be due to the extension of the temporal myopic crescent towards the fovea.

It is interesting that Chihara and Sawada (1990) found the incidence of atypical nerve fibre layer defects, as examined by fundus photography in myopes ranging from -5 to -19D, with POAG, to be greater than in both a group of emmetropic POAG patients, and a group of normal myopes ranging from -5 to -20D. These atypical nerve fibre layer defects were

- inferior dominant defects - the inferior retinal nerve fibre layer was more commonly defective than the superior region in the myopic group with POAG . This may be due to either ectasia of the inferior fundus or hypoplasia of the nerve fibre layer.
- ectopic and multiple focal defects, especially if the insertion if the optic disc was oblique.

Ten out of 45 healthy myopic eyes exhibited a thin nerve fibre layer in the inferotemporal area. Focal nerve fibre layer defects were not observed in healthy myopic eyes (Chihara and Sawada 1990).

The above literature strongly suggests that myopia, in the absence of any disease, can affect the differential light sensitivity of the visual field. Evaluation of the normal myopic visual field may help in long-term follow-up and differential diagnosis of diseases, including glaucoma, causing visual field abnormalities. There are few studies which have investigated the myopic field with automated static perimetry, and none of these utilised the Humphrey Field Analyzer. This is particularly important as automated perimetry is becoming the standard method of visual field examination in clinical practice. Knowledge of typical threshold values and likely field defects occurring in various degrees of myopia would be invaluable. Advice should be made available to optometrists and ophthalmologists on effective screening of myopic patients to exclude the possibility of open angle glaucoma.

This research will not investigate further the causative factors for the association between glaucoma and myopia, but information regarding the optic disc appearance in myopia and expected visual field sensitivity is provided.

CHAPTER 2

Rationale for the research

2.1 AIMS

This research was instigated following a pilot study, performed by an undergraduate, which investigated the central 25° of the visual field by manual kinetic perimetry in a group of seven young, myopic subjects. Results showed regional constriction of isopters and an enlargement of the blind spot in myopes when compared with normal subjects. The region of the visual field showing constriction corresponded to the position of the myopic crescent.

It is well established that focal areas of chorioretinal atrophy associated with myopic degeneration, situated peripheral to the disc and peripapillary region, will produce visual field defects which correspond with the fundus changes observed ophthalmoscopically. It is not the intention of this research to correlate these isolated regions of myopic retinal degeneration with their corresponding defect in visual space.

The aim is to establish typical values for the differential light sensitivity of the central 30° field, as determined by automated static perimetry with the Humphrey Field Analyzer, over a wide range of myopia. Comparisons will be made with visual fields from normal, emmetropic eyes. The extent of peripapillary/myopic crescents will be considered and myopic subjects will be divided into groups, depending upon the appearance of the posterior pole and relative size of these peripapillary crescents. Data will be available to evaluate the following

- does the degree of myopia influence the sensitivity of the central field (Chapter 7)?
- is axial length related to the sensitivity of the central field (Chapter 7)?
- typical normal values for optic disc area, neuroretinal rim area, cup area and peripapillary crescent area over a wide range of myopia (Chapter 8)
- is the size of the optic disc, optic cup, neuroretinal rim and any myopic crescent related to
  i) axial length (Chapter 8)
  ii) refractive error (Chapter 8)?
- how is the size of the optic disc, and any myopic crescent, related to the size of the blind spot (Chapter 9).

Young healthy individuals, without any ocular pathology, were recruited for this study from the academic and undergraduate populations of City University, and the majority of

the myopic patients were obtained from the Contact Lens Department of Moorfields Eye Hospital. Myopic subjects with typical myopic fundus changes at the posterior pole, surrounding the optic disc, were included. Subjects with fundus changes other than peripapillary crescents or slight pallor at the posterior pole were excluded.

2.2 PLAN FOR EXPERIMENTAL WORK

At the commencement of this research, it became clear that the following procedures needed to be investigated and consolidated into the main project,

- the optimal investigation strategy for a new ultrasonographic instrument, the Allergan Humphrey Ultrasonic 830 biometer. This instrument was used to measure the anterior chamber depth, lens thickness and axial length of the human eye. Its repeatability was also assessed (Chapter 5).

- the extent of psychophysical learning with static automated perimetry. Previous reports on learning are discussed in Chapter 3 section 3.4. The majority of studies involved the examination of both eyes, usually within one visit. Results varied between investigators as to the degree, if any, of psychophysical learning. In this project only one eye from each subject, selected randomly will be examined, to ensure independence of results for each eye tested. As the intention of the project is to provide typical values for the differential light sensitivity in myopia, it was thought appropriate to examine the visual fields with a test point resolution higher than that afforded by a single standard central visual field program. This can be achieved by combining two separate programs on the automated perimeter. It is possible that the extent of psychophysical learning may be different when only one eye is examined with two programs within one visit. Therefore, the learning process was first investigated in a group of normal emmetropic subjects, performing two programs at each of three separate visits (Chapter 6).

- the exact calculation of the true size of a fundus feature from a photograph requires precise knowledge of the optical components of the human eye being examined and the magnification of the fundus imaging system employed. It is not normally possible to measure all of the optical components of the human eye, thus certain assumptions must be made as to its optical configuration. In Chapter 8 (section 8.2) a ray tracing technique is described in which a schematic eye can be devised for each subject to compute its influence on the image size of a retinal feature. The camera magnification, if not already known, can be explored experimentally using a model eye (Chapter 8, section 8.3)

The main aims of this research have been outlined above. Chapter 7 is concerned with the results from automated perimetry in emmetropes and myopes over a wide range of refractive errors. In the same subjects the area of the optic disc, optic cup, neuroretinal rim and peripapillary crescents are investigated in Chapter 8. The area of the blind spot measured by automated perimetry and its relation to the area of the optic disc and peripapillary crescent is studied in Chapter 9.

CHAPTER 3

Automated perimetry

3.1 INTRODUCTION

The development of automated perimetry has made possible the measurement of the visual field with a precision and consistency greater than that generally available with manual perimetry. One of the original benefits envisioned for automated perimetry was the improved detection of progressive visual field loss in diseases such as glaucoma. As experience with automated perimetry has grown, it has become apparent that there is no general agreement as to what constitutes progressive change in the visual field of patients, and there is no definitive differentiation between normal and early pathological fields.

The general consensus is that field defects can be detected earlier with automated perimetry as compared with traditional manual perimetry (Heijl and Krakau 1975b; Koerner *et al* 1977; Beck *et al* 1985b; Mills *et al* 1986). Possible explanations are the shorter stimulus exposures and the random nature of the testing procedures, therefore the patient does not benefit from directing their attention to the location of the stimulus, as they would with manual perimetry. Holmin and Krakau (1979) found field defects to be more extensive with a shorter stimulus exposure time.

3.2 PHYSIOLOGICAL FACTORS AFFECTING VISUAL FIELD EVALUATION

3.2.1 Fixation and eye movements

Eye movements limit the accuracy of the visual field test. There are two basic forms of eye movements, voluntary and involuntary. There are three types of the latter, tremor, slow drift and microsaccade (Greve 1973). Tate and Lynn (1977) suggested a technique whereby the stimulus location is adjusted to compensate for the eye movement. However, large eye movements limit its application. Periodic stimulation of the blind spot has been introduced to give a measure of stability of fixation (Heijl and Krakau 1975b).

3.2.2 Optical defocus

A defocused retinal image of a test spot will cause enlargement of the stimulus and a decrease in the light intensity of the stimulus. How this affects perimetric thresholds

depends upon the retinal region being stimulated. The increment thresholds over the central 30° are markedly affected by blur using stimulus size I (Fankhauser and Enoch 1962). Sloan (1961) noted a change in thresholds for test stimuli size I and II on the Goldmann perimeter, but with larger stimulus sizes (III, IV and V) this effect was not seen. Benedetto and Cyrlin (1985) demonstrated using the Octopus and Goldmann (size III stimulus) that induced blur of ±2D had no effect statistically or clinically, but with 3D of blur or more there was a rapid loss of central sensitivity. Weinreb and Perlman (1986) produced +1D and +2D of blur using the same stimulus size, and found the average reduction in sensitivity per location for the central 6° to be 1.26dB per dioptre of induced refractive error. This is close to the value of 1.4dB per dioptre of blur, independent of eccentricity out to 25°, calculated by Heuer *et al* (1987) along the 180° meridian nasally. Others have found the effects of defocus to be greatest upon the central area (Sloan 1961; Fankhauser and Enoch 1962; Benedetto and Cyrlin 1985). Herse (1992) examined the average retinal sensitivity profile for a series of blur conditions within the central 5°. A steeper profile resulted for a 3mm pupil than for an 8mm pupil. He also found for both pupil sizes a linear decrease in the foveal sensitivity and the average macular sensitivity with increasing blur from 0 to +3D. The rate of decline was greater for the 8mm pupil. Goldstick and Weinreb (1987) found the mean sensitivity of the central field measured with the Octopus perimeter to decline with +1D and +2D of blur. Refractive blur was induced using soft contact lenses by Collin *et al* (1993) and subjects were tested with the HFA out to an eccentricity of 60°. They found the mean deterioration of perimetric thresholds with positive lenses to be 1.27dB per dioptre of defocus, and 1.01dB per dioptre with negative lenses.

The effect of blur on perimetric thresholds beyond 30 to 40 degrees is minimal (Sloan 1961; Aulhorn and Harms 1972). This may be due to the fact that peripherally the retinal image is blurred and distorted by the oblique passage of light rays through the refractive media. To some extent this is counterbalanced by the greater spatial summation more peripherally.

Refractive correction of the central and paracentral areas may differ, and can give rise to refraction scotomas (Schmidt 1955; Fankhauser 1969; Odland 1967). Refractive effects may be introduced unknowingly by physiological factors, for example accommodative spasm or fatigue, which are more likely in the young uncorrected hyperope. Wood *et al* (1988b) showed that accommodative microfluctuations are a minor component of the short-term fluctuation in perimetric sensitivity. The use of corrective lenses may produce artefacts due to the edges of the lenses. Approximately 4% of the light is lost due to reflection at each air-glass interface, a problem magnified by the use of multiple lenses.

3.2.3 Pupil size

The pupil controls the amount of light entering the eye and changes in pupil diameter can improve or degrade retinal image quality. Subjective brightness of peripheral light rays is only about 15% of that of central rays due to the directional sensitivity of the retinal cones (Stiles and Crawford 1934). This is to some extent counteracted by the greater capacity for spatial summation of the peripheral retina relative to the central region. Decreasing the pupil size reduces the retinal illumination, which is roughly proportional to the square of the diameter of the pupil, or its area (Tate 1985).

The image quality of any optical system reflects the sum of the effects of refraction and diffraction. The former may improve or degrade image quality, but the latter will always degrade the image. Refractive degradations such as those produced by aberrations are worse with larger pupils, the reverse is true for diffraction. In normal eyes as the pupil diameter reduces to 2.5mm the image improves, any further reduction and the diffractive effect becomes significant (Campbell and Gubisch 1966). If the pupil diameter falls much below 2.4mm the combination of decreased resolving power along with changes in the adaptive state of the retina, and the potentially greater significance of media opacities, can markedly alter the visual field. Normal variations in pupil size are not sufficient to influence the perimetric profile (Bedwell and Davies 1977; Fankhauser 1979; Brenton and Phelps 1986). This is supported by the fact the Herse (1992) found the slope of the retinal sensitivity profile for the central 5° to be the same for a 3mm and 8mm pupil.

Pharmacologically induced miosis has been found to depress the static perimetric sensitivity of the central field by 0.14 log units with manual static perimetry (Bedwell and Davies 1977; McCluskey *et al* 1986) and by 0.2 log units with static automated perimetry (Fankhauser 1979). Mean deviation (MD), a visual field index described later, deteriorated by 0.67dB in normal subjects after instillation of 2% pilocarpine (Lindenmuth *et al* 1989). Mikelberg *et al* (1987) reported that a reduction in absolute pupil diameter, induced by thymoximine 0.5%, produced no statistically significant change in the visual field indices. However, a highly significant positive relationship was found between the proportionate change in pupil diameter and mean sensitivity. Wood *et al* (1988a), varied the pupillary diameter using both 0.5% thymoximine and 10% phenylephrine. An increase in retinal sensitivity occurred as the pupil size increased, and this effect was more pronounced peripherally, thus producing a flatter sensitivity profile. It was suggested that the greater capacity for spatial summation of peripheral regions could preferentially utilise the increased intraocular light scatter associated with larger pupils, and thus increase peripheral sensitivity. A decline in MD of 0.83dB in normal subjects was demonstrated after instillation of 1% tropicamide (Lindenmuth *et al* 1990). This was believed to be caused by chromatic and spherical aberration. Greve (1973)

described a case in which a pupil change from two to six millimetres had no noticeable influence on the level of the sensitivity curve using the Visual Field Analyser. Rebolleda *et al* (1992) demonstrated an improvement in the threshold sensitivities of glaucoma patients, receiving miotic therapy, after instillation of 10% phenylephrine.

3.2.4 Media opacities

Opacities degrade the image in two ways; one is by defocusing the image and the other is by increasing the amount of light scatter. Cataracts have been shown to produce a generalised reduction in the sensitivity of manual static perimetry, with the central field being more affected (Greve 1973). Radius (1978) pointed out that while an I2e Goldmann isopter could be affected by trivial opacities, the other isopters were relatively unaffected. Intraocular light scatter causes attenuation of the light sensitivity in automated perimetry especially at lower background luminances (Greve 1973; Klewin and Radius 1986; Wood *et al* 1987b and c). For the Octopus automated perimeter the magnitude of this attenuation increased as a function of eccentricity (Wood *et al* 1987b).

3.2.5 Age

The superior region of the central visual field is influenced by age to a greater extent than the inferior field (Katz and Sommer 1986; Haas *et al* 1986). Decline with age is believed by some investigators to be homogenous for the central field (Brenton and Phelps 1986; Bebie 1985; Greve 1973). However, others have demonstrated both a depression and steepening of the hill of vision with age which is linear, for both automated perimetry (Katz and Sommer 1986; Jaffe *et al* 1986; Heijl *et al* 1987a and d; Iwase *et al* 1988), and manual perimetry (Drance *et al* 1967). This deterioration has been calculated to be between 0.4 to 0.6dB/decade (Haas *et al* 1986; Brenton and Phelps 1986) and to increase to 1dB/decade at 30° eccentricity (Heijl 1987). Flanagan *et al* (1993a) reported mean sensitivity to decline by 0.9dB/decade in normals. Collin *et al* (1988) however, found the rate of decline in sensitivity to increase with age in an un-homogenous manner. An accelerated loss of sensitivity has been demonstrated in normal subjects above the age of 55 years, with a decline in mean sensitivity of 0.34dB/decade in younger subjects, and 2.37dB/decade in subjects older than 55 years (Vivell *et al* 1993). Iwase *et al* (1988) reported mean sensitivity of the central 30° with the HFA to remain constant until the age of 37.4 years in normal subjects, and that above the age of 39 years mean sensitivity declined by 1.2dB/decade. They showed that in the majority of test locations the decline with age started between the ages of 24 and 44 years. Matsumoto *et al* (1991) described a more pronounced reduction in the mean sensitivity of the central 10° with age when smaller stimuli are used, being about1dB/ decade for stimulus size I and 0.5dB/decade for a size V stimulus. Increased nerve fibre layer drop-out and an increased cup-disc ratio

with age in normal subjects (Sommer *et al* 1984) are believed to be the cause of this loss of sensitivity. In addition, there is histopathologic evidence suggesting increased optic nerve atrophy with age (Balazsi *et al* 1984a).

3.2.6 Eccentricity

Retinal sensitivity has been shown to decline with eccentricity in both manual (Sloan 1961; Aulhorn and Harms 1972; Johnson *et al* 1978) and automated perimetry (Wild *et al* 1986 and 1987; Wood *et al* 1986 and 1988a; Goldstick and Weinreb 1987; Heuer *et al* 1989; Flanagan *et al* 1991). The sensitivity profile has been reported to be flatter in automated perimetry with larger stimulus sizes (Wood *et al* 1986; Wild *et al* 1987; Flanagan *et al* 1991) and lower background luminances (Flanagan *et al* 1991). Increasing the pupil size has been shown to reduce the effect of sensitivity decline with eccentricity (Wood *et al* 1988a). For the central 6° the retinal sensitivity was shown to decline by -0.377dB/degree on the Octopus by Weinreb and Perlman (1986), and Herse (1992) for the central 5° on the Humphrey Field Analyzer (HFA) calculated the gradient to be -0.75dB/degree. For the central 30° Brenton and Argus (1987) discovered the sensitivity to decline by -0.24dB/degree using the Octopus, and by -0.22dB/degree using the HFA. These are similar to the values reported by Heuer *et al* (1989), for the Octopus -0.29dB/degree, and -0.44dB/degree for the HFA.

3.3 Fluctuations in the Visual Field

It is accepted that the main source of error in the determination of static threshold sensitivity comes from the statistical nature of the patient responses. Threshold luminance can be statistically defined as that luminance which is perceived with 50% probability. In order to raise the probability of a seen response from 16% to 84% the stimulus luminance has to be raised by a factor of approximately two to four (Fankhauser and Bebie 1979). The accuracy of thresholds derived from 5 to 7 presentations, which is the routine in static procedures, must necessarily be poor. The probability for the stimulus to be differentiated from the background illumination is a function of its luminance, size and duration. Automated perimetry has minimised the influence of the perimetrist on the outcome of the examination, but the subjective components associated with the determination of any psychometric function still remain. These latter factors have been discussed with reference to manual perimetry (Aulhorn and Harms 1972; Tate and Lynn 1977), whilst the statistical nature of the response has been studied in relation to automated perimetry (Spahr 1975; Bebie *et al* 1976b; Flammer *et al* 1984a). The clinical relevance of these fluctuations is that they must be considered when analysing the significance of depressed visual sensitivities, to distinguish between true pathological defects and fluctuation.

3.3.1 Intra-subject fluctuations

If the visual threshold is measured several times at a location the result is not always identical. This variability of the threshold has been termed fluctuation, and is divided into short-term and a smaller long-term component (Bebie *et al* 1976a and b). Short-term fluctuation (SF) is the variation within a single examination. It depends largely upon the uncertain responses for stimuli near threshold, which is described by the frequency-of-seeing curve. The amount of fluctuation is influenced by the visual sensitivity, patient reliability, and the strategy employed by the instrument (Bebie *et al* 1976a).

SF has been shown to be greatest in the superior field and to increase with increasing eccentricity, especially for eccentricities beyond 30° (Jaffe *et al* 1986; Nelson-Quigg *et al* 1989). Wall *et al* (1993) found SF to increase with eccentricity in an exponential manner. Abnormal fields or abnormal areas of the visual field exhibit an increase in SF (Gloor *et al* 1984; Flammer *et al* 1984a and b; Werner and Drance 1977; Stürmer *et al* 1985; Langerhorst *et al* 1985; Piltz *et al* 1986; Heijl *et al* 1987c). It is now accepted that an early indication of visual field loss may be an increase in the localized fluctuation (Heijl 1985a; Werner and Drance 1977; Werner *et al* and 1987; Hoskins *et al* 1987; Heijl 1989). Flammer *et al* (1984b), Heijl *et al* (1989c) and Weber and Rau (1992) confirmed a strong association between the threshold level and threshold fluctuation, implying that fields with damage should always exhibit higher fluctuations. Brenton and Phelps (1986), contrary to other investigators (Holmin and Krakau 1979; Flammer *et al* 1984b, Starita *et al* 1987a), did not find a relationship between mean sensitivity of the central field and SF. Werner *et al* (1982) demonstrated SF to be greater for the central 5° in a group of patients with normal visual fields but elevated intraocular pressures, than in a group of normal controls. This agrees with Flammer *et al* (1984a), who used a program which extended 21° horizontally and 15° vertically from fixation. Using the same program, pupil size, except in glaucoma patients, and stimulus location in normals and glaucoma suspects, was found not to affect SF (Flammer *et al* 1984a and b). A relationship between SF and the number of false positive and false negative responses has been reported (Flammer *et al* 1984b). Whilst a relationship was revealed between SF and age by Autzen and Work (1990) this is at variance with other studies (Heijl *et al* 1989a; Brenton and Phelps 1986; Flammer *et al* 1984a and b; Werner *et al* 1982; Nelson-Quigg *et al* 1989). Katz and Sommer (1987) believe SF to be less affected by age than long-term fluctuation (see below), but that both increased significantly with age, and the longer the time interval between tests the more the time related variability increases. Increasing the brightness of the fixation target during testing (Safran *et al* 1992), and decreasing the background luminance to mesopic levels (Langerhorst *et al* 1991; Crosswell *et al* 1991) can increase the value of SF. Crosswell *et al* (1991) and Starita *et*

al (1987b) found that background luminances commonly employed by automated perimeters do not influence SF significantly. Increasing the size of the test stimulus reduces SF (Zulauf and Caprioli 1993; Wall *et al* 1993). Stimulus duration from 0.065 to 0.5 seconds were found not to affect SF (Pennebaker *et al* 1992).

SF is calculated as the root mean square of repeated thresholds at a number of points, and it has been found to lie within 44% of the true SF with a 95% confidence interval (Bebie *et al* 1976b).

$$SF = \sqrt{\frac{1}{m}\sum_{i=1}^{m}\frac{\sum_{r=1}^{R}\{x_{ir} - x_i\}^2}{R-1}}$$

where

m = number of locations with multiple determinations

r = particular repetition of a threshold

R = total number of threshold repetitions at a given location

x_{ir} = measured threshold at location i and repetition r

x_i = mean of R thresholds at location i

Generally the thresholds are only repeated once therefore R = 2. Chauhan *et al* (1991) demonstrated an increase in the local SF but not global SF when the number of threshold repetitions is increased from 2 to 5. They concluded that programs which determine the threshold only twice at a given location may underestimate the local fluctuation. Variability of SF has been shown to decrease as the number of locations with repeated thresholding increase (Casson *et al* 1990). In the Humphrey Field Analyzer it is calculated from double threshold determinations at 10 specified locations within 21° eccentricity. Flanagan *et al* (1993b) suggested using all the available double determinations of threshold to give a better estimation of the intratest variability.

An alternative determination for SF was proposed by Mills and co-workers (Schulzer *et al* 1990; Mills *et al* 1991), and does not require repeated testing. A polynomial was utilised to estimate the visual field surface and deviations of the measured field from this estimated field were used to assess the variance. The log of the estimated SF was within ±6.5% of the root mean square calculation. However, as the field became more defective it was more difficult to fit a polynomial to it.

Long-term fluctuation (LF) is an additional component of the variability encountered when tests are performed on different days (Bebie *et al* 1976b). It is due to changes in

the physiological state of the visual system. Long-term fluctuation is divided into a homogeneous component in which all the locations undergo a change in threshold in unison, and a heterogeneous component where the various locations do not change by the same amount (Bebie *et al* 1976a and Flammer *et al* 1983). A statistical relationship has been shown to exist between SF and LF (Flammer *et al* 1984c; Boeglin *et al* 1992). LF has been reported to

- be higher in glaucoma patients (Gloor *et al* 1980, Flammer *et al* 1984a) and glaucoma suspects (Flammer *et al* 1984c)
- increase with eccentricity in normal fields (Parish *et al* 1984; Lewis *et al* 1986; Heijl 1977b; Heijl *et al* 1987a and d) - particularly in the superior quadrant (Katz and Sommer 1987)- and glaucoma fields (Heijl *et al* 1989c; Magee *et al* 1987)
- to increase with progressive field loss (Werner *et al* 1987; Heijl *et al* 1989c and 1991; Boeglin *et al* 1992).

Zulauf *et al* (1991a) calculated LF, defined as the statistical variance of repeated measurements at each test location, to increase by $0.5dB^2$ for every decibel loss in sensitivity and by $0.1dB^2$ for each degree of eccentricity in a group of clinically stable glaucoma patients. Interestingly, in studies of glaucoma patients (Werner *et al* 1991; Boeglin *et al* 1992), the effect of test point location on LF largely disappeared after correcting for the differences in sensitivity in different regions of the visual field. Rutishauser *et al* (1989), however, did not find LF to increase with eccentricity. LF was unaffected by stimulus durations from 0.065 to 0.5 seconds in the study of Pennebaker *et al* (1992). According to Boeglin *et al* (1992) LF appears to be unrelated to age, but Katz and Sommer (1987) found a significant increase in LF with age. Heijl *et al* (1987d) and Werner *et al* (1987) showed these intertest threshold differences to be non-Gaussian. A variance of more than 4dB may occur at a single location in a normal field between tests (Wilensky and Joondeph 1984; Lewis *et al* 1986) and between 7-15% of locations may differ by 6dB or more (Keltner *et al* 1985). Werner *et al* (1987) suggested that a location needs to deteriorate by at least 6.4dB to constitute real change.

A summary of the magnitude of the mean short- and long-term fluctuations found in studies on normal subjects is given in table 3.1.

3.3.2 Inter-subject variation

Inter-subject variability exists and has been demonstrated to increase with eccentricity, (Brenton and Phelps 1986; Wild *et al* 1986; Heijl 1987; Heijl *et al* 1987a and d; Rutishauser *et al* 1989; Gundersen *et al* 1993) particularly in the superior field (Katz and Sommer 1986; Crosswell *et al* 1991), age (Brenton and Argus 1987) and pathologically

disturbed fields (Holmin and Krakau 1979; Flammer *et al* 1984 a and b; Wilensky and Joondeph 1984; Parish *et al* 1984; Lewis *et al* 1986; Katz and Sommer 1986; Hoskins *et al* 1987; Werner *et al* 1987). It has been found to be of the order of 1.91dB (Crosswell *et al* 1991), and typical values lie between 1.9 to 6dB. Werner *et al* (1982) examined this variability within the central 5°, and found it to be greater in glaucoma patients with normal visual fields but elevated intraocular pressures, as compared with normal subjects. In the same study no relationship with age could be demonstrated for the central 15°. Inter-subject variability decreases with training (Heijl *et al* 1989a), and a large proportion of the inter-individual variation can be explained by perimetric reliability (Heijl *et al* 1987c and d). If fields with good reliability scores are considered this variability reduces (Heijl *et al* 1987c). Intersubject variability decreases when larger test stimuli are used (Gundersen *et al* 1993).

Table 3.1. Summary of the mean short- and long-term fluctuations within the central field found in 16 studies on normal subjects

Investigators	**Perimeter**	**AGE** years	**No. of subjects**	**SF** dB	**LF** dB	**LF(HO)** dB	**LF(HE)** dB
Bebie *et al* 1976b	Octopus	10-70	11	1.8	1.7	1.0	1.3
Flammer *et al* 1984a	Octopus	mean 58	43	1.6	-	0.5	0.2
Rabineau *et al* 1985	Octopus	28-42	9	1.4-2.2	-	-	-
Brenton & Argus 1987	HFA	22-55	36	1.3	-	0.5	1.3
Brenton & Argus 1987	Octopus	22-55	36	1.6	-	0.6	1.6
Brenton *et al* 1986	HFA	22-47	20	1.65	-	-	-
Brenton & Phelps 1986	HFA	20-86	102	1.86	-	-	-
Katz & Sommer 1987	HFA	26-76	26	1.4	3.3	-	-
Heijl *et al* 1987c	HFA	-	84	1.57			
Heijl *et al* 1987d	HFA	20-80	95	1.42	1.6-6.0		
Iwase *et al* 1989	HFA	10-60	100	1.34			
Lindenmuth *et al* 1990	HFA	24-36	18	1.39			
Autzen & Work 1990	Octopus	50-83	33	1.76	-	-	-
Crosswell *et al* 1991	HFA	31.6±8.3	20	1.61	-	0.13	1.71
Chauhan *et al* 1991	Octopus	mean 57	10	1.48	-	-	-
Flanagan *et al* 1993a	HFA	23-83	98	1.36	-	-	-

SF = short-term fluctuation; LF = long-term fluctuation, HO = homogenous component, HE = heterogeneous component, HFA = Humphrey Field Analyzer

3.3.3 Inter-ocular differences

Brenton *et al* (1986) suggested comparing a diseased eye with the fellow normal eye. The normal inter-ocular differences ranged from 0dB to 9dB per test location. Greater differences occurred more frequently in the superior field and the standard deviation of these differences increased with eccentricity. They concluded that differences of 1.4dB in the mean sensitivity of the field should occur in less than 1% of normal subjects and that a 6dB difference should occur at fewer than 1% of the test locations. Zulauf *et al* (1991b) stated that asymmetry of more than 2dB in mean sensitivity between the eyes is suspicious of early disease.

3.4 LEARNING

It has been known for some time that there is a learning process with psychophysical testing (Low 1946; Haider and Dixon 1961). Aulhorn and Harms (1972) reported an increase in sensitivity of one log unit following 20 consecutive manual static perimetric threshold tests in one day. The presence of a learning process with subjects new to automated perimetry is well established (Greve 1973; Heijl and Krakau 1975a; Hodapp 1985; Wood *et al* 1987a), and is independent of the subject's age (Heijl *et al* 1989a). It is usually demonstrated as an improvement in the mean sensitivity, mean deviation, and both short- and long-term fluctuations. Consequently, one baseline visual field test may be insufficient, as a later reduction in the field sensitivity may be masked by perimetric learning. A number of investigators believe most of the learning to be complete after the performance of the first or second field tests (Flammer *et al* 1984a; Wilensky and Joondeph 1984; Hoskins *et al* 1988; Heijl *et al* 1989a). However, learning has been shown to continue beyond the first two field tests in some subjects, particularly if their baseline sensitivity values are low (Wood *et al* 1987a; Heijl *et al* 1989a; Wild *et al* 1989; Guttridge *et al* 1990). Kosoko *et al* (1986) failed to demonstrate a learning process with the Humphrey Field Analyser. However, only the test times between right and left eyes were compared as an indication of a learning or fatigue effect. Others have considered any improvement in sensitivity to be counterbalanced by a decrease in sensitivity associated with a fatigue effect, resulting from the duration of the examination (Katz and Sommer 1986; Brenton *et al* 1986). Baum and Schwartz (1992) did not find any improvement in the mean threshold values for the first four central fields performed with an Octopus perimeter.

The learning effect varies with visual field test location, becoming greater with increasing eccentricity, particularly beyond 30° and in the superior region of the field, in both normal subjects (Wood *et al*, 1987a; Heijl *et al* 1987c and 1989b) and glaucoma suspects

(Wild *et al*, 1989). This may arise from the patient learning to consciously raise the upper lid. A confounding factor is that the peripheral points tend to be measured towards the end of the test program. Wild *et al* (1989) and Searle *et al* (1991a and b) revealed a transfer of learning from the first to the second eye tested as an increase in mean sensitivity of the central field and the superior quadrant. The second eye tested produced less pronounced improvement over time as compared with the first. A retention of the learning was demonstrated after a period of two weeks (Searle *et al* 1991a) and nine months (Wild *et al* 1991). Indeed this transfer effect may also be influenced by fatigue resulting from the length of the examination itself (Heijl 1977a; Heijl and Drance 1983a and b). Heijl *et al* (1989a) and Wild *et al* (1991) state that following a training period, the presence of a learning effect at long-term follow up is small and can be ignored in the clinical context.

Learning effects have also been demonstrated in glaucoma suspects (Werner *et al* 1990; Adelson *et al* 1988), clinically stable glaucoma patients (Niles and Trope 1988) and in a retrospective study of glaucoma patients (Gloor *et al* 1981). Werner *et al* (1988b) in agreement with Grammer *et al* (1986) found little evidence of a learning process in stable glaucoma patients. However, in the former study a small learning effect was evident on SF.

3.5 FATIGUE

Increased effort and the attentional demands present in automated perimetry may adversely influence the sensitivity and reliability of visual field test results. Current test strategies have been devised under the assumption that the visual field sensitivity and response errors do not vary during the examination (Bebie *et al* 1976a and Fankhauser *et al* 1972). An increase in the contrast threshold with continuous testing has been demonstrated for 15 minutes (Jaffe *et al* 1986; Langerhorst *et al* 1987b), 30 minutes (Heijl 1977a; Heijl and Drance *et al* 1983a and b; Johnson *et al* 1988) and 60 minutes (Mills *et al* 1987; Heijl 1977a). Johnson *et al* (1988) found maximum sensitivity loss after 8-10 minutes of testing, the magnitude of which became larger with increasing eccentricity. However, Rabineau *et al* (1985) could not demonstrate a fatigue effect after 2 to 3 hours of profile automated perimetry in normals. Their conclusion was that a session of up to one hour does not significantly influence the threshold result, thus a 30 minute test should give reliable data from a normally attentive individual. Inspection of their data indicates a small average sensitivity loss over time for the central 30° with considerable individual differences. Also, their study included a small sample (n=8) of young normal individuals, half of whom were trained psychophysical observers. Their findings are not necessarily at variance with the results of other investigations. Heijl (1977a) did not report any significant difference in the fatigue effect as a function of

visual field eccentricity, but this study only extended to 15° eccentricity. Langerhorst *et al* (1987b) reported local fatigue to be greater than global fatigue, with a slight age dependency. Stürmer *et al* (1985) found SF to increase with increasing test duration in pathological fields. Fatigue effects which tend to increase with examination duration and which are greatest in or adjacent to relative scotomata have been reported in glaucoma (Heijl 1977a; Holmin and Krakau 1979; Heijl and Drance 1983b; Johnson *et al* 1988; Langerhorst *et al* 1987b) and in cases of optic neuropathies (Wildberger and Robert 1988). This may explain, to some extent, the enhancement or exaggeration of visual field defects with automated perimetry as compared with manual perimetry (Koerner *et al* 1977).

There is evidence for intra- and inter-test fatigue effects (Brenton *et al* 1986; Wild *et al* 1989; Hudson *et al* 1992; Coman *et al* 1994). Wild *et al* (1989) tested suspect glaucoma patients, naive to automated perimetry, examining the right eye followed by the left eye. The left eyes did not show the improvement in sensitivity, learning effect, over time as did the right eyes. At long-term follow up a statistically significant increase in the number of stimulus presentations, SF and a decrease in the sensitivity values in the mid-periphery of the left eyes (second eye tested) was interpreted as a fatigue effect (Wild *et al* 1991). A customised program consisting of 3 phases each lasting about 5 minutes exposed a decline in mean sensitivity and an increase in SF after the first phase. This fatigue effect continued for the remaining two phases, and was more pronounced in the second eye tested (Searle *et al* 1991a and b). Coman *et al* (1994) have also shown between eye fatigue effects.

3.6 Optimal configuration of test locations

Fankhauser and Bebie (1979) concluded that a grid formation of test locations is superior to points aligned along meridians and that averaging thresholds from two results aids the separation of true scotomata from pseudodefects. They also calculated the statistical probability of identifying 4° defects using a 6° grid to be 35%. To obtain 100% probability of detection the defects would need to be at least 8.4° in diameter. For detection purposes a 6° grid spacing is optimal (Fankhauser and Bebie 1979; Weber 1987; Heijl 1989). Fankhauser and Bebie (1979) pointed out that the detection probability of tiny scotomata of 1° radius or less, is very low irrespective of the grid configuration. Greve (1975) demonstrated that to detect a 3° circular defect, within the central field, with a probability of 95%, a total of 452 stimuli would be needed. However, since the purpose of the visual field examination is to detect field defects in a relatively short time, a compromise must be established. Interestingly, King *et al* (1986) demonstrated that a grid resolution of 6° is still inadequate for identification of scotomata of the size and depth of the physiological blind spot in the central field. Weber

and Dobek (1986) using the HFA deduced the optimal grid separation for detecting glaucomatous loss to be 3° within the central 10°, 4.2° between 10° and 20° eccentricity and 6° from 20° to 30° eccentricity. For detection purposes a stimulus size no less than 0.5° has been recommended (Fankhauser and Bebie 1979). Spatially adaptive programs are another alternative, a higher resolution is only used around locations with depressed thresholds (Häberlin *et al* 1980; Funkhauser *et al* 1988a and b). This saves time compared with a finer grid over the entire area.

CHAPTER 4

Design of the Humphrey Field Analyser 630

4.1 CONSTRUCTION AND CONCEPTS

The Allergan Humphrey Field Analyser (HFA) is an automated computer-driven projection perimeter providing a choice of threshold, screening and suprathreshold programs (Heijl 1985b). Visual field test results can be stored on computer discs as well as printouts. The stimulus is projected on to a hemisphere with a 33cm radius. Background luminance is fixed at 31.5 asb (10cd/m²,) while stimulus luminance can be varied over a 5.1 log unit range (0.08-10,000 asb) through a set of fixed neutral density filters plus a filter wedge. The decibel (dB) is the unit of threshold measurement on the HFA which is:

$$1dB = 10 \cdot \log(L_b/\Delta L) + 25$$

where L_b is background luminance, and ΔL is the luminance difference between stimulus and background (Weber and Rau 1992). Decibel values refer to retinal sensitivity rather than to stimulus intensity.

Table 4.1. Technical specifications of the HFA 630

Stimulus specifications	mode of presentation	static and random
	duration	0.2 seconds
	source	incandescent lamp
	intensities	0.08-10,000 asb
	intensity range	5.1 log units
	size	0.25-64mm²
	colours	white, blue, red, green
Background	surface shape	hemisphere, 33cm radius
	luminance	31.5 asb
Computer		Intel 8088 processor
Input unit		cathode ray tube/light pen
Output unit		Impact printer + CRT
Disc system		Two 5.25" floppy disc drives
Fixation monitoring		Blind spot + telescope

Stimulus positioning is automatically checked and adjusted at the beginning of each test. Edge detectors recheck correct mirror positioning each time the mirror passes the positions corresponding to the vertical and horizontal meridians of the visual field.

Currently the 'up and down staircase method', as utilised by the HFA, is believed to be the optimal threshold testing strategy (Cornsweet 1962; Sphar 1975; Heijl and Krakau 1975a; Krakau 1978; Heijl 1984; Hoskins and Migliazzo 1985). To obtain threshold the light intensity level descends/ascends by 4dB until the first reversal (from seen to not seen or vice versa), and then ascends/descends by 2dB until the second reversal. The last seen value is recorded as threshold. This testing strategy only was employed throughout the experimental work reported in this thesis.

Initially one primary point in each quadrant is tested twice, $x = 9$ and $y = 9$ (Haley 1987). These four points are used as starting levels for establishing threshold for neighbouring points, which are assumed to drop by 0.3dB for each degree of eccentricity. Results from secondary points are then used as starting levels (adjusted for eccentricity) for their neighbouring points (Heijl 1977b). If the measured threshold at a point differs by more than 0.4 log units from the expected value (which is based on the threshold of the neighbouring point) the threshold is measured again. Stimuli are presented randomly, which has been found to improve the stability of patients' fixation (Heijl and Krakau 1975a and b; Heijl and Krakau 1977), probably because the stimulus duration is too short for the patient to benefit from directing their attention to it, unlike manual kinetic perimetry.

4.2 RELIABILITY PARAMETERS

A patient's responses can be affected by factors such as mood, attention, nervousness, age and co-operation (Greve *et al* 1976; Brusini *et al* 1985). The reliability indices are an attempt to measure the patient's performance.

Fixation of the patient is monitored by random stimulation of the blind spot with a supraliminal stimulus, the size of which can be varied (Heijl and Krakau 1975a and b). A telescope enables the patient's eye to be viewed during testing and aids positioning the patient's pupil at the centre of the hemisphere. At the beginning of every test the position of the patient's blind spot is assumed to be in the average anatomical position. If the blind spot is not in its usual position it is re-plotted. If the patient responds to a supraliminal stimulus projected into the blind spot a fixation loss error is recorded. However, a distinction is not possible between a fixation loss (FL) and a false-positive (FP) error. A FP error occurs when the patient responds in the absence of stimulus presentation. At

random intervals a suprathreshold stimulus is presented in an area already tested. If the patient fails to respond to this stimulus a false-negative (FN) error is recorded. Field tests are flagged as unreliable if FL > 20% or if FP or FN >33%.

Several studies have reported a larger than expected number fields not meeting the reliability criteria set by the HFA for fixation losses (Nelson-Quigg *et al* 1989; Katz and Sommer 1988 Katz *et al* 1991; Bickler-Bluth *et al* 1989). For the other two reliability indices reports are varied in this regard. Recently it was shown that the reliability indices can be substantially reduced by proper training of technicians administering automated perimetry (Sunabrai *et al* 1991). Johnson and Nelson-Quigg (1993), in a prospective study of normal subjects, ocular hypertensive and early glaucoma patients, found fixation losses to be the main source of unreliable fields, but that in most cases fields are reliable.

Investigators have demonstrated that FN (Heijl *et al* 1987c; Starita *et al* 1987a; Katz and Sommer 1988; Katz *et al* 1991; Johnson *et al* 1988), FP (Johnson *et al* 1988) and FL (Heijl 1977a and b) errors are more common in glaucomatous than in normal subjects. This may be due to increased visual fatigue and variability with diseased eyes (Werner *et al* 1982; Flammer *et al* 1984a and b). However, the rates of FP (Flammer *et al* 1984a; Heijl *et al* 1987c and Katz and Sommer 1988) and FN errors (Flammer *et al* 1984a) have also been reported to be the same in normals and glaucoma patients.

Cascairo *et al* (1991) compared the mean deviation (defined later) in subjects who had performed a field test to the best of their capabilities, with subsequent field tests with the subject making deliberate FP, FN and FL errors. Mean deviation decreased (an improvement in the threshold level) and threshold variability increased with 20% or more FN errors. When the prevalence of FL and FP was 33%, mean deviation decreased but the threshold variability remained unchanged. In normals a higher FN rate was found to be associated with an apparent increase in localised defects, but FL rate did not exert any effect (Katz and Sommer 1990). More depressed visual sensitivities seem to produce a greater FP rate (Flammer *et al* 1984b), but Katz and Sommer (1990) demonstrated in normals that a higher FP rate was found in fields with less depressed thresholds. Glaucoma patients with higher FL and FP rates have fields with higher sensitivity values and fewer localised defects, whereas the opposite occurred with a higher FN rate, when compared with patients having good fixation and low FP and FN rates (Katz and Sommer 1990; McMillan *et al* 1992). Unreliable fields from glaucoma patients display an increased threshold variability between tests (McMillan *et al* 1992). Bennett *et al* (1991) recorded the difference in mean deviation between two fields to be unrelated to reliability indices. Age does not appear to have any effect on any of the reliability parameters in either normal nor defective fields (Bickler-Bluth *et al* 1989; Flammer *et al* 1984b).

4.3 STATPAC

This is the statistical package available with the HFA. It offers statistical analysis in three formats, single field analysis, overview and change analysis, which are available for the central 24° and 30° threshold test programs only. Firstly the global indices shall be described.

4.3.1 Global indices

These were first developed by Bebie and Fankhauser (1982) for the Octopus perimeter and described by Flammer *et al* (1985) in the analysis of glaucomatous fields. These ideas were further developed by Heijl *et al* (1987b) for the HFA. The global indices from the HFA, apart from mean sensitivity, are weighted for the variability at each location. Dividing the global index by the normal inter-subject variance minimises the values for the global indices in normals.

Mean sensitivity

The mean sensitivity (MS) is the arithmetic mean of the differential light sensitivity of all tested locations in the field.

$$\mathrm{MS} = \frac{1}{n}\sum_{i=1}^{n}\frac{1}{m}\sum_{k=1}^{m}\bar{x}_{ik}$$

$\bar{x}_{ik}$ = threshold value at test location i, replication k , m is the number of replications and n is the number of locations.
MS is more sensitive to diffuse field damage, and defects in small areas have little effect on MS. STATPAC can perform a linear regression analysis on MS if between five to sixteen central threshold field tests are available.

Mean deviation (MD)

MD is a weighted average deviation of the measured field from the normal reference field. It is the arithmetic mean of the differences between measured values and normal age-corrected reference field values at the tested locations (Heijl *et al* 1987b). Weighting by the normal variance is an attempt to take into consideration the variability of threshold at each stimulus location.

$$\mathrm{MD} = \left\{\frac{1}{n}\sum_{i=1}^{n}\frac{x_i - N_i}{s_i^2}\right\} \Big/ \left\{\frac{1}{n}\sum_{i=1}^{n}\frac{1}{s_i^2}\right\}$$

where N_i is the normal reference threshold and x_i is the measured threshold at point i, and s_i^2 the variance of the normal field at point i. MD estimates the uniform part of the deviation of the measured field from the age-corrected normal reference field. With increasing field defects MD becomes an increasing negative number. Langerhorst *et al* (1987a), found MD to be a better estimator of the visual field behaviour over time than MS. If five to sixteen fields are available a linear regression analysis can be performed on MD. One of two messages, 'MD slope not significant' or 'MD slope significant', will be printed below the results.

Short-term fluctuation (SF)

SF is a weighted mean of the standard deviations at ten points where the threshold is determined twice.

$$SF^2 = \left\{\frac{1}{10}\sum_{j=1}^{10} s_j^2\right\}\left\{\frac{1}{10}\sum_{j=1}^{10}\frac{(x_{j1}-x_{j2})^2}{2s_j^2}\right\}$$

where x_{j1} is the first and x_{j2} is the second threshold value at location j. The normal intra-test variance is denoted by s_j^2, dividing by this was stated to minimise SF^2 in normals (Heijl *et al* 1987b). SF is calculated from double determinations at ten specified locations within 21° eccentricity.

Pattern standard deviation (PSD)

PSD is a weighted standard deviation of the point-wise differences between the measured and normal reference field. PSD estimates the non-uniform part of the deviation. It is an attempt to express any deviation of the shape of the measured field from the shape of the reference field. PSD is always positive and increases when localised field defects develop and progress. Weighting by $1/s_i^2$ was stated to minimise PSD^2 in normals.

$$PSD^2 = \left\{\frac{1}{n}\sum_{i=1}^{n} s_i^2\right\}\left\{\frac{1}{n-1}\sum_{i=1}^{n}\frac{(x_i - N_i - MD)^2}{s_i^2}\right\}$$

Corrected pattern standard deviation (CPSD)

CPSD estimates that part of the non-uniform deviation which is not caused by SF. CPSD

aims to differentiate between real deviations and those due to scatter.

$$CPSD^2 = PSD^2 - k \times SF^2$$

Alongside the global indices a probability value is printed. This estimates the likelihood of the index lying outside normal limits.

4.3.2 Data presentation

Traditionally, perimetric data has been represented by various forms of graph. With automated perimetry the numerical data can be represented in a variety of forms. The single field analysis printout of STATPAC is most commonly used (figure 4.1). The various components of this plot shall be described. With every printout the date, patient name, program used, testing strategy, conditions of test, reliability indices, questions asked (number of stimuli presented), test duration, and time of test are recorded. The HFA prints an XX after any of the reliability indices that fall outside established limits for reliability.

4.3.3 Numeric

In the numeric format (figure 4.1, top left), threshold sensitivities are printed in decibel (dB) units. Each decibel sensitivity corresponds to a given stimulus intensity at that location. This format provides the most accurate information, but it is difficult to interpret (Greve 1982).

4.3.4 Gray scale

Gray scale plots (figure 4.1, top right), in which the sensitivity values are represented by a gray symbol, are easy to interpret. Fankhauser *et al* (1972) first introduced interpolation for static perimetry and the gray scale display. Ten gray levels are available, and a key is printed at the bottom of every visual field printout. Interpolated sensitivities are derived from measured sensitivities at neighbouring locations, and are only slightly less accurate than direct measurements when the inter-stimulus separation does not exceed 6° (Fankhauser and Bebie 1979). However it has been shown that this form of data presentation can be inaccurate depending upon the interpolation procedure (Weber and Geiger 1989).

4.3.5 Total deviation plots

Firstly a normal field contour is constructed by the HFA using the second-most sensitive value of the four primary points (one in each quadrant), or of five points if the foveal threshold has been measured. Differences from this normal plot and the measured field are displayed in two formats, numeric and grayscale. In the upper plot numerical values (figure 4.1, middle left) represent the depth in decibels of any defect relative to the age corrected normal threshold values at each location. These values are converted into grayscale symbols (figure 4.1, bottom left). A key is given to the right of the plot, 'probability symbols'. The probability significance levels are 5%, 2%, 1%, and 0.5%. If for example a location is identified with $p<5\%$, it means that less than 5% of the normal population deviates from the norm by the value found at that location (Haley 1987). The darker the symbol the less likely it is that the field is normal at that location. A variation of this plot is the defect depth, in which values within 4dB of the age related normal reference field are displayed as 'o' and larger deviations are expressed in decibels

4.3.6 Pattern deviation plots

The last two plots on the right of figure 4.1 are the 'pattern deviation plots'. These are similar to the total deviation plots, except STATPAC has adjusted the test results for any change in the height of the hill of vision. This is to try and separate diffuse from localised changes. For example, if the total deviation plot shows many darker symbols which are less frequent in the corresponding pattern deviation plot, this indicates that the field loss is mainly due to a general reduction in sensitivity with few localised defects.

Finally, a short list labelled 'global indices' appears on the far right of the page. The p values for each global index give the probability of the index being outside normal limits. For example, if for MD the value $p < 2\%$ is given, less than 2% of the normal population show an MD larger than the value found in the test.

A variation of the above is the three-in-one printout, which includes the gray scale, numeric and total deviation map. The summation of all threshold values in each quadrant is presented just outside each quadrant of the field.

4.3.7 Profile

Profile printouts can be used to evaluate meridional cuts through the visual field (figure 4.2)
Additional printouts are available for the results from screening tests performed by the HFA but are not described here.

4.3.8 Overview and change analysis printouts.

STATPAC's overview printout can show the results of up to 10 tests in chronological order (figure 4.3). Four formats are plotted, grayscale, numeric, total deviation and pattern deviation. Like the overview the change analysis shows the STATPAC analysis of up to 10 tests. STATPAC presents the change analysis in the form of a box plot analysis of the test results and a summary of the four global indices. The purpose of this is to try to identify any trends over time (Haley *et al* 1987). The box plot will not be discussed further because no use is made of it hereafter.

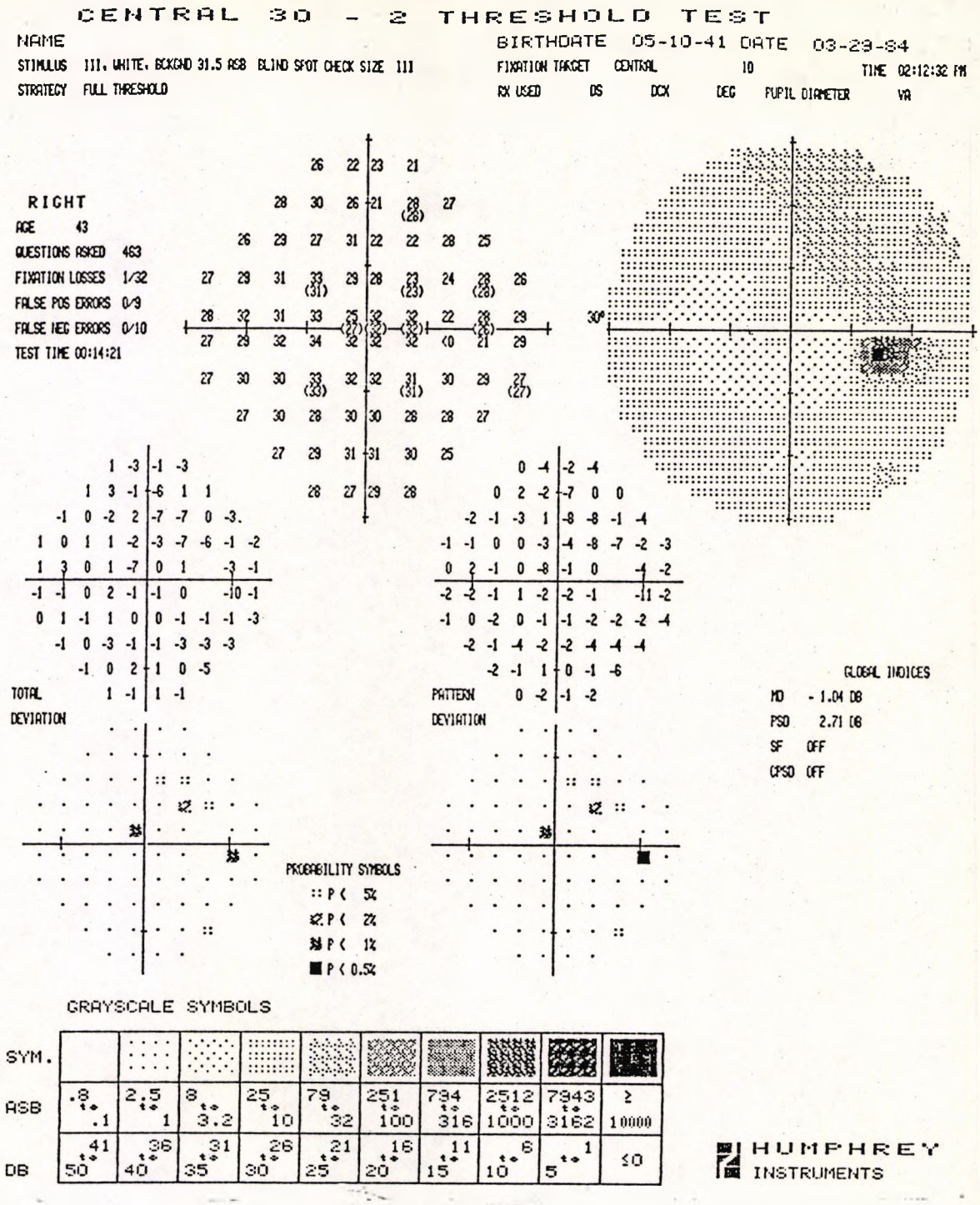

Figure 4.1. Standard printout from the HFA for the central 30-2 program.

CENTRAL 30 - 2 THRESHOLD TEST

STIMULUS III, WHITE, BCKGND 31.5 ASB NAME
BLIND SPOT CHECK SIZE III ID BIRTHDATE 03-19-28
FIXATION TARGET CENTRAL DATE 05-19-86 TIME 12:51:33 PM
STRATEGY FULL THRESHOLD PUPIL DIAMETER 3 MM VA 20/50
RX USED +4.0 DS DCX DEG

RIGHT

FIXATION LOSSES 2/28
QUESTIONS ASKED 554
FALSE POS ERRORS 0/11
FALSE NEG ERRORS 1/17
FLUCTUATION 2.57 DB
FOVEA: 23 DB
TEST TIME 00:15:38

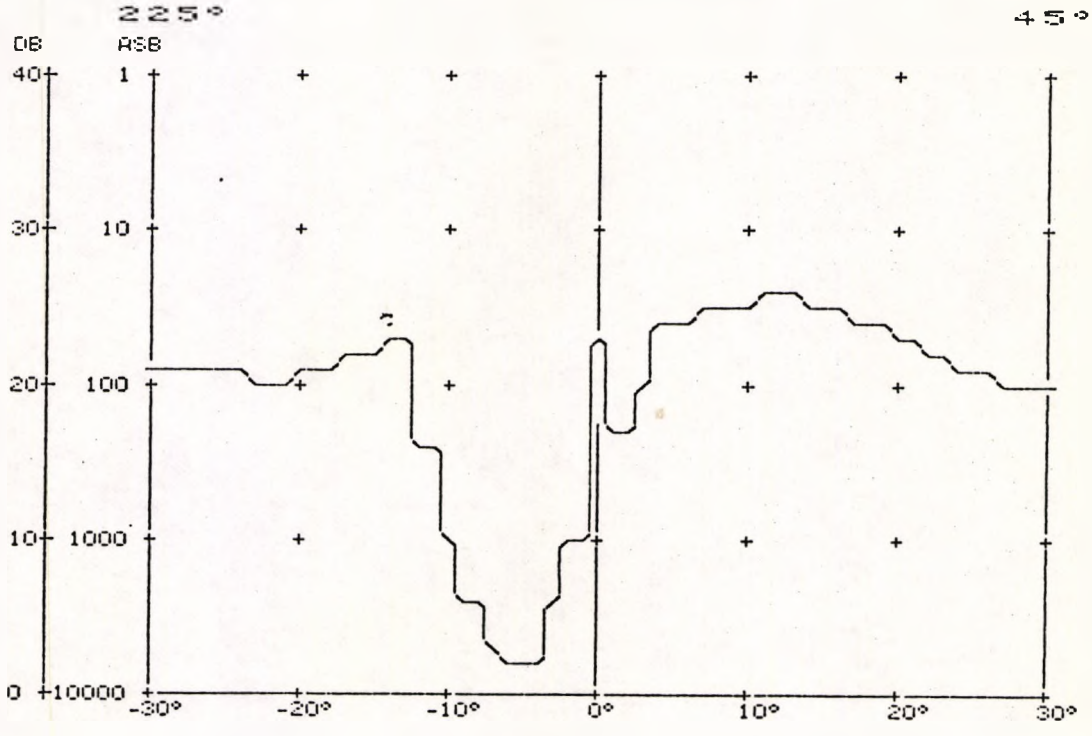

GRAYSCALE SYMBOLS

SYM.									
ASB	.8 to .1	2.5 to 1	8 to 3.2	25 to 10	79 to 32	251 to 100	794 to 316	2512 to 1000	7943 to 3162	≥ 10000
DB	41 to 50	36 to 40	31 to 35	26 to 30	21 to 25	16 to 20	11 to 15	6 to 10	1 to 5	≤0

ALLERGAN HUMPHREY

Figure 4.2. Profile printout from the HFA.

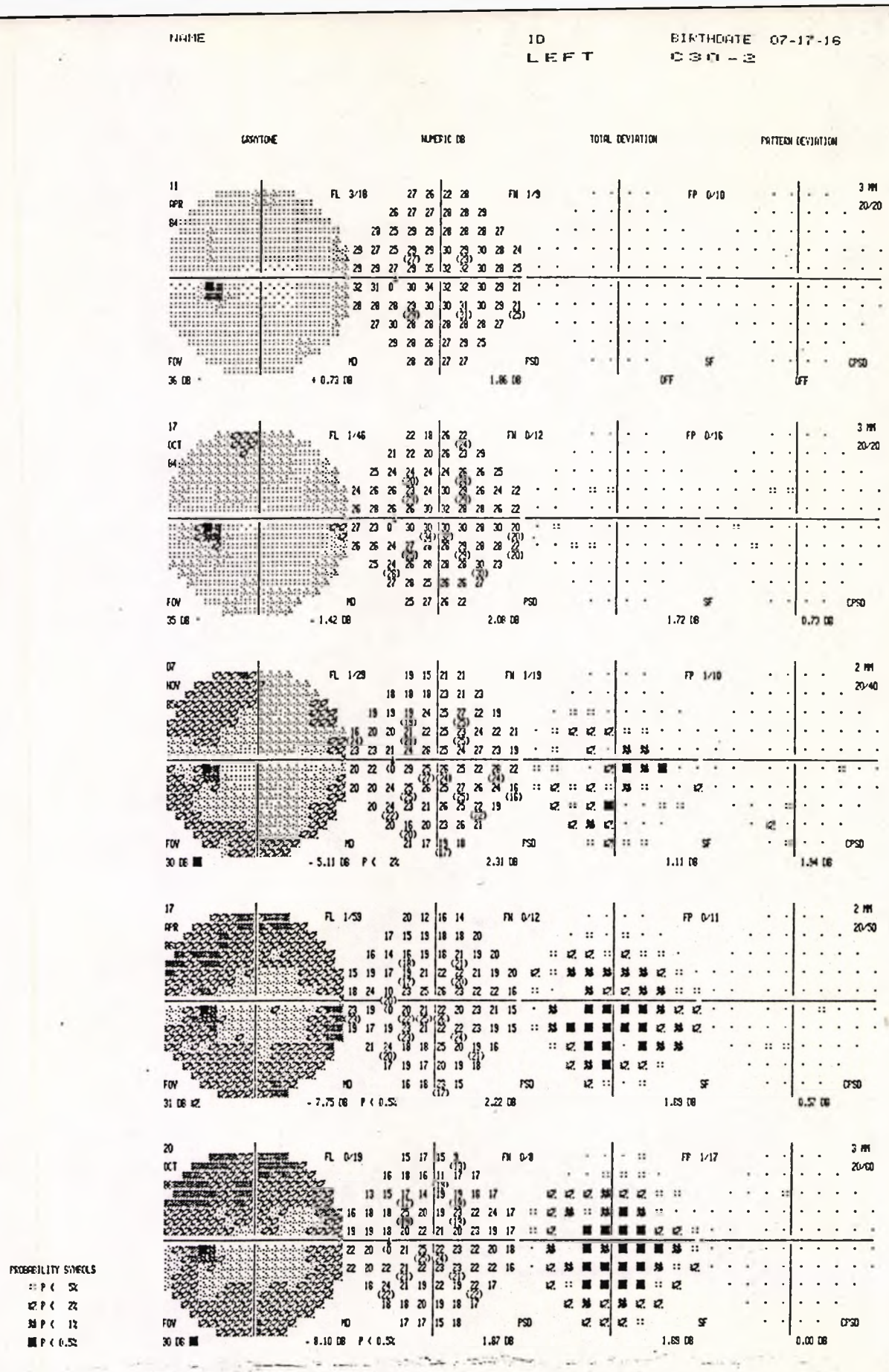

Figure 4.3. Overview printout from the HFA.

CHAPTER 5

Clinical evaluation of the Allergan Humphrey Ultrasonic Biometer 820

5.1 INTRODUCTION

At the outset of this work the recently marketed Allergan Humphrey 820 ultrasonic biometer became available for use in this study. At that time there was no published data relating to instrument accuracy, apart from unsupported manufacturer's data. Before this biometer could be incorporated into this study its repeatability and reproducibility had to be established. Information regarding the instrument's repeatability and reproducibility are vital aspects of instrument accuracy which are usually omitted from clinical assessments of biometers. Such an investigation should be performed before, or concurrently with, comparisons between instruments (Altman and Bland 1983). The ease of use of the biometer was assessed by comparing an experienced with an inexperienced experimenter.

Ultrasonic biometry was first performed on the eye by Mundt and Hughes (1956). Baum (1956) reported no adverse effects on ocular tissue from low-intensity pulsed ultrasonography as opposed to the radiographic methods employed by Sorsby and O'Connor (1945) and Stenstrom (1946). The use of ultrasound on the eye is widespread in diagnostics and in measurement of ocular dimensions.

5.2 MATERIALS AND METHODS

5.2.1 Instrumentation

The Allergan Humphrey model 820 ultrasonic biometer (figure 5.1) was employed. The manufacturer's specifications state the probe to contain a focused transducer with a frequency of 10MHz, which can be hand held or mounted on a slit lamp using the cone holder of the Goldmann applanation tonometer. The calibrated sonic velocities are,

Vitreous and aqueous	1532 m/sec
Lens	1640 m/sec
Aphakic mean velocity	1533 m/sec
Pseudo phakic mean velocity	1553 m/sec

These values are in accordance with Jansson and Sundmark (1961) and Jansson and Kock (1962).

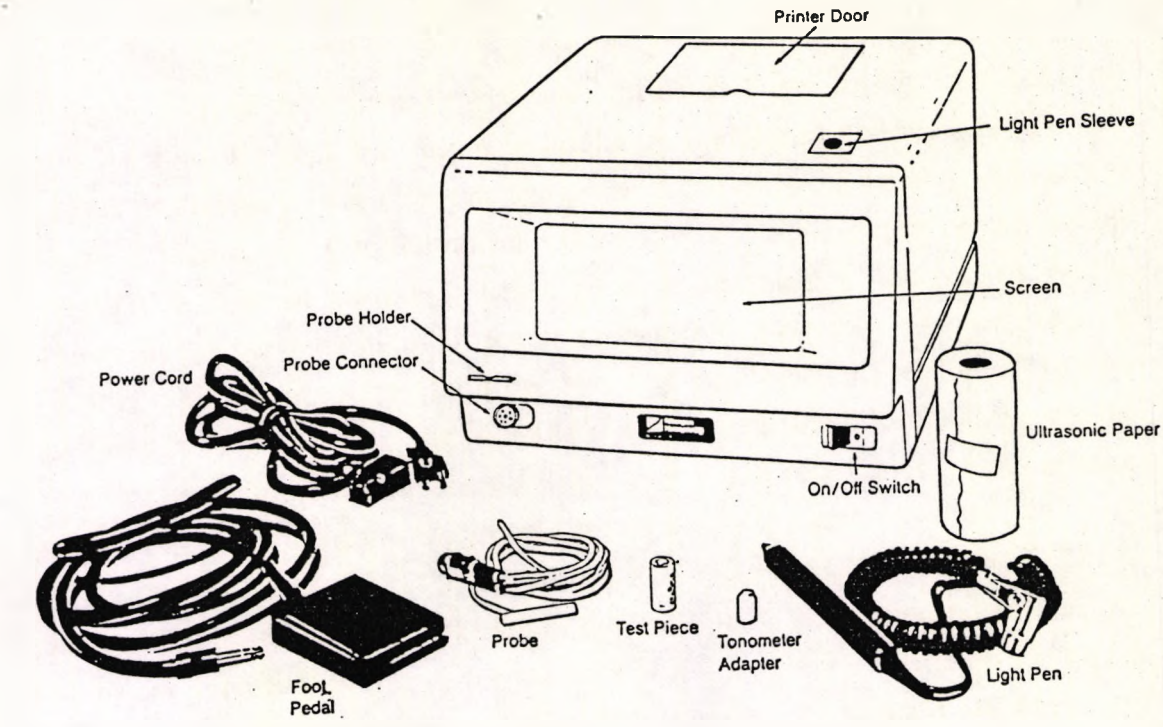

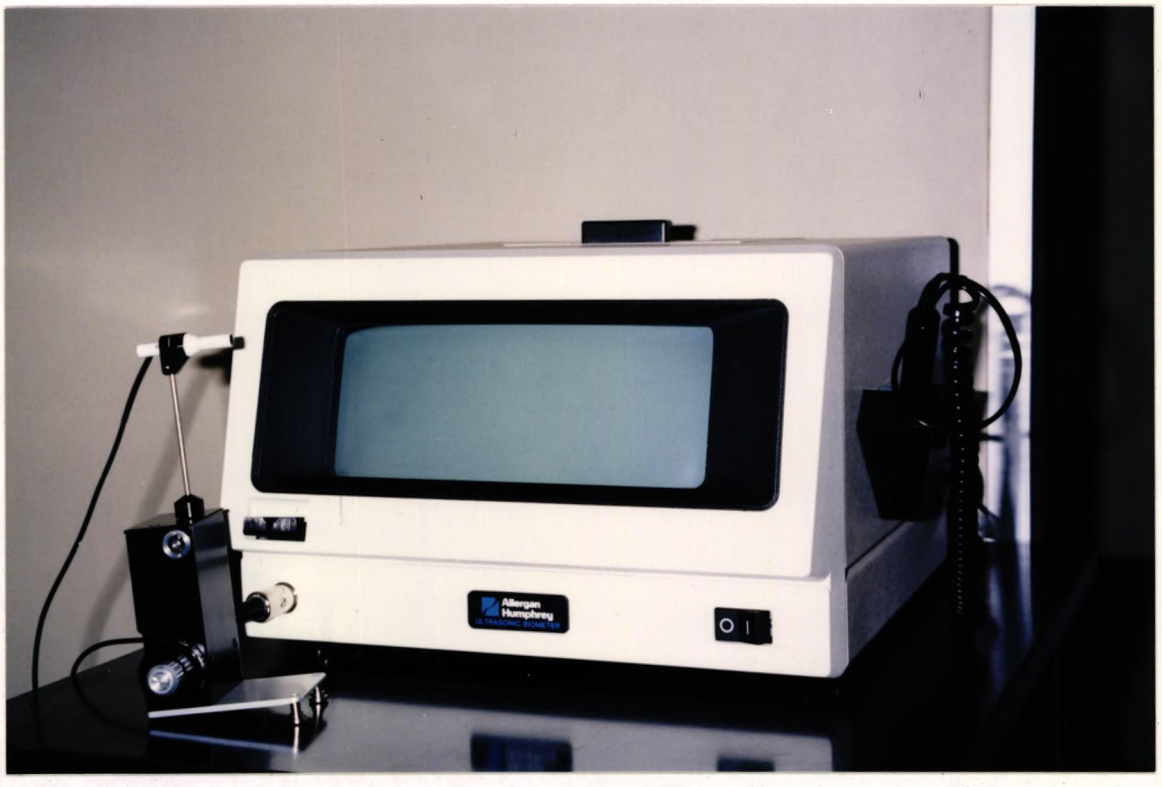

Figure 5.1. Photograph and schematic diagram of the Allergan Humphrey 820 ultrasonic biometer.

The amplification of the response signal (gain) of the biometer can be increased from zero to 100% in 10% steps. It is recommended by the manufacturer to begin at 60% gain and adjust as necessary. When the gain and probe alignment are optimal the echospikes are clean and sharp with lens and retinal echoes of almost equal amplitude. An audible sound indicates corneal contact at which point, if alignment is correct, an A-scan measurement will be momentarily frozen on the screen (indicated by a higher bleep). If the A-scan fulfils the above criteria it can be stored by a quick depression of the foot pedal. Stored measurements can be reviewed and erased if desired. Readings were taken only at first contact to minimise corneal indentation. Consistent values for the anterior chamber depth are an indication that corneal indentation is constant.

The model 820 offers three measurement modes: automatic, semi-automatic and manual. These modes differ in their criteria for an acceptable scan and the way scans are frozen and stored. In all three modes one can store the current A-scan with a quick depression of the foot pedal. In this study the semi-automatic mode was used. In this mode the amplitude criteria are relaxed by 25% from the criteria imposed by the automatic mode and the instrument analyses less data before presenting a frozen A-scan.

5.2.2 Procedure

Calibration of the biometer was checked at the beginning of every session by measuring the test block supplied with the instrument.

Thirty subjects (60 eyes) free from ophthalmological abnormality, aged 24 to 57 years (mean 37 years) were examined on two separate occasions to evaluate repeatability and reproducibility. Ten of the subjects (20 eyes) returned for a further three sessions to assess the intersession variability. Mean spherical refractive error was within ±6.00DS and no subject had a cylindrical error greater than 3.25DC. The examination procedure was as follows,

- keratometry was performed using the Topcon keratometer. Eyes reflecting distorted mires were excluded
- contact lens wearers left their lenses out on the day of measurement
- one drop of 0.4% benoxinate hydrochloride was instilled in each eye. The biometer probe was housed in the holder for the cone used in Goldmann applanation tonometry and the pressure set to 1g. Application of the probe should be perpendicular to the central cornea, along the visual axis. This was assisted by the corneal reflection of the probe fixation light as it approached the cornea. Accommodation was controlled by the non-tested eye fixating a pen torch at 4 metres

To reduce the number of probe applications, only two different gain settings were used. 60% gain was always used for subjects right eyes and 40% for the left eyes. Right eyes were always measured first. Steele *et al* (1992) have shown the effect of the order of eye measured to be insignificant. To assess reproducibility, measurements were taken by two experimenters, one experienced in the use of the Humphrey 820 biometer, and the other inexperienced. The order of the experimenters was randomised and each obtained an average from 5 readings on each eye. After biometry a slit lamp examination was performed as a precaution.

5.3 STATISTICAL ANALYSIS

5.3.1 Repeatability

This is the intra-experimenter variation. Results from each experimenter are analysed separately comparing sessions 1 and 2. Graphs were drawn for pairs of data obtained by each experimenter on the two occasions, and correlation coefficients were evaluated. These measure the association between pairs of data, rather than the agreement between them. However, the proximity of the points to the regression line does give some indication of the agreement. As a preferred alternative to the correlation approach the differences between paired values obtained at sessions 1 and 2 were plotted against their mean for each ocular dimension. These plots allow investigation of any relationship between the measurement error and the true value. The true value is unknown and the mean of the measurements is the best estimate (Bland and Altman 1986). It would be a mistake to plot the differences against either value separately because the difference will be related to each, a well known statistical artefact (Altman and Bland 1983).

The coefficient of repeatability can be calculated, defined by British Standards Institute (BS 5497) to be twice the standard deviation (SD) of the mean difference. Thus by definition 95% of the values will fall between ±2SD. Provided that the differences within ±2SD would not be clinically important one can say there is good repeatability between the two measures.

5.3.2 Reproducibility

Many factors can affect a measurement such as observer, time of day, position of subject, laboratory used etc. A distinction is made between repeatability and reproducibility, which is examining how results vary under different conditions. The inter-experimenter variation was examined for session one, comparing the inexperienced (E2) with the experienced (E1) experimenter. Graphs for pairs of data, correlation coefficients and regression lines were examined as for repeatability. The differences between paired

values were plotted against their mean. The mean of the differences is calculated together with its SD to construct the 95% limits (Bland and Altman 1986).

5.3.3 Inter-session variability

A two-way analysis of variance with 'subjects' and 'session' as the main effects was used. Apart from the expected differences between subjects the objective of this model is to detect the presence of any significant difference between sessions and any interaction effect (i.e. a 'variable bias' between sessions for subjects). However, this design does not allow for the fact that the same subjects are examined by two experimenters over each of the five sessions. Thus a two-factor design with repeated measures on one factor (Winer 1972) was performed. This modifies the partition of the variability of the within-cell structure allowing, under the correct conditions, a more sensitive detection of a difference in either the session effect or interaction effect.

5.4 RESULTS

The repeatability results are presented in table 5.1 and figures 5.2 and 5.3. Typical examples are given, with emphasis placed upon the axial length results as these showed greatest variability. Although only two examples of scattergraphs are shown, the other scattergraphs were virtually identical to those in figure 5.2, which reflects the inadequacies of this method of analysing the data.

Correlation coefficients were high in every case, invariably 0.95 or above, but they do not give any indication of the actual agreement. Difference plots showing the 95% confidence limits for the mean of the differences (figure 5.3) allow a more valid assessment of the agreement. Individual data points should be evenly distributed above and below the mean at all x values. Typical examples are given in figure 5.3, which show an acceptable spread about the mean, with one exception, figure 5.3d. In addition there should not be any 'funnelling effect'. There is little evidence of funnelling in any of the examples illustrated, with the possible exception of figure 5.3f, where there may be a slight tendency for the points to appear to spread out as the axial length increases. This would imply that the repeatability declines as this dimension increases. However this is not conclusive due to the few data points available. The increase in curvature of the posterior pole in longer eyes (Shammas and Milkie 1989) may account for any 'funnelling effect'. It is analogous to measuring a cup with a wide ruler. The 95% confidence limits for AC depth are +0.12/-0.13mm, for lens thickness +0.11/-0.13mm, for axial lengths for right eyes +0.17/-0.19mm, and axial length for left eyes +0.26/-0.40mm.

Table 5.1. Repeatability results comparing session 1 and session 2 for experimenter 1 (E1) and experimenter 2 (E2).

Ocular dimension		mean difference (mm)	standard deviation (mm)	95% confidence limits (mm)
Anterior chamber depth				
RE	E1	-0.009	0.058	+0.107/-0.125
RE	E2	-0.012	0.050	+0.088/-0.112
LE	E1	0.001	0.062	+0.125/-0.123
LE	E2	-0.003	0.058	+0.113/-0.119
Lens thickness				
RE	E1	-0.002	0.053	+0.104/-0.108
RE	E2	-0.001	0.058	+0.115/-0.117
LE	E1	-0.012	0.060	+0.108/-0.132
LE	E2	-0.006	0.059	+0.112/-0.124
Axial length				
RE	E1	-0.012	0.090	+0.168/-0.192
RE	E2	-0.010	0.078	+0.146/-0.166
LE	E1	-0.072	0.166	+0.260/-0.404
LE	E2	0.006	0.127	+0.260/-0.248

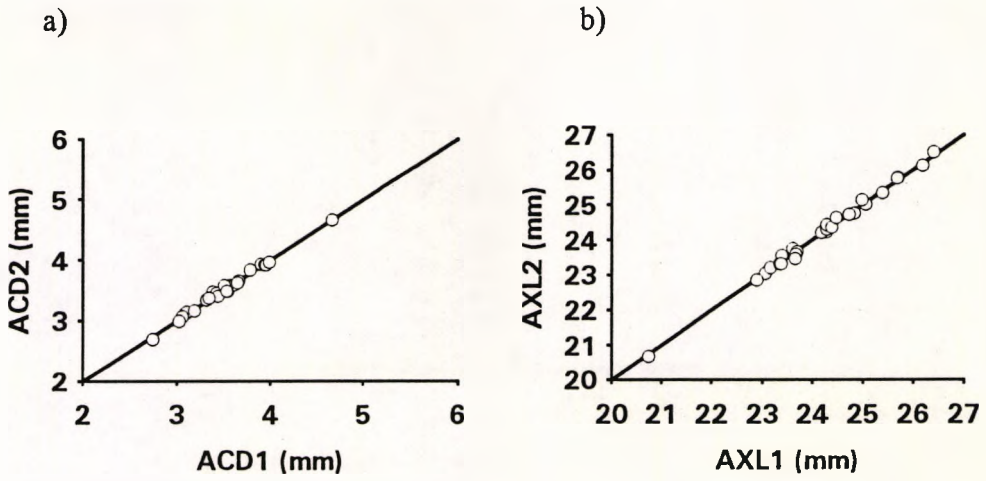

Figure 5.2. a) anterior chamber depth for session 2 (ACD2) plotted against session 1 (ACD1) for experimenter 2, left eyes; b) axial length for session 2 (AXL2) plotted against session one (AXL1), for experimenter 1, right eyes.

Reproducibility results are presented in table 5.2 and four typical graphs in figure 5.4. These results show that reproducibility was at an acceptable level for all ocular dimensions. From the repeatability and reproducibility results it is clear that the measurement of left axial lengths show greatest variability. Using the 40% gain there is a greater chance of error when the biometer automatically assesses the retinal echospike, which with the lower gain setting tends to be confused with echospikes from surrounding tissue interfaces at the posterior pole. A similar observation was made by Oksala and Varonen (1964). With the 60% gain the retinal echospike is more clearly defined and more easily distinguished. If we exclude all the left axial length results the maximum 95% limits for repeatability become +0.17/-0.19mm and those for reproducibility +0.19/-0.18mm. Similar reproducibility results were obtained for session 2.

The results for the inter-session analysis show no evidence of any significant session or interaction effects over the 5 sessions. Finally a two-factor model with 'subjects' and 'experimenter' as the main effects was used. No significant difference was found between the experimenters over the five sessions. For all cases the F-test was not significant, $p>>0.1$. Assumptions underlying the two-way analysis were checked throughout. Cochran's test (Winer 1972) determined the equality of cell variances. Graphical analysis of residuals verified the independence and normality. However, detailed inspection of the latter (using the Shapiro-Wilk test, Dunn and Clark 1974) indicated some non-normality in the case of axial lengths. Scheffe (1959) has shown that this is not a serious violation especially in cases such as this where each cell within the design has an equal number of observations.

Slit lamp examination showed minimal or, in the majority of cases, no corneal staining.

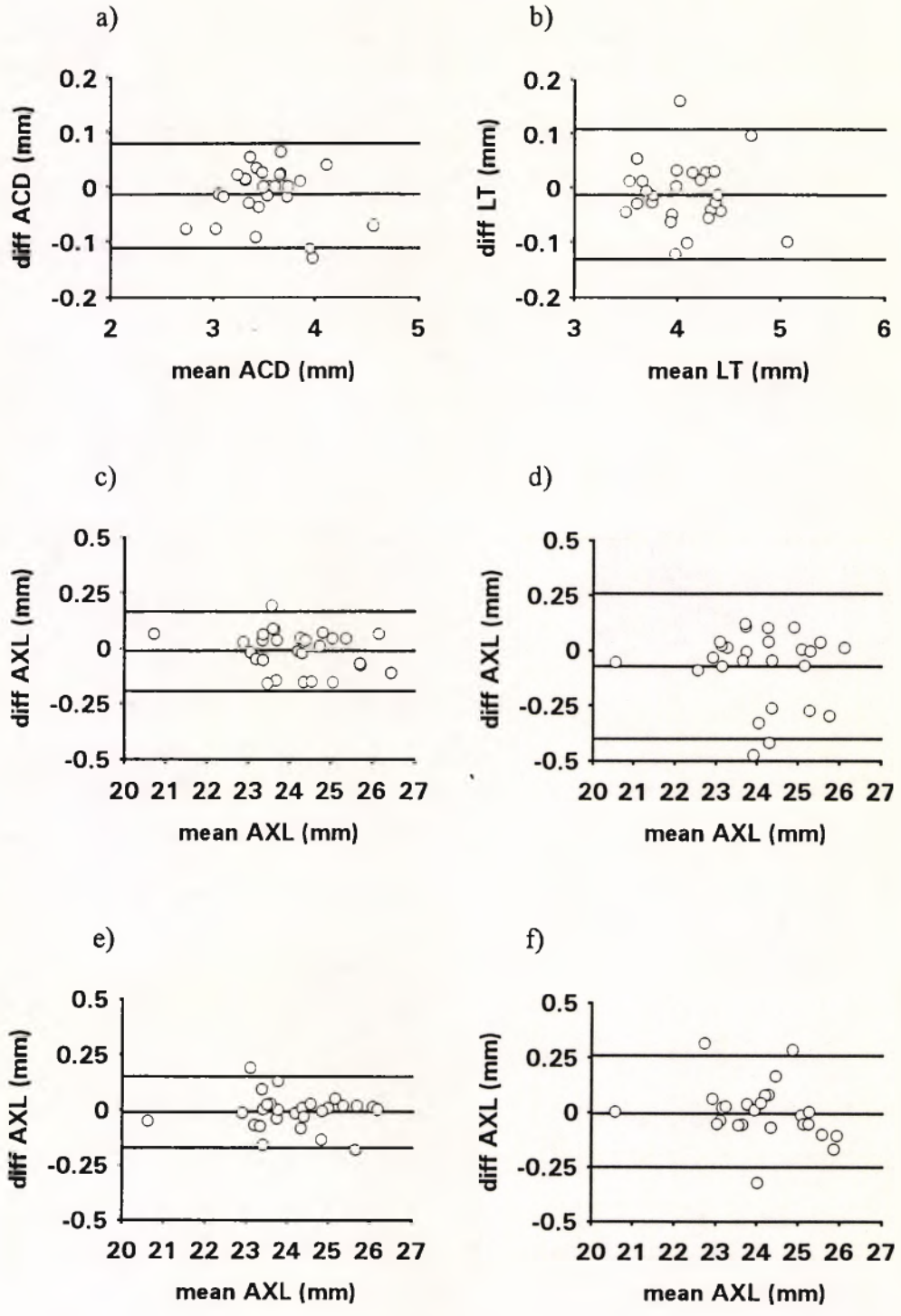

Figure 5.3. Differences between paired values for sessions 1 and 2 plotted against their mean for a) experimenter 2, right eyes, b) experimenter 1, left eyes, c) experimenter 1, right eyes, d) experimenter 1, left eyes, e) experimenter 2, right eyes, f) experimenter 2, left eyes. The horizontal lines represent the mean difference and 95% confidence limits. ACD = anterior chamber depth, LT = lens thickness, AXL = axial length.

Table 5.2. Reproducibility comparing experimenter 2 with experimenter 1 for session 1.

Ocular dimension	mean difference (mm)	standard deviation (mm)	95% confidence limits (mm)
Anterior chamber depth			
RE	0.001	0.070	+0.141/-0.139
LE	-0.015	0.056	+0.097/-0.127
Lens thickness			
RE	-0.020	0.068	+0.166/-0.156
LE	0.009	0.054	+0.117/-0.099
Axial length			
RE	0.004	0.093	+0.190/-0.182
LE	-0.015	0.117	+0.219/-0.249

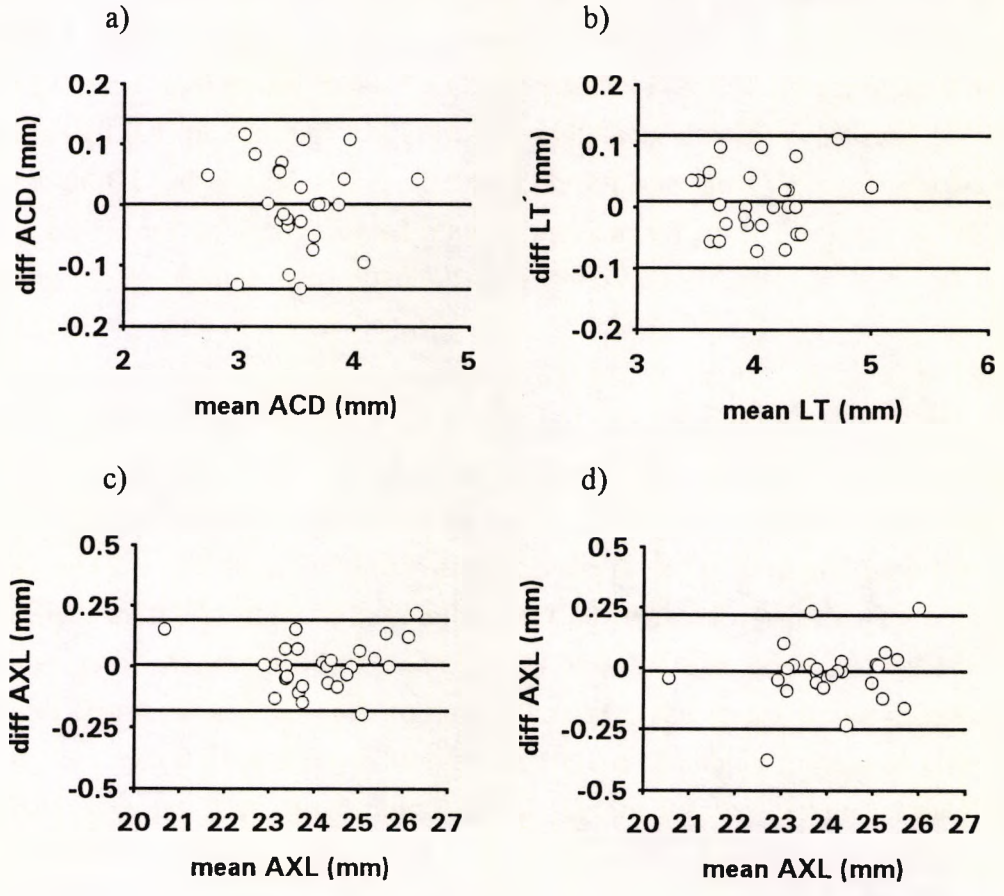

Figure 5.4. Differences between paired values obtained by the two experimenters plotted against their mean value for session 1. a) and c) right eyes, b) and d) left eyes. The horizontal lines represent the mean difference and the 95% confidence limits. ACD = anterior chamber depth, LT = lens thickness, AXL = axial length.

5.5 DISCUSSION

Accurate measurement of the optical dimensions of the eye is of great importance, not only in this study but also, for example, in determining intraocular lens (IOL) calculations, monitoring patients with axial elongation or studying the ocular dimensions in different eye conditions. Van Alphen (1961) found that a 1mm change in axial length varied the refraction by 2.43D. However, according to Elenius and Sopanen (1963), for the average aphakic eye 0.50D corresponds to 0.35mm in axial length, and Storey (1982) states that 0.3mm is equivalent to 1.00D.

With the solid probe used in this study, the effect of corneal applanation upon the axial length needs to be considered. It has been shown in previous studies that the axial length determinations obtained with a contact technique are somewhat shorter than those obtained with an immersion technique (Shammas 1984, Artaria 1986, Schelenz and Kammann 1989; Olsen and Nielsen 1989; Olsen 1989; Snead *et al* 1990). Steele *et al* (1992), demonstrated the degree of corneal applanation to be approximately 0.1mm with the biometer used in this study. This corresponds to an error of approximately 0.36D in calculated IOL power, and should be taken into account when empirical corrections are made in IOL calculation. However, Olsen (1989) calculated the axial length optically in pseudophakes, and demonstrated a better agreement between this and the Sonometrics applanation technique than with the Kretz immersion technique.

Jansson (1963) obtained repeatabilities of ±0.108mm for AC depth, ±0.135mm for lens thickness and ±0.114mm for axial length using immersion biometry; Binkhorst (1981) calculated the repeatability for the Sonometrics digital rule to be ±0.12mm, Storey and Rabie (1983) obtained repeatabilities of ±0.14mm for AC depth, ±0.16mm for lens thickness and ±0.18mm for vitreous chamber depth and axial length using the Kretz, and McBrien and Millodot (1987) using the Storz ±0.107mm for axial lengths measurements. Johns (1979), Ossoining (1983) and Hauff (1983) state an accuracy of 0.1mm for axial length. These values are similar to those obtained in this study. However the methods of analysis varied for the different studies therefore it is difficult to directly compare them. Other authors have used the optical determination of the axial length in aphakes/pseudophakes as the value with which to compare the ultrasonic measurement (Binkhorst 1981; Storey 1982; Rabie and Storey 1984; Olsen 1989). Since this study was completed and published Zadnik *et al* (1992) have published repeatability data using the Allergan Humphrey 820 biometer in a group of children, where the biometer probe was hand held. They found repeatability, using the same method of analysis, to be ±0.29mm for AC depth, ±0.20mm for lens thickness and ±0.37mm for vitreous chamber depth, figures which are slightly higher than the results in this study. It is likely that using the biometer in a hand held fashion with children would give less repeatable results.

Manufacturers claim an instrument accuracy for the model 820 biometer of ±0.034mm and patient measurement accuracy of ±0.10mm. Hence optimum accuracy can be expected to be ±0.134mm, with which our results compare favourably for both repeatability and reproducibility. Furthermore, the intersession results show no significant difference in any ocular dimension over the 5 sessions for either experimenter. It is likely that repeatability and reproducibility would be lower for the same level of gain in an elderly cataractous population.

As explained above the lower gain appeared less accurate for axial length determination. To achieve optimum results the gain should be set to 60% and adjusted as required to obtain maximum peaks on the ultrasonogram. This was the procedure adopted in the main study. It was observed that for corneal astigmatism over 2.00D, it was more difficult, in some cases, to obtain repeatable/reproducible results.

5.6 Conclusions

Ocular dimensions obtained using the Allergan Humphrey Ultrasonic Biometer 820 were repeatable and reproducible within acceptable limits. Its ease of use was illustrated by the comparatively excellent performance of the inexperienced experimenter.

CHAPTER 6

Investigation of learning in serial fields in normal subjects

6.1 AIMS

The primary aim of this study was to establish the optimum protocol for the subsequent investigation which examined the sensitivity of the central field in myopia, using a grid resolution of 4.2°. This resolution can be obtained by combining the 30-2 and 30-1 central programs of the HFA. The initial intention was to perform both central test programs, on one eye, within one session with a short rest period between tests of at least 15 minutes. The extent of the learning process needed to be evaluated when only one eye is examined, and two central field programs are performed in close succession at each visit. Knowledge of the number of visits (between 5 and 7 days apart) to complete the learning process was required. The study method described below was specifically designed with the follow-up investigation in mind.

A secondary aim of this study was to compare the ability of an alternative form of analysis to detect a learning process in normal subjects with the analysis of the STATPAC global indices of the HFA. An image processing filter was applied to the visual field data to reduce the effect of inherent variability (Fitzke and Kemp 1989). Spatial representations of the learning process are presented, both before and after the use of the filter process.

6.2 MATERIALS AND METHODS

The sample consisted of thirty volunteers (age 19 to 33 years, mean 24.5 years) inexperienced in automated perimetry and free from any ophthalmological abnormality. Each subject attended for three visits on separate days. At each visit the subject underwent two 30-2 programs on one eye, selected at random, using the Humphrey Field Analyzer 630. This program tests 76 locations within the central 30°, separated by 6° and offset symmetrically from the horizontal and vertical midlines (figure 6.5). A rest period of 10 to 15 minutes was given between fields. Thus a total of six fields was obtained for each subject. Only one eye was tested to avoid the confounding effects of a transfer of learning from one eye to the other (Wild *et al* 1991).

6.2.1 Conventional analysis of serial fields

As experience with automated perimetry has grown, it has become apparent that there is no general agreement as to what constitutes progressive change in the visual field of patients or how to detect it. One major problem in detecting change or early field defects, is that the visual field, as measured by an automated perimeter, is subject to variability or fluctuations as explained in Chapter 3. Separating true change from fluctuation poses a problem in data analysis. Depressions of 6dB or more (Sommer *et al* 1985) and small clusters of moderately significantly depressed points may occur in normal subjects (Heijl and Asman 1989b; Chauhan *et al* 1989). Another problem with detecting change in automated perimetry is the large amount of numeric data generated. It is difficult for the clinician to analyse these visual fields by simple inspection. As a result various types of data reduction (global indices) and statistical tests have been applied.

Statistical tests on the global indices such as analysis of variance (Hirsch 1985), and linear regression (Holmin and Krakau 1982; Gloor and Vökt 1985; Mikelberg *et al* 1986a; Hoskins *et al* 1987; Wu *et al* 1987) have been proposed to detect changes over time. At least five field test have been recommended for temporal evaluations (Schwartz and Nagin 1985; Wu *et al* 1987). The appropriateness of these statistical methods used to compare the sample means is questionable. To compare each mean as if from an independent sample is certainly invalid. A paired t-test is also inappropriate because of the multiple comparisons involved.

Typically, the effect of learning on sensitivity is observed as an improvement in MD, MS or SF with successive field tests. A sample mean for MD and MS is calculated for each field test. The significance of differences between fields is investigated using hypothesis testing, and temporal trends are illustrated diagrammatically (Wood *et al* 1987a; Wild *et al* 1989 and 1991; Werner *et al* 1988b and 1990; Heijl *et al* 1989a; Autzen and Work 1990).

A two way ANOVA with subjects and field test as the main factors, is a suitable and robust method. Although it does not require the data to be normally distributed, neither overall or within a group, the residuals are expected to have a normal distribution (Altman 1991). This was adopted as a starting point for this study.

6.2.2 Alternative pointwise analysis of serial fields

Consider one subject and their field data from test n and test (n+1). If threshold values at each location in test n are subtracted from their corresponding values in test (n+1) the

difference at each location can be identified as,

positive {an increase in sensitivity from test n to test (n+1)},

negative {a decrease in sensitivity from test n to test (n+1)},

or no change

This process was repeated for all locations, excluding the two blind spot locations (figure 6.5). The index LP (the learning proportion) is defined as the ratio of the number of locations which have increased in sensitivity between tests n and (n+1) to the total number of locations that have changed in sensitivity. This index was calculated for field tests 1 to 2, 2 to 3, 3 to 4 etc. In the absence of learning it would be expected that half of those locations showing a change in sensitivity would increase, and half would decrease, from one test to the next. Thus LP should equal 0.5. If a greater proportion of points increase in sensitivity from one test to the next (a learning effect) the value of LP would increase, thus LP would be greater than 0.5. A sample mean LP and a 95% confidence interval were constructed for each test from all 30 subjects. These values were plotted and compared with the null hypothesis, LP = 0.5.

6.3 RESULTS

Mean values and standard deviations (SD) for all global indices across the 6 field tests are given in table 6.1. A plot of the sample means of MD is given in figure 6.1. This shows some of the characteristics of the typical learning curve obtained from subjects new to automated perimetry. MD improves, as expected, from the first to the second field test. However, an apparently greater improvement in sensitivity occurs between tests 3 and 4.

However such plots are limited in their ability to describe fully the variability of subjects' responses. For example it should be noted that the error bars do not encompass all the observations obtained. The inadequacy of such plots to fully describe the variability is discussed in detail by Matthews *et al* (1990). To further illustrate the diversity of individual responses typical examples from nine subjects are presented in figure 6.2.

It is difficult to draw firm conclusions from the results shown in figure 6.1. From the two-way ANOVA, with subjects and test as the main factors, no significant differences between the sample means were found (F-test; $p = 0.14$). A tentative conclusion would be that, based on an analysis of MD, there is no clear evidence of a learning effect.

Table 6.1. Sample mean ± SD for the global indices in dB across the six field tests.

Global Index	Visual field test					
	1	2	3	4	5	6
MS	28.74 ± 1.08	29.02 ± 1.17	28.86 ± 1.27	29.05 ± 1.09	29.14 ± 1.00	29.09 ± 1.02
MD	-2.15 ± 1.01	-1.92 ± 1.05	-1.89 ± 0.97	-1.57 ± 1.17	-1.50 ± 0.84	-1.67 ± 0.94
SF	1.42 ± 0.35	1.45 ± 0.67	1.35 ± 0.59	1.30 ± 0.42	1.19 ± 0.29	1.32 ± 0.47
PSD	2.30 ± 0.79	2.11 ± 0.66	2.24 ± 0.93	2.09 ± 0.58	2.07 ± 058	2.10 ± 0.78
CPSD	1.37 ± 0.94	1.22 ± 0.80	1.44 ± 0.74	1.37 ± 0.89	1.34 ± 0.88	1.30 ± 0.94

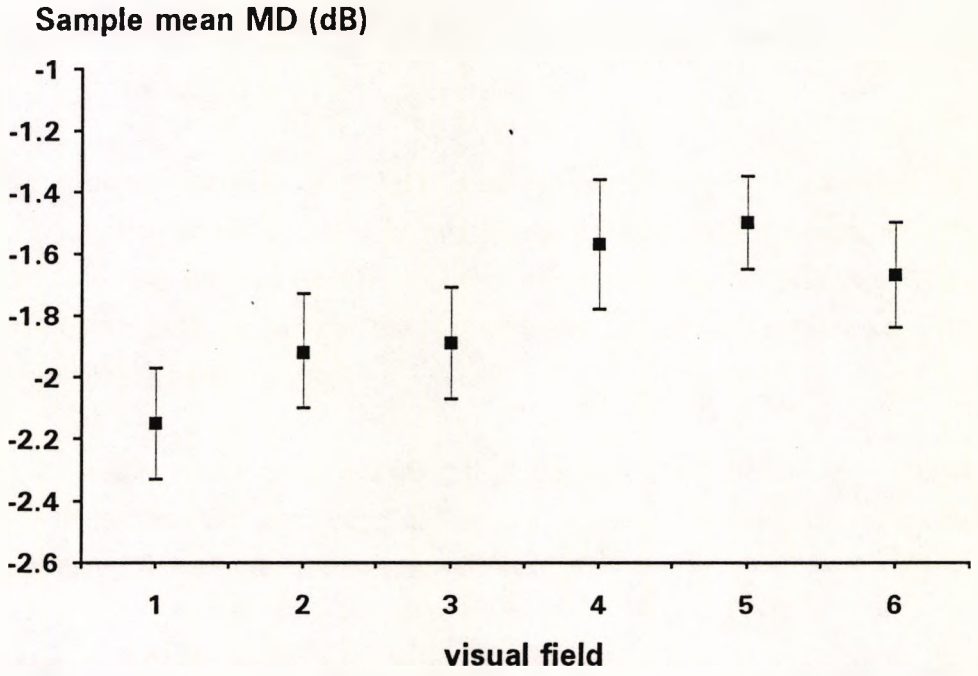

Figure 6.1. Sample mean of the mean defect, MD ± SE, for 30 subjects plotted against successive field tests.

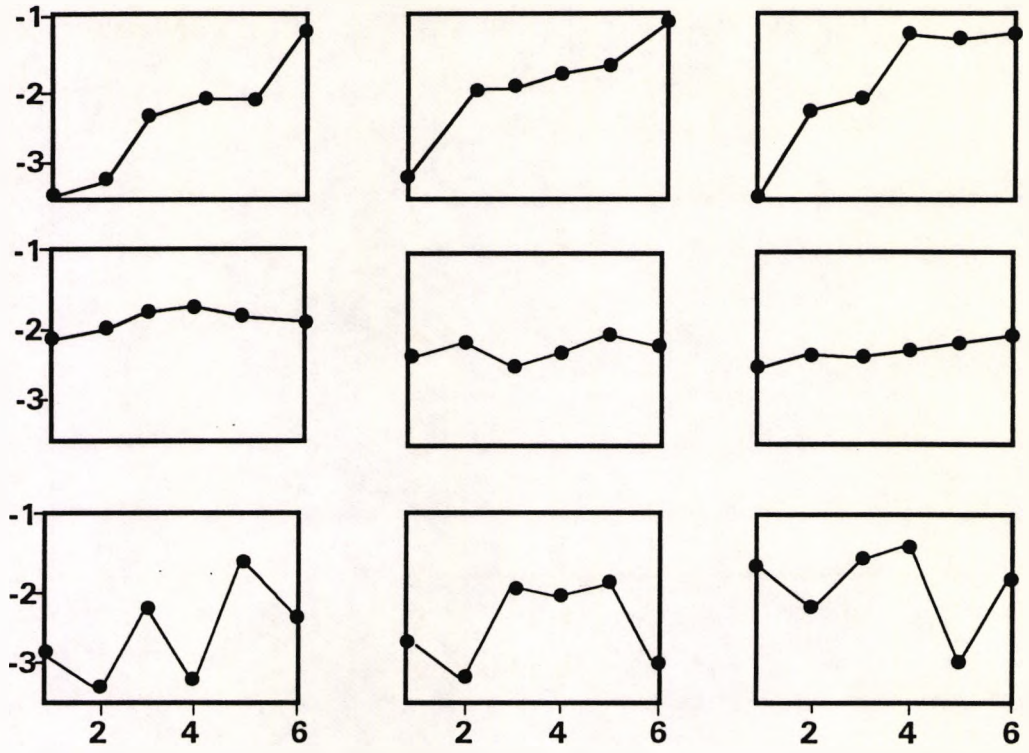

Figure 6.2. Mean defect, MD plotted against successive field tests for 9 subjects.

Any arithmetic mean, such as MD, is adversely affected by extreme values. Intuitively there are likely to be several influential outliers (values which are incompatible with the rest of the data set) in a field from an inexperienced subject. Therefore, MD may not be the optimum index to describe the general improvement in sensitivity associated with the learning phenomenon.

Similar results were obtained using MS (figure 6.3), SF, PSD and CPSD. Again there were no statistically significant differences between the sample means. These global indices are subject to the same criticisms as MD.

A plot of LP for the sample is shown in figure 6.4. The space between the bar representing the 95% confidence interval for LP for field tests 1 to 2 (n = 1) and the expected value of 0.5 implies that the ratio is significantly larger than 0.5 between tests 1 and 2 ($p = 0.01$). There are no other significant differences since the expected value is encompassed by the 95% confidence intervals for the remaining cases. This suggests a learning effect between tests 1 and 2 only.

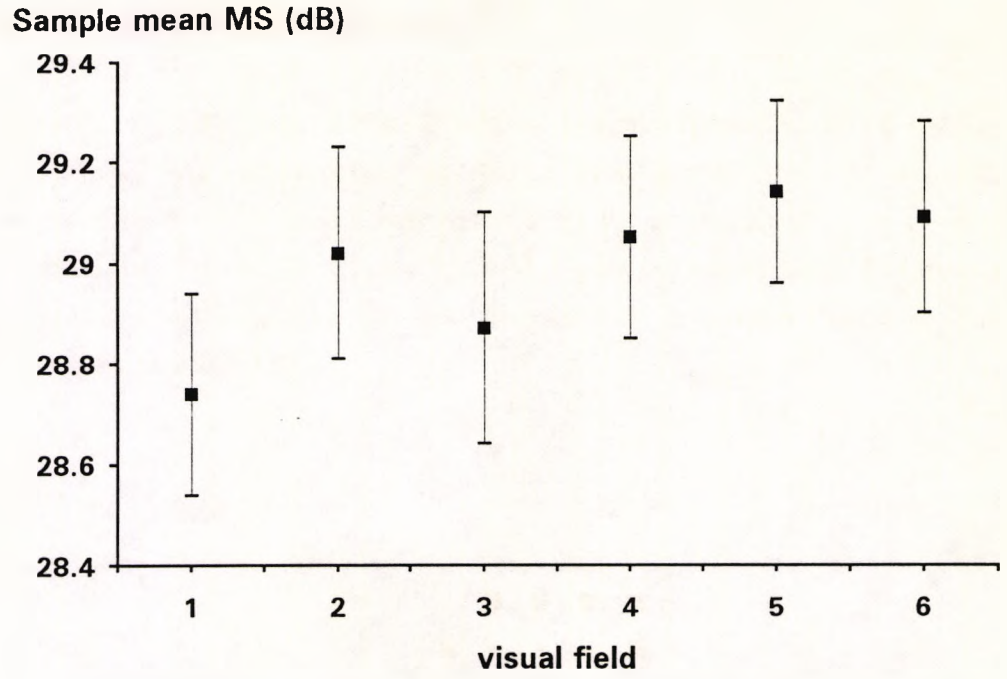

Figure 6.3. Sample mean of the mean sensitivity, MS ± SE, for 30 subjects plotted against successive field tests.

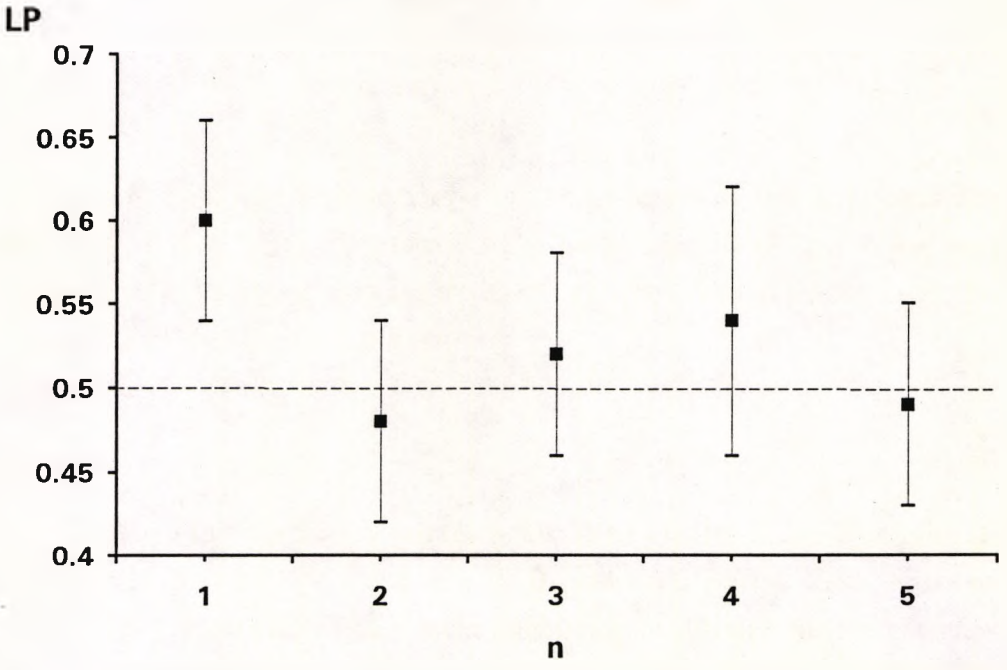

Figure 6.4. Sample mean of learning proportion, LP, with 95% confidence intervals, for all 30 subjects plotted for successive field tests. LP is calculated for field tests n to n+1, where n = 1 to 5.

6.4 SPATIAL REPRESENTATIONS

Considering field tests 1 and 2 only, a spatial representation of the learning was constructed. At each location the change in sensitivity (positive or negative) in dB between field test 1 and 2 was determined for each subject. The mean change per location for all 30 subjects was calculated. Figure 6.5 shows the 25% (upper quartile) of locations with the greatest increases in sensitivity. The mean change at these locations ranged from 0.8 to 3dB.

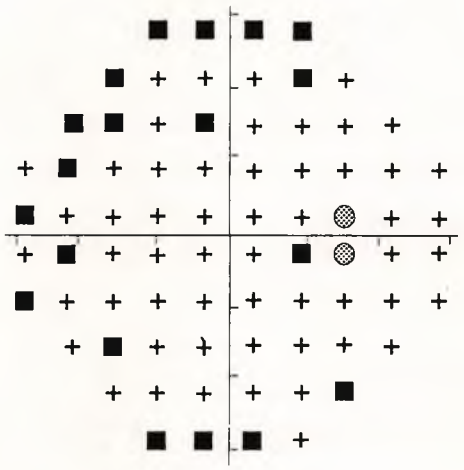

Figure 6.5. Pointwise representation of the increases in threshold sensitivity between field tests 1 and 2, for 30 subjects. The black squares represent the upper 25% of locations with the largest increase in sensitivity. The grey circles represent the blind spot locations excluded from the analysis.

The variability of threshold responses tends to be greater in these peripheral regions of the field (Heijl *et al* 1989c and 1987d; Brenton and Phelps 1986; Katz and Sommer 1986). This presents difficulties when attempting to distinguish true change from intra-test (short-term fluctuation), inter-test (long-term fluctuation) or inter-individual variations. An attempt was made to describe this variability by using a spatial filter process, to remove possible erroneous results (outliers) from the data set. An image (spatial) processing filter can be used to enhance or smooth the data. The filter employed is illustrated in figure 6.6 which shows a location with threshold sensitivity y, surrounded by 8 neighbouring points. The mean threshold sensitivity of the surrounding eight

locations is calculated and subtracted from *y*, taking the absolute value of this difference to be D_i. This process was repeated for all locations in the 30-2 program for tests 1 and 2 only. This filter is a simple version of a technique employed in image analysis (Fitzke and Kemp 1989). For locations at the edges of the field there will be fewer, albeit sufficient, contiguous locations making a contribution.

x1	x2	x3
x8	y	x4
x7	x6	x5

$$D_i = \left| y_i - \frac{\sum x_j}{n} \right| \quad \text{where i = 1 to 74}$$

Figure 6.6. Schematic representation of the 3x3 spatial filter acting on the central location with threshold sensitivity *y*, surrounded by 8 neighbouring locations.

The frequency distribution for D_i was plotted. An arbitrary cut- off point was taken to exclude the upper 10% of values for D_i. For values of D_i within this zone, the original value of *y* is replaced by the mean of the surrounding locations. The resulting filtered data was analysed as above to determine the 25% (upper quartile) of locations now showing the greatest increases in sensitivity (figure 6.7). The mean change at these locations ranged from 0.4 to 2dB. These are observed to be more randomly distributed over the central field. The filtered version has de-emphasised the increases occurring towards the periphery of the central field, allowing locations situated more centrally to become apparent.

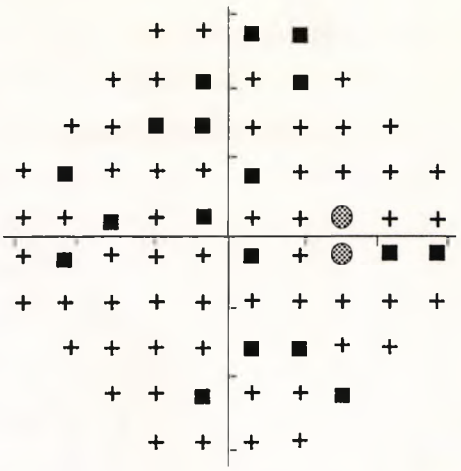

Figure 6.7. Spatial representation of the increases in threshold sensitivity between fields test 1 and 2, for 30 subjects, after the spatial filter was applied. The black squares represent the upper 25% of locations with the largest increase in sensitivity. The grey circles represent the blind spot locations excluded from the analysis.

6.5 Discussion

Analysis of the global indices did not reveal any significant improvement between fields test 1 to 6. However, LP demonstrated a learning process, in agreement with previous studies (Heijl 1989a; Wild *et al* 1989), between field tests 1 and 2 only.

- Before applying the filter a spatial representation of the increases in threshold sensitivity showed that those locations changing most between the first two tests were predominantly in the periphery of the central field program, particularly in the superior field. This is in agreement with previous studies on learning (Wood *et al* 1987a; Wild *et al* 1989; Heijl *et al* 1989b; Adelson *et al* 1988). One possible explanation that has been suggested for the greater learning in these regions of the field is that the patient may learn to consciously raise the upper lid. However, after the spatial filter was applied to remove possible outliers in the data, the configuration of the learning appeared more randomly distributed over the central field. Improvements in sensitivity became evident in more central locations. This technique of utilising the dependence which exists between adjacent locations has potential in detecting or removing the variability present in visual field data.

In many analyses of visual field data some form of data reduction is used. MD and MS are examples of data reduction which quantify and summarise the state of the field. They

are widely understood and are considered statistically robust, but have limitations and disadvantages as described above. The suitability of these statistical methods typically used to compare the sample means is questionable, because of the lack of normality and independency of the data.

Some researchers have assumed threshold values in normal subjects to be normally distributed at individual test locations (Greve 1973; Bebie 1985; Le Blanc 1985; Fankhauser and Bebie 1979; Hirsch 1985; Bebie *et al* 1976b; Schwartz and Nagin 1985), and the range of threshold values have been assumed to be uniform across the field. Other investigators have found pointwise variations of LF, inter-subject variations (Katz and Sommer 1986; Heijl 1987; Werner *et al* 1987), deviations from age-matched normal threshold values (Heijl 1987; Heijl *et al* 1987b and d) and deviations at a point from its mean value particularly in relative scotomas (Flammer and Zulauf 1985) to exhibit non-Gaussian behaviour.

Each threshold value within a single test is dependent upon the threshold of surrounding test locations, and repeated visual field tests for the same subject are certainly not independent. As pointed out by Werner *et al* (1988a), an analysis of variance to examine changes at individual locations over time is very likely to produce significant trends, because the large number of degrees of freedom will inflate significance levels. The two-way ANOVA used in this study on the global indices is a suitable and robust method (Altman 1991).

The advantage of LP, when compared with the global indices, is that it is not influenced by extreme values. Values of LP were normally distributed about the mean value. On the other hand, LP joins with the global indices as a further example of data reduction, and as such must inevitably lead to some loss of information.

Interestingly the proportion of unchanged locations between visual field tests correlated well with both the reliability indices and number of questions asked during testing, and may provide an alternative method of assessing reliability. If such a correlation were confirmed test time could be reduced by eliminating the need for false positive and false negative catch trials.

6.6 Conclusions

This study has demonstrated that when two field tests are performed in close succession on one eye on three separate visits, a significant learning effect is found between the first two tests only. On this basis, in all subsequent field examinations (Chapter 7) the first two fields plotted for each subject were discarded to account for learning.

The learning proportion (LP) and filtered spatial representations of serial visual fields may, with further development, be used for the long-term follow up of pathological visual fields, but the decline in sensitivity with age would need to be taken into consideration. This could facilitate the extraction of true progression from the 'noise' within serial glaucomatous visual fields. The alternative approaches suggested here are clearly not definitive, however, development of these ideas could enhance the analysis of serial visual fields.

CHAPTER 7

Influence of myopia upon the differential light sensitivity of the central visual field

7.1 AIMS

There is limited quantitative information regarding the possible changes in the myopic central visual field as measured by automated perimetry. The aim will be to establish typical values for the differential light sensitivity of the central 30° field as determined by automated static perimetry with the Humphrey Field Analyzer, over a wide range of myopia. Comparisons will be made with visual fields from normal, emmetropic eyes. The extent of peripapillary/myopic crescents will be considered and myopic subjects will be divided into groups, depending upon the appearance of the posterior pole and relative size of these peripapillary crescents. Subjects with myopic retinal degenerations, other than peripapillary crescents, were not included in this study. Data will be available to evaluate the following

- is the sensitivity of the central field influenced by the degree of myopia?
- is the sensitivity of the central field related to axial length?

Previous studies using automated perimetry were discussed in Chapter 1 section 1.4. However, none of these studies utilised the HFA.

7.2 MATERIALS AND METHODS

7.2.1 Subject selection and initial examination

Subject numbers were selected for the study as follows,

- 30 subjects who were either hypermetropes, emmetropes or myopes with less than 1D of myopia (mean spectacle refractive error)
- 33 subjects with more than 1D of myopia but without peripapillary crescents
- 64 subjects with more than 1D of myopia with peripapillary crescents, 30 of these subjects had more than 8D of myopia.

The sample comprised 127 healthy subjects, aged 16.5 to 35.4 years, free from any

ocular or systemic medication, with a range of refractive error from +4D to -25.75D. Subjects were ophthalmologically normal, apart from peripapillary fundus changes associated with myopia. A young subject population was chosen deliberately to avoid the results being affected by age-related ocular changes which influence the differential light sensitivity. Individuals were recruited from two sources. The majority of the myopes were patients attending for routine contact lens aftercare examinations at the Contact Lens Department of Moorfields Eye Hospital. The remaining subjects were recruited from the academic and undergraduate populations of City University. Inclusion criteria were as follows,

- visual acuity 6/9 or better
- spectacle astigmatism less than or equal to 3.00DC
- intraocular pressure less than or equal to 20mmHg by Goldmann applanation tonometry

contact lens wearers

- if contact lenses were habitually worn, it was compulsory for them to be fitting correctly, and be in good condition
- no disturbance of the cornea with or without fluorescein staining
- no signs of any previous corneal inflammation
- no corneal oedema
- no distortion of the keratometer mires.

7.2.2 Biometry of the eye and fundus photography

1. Prior to instillation of any eye drops the corneal front surface radius was measured with the Allergan Humphrey 410 automated keratometer, and an average from five readings obtained.
2. One drop of 0.4% benoxinate was instilled into one eye only, selected randomly. A-scan biometry was performed using the Allergan Humphrey 820 ultrasonic biometer in the semi-automatic mode with 60% gain as a starting level (Chapter 5). Five measurements were taken and the average calculated for, anterior chamber depth, lens thickness and axial length. After ultrasonography the eye was examined with a slit lamp microscope to ensure no insult had occurred to the corneal epithelium.
3. One or two drops of 1% tropicamide were instilled into the same eye and a cycloplegic refraction carried out.
4. Fundus photography of the optic nerve head region was performed with the Carl Zeiss Jena fundus camera.

7.2.3 Division of subjects into groups

The frequency (Huang *et al* 1987; Curtin and Karlin 1971; Jonas *et al* 1988d; Pierro *et al* 1993) and size (Stenstrom 1946; Otsuka 1967; Huang *et al* 1987) of crescents increases with the degree of myopia and with axial length elongation. Peripapillary crescents may indicate a region of the posterior pole adjacent to the optic disc which exhibits greater axial extension, and the function of the respective retinal nerve fibre bundles may be affected by this axial elongation. Thus, myopes with larger crescents may have experienced more axial elongation than myopes without crescents, or those with relatively smaller crescents. Axial extension may cause disarrangement of the retinal elements, which ultimately will influence their visual performance, as it has been shown that the receptors are directionally sensitive to light (Stiles and Crawford 1934).

It was hypothesised that subjects with relatively larger peripapillary crescents will show the greatest deficit in visual performance of the retinal elements, as measured by the differential light threshold, when compared with subjects without peripapillary crescents or with smaller crescents. Subjects were divided into four groups with this hypothesis in mind, and their visual field results compared,

group 1 - hypermetropes, emmetropes, and myopes with less than 1D of myopia without peripapillary crescents
group 2- myopes with more than 1D of myopia without peripapillary crescents
group 3- myopic eyes with relatively smaller peripapillary crescents
group 4- myopic eyes with relatively larger peripapillary crescents

Allocation of subjects to group 1 was without difficulties. However, dividing the remaining subjects into groups 2, 3 and 4 was troublesome. Identification and delineation of crescent formation at the optic disc border was problematic, due to the marked inter-subject variability of peripapillary changes. With less obvious crescents it was sometimes difficult to decide whether a myopic crescent was actually present, or whether the feature along the disc border was some other tissue irregularity. In some cases the crescent margins were very indistinct, and it was not possible in all cases to accurately differentiate between scleral and choroidal crescents. Separating subjects into groups 3 or 4 was achieved by an arbitrary division according to crescent size. Subjects were ordered in an ascending fashion according to the size of the crescent expressed as a percentage of the disc area. The first half, with smaller crescents, were assigned to group 3 and the second half to group 4.

7.2.4 Visual field examination

Differential light sensitivity of the central 30° was examined using the threshold strategy with test programs 30-2 and 30-1 (figure 7.1). Both programs have a grid separation of 6°, and when combined, they yield a test point resolution of 4.24°.

All subjects were inexperienced in automated perimetry. In Chapter 6 a study investigated the learning process with automated perimetry when two programs are performed, in close succession, on one eye only. It was concluded that in general the learning process is complete after the subject has undergone two central programs. This procedure was adopted for this study. All subjects received two training test programs, one 30-2 and one 30-1, on the HFA within one session. At a second session, between 7 and 10 days later, the same programs were repeated. In each instance 5 minutes adaptation to the background was given, and the foveal threshold was measured at the beginning of each program. A rest period was given of at least 15 minutes between tests. The order of field tests was randomised. Subjects were given the option to pause during the examination, if they felt fatigued, by continuously depressing the response button immediately after responding to a light stimulus. At intervals throughout the examination subjects were given verbal encouragement and an estimate of testing time still remaining.

Subjects wore their usual mode of visual correction for the field examination, either contact lenses or spectacles. If a spectacle correction was needed a trial lens was used and the vertex distance recorded. An optical appliance was not used if the mean refractive error was between ±1D. In group 2, 30% wore contact lenses and 50% glasses, in group 3, 50% wore contact lenses and 45% glasses, and in group 4, 71% wore contact lenses and 29% glasses. The highest myopic correction in spectacles was 14D

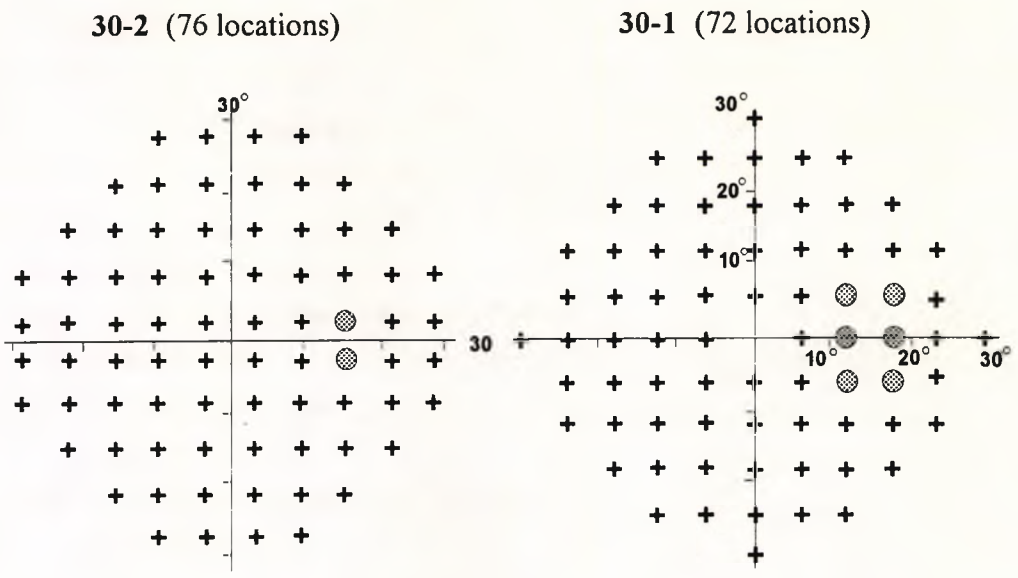

Figure 7.1. Test locations of programs 30-2 and 30-1 of the HFA. Grey circles indicate those locations assumed by the HFA to fall within the normal blind spot .

7.2.5 Statistical analysis

From the hypothesis described in section 7.2.3, the purpose of the statistical analysis is two-fold. Firstly, to identify any significant differences between the visual performance of the 4 subject groups, as measured by automated static perimetry, and secondly, to investigate the strength and nature of any linear relationship which may exist between visual performance and axial length, or between visual performance and ocular refraction. Analysis of the visual field was performed after excluding results from the blind spot locations. Points considered as belonging to the blind spot by the HFA are shown in figure 7.1 above.

Global indices MS, MD, PSD, CPSD and SF were calculated for each subject by the STATPAC program of the HFA. A one way analysis of variance (ANOVA) together with the least significant difference multiple comparison procedure was used to identify any significant differences between groups' mean global indices. This is an acceptable and robust method and the least significant difference multiple comparison procedure controls the overall Type I error rate (Altman 1991). Correlation was employed to investigate any linear association between the global indices and axial length and ocular refraction, followed by linear regression using the least squares method. Plots of the residuals were examined to assess the goodness of fit of the linear regression. These plots should show an even scatter of the points at all x values. Values for R^2 of 0.6 and above, from the correlation analysis, are considered as acceptable.

Single field analysis printouts from the HFA were visually evaluated for each subject. The two programs were viewed in conjunction with each other. This is preferable to a merged printout of the two programs, because probability maps are unavailable in this mode.

In addition to the global indices, the visual field was divided into regions to investigate any regional differences between the groups. Points falling along the dividing lines between regions were excluded. Three types of regional maps were devised,

- **three annuli of 10 ° radius** (figure 7.2a),
  1 = inner, 21 locations
  2 = middle, 42 locations
  3 = outer, 80 locations

- **four meridional quadrants** (figure 7.2 b),
  1 = upper-temporal, 31 locations
  2 = upper-nasal, 32 locations
  3 = lower-nasal, 32 locations
  4 = lower-temporal, 29 locations

- **four sectors outside 10°** (figure 7.2 c),
  2 = superior, 28 locations
  3 = nasal, 28 locations
  4 = temporal, 22 locations
  5 = inferior, 28 locations

Area 1 in figure 7.2c is equivalent to the inner 10° annulus described above.
In addition to these field regions the foveal sensitivity was also evaluated. The mean sensitivities for the regions were analysed between the groups by the same methods used for the global indices.

a) 10° Annuli

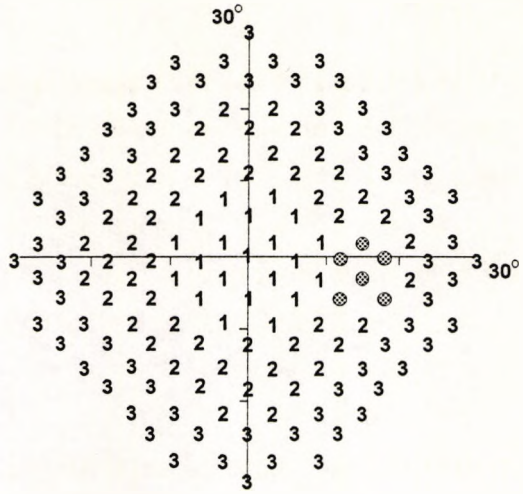

b) Quadrants

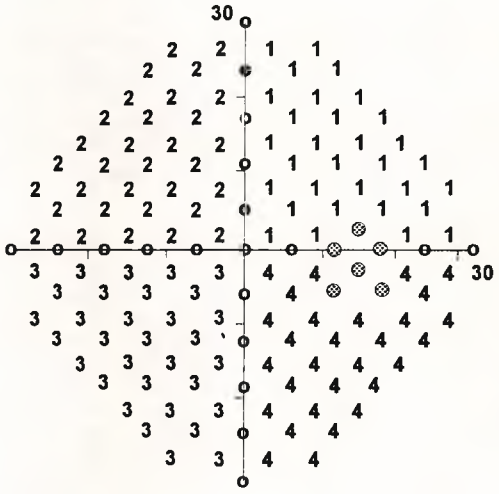

c) Sectors

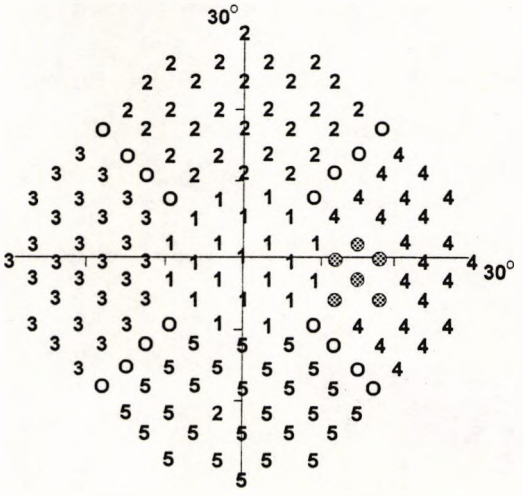

Figure 7.2. Regional maps devised for the central field for a right eye. Grey circles indicate those points assumed to fall within the normal blind spot, and these are not incorporated in the analysis. Locations along dividing lines between regions are indicated by 'o', and are excluded for that particular regional analysis.

7.3 Results

Two subjects failed to meet the criteria set by the HFA for reliability indices for both central test programs, and they were excluded from the study. The remainder met the criteria, and all reliability indices were within 20%. Three subjects did not complete the study, leaving a total of 122 subjects. The number of subjects, age, mean ocular refraction and axial length for each group is given in table 7.1. Ocular refraction was calculated as described in Chapter 8, section 8.2.2.3(b).

Table 7.1. Number of subjects in each group, together with the means for age, ocular refraction and axial length. Values in parenthesis indicate the range.

Group	number of subjects	mean age (years)	mean ocular refraction (D)	mean axial length (mm)
1	30	22.42 (19.1-26.8)	+0.21 (4.3 to -0.9)	22.63 (22.0-25.4)
2	30	22.62 (19.0-32.8)	-2.67 (-1 to -5)	24.63 (23.0-26.6)
3	31	22.97 (18.5-35.4)	-6.10 (-1.4 to -12.8)	26.38 (23.5-29.4)
4	31	22.47 (18.9-35.2)	-10.92 (-4 to -20.3)	28.47 (24.4-34.6)

In group 4 the crescent area, expressed as fraction of the optic disc area, was at least 40% of the optic disc area, with a maximum of 6x disc area. In group 3 the area of the crescent ranged from 5% to 35% of the optic disc area.

7.3.1 Global indices

ANOVA results

Mean values (±SD) for all the global indices for the sample are given in table 7.2. A one way ANOVA followed by the least significant difference multiple comparison procedure yielded the following,

- no significant differences between groups 1 and 2 for any global index
- group 4 demonstrated a significant difference from the other three groups for MS,

MD, PSD and CPSD ($p<0.01$). SF differed significantly between groups 4 and 1 only ($p<0.05$)

- group 3 showed a statistically significant difference from group 1 ($p<0.01$) and group 2 ($p<0.05$) for MS and MD only.

Table 7.2. Mean value (±SD) of the global indices for the four groups

group	MS (dB) (±SD)	MD (dB) (±SD)	PSD (dB) (±SD)	CPSD (dB) (±SD)	SF (dB) (±SD)
1	29.21 (±1.29)	-1.75 (±1.19)	1.95 (±0.45)	1.28 (±0.51)	1.19 (±0.42)
2	28.88 (±1.07)	-1.97 (±1.02)	1.95 (±0.37)	1.12 (±0.55)	1.32 (±0.27)
3	27.66 (±1.66)	-3.05 (±1.59)	2.06 (±0.42)	1.38 (±0.59)	1.26 (±0.25)
4	25.95 (±2.93)	-4.64 (±2.77)	2.61 (±0.90)	1.91 (±1.08)	1.39 (±0.27)

Correlation and linear regression results

Plots of the residuals were satisfactory in most cases, except for SF in all cases, and PSD in groups 1 and 2. Despite this the analysis was completed in these unsatisfactory cases but results were treated with caution as the underlying assumptions were not met. Values for R^2, p, and gradients of the regression line, are presented.

Groups 1 and 2

- analysis did not reveal any significant correlation between any of the global indices with either axial length or ocular refraction.

Group 3

- MD and MS declined significantly as axial length increased and as mean ocular refraction became more myopic, however, because the R^2 values are low, these results should be interpreted with caution (see table 7.3).
- SF, PSD and CPSD did not exhibit any significant linear correlation with either axial length or ocular refraction.

Group 4

- MD and MS declined significantly as axial length increased and as mean ocular refraction became more myopic ($p<<0.01$). In this group the R^2 values are much

higher than for group 3 (table 7.3). MD deteriorated by 0.80dB/mm ($R^2 = 0.76$) with increasing axial length, and with increasing myopia by 0.44dB/D ($R^2 = 0.67$). MS deteriorated by 0.83dB/mm ($R^2 = 0.72$) with increasing axial length, and with increasing myopia by 0.47dB/D ($R^2 = 0.66$)

- although significant *p* values were found for correlations between either PSD, or CPSD, with axial length and ocular refraction, all R^2 values are low, lying between 0.31 to 0.48 (table 7.3).
- SF did not exhibit any significant linear relationship with axial length nor ocular refraction.

Graphical examples are given for MD, MS and PSD plotted against axial length and ocular refraction for all subjects in figures 7.3 to 7.5.

Table 7.3. Summary of the results of correlation and linear regression of the global indices against axial length and ocular refraction for groups 3 and 4.

Global index	**axial length**			**ocular refraction**		
Group 3	**R^2**	***p* value**	**gradient dB/mm**	**R^2**	***p* value**	**gradient dB/D**
MD	0.16	0.03	-0.46	0.24	0.004	+0.26
MS	0.21	0.01	-0.55	0.25	0.004	+0.28
PSD	0.08	0.13	+0.09	0.11	0.06	-0.05
CPSD	0.02	0.43	+0.06	0.06	0.18	-0.05
SF	0.09	0.09	+0.06	0.05	0.25	-0.02
Group 4						
MD	0.76	<<0.01	-0.80	0.67	<<0.01	+0.44
MS	0.72	<<0.01	-0.83	0.66	<<0.01	+0.47
PSD	0.44	<<0.01	+0.20	0.32	<<0.01	-0.10
CPSD	0.48	<<0.01	+0.25	0.31	0.001	-0.12
SF	0.04	0.31	+0.12	0.08	0.12	-0.01

a)

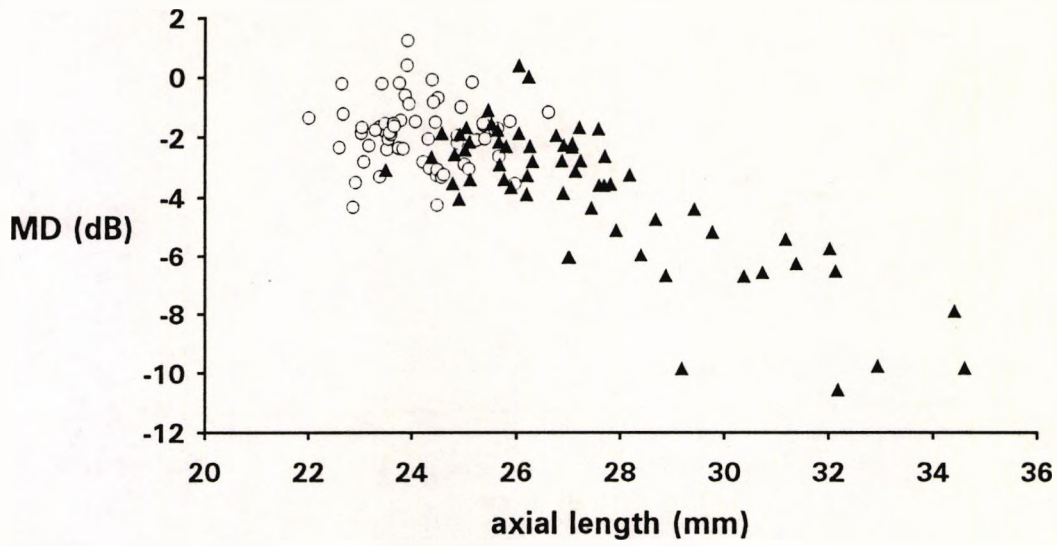

b)

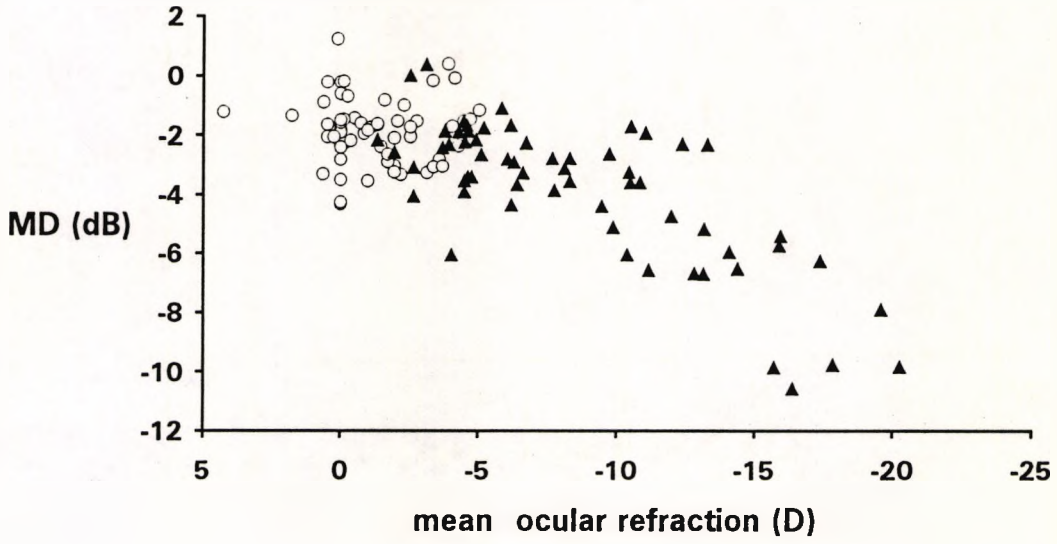

Figure 7.3. MD plotted against a) axial length and b) ocular refraction for the entire sample. Open circles represent subjects without peripapillary crescents, and the solid triangles represent subjects with peripapillary crescents.

a)

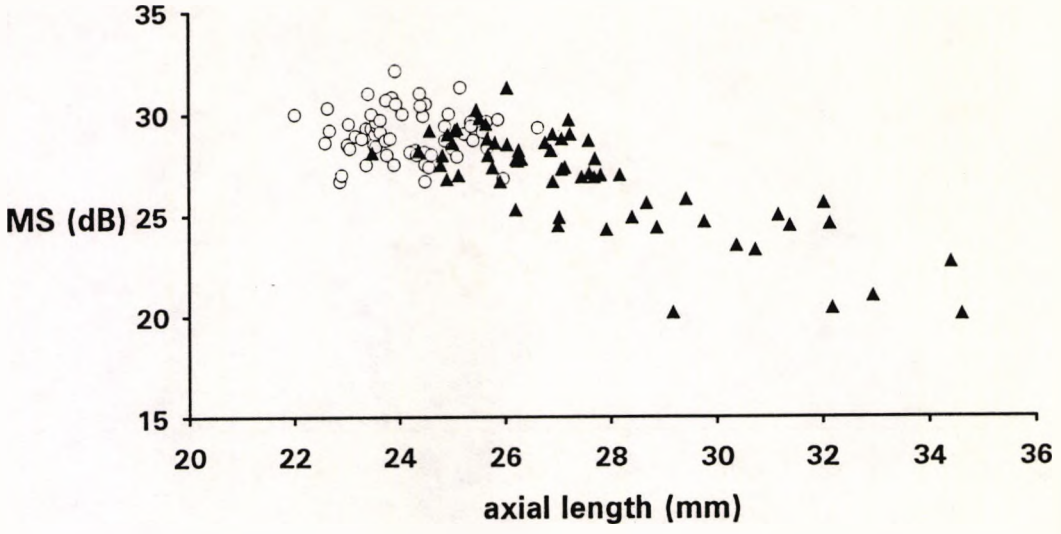

b)

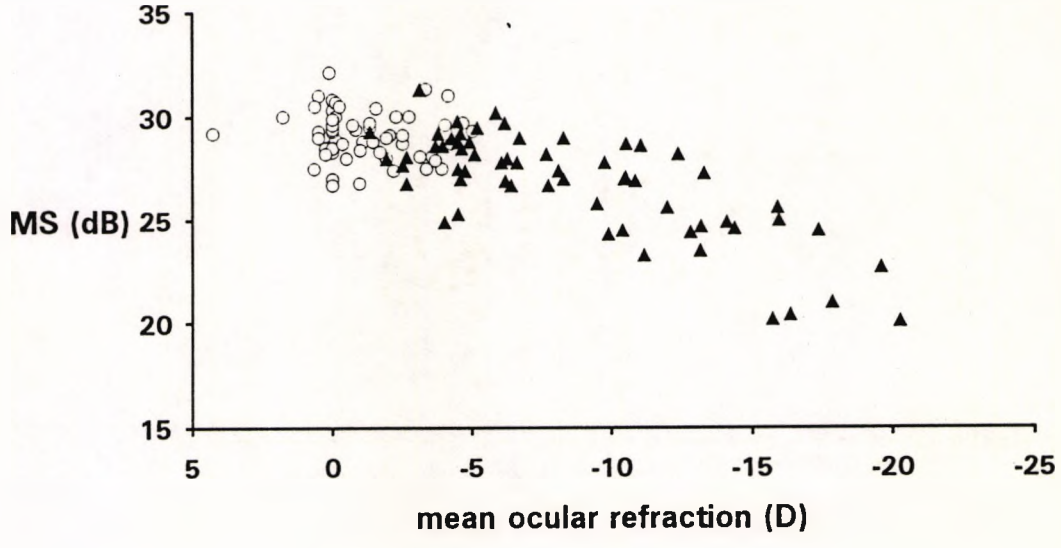

Figure 7.4. MS plotted against a) axial length and b) mean ocular refraction for the entire sample. Open circles represent subjects without peripapillary crescents, and the solid triangles represent subjects with peripapillary crescents.

a)

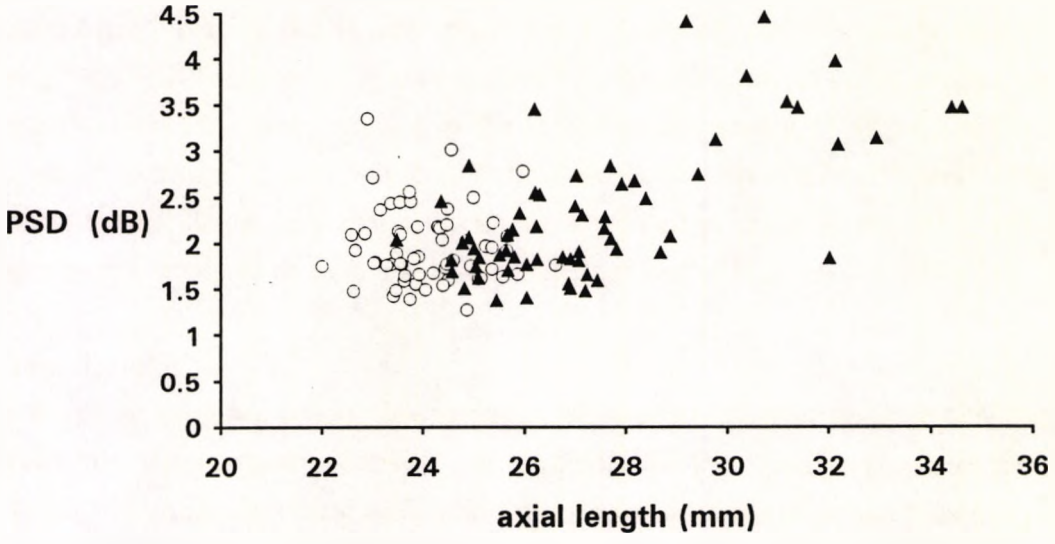

b)

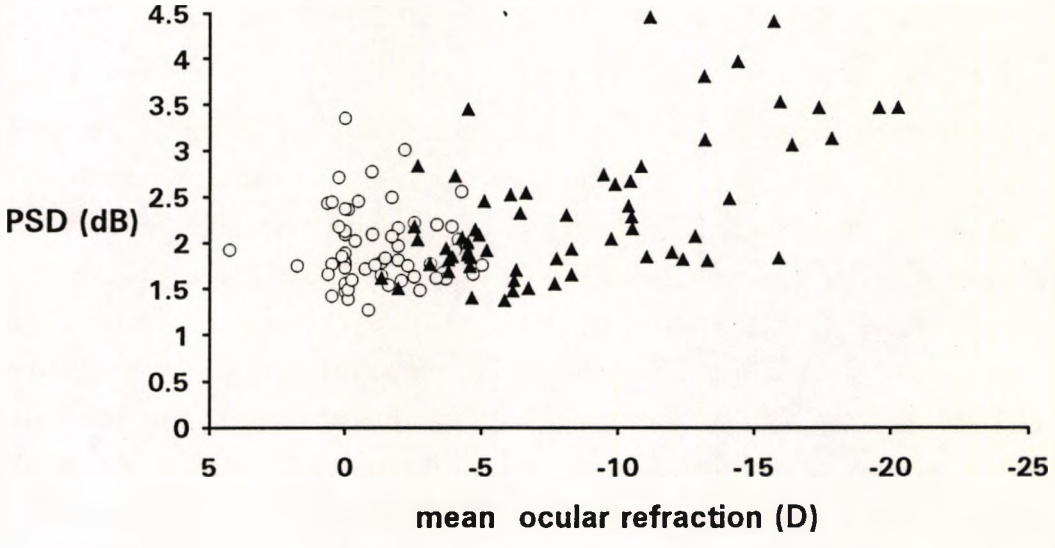

Figure 7.5. PSD plotted against a) axial length and b) ocular refraction for the entire sample. Open circles represent subjects without peripapillary crescents, and the solid triangles represent subjects with peripapillary crescents.

7.3.2 Humphrey single field analysis printouts

Single field analysis printouts were examined separately for the 30-1 and 30-2 programs. In all groups, including the emmetropic group 1, locations were frequently identified as significant in the total deviation plot for $p<5\%$, either in clusters or as isolated points. These locations have been ignored in the following assessment of single field analysis printouts which concentrates on the other three probability levels (2%, 1% and 0.5%). In addition to the single field analysis printout a merged printout of the 30-1 and 30-2 programs was obtained to examine the combined gray scale and defect depth plots.

Groups 1 and 2

There was no evidence of any field defects on inspection of gray scale or defect depth plots, other than a minor decrease in sensitivity in the outer annulus, particularly superiorly. In some subjects small clusters of up to 4 locations were identified for $p<2\%$ in the total deviation probability plot. Approximately half of the subjects had one location identified for $p<1\%$ or 0.5% in one field only. In all subjects, the pattern deviation probability plot never displayed more than two locations at any one of the four significance levels. In summary, neither group showed any significant changes in the field.

Group 3

Gray scale and defect depth plots suggested a reduction in sensitivity of the superior field, particularly at the outer edges of the field. Locations in the total deviation plot identified for $p<0.5\%$ were infrequent, with a maximum of two points in any one field. However, those for $p<2\%$ or 1%, occurred more frequently than in groups 1 and 2. They occurred either in isolation, as small clusters, or scattered within the field. In one subject they were clearly associated with the blind spot. It was not possible to ascertain with certainty any area of the field as being predominantly affected. Comparing the superior and inferior hemifields the superior field showed more defective locations in 5 subjects, and the inferior field in 7 subjects. There was no evidence of any arcuate scotomas or nasal wedge defects. The pattern deviation plot was unremarkable in most cases.

MD was flagged as abnormal, for at least $p<0.1$, in 18 subjects, but PSD and CPSD were flagged as abnormal in only 3 subjects.

Between 15 and 20 locations in each total deviation plot were identified at the 1% and/or 2% levels and between 2 and 7 locations identified at the 0.5% level, in the central area of the field in 4 subjects. STATPAC reported a general reduction in sensitivity in these four cases. Only one of these subjects exhibited significantly depressed locations in the pattern deviation plot, which were clearly associated with the blind spot. In one other

subject the glaucoma hemifield test was borderline, and yet the total and pattern deviation plots showed only one depressed location for $p<0.5\%$.

The glaucoma hemifield signifies a difference in sensitivity between the superior and inferior hemifields (Asman and Heijl 1992) and is only available for the 30-2 program.

Group 4

Gray scale and the defect depth plots appeared to indicate a decline in sensitivity of the superior hemifield, particularly towards the periphery of the plot. Thirteen subjects exhibited enlargement of their blind spots. Often the blind spot appeared to extend temporally. Locations identified at the 1% and 2% levels in the total deviation plot were not infrequent. They occurred either at scattered locations, adjacent to the blind spot or in small clusters. The sensitivity decline in the superior hemifield which were observed in the gray scale and defect depth plots were frequently not confirmed in the corresponding total deviation probability plots. This disparity is probably due to the weighting procedure employed to construct the empirical probability plot, which attempts to account for the increasing threshold variability with increasing eccentricity.

MD was classified as abnormal, for at least $p<0.1$, in 21 subjects while PSD was abnormal in 12 subjects, and CPSD in 11 subjects.

STATPAC reported the glaucoma hemifield test to be borderline in 3 subjects, outside normal limits in 2 subjects, and a general reduction in sensitivity in 9 subjects. These 14 subjects suffered this decline within the central 20° of the field according to the total deviation plot, with 4 to 25 locations at $p<0.5\%$ level, surrounded by points for $p<1\%$ and 2%. They also demonstrated marked enlargements of their blind spots. In a few cases the blind spot appeared to extend towards the fixation point. In 8 of these subjects the total probability plot showed a marginally higher number of defective locations in the inferior field than in the superior field. The corresponding pattern deviation plots identified significantly depressed locations in the outer region of the central plot in 2 subjects, around the blind spot in 8 subjects, and a cluster of 4 locations below fixation in one subject ($p<0.5\%$). In 20 subjects the pattern deviation plot was unremarkable. There was no evidence of any arcuate scotomas or nasal wedge defects.

Some examples of visual field plots with the corresponding fundus photograph are given in Appendix A1.

There were no major differences between the results of the 30-1 and 30-2 plots. They complemented each other and helped confirm the presence/absence of a defective field region in uncertain cases.

7.3.3 Regions of the central field

ANOVA results

Sample mean sensitivities (±SD) for the fovea and the regions are given in table 7.4. Using a one way ANOVA with the least significant difference multiple comparison procedure the following results were obtained,

- mean sensitivities for all regions of the field did not differ significantly between groups 1 and 2
- group 4 differed statistically significantly from all the other groups for all regions ($p<0.01$)
- comparisons between group 3, and groups 1 and 2 are summarised in table 7.5. It is noteworthy that between groups 2 and 3 the only region significantly different at the 0.01 level is the upper-temporal quadrant
- mean foveal sensitivity in groups 3 and 4 was significantly different from that in groups 1 and 2 ($p<0.01$).

Correlation and linear regression results

Groups 1 and 2

- correlation analysis did not reveal a significant relationship between mean sensitivity and either axial length, or ocular refraction, in any region of the field.

Group 3

- correlation analysis revealed a significant relationship at the 5% level, at least, between mean sensitivity and either axial length or ocular refraction, for all regions except between the inferior sector and axial length, and between the fovea and ocular refraction. As axial length or degree of myopia increase, the mean sensitivity of each field region deteriorates. However, results need to be interpreted conservatively because the R^2 values are low. Values for R^2, p and the regression gradients are given in table 7.6.

Group 4:

- correlation between mean sensitivity and both axial length and ocular refraction was highly significant in all cases ($p<<0.01$). As axial length increases and the degree of myopia increases, the mean sensitivity of each field region declines. The correlation analysis generally yielded much higher R^2 values than for group 3, the notable exceptions being mean sensitivity of the outer annulus with either axial length or ocular refraction which gave the lowest R^2 value of 0.29.

Table 7.4. Mean sensitivities (dB±SD) for the field regions for the sample.

Field region	group 1	group 2	group 3	group 4
fovea	37.33 ± 1.75	37.23 ± 1.52	35.97 ± 1.94	35.10 ± 2.55
Annuli				
inner	32.11 ± 1.03	31.89 ±0.84	30.84 ±1.34	29.12 ±2.86
middle	30.26 ±1.09	29.78 ±1.03	28.80 ±1.51	27.11 ±2.82
outer	27.78 ±1.71	27.51 ±1.39	26.35 ±1.91	23.83 ±5.13
Quadrants				
upper-temporal	28.79 ±1.56	28.46 ±1.29	26.88 ±2.26	24.68 ±3.40
upper-nasal	28.55 ±1.64	28.15 ±1.50	26.95 ±1.98	25.14 ±3.06
lower-temporal	30.27 ±1.07	30.01 ±1.09	28.92 ±1.38	26.95 ±3.33
lower-nasal	29.31 ±1.40	28.87 ±1.06	28.01 ±1.52	26.70 ±2.81
Sectors				
superior	27.12 ±1.86	26.65 ±1.71	25.07 ±2.62	23.19 ±3.17
inferior	28.81 ±1.30	28.46 ±1.13	27.76 ±1.55	26.35 ±2.69
nasal	28.59 ±1.66	28.37 ±1.30	27.31 ±1.81	25.70 ±3.18
temporal	29.86 ±1.37	29.50 ±1.18	28.03 ±1.94	25.63 ±3.75

Table 7.5. Summary of the one way ANOVA with the least significant difference multiple comparison procedure for mean sensitivity between group 3 and groups 1 and 2.

Field region	**group 3 and group 1**	**group 3 and group 2**
fovea	p <0.01	p <0.05
Annuli		
inner	p <0.01	p <0.05
middle	p <0.01	p <0.05
outer	NS	NS
Quadrants		
upper-temporal	p <0.01	p < 0.01
upper-nasal	p <0.01	p < 0.05
lower-temporal	p <0.01	p < 0.05
lower-nasal	p <0.01	NS
Sectors		
superior	p <0.01	p <0.05
inferior	p <0.05	NS
nasal	p <0.05	NS
temporal	p <0.01	p <0.05

Table 7.6. Summary of the results of correlation and linear regression for mean sensitivity against axial length and ocular refraction for group 3.

	Axial length			Ocular refraction		
Field region	**R^2**	***p* value**	**gradient dB/mm**	**R^2**	***p* value**	**gradient dB/D**
fovea	0.18	0.019	-0.60	0.11	0.085	0.20
Annuli						
inner	0.27	0.003	-0.51	0.25	0.004	+0.22
middle	0.21	0.010	-0.51	0.29	0.002	+0.27
outer	0.21	0.009	-0.64	0.24	0.005	+0.31
Quadrants						
upper-temporal	0.25	0.004	-0.83	0.24	0.005	+0.37
upper-nasal	0.21	0.009	-0.67	0.28	0.002	+0.35
lower-temporal	0.17	0.022	-0.42	0.18	0.017	+0.19
lower-nasal	0.19	0.015	-0.48	0.28	0.002	+0.27
Sectors						
superior	0.17	0.021	-0.80	0.24	0.005	+0.43
inferior	0.12	0.061	-0.39	0.15	0.029	+0.20
nasal	0.18	0.017	-0.56	0.26	0.004	+0.30
temporal	0.23	0.006	-0.69	0.16	0.025	+0.26

Table 7.7. Summary of the results of correlation and linear regression for mean sensitivity against axial length and ocular refraction for group 4. In all cases the correlation was significant for $p<<0.01$.

	Axial length		Ocular refraction	
Field region	**R^2**	**gradient dB/mm**	**R^2**	**gradient dB/D**
fovea	0.41	-0.54	0.32	+0.28
Annuli				
inner	0.81	-0.86	0.63	+0.44
middle	0.77	-0.83	0.71	+0.46
outer	0.29	-0.93	0.29	+0.53
Quadrants				
upper-temporal	0.63	-0.89	0.59	+0.51
upper-nasal	0.66	-0.83	0.62	+0.47
lower-temporal	0.71	-0.94	0.63	+0.52
lower-nasal	0.66	-0.77	0.60	+0.43
Sectors				
superior	0.55	-0.79	0.56	+0.46
inferior	0.65	-0.72	0.60	+0.41
nasal	0.63	-0.85	0.58	+0.47
temporal	0.60	-0.97	0.56	+0.55

7.3.4 Further analysis

Inspection of the data in figure 7.3 clearly shows MD to decline with increasing axial length and increasing myopia. This decline begins at about 26mm of axial length and 5D of myopia. To investigate this further, in addition to the existing classification of subjects according to the presence or absence of a myopic crescent, two alternative arbitrary classifications were made according to axial length, and ocular refraction. However, as the subjects were not recruited specifically for this type of analysis, numbers are uneven across the groups and small in some groups. Mean age and number of subjects in each category is given in table 7.8. Two subjects had an axial length greater than 34mm and one subject more than -20D of myopia, therefore the last group for both axial length and ocular refraction was extended in each case to include these two subjects.

Table 7.8. Number of subjects in each category, and mean age within the groups.

Category	group label	number of subjects	mean age (years)	age range (years)
Axial length (mm)				
22.00 - 24.00	i	32	22.84	19.50-30.17
24.01 - 26.00	ii	47	21.66	19.00-26.17
26.01 - 28.00	iii	26	25.85	17.83-35.42
28.01 - 30.00	iv	7	23.23	16.50-27.17
30.01 - 32.00	v	4	28.77	22.67-33.25
32.01 - 34.60	vi	6	25.27	18.92-31.00
Ocular refraction (D)				
+5.00 to 0.00	A	22	22.31	20.25-26.75
0.01 to -5.00	B	58	22.67	19.00-35.25
-5.01 to -10.00	C	19	23.72	17.83-35.42
-10.01 to -15.00	D	15	26.38	16.50-35.00
-15.01 to -20.25	E	8	24.76	18.92-31.00

A one way analysis of variance (ANOVA) combined with the least significant difference multiple comparison procedure was employed to identify any significant differences between the indices across the axial length and ocular refraction categories.

Global indices

Mean values (±SD) for the global indices are given in tables 7.9 and 7.10.

Results from the one way ANOVA for axial length revealed the following,

- groups i and ii did not exhibit any significant differences for any global index.
- groups iv, v and vi were always significantly different from groups i, ii and iii for MD, MS, PSD, CPSD ($p<0.01$).
- group iii differed from group i for MD and MS, and from group ii for MS only ($p<0.01$).
- SF did not differ significantly between the groups except between group i and iv ($p<0.05$).

Differences between groups iv, v, and vi were significant in the majority of cases but these findings should be treated with caution because of the small sample sizes.

A one way ANOVA for ocular refraction revealed the following,

- groups A and B did not differ from each other for any global index.
- group C differed from group B for MS and MD ($p<0.05$), and from group A for MS ($p<0.01$), and MD ($p<0.05$).
- groups D and E were significantly different from all other groups for MD, MS, PSD and CPSD ($p<0.01$).
- groups D and E were significantly different from each other for MD, MS, PSD ($p<0.01$) and CPSD ($p<0.05$).
- SF differed significantly between groups A and E only ($p<0.01$).

Results from group E should be regarded with caution because of the small sample size.

Table 7.9. Mean value (±SD) for the global indices for each axial length category.

Axial length (mm)	MS (dB) (±SD)	MD (dB) (±SD)	PSD (dB) (±SD)	CPSD (dB) (±SD)	SF (dB) (±SD)
i 22.00-24.00	29.11 (±1.19)	-1.69 (±1.13)	1.97 (±0.43)	1.23 (±0.53)	1.25 (±0.39)
ii 24.01-26.00	28.73 (±1.14)	-2.25 (±0.97)	1.94 (±0.37)	1.16 (±0.55)	1.27 (±0.29)
iii 26.01-28.00	27.64 (±1.62)	-2.86 (±1.53)	2.07 (±0.50)	1.38 (±0.65)	1.26 (±0.22)
iv 28.01-30.00	24.66 (±2.14)	-5.75 (±2.12)	2.77 (±0.83)	2.08 (±0.78)	1.52 (±0.46)
v 30.01-32.00	24.08 (±0.81)	-6.23 (±0.58)	3.81 (±0.45)	3.42 (±0.51)	1.39 (±0.15)
vi 32.01-34.60	22.40 (±2.29)	-8.38 (±1.97)	3.16 (±0.72)	2.59 (±0.75)	1.43 (±0.19)

Table 7.10. Mean value (±SD) for the global indices for each ocular refraction category.

Ocular refraction (D)	MS (dB) (±SD)	MD (dB) (±SD)	PSD (dB) (±SD)	CPSD (dB) (±SD)	SF (dB) (±SD)
A +5.00 to 0.00	29.11 (±1.41)	-1.85 (±1.32)	2.00 (±0.45)	1.28 (±0.51)	1.26 (±0.46)
B 0.01 to -5.00	28.72 (±1.26)	-2.09 (±1.16)	1.96 (±0.42)	1.21 (±0.58)	1.26 (±0.27)
C -5.01 to -10.00	27.86 (±1.45)	-2.93 (±1.08)	2.00 (±0.44)	1.25 (±0.65)	1.27 (±0.23)
D -10.01 to -15.00	25.95 (±1.83)	-4.47 (±1.89)	2.64 (±0.84)	1.99 (±1.03)	1.32 (±0.20)
E -15.01 to -20.25	22.43 (±2.32)	-8.16 (±2.10)	3.30 (±0.71)	2.71 (±0.67)	1.59 (±0.37)

These findings support statistically the visual impression from figures 7.3, 7.4 and 7.5, that worsening of the global indices begins to reach significance in subjects with axial lengths above 26mm, and in subjects with more than 5D of myopia. Analysis of the visual field regions using the same subject categories yielded, as expected, very similar results for significant differences between the groups. These results are summarised in the Appendix A1.1.

Correlation and linear regression performed on subjects with axial lengths longer than 26mm (43 subjects), and more than 5D of myopia (42 subjects) for all the visual field parameters yielded, not surprisingly, very similar results to those obtained for the original group 4 (myopes with relatively larger peripapillary crescents). The axial length group contained 24 subjects from the original group 4, and the ocular refraction group contained 25 subjects from group 4. The number of subjects common to the axial length and ocular refraction group is 37, 17 of whom came from group 4. For completeness a summary table of the regression analysis is given in Appendix A1.1, table A1.1.

7.4 Discussion

7.4.1 Global indices

Central visual field sensitivity declines as the degree of myopia and axial elongation increases. Subjects with larger areas of peripapillary crescents (group 4), who also tend to be subjects with longer axial lengths and higher myopia, suffered the greatest depression of their visual fields, as measured by the global indices, than the other subjects (groups 1 to 3). MD and MS are indicators of generalised change, whereas PSD and CPSD indicate non-uniformity within the field, and are believed to represent the presence of localised depressions. From tables 7.2 and 7.3, this depression of the field with increasing myopia appears to be more generalised than local, as changes in MD and MS appear more marked than those of the other indices. This is supported by the number of subjects' fields in which MD is flagged as abnormal by STATPAC for at least $p<0.1$, compared with the other indices in groups 3 and 4. Values for PSD and CPSD in groups 1, 2 and 3 are in very good agreement with those of Iwase *et al* (1989) in normals (1.94 ± 0.48dB for PSD, and 1.11 ± 0.61dB for CPSD), whereas values in group 4 are higher in this study being 2.61 ± 0.90dB for PSD and 1.91 ± 1.08dB for CPSD. This supports the evidence of a localised component of the field depression in addition to the generalised loss in group 4. However, Heijl *et al* (1987c) in a group of normal subjects reported higher values for PSD (2.42 ± 1.13dB), which is close to the value in group 4. Chihara and Sawada (1990), using the Octopus automated perimeter for the central field, found MD to be abnormal in 5 out of 45 subjects with myopia, ranging from -5 to -19D (mean age 46.9 years). Their myopes had peripapillary crescents no larger than 1.5 disc diameters and had no other fundus changes.

When categorised by axial length and ocular refraction, subjects with axial lengths beyond 26mm or myopia more than 5D showed statistically significantly depressed values for MS and MD when compared with subjects with axial lengths below 26mm and myopia less than 5D. These findings support the visual impression in figures 7.3, 7.4 and 7.5. Subjects with axial lengths beyond 28mm or myopia more than 10D have, in addition, statistically significantly depressed values for PSD and CPSD when compared with subjects with shorter axial lengths and less myopia. From these findings it would seem that as axial length and myopia increase a generalised depression is observed to which a non-uniform component of field loss becomes apparent as the myopia increases further. It is difficult to place a precise cut-off point for axial length or degree of myopia above which perimetric thresholds are likely to be significantly depressed. However, it is reasonable to conclude that subjects with axial lengths beyond 28mm are very likely to show a deterioration in their global indices, particularly MD and MS, when compared with age-matched normal subjects with axial lengths below 26mm.

From table 7.3 it can be seen that the coefficients of determination in group 4 are sufficiently high to suggest that linear regression may be of some value in predicting MD and MS for medium and high myopes. To illustrate this approach, results from table A1.1 in appendix A1 are used. These data were obtained by dividing the sample (a) into subjects with axial lengths above or below 26mm, and (b) into subjects with ocular refractions above or below -5D. A myope with an axial length of 29mm for example, would be predicted to exhibit a decline in MD of approximately

$$(29-26)x(-0.90)dB = -2.70dB$$

when compared with a subject of the same age having an axial length less than 26mm. Similar calculations can be performed in subjects knowing their ocular refraction. For example a myope of -14D would be predicted to exhibit a decline in MD of approximately

$$[-14-(-5)]x(+0.48)dB = -4.32dB,$$

when compared with a subject of the same age with less than 5D of myopia (table A1.1).

Values for MD in the non-myopic control group 1, and the low myopes in group 2, are perhaps lower than expected for normal subjects, (mean MDs of -1.75dB and -1.97dB respectively). However, these values are supported by a previous study with a different subject population of the same age on the same instrument (Chapter 6), and another study using a different HFA (Guttridge 1993 unpublished data, personal communication). Subjects were young, normal, healthy individuals with no ocular pathology (past or present), and it is highly unlikely that the entire sample in the non-myopic and lower myopic group contained subjects with abnormally reduced visual thresholds due to an unknown cause. It is more probable that the age-corrected normal data stored within the HFA was constructed from a sample with different differential light thresholds from those in this study. From Heijl *et al* (1987b) it is not clear how many subjects were included from each decade to compose the normal reference field. However, the sample mean MS of 29.21dB for the central field of the non-myopic group in this study is similar to that found in other investigations. Published normal values for MD and MS for the HFA are given in table 7.11.

Table 7.11. Mean global index values ± SD (if given) for HFA central fields of normal subjects.

Investigators	age range / mean ±SD	number of subjects	mean MS ± SD (dB)	mean MD ± SD (dB)
Brenton & Phelps 1986	20-29	17	30.4 ± 1.5	-
	30-39	18	29.9 ± 1.4	
Lewis *et al* 1986	31-58	6	31.63	-
Heijl *et al* 1987c	not stated	84		-0.05 ± 1.73
Collin *et al* 1988	22.1 ± 1.6	25	28.13 ± 3.88	-
Iwase *et al* 1989	10-60	100	-	-0.36 ± 1.12
Katz & Sommer 1990	mean 53	252	-	-0.27
Lindenmuth *et al* 1990	24-36	18	-	-0.95
Flanagan *et al* 1993a	49.6 ± 16.9	98	27.24 ± 2.84	-

Values for SF in this entire sample are in agreement with previous studies on normal subjects (Bebie *et al* 1976b; Flammer *et al* 1984b; Rabineau *et al* 1985; Brenton and Argus 1987; Brenton *et al* 1986; Brenton and Phelps 1986; Katz and Sommer 1987; Heijl *et al* 1987d; Iwase *et al* 1989; Autzen and Work 1990; Crosswell *et al* 1991; Chauhan *et al* 1991; Flanagan *et al* 1993a). SF did increase significantly between groups 1 and 4, and this may be either the result of an association between SF and lower visual threshold values (Flammer *et al* 1984b, Heijl *et al* 1989c; Weber and Rau 1992), or because SF is found to be higher in abnormal fields or abnormal areas of the field (Gloor *et al* 1984; Flammer *et al* 1984a and b; Werner and Drance 1977; Stürmer *et al* 1985; Langerhorst *et al* 1985; Piltz *et al* 1986; Heijl *et al* 1987c).

Table 7.2 shows an increase in the standard deviation from groups 1 and 2, to groups 3 and 4, for the group means of global indices. As the degree of myopia increases the field becomes more disturbed, and the extent of this disturbance varies between individuals, giving these larger standard deviations for the group means (see also tables 7.4, 7.9 and 7.10). This can be interpreted as an increase in the intersubject variability. Intersubject variability has previously been shown to increase in disturbed regions of the field (Gloor *et al* 1984; Flammer *et al* 1984a and b; Werner and Drance 1977; Stürmer *et al* 1985; Langerhorst *et al* 1985; Piltz *et al* 1986; Heijl *et al* 1987c) and in abnormal fields (Holmin and Krakau 1979; Flammer *et al* 1984a and b; Wilensky and Joondeph 1984; Parish *et al* 1984; Lewis *et al* 1986; Katz and Sommer 1986; Hoskins *et al* 1987; Werner *et al* 1987).

7.4.2 HFA printouts

Significantly depressed points were found in normal fields, and this finding is supported by previous studies (Wilensky and Joondeph 1984; Keltner *et al* 1985; Sommer *et al* 1985; Lewis *et al* 1986; Heijl and Asman 1989b; Chauhan *et al* 1989). From the single field analysis and merged printouts it is evident that myopes with peripapillary crescents demonstrated a depression of the differential light thresholds, particularly those in group 4. STATPAC reported a generalised reduction in sensitivity in more subjects in group 4 than in group 3. In addition, the glaucoma hemifield test was borderline in one subject in group 3 and 3 subjects in group 4. In the latter group, it was outside normal limits in two other subjects. This signifies a significant difference in sensitivity between the superior and inferior hemifields. The gray scale and defect depth printouts suggest a greater involvement of the superior hemifield, but the probability plots show a more generalised loss in sensitivity. In agreement with previous studies an enlargement of the blind spot was observed (Nakase *et al* 1987a; Masukagami *et al* 1987; Jonas *et al* 1991; Martin-Boglind 1991), but this was evident in group 4 only.

7.4.3 Field regions

Results set out in table 7.4 show a reduction in the thresholds for all regions from group 1 through to group 4. This decline in the central visual field sensitivity is significant in all cases when comparing group 4 with the other three groups. Group 3 differed significantly from groups 1 and 2 in the majority of cases. Between groups 2 and 3 the upper-temporal quadrant was the only region different for $p<0.01$ (table 7.5). The value for the foveal threshold in groups 1 and 2 is in good agreement with previous studies on subjects of a similar age (Brenton and Phelps 1986; Lindenmuth *et al* 1990 and 1989; Herse 1992).

From inspection of table 7.4 it is difficult to conclude which regions are predominantly affected. Regarding each regional map separately, the lowest sensitivities in all groups are found in the outer-annulus, the superior hemifield (combining the upper temporal and nasal quadrants), and superior sector in all groups. The lower value for the outer annulus is expected, because it is well established that visual sensitivity declines with the distance from fixation (Sloan 1961; Aulhorn and Harms 1972). It is interesting to observe the differences between the mean sensitivities of certain field regions within the groups, particularly between the inner and outer annuli, the upper and lower hemifields, and the superior and inferior sectors. From table 7.12 it is evident that these differences are larger in group 3 compared with groups 1 and 2, and in group 4 compared with group 3. Henson *et al* (1984) has explained asymmetric depressions of the superior field by

eyelashes or brows interfering with the measurement of retinal sensitivity. It is possible that a lower position of the upper lid as the subject became fatigued could produce such effects. However, this does not explain the increasing difference between the superior and inferior hemifields from group 1 through to group 4.

Table 7.12 Differences between selected field regions in the four groups.

Difference between regions	**Group 1 dB**	**Group 2 dB**	**Group 3 dB**	**Group 4 dB**
Annuli				
inner - outer	4.33	4.38	4.49	5.29
Hemifields				
inferior - superior	1.12	1.14	1.55	1.92
Sectors				
inferior - superior	1.69	1.81	2.69	3.16

This suggests an increase in the non-homogeneity of the field. It appears that the decline in field sensitivity in groups 3 and 4 preferentially affects the superior hemifield and superior sector, and the outer annulus in group 4.

Depression of the upper-temporal quadrant in group 4 agrees with previous studies reporting upper-temporal field defects with the manual investigations of the visual field in myopes who in addition had tilted discs and inferior-nasal fundus ectasia (Rucker 1946; Caccamise 1954; Schmidt 1955; Berry 1963; Riise 1966; Odland 1967; Graham and Wakefield 1973; Young *et al* 1976). These studies also reported bitemporal field defects which were not investigated in this study. Huang and Tokoro (1990) using the Octopus automated perimeter demonstrated a reduction of the light sensitivity in group of 71 subjects, aged 12-64 years, with more than 8.25D of myopia and tigroid fundus changes only, as compared to a non-myopic control group, and the upper-temporal quadrant was significantly more affected than the other quadrants. Chihara and Sawada (1990) using the Octopus found mid-peripheral regions of the central 30° to be particularly affected, this was not the predominant finding in this study.

The lower sensitivity of the upper-temporal quadrant in group 4 and superior sector in groups 3 and 4 is probably related to the preferential ectasia of the lower-nasal retina associated with axial elongation in myopia (Curtin 1988). In many of the subjects in group 4, and some in group 3, the choroidal vasculature was more visible in the inferior and nasal retinal areas as compared with the rest of the retina. This indicates a thinning

and/or stretching of the retina, or a lack of pigmentation of the retinal pigment epithelium.

The correlation analysis presented in tables 7.6 and 7.7 shows a much stronger linear association for group 4 than for group 3 for the mean sensitivities of field regions with both axial length and ocular refraction. However, the exceptions in group 4 are the fovea and outer annulus for which the R^2 values are particularly low. In group 3 the rate of sensitivity decline with both axial length and increasing myopia, as indicated by the gradients of the regression lines, is remarkably higher for the upper-temporal quadrant and superior sector. The difference between the gradients in group 3 is quite striking in some cases, for example, upper- versus lower-temporal quadrants, and superior- versus inferior-sector. For all regions the rate of loss is greater in group 4 than in group 3 except for the fovea, superior sector and the upper-temporal quadrant which are very similar in these two groups. In group 4 the gradients do not differ markedly. It would appear that myopes with relatively smaller crescents (subjects with shorter axial lengths and less myopia) show the most rapid decline in sensitivity in the upper-temporal and superior sectors. However, in subjects with larger peripapillary crescents, longer axial lengths and more myopia, the rate of decline seems to be very similar in all regions of the field. In group 4 the temporal sector has the steepest gradient, and this may be related to the larger area of the peripapillary crescent in group 4 myopes, which may affect the visual sensitivity at locations beyond the margins of the normal blind spot. The HFA printouts demonstrated enlarged blind spots in group 4 subjects.

These regional maps are not definitive, and other regional maps may have given slightly different results. From the above findings it is reasonable to conclude that the sensitivity loss in myopia is generalised with localised components in higher degrees of myopia. In group 3 subjects the rate of loss is greater in the superior sector and upper-temporal quadrant but in group 4 the rate of loss is very similar over the entire field. Interestingly, Huang (1993) using the Octopus perimeter recently reported a significant correlation between the field loss of the central field and the degree of myopia and axial length, and the regions most affected were the upper-temporal quadrant and the annulus from 11-20° eccentricity.

The difference observed between the superior and inferior hemifields partially agrees with the report of thinning of inferior nerve fibre bundle in normal myopic eyes (Chihara and Sawada 1990), but this was mainly seen in the inferior-temporal retina which corresponds to the upper-nasal field region.

Greve and Furuno (1980) found a variety of field defects in a group of myopes with glaucoma. Of these only the upper-temporal defect, and enlarged blind spot were found

in this study. Other defects which included typical and atypical nerve fibre bundle defects were not found in this study.

Results from the axial length and ocular refraction categories for the field regions yielded very similar results as for the global indices and shall not be discussed further.

Several possible explanations for visual field sensitivity deterioration in myopia are suggested below

- fundus ectasia may give rise to refraction scotomas (Schmidt 1955; Odland 1967)
- structural changes in the retina-choroid complex, which can not be observed ophthalmoscopically, may influence the performance of the visual receptors
- axial elongation will cause stretching of the retina, and the receptor spacing may be increased, resulting in fewer receptors per unit area as compared with an emmetropic eye. For the same stimulus size, fewer receptors will be stimulated in a myopic eye as compared with a non-myopic eye, and as a result the stimulus is less likely to elicit a response
- axial elongation may induce distortion and/or misdirection of the receptors. It is known that the receptors are very directionally sensitive to light. If they are misdirected they will not respond optimally
- minification of the stimulus by the negative prescription may cause attenuation of threshold

Another possible factor is the axial length of the eye, which may affect the retinal illuminance sufficiently to alter retinal adaptation. It is known that the effective illuminance of the retina is inversely proportional to the square of the distance from the second principal point of the eye to the retina, k' (Le Grand 1968). If we take the two extremes in this sample the shortest value for k' is 19.877 and the longest 32.656, which is a 1.64 fold increase in k' (calculation of k' is described in Chapter 8 section 8.2.2.3). Assuming all other factors to be constant such as transmission of the ocular media and pupil size, retinal illuminance will decrease in the longer eye by $(1/1.64)^2 = 0.371$ of that in the shorter eye. If we let the shorter eye have retinal illuminance of 1 unit then the retinal illuminance in the longer eye will reduce by (1-0.371) units which is 0.629 units. The decibel unit of measure $10.\log\Delta L$, thus 10.log(0.629) gives 2.0dB. This difference in the retinal illuminance is very low and can safely be ignored in the clinical context. Heuer *et al* (1989) have demonstrated using the HFA in subjects with fully dilated pupils, that retinal adaptation needs to be reduced by at least 1.5 log units (15dB) to significantly affect threshold within the central 30°. Although Klewin and Radius (1986) found significant changes in threshold with neutral density filters of 0.5 log units with the Octopus automated perimeter which has a lower background luminance of 4asb, no

attempt was made to control pupil diameter.

Changes in the visual field of normal myopic individuals are possible confounding factors in the clinical screening for, and diagnosis of field defects. This is of particular relevance to optometrists and ophthalmologists when screening and monitoring the progress of POAG. Apart from the global indices being flagged by the HFA STATPAC, the comments given on the printout could be interpreted as characteristic of glaucoma. None of the subjects in this study had a known positive family history of glaucoma. All were young, and without any history of ocular pathology. In addition, in all cases the optic discs were normal in appearance for a myopic eye, and the intraocular tensions were below 20mmHg. It is very unlikely that there were any glaucoma sufferers in the sample. Guidelines for practitioners would be helpful to avoid myopic field changes being confused with other types of field loss, including glaucoma. Obviously, any other ocular findings must be considered together with the visual field data. The following guidelines are proposed according to the findings in this study of the central field

- myopes with axial lengths above 26mm and more that 5D of myopia may show deficits in the visual threshold in comparison with normals of the same age as measured by the global indices and regional mean sensitivities.
- the regression gradients discussed above can be utilised to predict the value of the global indices or regional mean sensitivities, providing the myopic refraction or axial length is known. It should be noted however, that changes in myopic individuals with age have not been investigated, but as myopia progresses the global indices and mean sensitivities of field regions may deteriorate.
- the field loss is mainly generalised with a localised component. As the myopia increases the difference between the mean sensitivity of the superior and inferior hemifields becomes larger. Once again the regression gradients can be utilised to estimate the sensitivity in field regions for subjects of the same age as in this study.
- superio-temporal defects may be due to fundal ectasia which may give rise to a refraction scotoma. This can be investigated by re-testing the field with increasingly negatively powered lenses. Careful ophthalmoscopy may reveal a difference in the level of the retina.
- if an individual has a crescent which is approximately half the size of the optic disc or more, as in group 4, a reduction in the differential light thresholds is more likely.
- a difference between the superior and inferior hemifields was reported in this research by the Humphrey STATPAC program. This type of field abnormality is typical of glaucoma. However, paracentral or arcuate scotomas or nasal wedge defects were not found in this group of myopes.

It must be remembered that isolated or arcuate scotomas can occur in myopia in

conjunction with chorioretinal degeneration, in which case the field defects should parallel ophthalmoscopic findings. Enlargement of the blind spot does occur in myopia and this aspect is covered in Chapter 9. A single threshold program such as the 30-2 is sufficient for screening purposes.

The distinction between field defects due to myopia and those due to POAG is not easy. As reviewed in Chapter 1, section 1.5.1, there is an association between myopia and glaucoma. Greve and Furuno (1980), using Goldmann kinetic perimetry investigated field loss in myopes with glaucoma. They reported a variety of field defects, some of which were found in this study. Recently, Poinoosawmy *et al* (1994) using the HFA reported myopes with either normal tension or high tension glaucoma to exhibit field defects predominantly in the inferior hemifield. However, it is not evident from their abstract whether the field loss associated with myopia in the absence of glaucoma was considered. A longitudinal study of the visual field in myopes encompassing subjects below and above the age of 35 years would be useful. Although myopes with raised intraocular pressures could be identified and classified as high pressure glaucoma patients, it may be difficult to classify a myopic subject as a normal tension glaucoma patient because the field loss may be due to the myopia. This is further confounded by the difficulty in assessing myopic optic discs.

CHAPTER 8

Dimensional assessment of the optic nerve head and peripapillary region

8.1 AIMS

As outlined in Chapter 2 the aim of this chapter is to evaluate the following

- a method for determining the true size of a retinal feature from its photographic image. Exact calculation of the true size of a fundus feature from a photograph requires precise knowledge of the optical components of the human eye being examined and the magnification of the fundus imaging system employed. The latter, if not already known, can be explored experimentally using a model eye (section 8.3). However, it is not normally possible to measure all of the optical components of the human eye, thus certain assumptions must be made as to its optical configuration. This aspect is considered below in section 8.2
- typical normal values for optic disc area, neuroretinal rim area, cup area and peripapillary crescent area over a wide range of myopia and to compare these with previous studies (section 8.4)
- whether the size of the optic disc, optic cup, neuroretinal rim and any myopic crescent is related to axial length and refractive error (section 8.4)?

From the data available it will be possible to assess any inter-relationship between optic disc area, cup area, and neuroretinal rim area. In addition, the peripapillary crescent area in relation to the area of the optic disc will be assessed.

It is important to know the dimensional characteristics of the normal optic disc as this may help in the differential diagnosis of normal and pathologically disturbed optic nerve heads. For example, it has been shown that the neuroretinal rim area is superior to cup-disc ratio in distinguishing glaucomatous eyes from normal eyes and eyes with ocular hypertension (Airaksinen *et al* 1985a; Drance and Balazsi 1984; Jaeger 1983; Jonas *et al* 1987). Typical dimensional values for a normal emmetropic optic disc are different from those of an optic disc of a highly myopic eye (Jonas *et al* 1988d). In highly myopic eyes the optic nerve head has a distinctly different ophthalmoscopic appearance. Assessment of any cupping is hindered by the forward displacement of the cribriform plate in myopes, observed by Donders (1864), and the oblique insertion of the optic disc (Brown and Tasman 1983). Peripapillary crescents are not exclusive to myopia, for example atrophy of the peripapillary region in the form of either pigmented or non-pigmented

crescents and haloes has been described in association with glaucoma (Primrose 1971; Wilensky and Kolker 1976; Heijl and Samander 1985; Anderson 1983; Jonas *et al* 1992a). Cup size, disc size and the presence of peripapillary atrophy are thought to indicate increased vulnerability of an optic nerve head to glaucomatous damage (Anderson 1987; Armaly 1970; Chi *et al* 1988).

8.2 RAY TRACING TECHNIQUE FOR DETERMINING THE TRUE SIZE OF A RETINAL FEATURE

8.2.1 Introduction

Anomalies and diseases of the optic nerve are often associated with specific alterations to the topography of the optic nerve head. Quantification of the optic nerve head surface may be helpful in diagnosis and subsequent follow-up. Clinically detectable structural damage to the optic nerve head and nerve fibre layer are believed, by some investigators, to precede measurable visual field loss in glaucoma (Quigley *et al* 1982; Airaksinen *et al* 1985c; Caprioli *et al* 1987). One area of research in glaucoma has involved assessment of the optic disc, in particular the area of the neuroretinal rim, which is believed to reflect the number of nerve fibres in an eye (Radius and Pederson 1984; Airaksinen *et al* 1985a and b). Optic disc area and neuroretinal rim area have to be computed from measurements made from fundus photographs and calculations which take account of the magnification of the camera employed and the dioptric power of the eye photographed (Bengtsson 1976; Bengtsson and Krakau 1977 and 1992; Littmann 1982 and 1988).

Firstly the methods proposed by Littmann (1982) to determine the true size of a retinal feature are described. His technique has been widely used. Secondly, alternative methods are presented.

8.2.2 Methods and analysis

8.2.2.1 Littmann's procedure

Assuming axial ametropia and with particular reference to the Zeiss Oberkochen telecentric fundus camera, Littmann (1982) devised a technique for determining the true size of a given fundus feature. Littmann's formula is

$$t = 1{\cdot}37qs \qquad (1)$$

This relates the true size t of a retinal feature to the measured size s of its image on the fundus camera film. The factor q, which needs to be determined, is a variable dependent on the optical dimensions of the given eye. On the assumption of axial ametropia as the norm and taking Gullstrand's schematic eye as a model, Littmann devised a method of estimating q from only two known quantities: the corneal radius (r_1) and the ametropia (A) at the corneal vertex. Although equation (1) can be applied in principle to any fundus camera of known telecentric design, the numerical factor 1·37 is not a constant. It applies only to the West German Zeiss instrument used by Littmann. If there are any other

telecentric models, different values of the numerical factor would almost certainly pertain. It should also be noted that equation (1) refers to linear, not to area magnification. If s^2 represents a measured area on the camera film and t^2 the corresponding area of a retinal feature, equation (1) should be replaced by

$$t^2 = (1{\cdot}37q)^2 s^2 \qquad (1A)$$

For example, if

$$s^2 = 17{\cdot}4\text{mm}^2 \text{ and } q = 0{\cdot}315$$
$$t^2 = (1{\cdot}37 \times 0{\cdot}315)^2 \times 17{\cdot}4 = 3{\cdot}24\text{mm}^2$$

Littmann's first method of arriving at q required the use of a nomogram or network chart printed in two sections - figures 2 and 3 of his 1982 paper (Littmann 1982). This gives a direct reading of q from the grid location representing the known values of r_1 and A. In a later paper (Littmann 1988), Littmann offered an alternative to the use of his nomogram. Instead, the value of q was to be obtained by calculation from the formula

$$100q = aA^2 - bA + c \qquad (2)$$

The requisite values of a, b, and c, all varying with r_1, could be obtained from a table provided. Values of r_1 ranged from 6·0 to 10·0mm at intervals of 0·2mm, in general requiring interpolation at intermediate values of r_1.

This development by Littmann prompted the thought of a further step forward by making reference to tables unnecessary. An original scheme fulfilling this purpose is now presented. To facilitate explanation, four lines from the middle of Littmann's table of the co-efficients a, b, and c are here reproduced, with due acknowledgements, as table 8.1.

Table 8.1. Extract from Littmann's own table 1 (Littmann 1988).

r_1 (mm)	a	b	c
7.6	0.0091	0.5739	29.49
7.8	0.0096	0.5932	30.01
8.0	0.0100	0.6126	30.52
8.2	0.0105	0.6322	31.02

Inspection of the complete table shows that the three co-efficients all increase with r_1 at different rates. Nevertheless, in each one of them taken separately, the increments are nearly constant, especially when r_1 falls within the range 7·0 to 9·0 mm, which covers the great majority of eyes. This makes it possible to express a, b, and c as simple functions of r_1 such as the following,

$$a = 0.0100 + 0.00236(r_1 - 8) \quad (3)$$

$$b = 0.6126 + 0.0968(r_1 - 8) \quad (4)$$

$$c = 30.52 + 2.57(r_1 - 8) \quad (5)$$

The ametropia A can be calculated from

$$A = \frac{F_{sp}}{1 - 0.001v F_{sp}} \quad (6)$$

in which F_{sp} is the spectacle correction at the measured distance v mm from the corneal vertex. For a numerical example, suppose r_1 to be 7·6mm and A to be -8.00D. Round figures have been chosen to simplify the nomogram reading of q, which is found to be in the neighbourhood of 0.346. For r_1 = 7.6, equations (3) to (5) give a = 0.0091, b = 0.5739, and c = 29.49, as in the table itself. Equation (2) then becomes

$$100\,q = 0.0091 \times 64 - (0.5739 \times -8) + 29.49$$

whence $q = 0.347$

The intuitive procedure with an astigmatic eye would be to take F_{sp} as the mean of the two principal powers of the spectacle corrections, S and $(S+C)$, ignoring the cylinder axis. Thus,

$$F_{sp} = S + 0.5C$$

from which A can then be calculated. Similarly, r_1 would be taken as the mean of the two recorded corneal radii, again irrespective of axis direction. Without going into details, it can be said that a thorough optical analysis would endorse this intuitive approach.

A second nomogram was devised by Littmann (1982) which utilised the axial length of the subject if known. Computation of this nomogram is explained in Appendix A2.2.

8.2.2.2 The telecentric principle and the factor *q*

Bengtsson and Krakau (1977) described the process of aligning the Zeiss fundus camera in front of a human eye to ensure that it is in the correct position for the telecentric principle to apply. As Littmann did not explain the rationale of his procedure and its dependence on a telecentric camera system, the true nature of the factor *q* did not emerge.

The essential features of the telecentric design are illustrated in figure 8.1, in which a subject's hypermetropic eye is represented by a 'reduced' single-surface eye whose single principal point P coincides with the corneal vertex.

The component of the camera's optical system nearest the subject's eye may be termed the condenser, shown in figure 8.1 as a 'thin' lens with its optical centre at O and its anterior principal focus (F) coincident with P. Thus, a ray such as HJ parallel to the optical axis XX and travelling from left to right would be refracted so as to meet the axis at P, as shown. The ray QP from a retinal point Q gives rise to the refracted ray PE which meets the condenser at E. After refraction by this lens, the emergent ray EG will be parallel to the optical axis, like HJ. At this stage the image of Q must lie along EG.

Its exact location is easily found in two steps. First, on refraction by the eye itself, an image Q'_1 will be formed in the plane of the eye's far point M_R, which is conjugate with the retina. As shown in figure 8.1, Q'_1 lies on the path of the refracted ray PE produced backwards to the far point plane. Next, Q'_1 becomes an object for the condenser. A construction line from Q'_1 through the optical centre O of the condenser meets the refracted ray EG at the second image point Q'_2.

As shown in figure 8.2, the same procedure for locating Q'_1 and Q'_2 can be applied to the myopic eye. This is now represented by a three-surface schematic eye because the reduced eye is too simple a model for continued use here. The schematic eye has two principal points, the first at P and the second at P′. According to the Gaussian system, the distance *k* to the eye's far point is measured from P and the distance *k′* to the retina is measured from P′. Ocular refraction is the reciprocal of the distance *k*. Unless otherwise stated, all future references to *k* and *k′* are to be taken in the Gaussian sense.

If an incident ray is directed towards P, the refracted ray emerging from the crystalline lens will appear to have originated from P′. These Gaussian construction rays, like actual ones, are reversible.
The conjugate angles *U* and *U′* in figures 8.1 and 8.2, if small, can be taken as obeying the simplified law of refraction, so that

$$U' = U/n \tag{7}$$

in which n is the refractive index of the final ocular medium. This may be taken as 1.336, a generally accepted value.

The telecentric optical system is designed such that the ratio of the image size s on the camera film to the distance y (OE) is a constant, at least over a wide range of ametropia. Also, since the distance OP can be assumed to remain constant, the only variable governing y is the angle $U°$ between the refracted ray PE and the optical axis. The telecentric design thus gives rise to the relationship

$$s = U°/p \tag{8}$$

in which p is a constant for a particular model of the instrument. Figure 8.2 represents the simple case in which the retinal object QM′ of height t is situated on the optical axis. If t is very small, paraxial approximations may be used. The object height t can then be expressed as

$$\begin{aligned} t &= k'U' = k'U/n \qquad (U \text{ in radians}) \\ &= k'U°/57.296n \qquad (U \text{ in degrees}) \end{aligned} \tag{9}$$

With n as 1·336, equation (9) becomes

$$\begin{aligned} t &= k'U°/76.547 \\ &= 0.01306\, k'U° \end{aligned} \tag{10}$$

Finally, equations (8) and (10) in conjunction lead to

$$t = p(0.01306\, k')s \tag{11}$$

Comparison of this expression with Littmann's - equation (1) above - shows that 1.37 is the value of p for the Zeiss fundus camera in question, while the middle term is equivalent to the variable q. That is to say,

$$q = 0.01306\, k' \tag{12}$$

which shows q to be a constant fraction (about one eightieth) of the crucial ocular dimension k'. The determination of k' is the problem to be solved. It has to be faced that k' and q cannot be determined directly but only evaluated to varying degrees of

approximation.

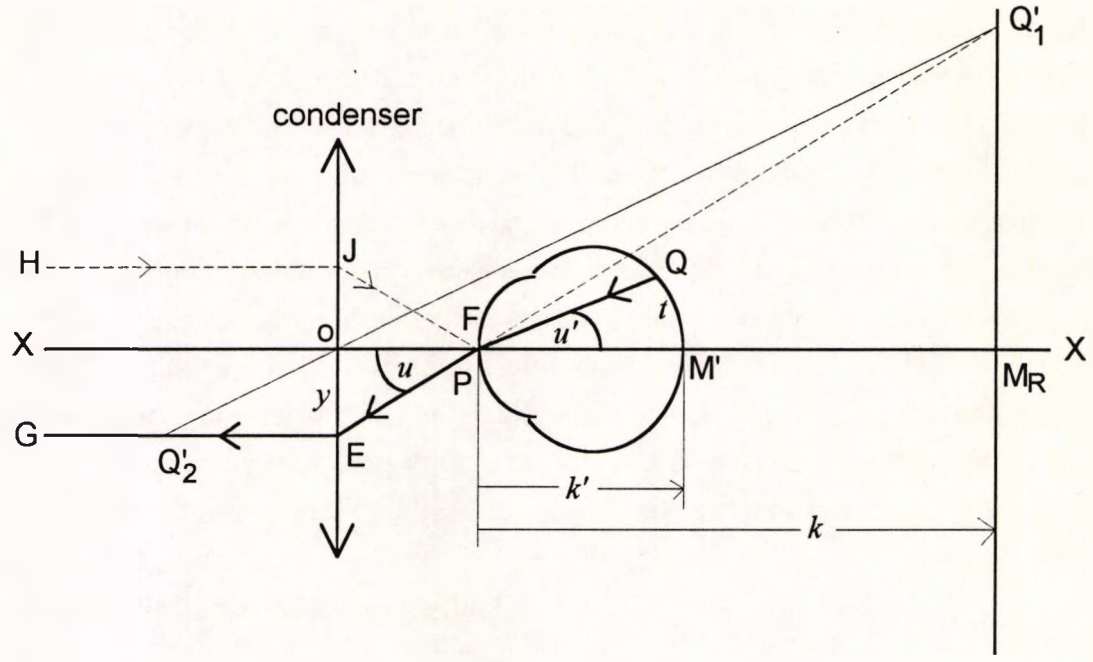

Figure 8.1. The telecentric principle illustrated for a hypermetropic 'reduced' single-surface eye

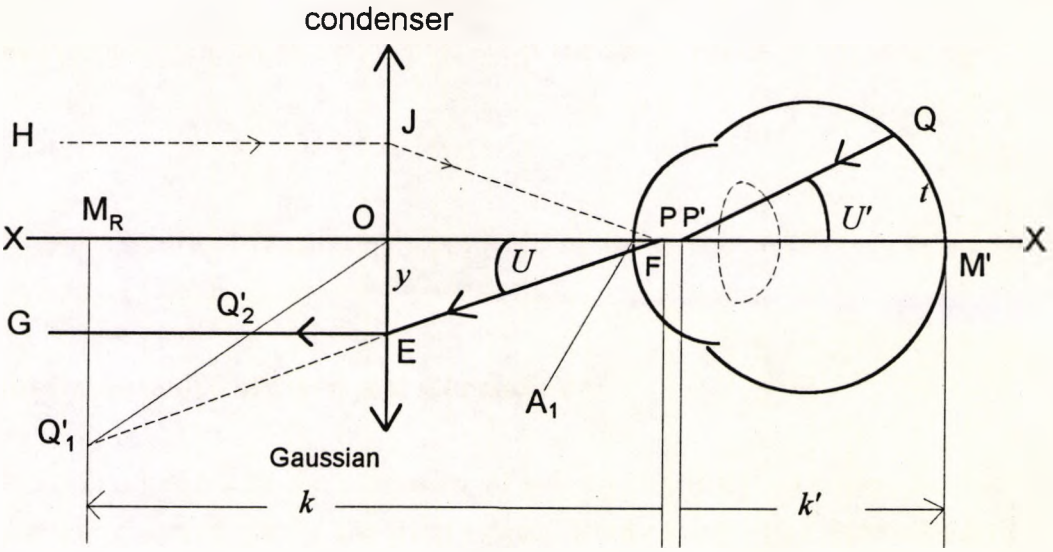

Figure 8.2. The telecentric principle illustrated for a myopic three-surface eye.

8.2.2.3 Alternative methods of evaluating q

All numerical approaches have to be based on a particular schematic eye as the model. Gullstrand's No.1 schematic eye chosen by Littmann has a two-surface cornea and a four-surface crystalline lens. For the methods to be described, the model to be used is the new three-surface schematic eye detailed by Bennett and Rabbetts in appendix B of their work (Bennett and Rabbetts 1989). It is proposed as a future replacement of the Gullstrand-Emsley three-surface eye now used throughout the text. The new Bennett-Rabbetts eye is not only adequate for the present purpose but is also dimensionally closer to the data now available. Instead of Gullstrand's low values of 58.64D and 19.11D for the equivalent powers of the eye and crystalline lens respectively, the corresponding values of the Bennett-Rabbetts eye are 60.00D and 20.83D respectively. Both eyes take 1.336 as the refractive index of the aqueous and vitreous humours.

(a) The adjusted axial length method

As shown in figure 8.2, the distance k' can be found by subtracting A_1P' from the eye's axial length x. In the Bennett-Rabbetts eye this distance is 1·82mm but is subject to individual variation. The position of both principal points, P and P′, is the result of a tug of war between the cornea and crystalline lens. Each exerts a pull on the principal points, proportional to its own power. Figure 12.6 in the work by Bennett and Rabbetts includes the differing values of A_1P' over a wide range of combinations of corneal and lens powers. These figures suggest that if 1.82mm is adopted as a standard value, individual variations are unlikely to exceed plus or minus 0.55mm. The resulting maximum error in q would be only the fraction 0.01306 of 0.55, that is, 0.007. A unique feature of this method is that the axial length of the eye is the only information required,

$$q = 0.01306\ (x - 1.82) \qquad (13)$$

A similar approach was recently proposed by Bengtsson and Krakau (1992), who take A_1P' to be 1.6mm.

(b) Construction of a personal schematic eye

A novel approach to the evaluation of q is to construct, on paper, a personal three-surface schematic eye for the given subject. Until recently, this undertaking would have required phakometry to provide data on the crystalline lens. This need can now be obviated by a procedure devised by Bennett (1988). In addition to the keratometer reading (r_1) and ametropia (A), the only other information required can be obtained from

A-scan ultrasonography: the anterior chamber depth (d_1), the axial thickness of the lens (d_2), and the vitreous depth (d_3). A surprisingly short computing scheme leads to F_L and F_E, the equivalent powers of the lens and eye respectively. A few added steps are needed to calculate A_1P', k', and q_0, the paraxial value of q given by this method.

The principle of Bennett's procedure is applicable to any three-surface schematic eye. All his own calculations and numerical examples were based on the optical constants of the Gullstrand-Emsley eye. The revised constants of the new Bennett-Rabbetts eye were used here in producing the results displayed in column (5) of table 3. Details of the complete computing scheme are given in Appendix A2.1.

Bennett's procedure contains an inherent source of error because it assumes the relative curvatures of the two surfaces of the crystalline lens to conform to a defined standard pattern. Nevertheless, extensive tables in his paper show that the resulting limits of error are unlikely to exceed ±1·00D for F_L and ±0·50D for F_E.

(c) Peripheral values of q

So far discussion has been limited to the paraxial value of q. Peripheral values can be found by ray tracing through the personal schematic eye. For this purpose the distance A_1P from the corneal vertex to the eye's first principal point P is needed. In figure 8.3, two incident rays are directed towards the point P, one making a greater angle U_G with the optical axis and the other the lesser angle U_L. The angle between the incident rays is denoted by ΔU. After refraction by the crystalline lens both rays appear to have proceeded from the immediate neighbourhood of P′ to meet the retina at Q_G and Q_L. The linear distance t between these points represents the size of a peripheral retinal feature to be photographed with the eye in its primary position. In this situation, the factor q was defined by Littmann as

$$q = t/\Delta U^{\circ} \qquad (14)$$

Any ray tracing program for co-axial spherical surfaces may be used. Details of the computing scheme used is given in Appendix A2.1.

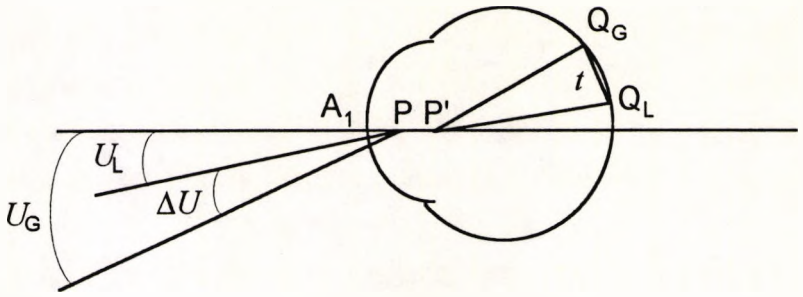

Figure 8.3. Chief rays contributing to image formation of a peripheral retinal feature of linear size *t*.

8.2.3 Results

Comparison of different evaluations of q

To provide a basis for comparing the numerical results given by the different methods of evaluating q, 12 subjects were included whose ocular dimensions including data from ultrasonography had been determined. The subjects, 6 of each sex and all with healthy eyes, were in the age span of 21-28 years with a mean of 23·5. To cover a wide range of ametropia, only one eye of each subject was included.

The relevant data for each eye are given in the upper part of table 8.2. In the lower part are details of the corresponding personal schematic eyes, together with k', q_0 and A_1P'. Results on the same subjects from all the methods described are presented in table 8.3. For convenient reference, subscript numerals or letters have been added to q to denote the method of calculation.

Column (2) of table 8.3 gives the values of (q_1) derived from the mathematical equivalent of Littmann's nomogram and tables. Columns (3) and (4) give the results of two alternative methods when the eye's axial length (x) is known. The first is Littmann's supplementary procedure (Littmann 1982 and 1988), also converted into a mathematical routine to obtain the values q_2. The second, (q_x) in column (4), is derived from equation 13.

Transferred from table 8.2, the results in column (5) show the paraxial values (q_0) obtained from the personal schematic eyes. Finally, the remaining columns tabulate peripheral values (q_P), and this calculation is demonstrated for one example in Appendix A2.1. To arrive at these figures three obliquely incident rays aimed at P as in figure 8.3 were traced through the personal schematic eyes, making angles U_1 with the axis of 8°,

16° and 24°. The points at which the finally refracted rays meet the retina may be denoted by Q_8, Q_{16}, and Q_{24}, with Q_0 coinciding with the fovea at M′. By calculating the linear distances t from Q_0 to Q_8, Q_8 to Q_{16} and Q_{16} to Q_{24}, values of q_P for each of these ranges were obtained from equation (14). The denominator ΔU_1 was 8° in each case.

Since every eye showed a similar pattern of declining values of q_P with increasing values of U_1, the possibility of a general expression was investigated. The ray tracing procedure was repeated on one of the eyes (No.4) for values of U_1 at 2° intervals from 0 to 32°, giving very small values of t. Examination of the first and second differences between successive values of t indicated a quadratic function, which took shape as

$$q_P = q_0 - 0{\cdot}000014\ U_1^2 \qquad (15)$$

in which U_1 is the larger of the two angles defining the location of t. In his 1982 paper Littmann had expressed the view that the reading of q yielded by his nomograms was sufficiently accurate within ±20° from the optical axis.

Table 8.2. Measured ocular dimensions of 12 subjects and calculated optical constants of the corresponding personalised schematic eyes

		Subject number											
		1	2	3	4	5	6	7	8	9	10	11	12
Given data	Symbol												
Spectacle correction	F_{sp}	+4.00	+1.62	+0.62	+0.62	-2.50	-4.87	-6.62	-8.25	-12.00	-14.50	-6.75/-1.50	-7.75/-2.25
Mean lens power	F_{sp}											-7.50	-8.87
Vertex distance	v	15	11	12	13	14	11	10	8	11	10	12	10
Ametropia	A	+4.16	+1.65	+0.62	+0.62	-2.42	-4.62	-6.21	-7.74	-10.60	-12.66	-6.88	-8.15
Corneal radius or radii	r_1	7.98	7.59	7.86	7.68	8.01	7.76	7.62	7.60	7.75	7.49	7.77; 7.37	8.12; 7.79
Anterior chamber depth	d_1	3.32	3.80	3.86	3.79	3.52	3.76	3.73	3.42	3.89	3.19	3.73	3.73
Axial lens thickness	d_2	3.47	3.74	3.50	3.78	3.63	3.86	3.64	3.64	3.81	4.64	3.57	3.92
Vitreous depth	d_3	15.89	14.47	16.56	15.81	17.94	17.49	18.96	19.80	19.89	18.42	18.90	19.27
Axial length of eye	x	22.68	22.01	23.92	23.38	25.09	25.11	26.33	26.86	27.59	26.25	26.20	26.92
Calculated values													
Equivalent power of eye	F_E	59.54	65.59	59.99	61.69	59.98	62.53	60.58	60.76	62.80	68.05	61.59	61.89
Equivalent power of cornea	F_1	42.11	44.27	42.75	43.75	41.95	43.30	44.09	44.21	43.35	44.86	44.39	42.26
Equivalent power of lens	F_L	21.01	26.66	21.30	22.38	21.96	23.94	20.48	20.31	24.32	29.00	21.37	24.30
Gaussian k'		20.93	19.87	22.04	21.44	23.20	23.06	24.55	25.16	25.50	23.99	24.39	24.80
A_1P'		1.75	2.14	1.88	1.94	1.87	2.05	1.78	1.70	2.09	2.26	1.81	2.12
$q_0 = 0.01306k'$		0.273	0.259	0.288	0.280	0.303	0.301	0.321	0.329	0.333	0.313	0.319	0.324

Linear dimensions in millimetres, powers in dioptres

Table 8.3. Comparison of different evaluations of q

		Axial length (x) known		**Personalised schematic eye**			
Subject No.	Littmann's method when (x) unknown	Littmann's extended method	Adjusted axial length*	Paraxial	Peripheral q_p when U_1 is		
					0-8°	8°-16°	16°-24°
	q_1	q_2	q_x	q_0	q_p	q_p	q_p
(1)	(2)	(3)	(4)	(5)	(6)	(7)	(8)
1	0.281	0.273	0.273	0.273	0.273	0.271	0.266
2	0.285	0.247	0.264	0.260	0.259	0.257	0.254
3	0.298	0.291	0.289	0.288	0.287	0.285	0.281
4	0.293	0.285	0.282	0.280	0.279	0.277	0.273
5	0.321	0.308	0.304	0.303	0.302	0.300	0.296
6	0.328	0.311	0.304	0.301	0.300	0.298	0.294
7	0.335	0.327	0.320	0.321	0.320	0.371	0.313
8	0.345	0.335	0.327	0.329	0.327	0.325	0.321
9	0.372	0.348	0.337	0.333	0.332	0.330	0.326
10	0.378	0.333	0.319	0.313	0.313	0.311	0.318
11	0.338	0.326	0.319	0.318	0.317	0.315	0.310
12	0.360	0.336	0.328	0.324	0.323	0.321	0.316

*$q_x = 0.01306(k' - 1.82)$

8.2.4 Discussion

Reliability of the results and practical convenience are probably the best criteria by which the various methods of determining q should be assessed. All the methods are open to error, both experimental and inherent. The latter variety arises from assumptions as to quantities not directly measurable.

The adjusted axial length method leading to equation (13) is arguably the most reliable and convenient of all. It requires no data other than the eye's axial length, not even the ametropia. As a result there is only one source of experimental error, which, on the basis of the results in Chapter 5, could realistically be taken as ± 0.20mm. The inherent error is the assumption of a constant value for A_1P', taken as 1.82mm. In the penultimate line of table 8.2 are the calculated values of A_1P' for the 12 given eyes. The lowest is 1.70mm and the highest 2.26mm. These are well within the ± 0.55mm limits of error already suggested. When the experimental errors are added, the total becomes ± 0.75mm. Finally, if 22mm is taken as a typical value of the Gaussian k', an error of ± 0.75mm can be expressed as a percentage error of ± 3.4%, which is quite low. This figure applies also to q because q is a constant fraction of k'.

The results obtained from the personal schematic eyes are in excellent agreement with those from the adjusted axial length method. Greater differences might have been expected because more data and more sources of experimental error are involved. Also, the calculating scheme itself has an inherent source of error. Although this method may not commend itself for routine clinical use, it does yield valuable data throwing light on the optics of the given eye. The values of F_E, F_L, and A_1P' recorded in table 8.2 were obtained by this method which evidently has a useful role to play in the field of ocular dioptrics.

Littmann's q_1 results based solely on r_1 and A cannot aspire to the degree of reliability made possible by a knowledge of the eye's axial length. Unfortunately, there is no way of avoiding the drawback that an eye with a given combination of r_1 and A can still have a wide range of possible axial lengths and corresponding values of k'. A report by Sorsby *et al* (1957), whose findings were broadly in line with previous studies, showed that in most refractive states the axial length could vary by as much as 4mm, sometimes more. A possible error of 4mm in the assumed value of k' would represent a percentage error of ±20% to ±13% as k' varies from 20 to 30mm.

A significant feature of the q_1 results is that they are invariably higher than all the other evaluations. Mansour (1990) found q_2 to give lower values for the size of the optic disc than q_1. The probable explanation is that Littmann took into account any excess or

deficiency of corneal power relative to the Gullstrand value of 43.05D, but otherwise assumed the ametropia to be caused by shortening or elongation of the eye's axial length. In effect, the unknown power of the crystalline lens was assumed to have Gullstrand's value of 19.11D. This is much lower than in any modern schematic eye as well as all those in table 8.2. Based on the resulting under-estimate of the eye's equivalent power, the axial length arrived at is too long and gives too high a value to q.

Supporting this explanation, the largest differences between q_1 and q_x occur in those eyes, Nos. 2, 9, 10, and 12, in which the lens power F_L has values exceeding 24D. The biggest difference of all is in eye No.10 with a lens power of 29D, which must be near the limit of credibility. Littmann's nomogram (1988) (his figure 4) gives 29·8mm as the estimated axial length of this eye whereas its measured length is only 26.25mm.

Nevertheless, if these four exceptional eyes are excluded, the mean difference between the q_1 and q_x results is fractionally less than 5% of the latter, which is remarkably small. Moreover, Littmann's procedure for improving the value of q_1 when the axial length is known produces results q_2 which for the most part differ only negligibly from the q_x values. Jonas *et al* (1988a) has shown, using the Littmann method, that the mean disc diameter/area for 100 normal optic discs was not significantly different from the mean size of the scleral canal of the optic nerve as determined in 107 enucleated fixed donor eyes. In all, Littmann must be credited with having devised a workable system of proven utility.

8.3 CONSTRUCTION OF A MODEL EYE TO INVESTIGATE THE MAGNIFICATION PROPERTIES OF THE CARL ZEISS JENA FUNDUS CAMERA

8.3.1 Introduction

The model eye to be described was needed for the initial purpose of investigating possible changes in the magnification of the Carl Zeiss Jena fundus camera as the degree of axial ametropia varies. Information regarding this camera's magnification was unavailable. The experimental procedure below allowed the magnification characteristics of this camera to be determined, establishing whether or not the camera is telecentric. This information is required in section 8.4, for the determination of the true area of the optic nerve head features and peripapillary crescents, from fundus photographs taken with this camera. A second camera, known to be telecentric, was also investigated for comparison.

As pointed out by von Rohr (1920) the first known model eye was made by Christoph Scheiner (1575-1650). The cornea, lens and curved fundus were made of glass or crystal and the anterior (but not the vitreous) chamber filled with water. Polyak (1941), cited by Levene (1966), gives a brief account of other early constructions. In more recent times, other models for experimental purposes have been devised by Airy (1828), Tscherning (1924), Fincham (1959), Gliddon (1929), Chalmers and Ryland (1906), Naylor and Arden (1947), Arell and Kolari (1978) and Kennedy *et al* (1983). Rosenthal *et al* (1980) and Lovasik (1983) constructed model eyes incorporating a micrometer screw to vary the vitreous depth to produce axial ametropia.

Normally, the lens is a solid construction of glass or plastics, but in Gliddon's (1929) model it consisted of two thin glass shells filled with a mixture of glycerine and water to obtain the desired refractive index. Hydrophilic materials of high water content for soft contact lens manufacture have refractive indices approximating to that of the corneal substance (approximately 1.376) but are unsuitable for model eyes.

8.3.2 Design and construction of the model eye

The design of the model eye is based on the main features of the new schematic eye proposed by Bennett and Rabbetts (1989). They are set out in table 8.4.

First model (Mark I)

For the cornea and lens, the gas permeable contact lens material Boston RXD was chosen. This has a mean refractive index of 1.435, which is closer to the value for the

human cornea than other currently available gas permeable materials. It is very close to the value chosen by Bennett and Rabbetts (1989) for the crystalline lens of their schematic eye. Distilled water was used for the two chambers. To obtain the desired surface powers, the radii of the Bennett-Rabbetts eye had to be modified. The essential dimensions of the Mark I model were accordingly as shown in table 8.5.

Table 8.4. Main features of the Bennett-Rabbetts schematic eye

Refractive Indices	
Aqueous and Vitreous Humours	1.336
Crystalline lens	1.416
Surface powers	
Cornea (single surface)	+43.08D
Lens: front surface	+7.82D
Lens: back surface	+13.28D
Equivalent powers	
Cornea	+43.08D
Crystalline Lens	+20.83D
Eye	+60.00D
Axial separations	
Anterior chamber depth	3.60mm
Axial thickness of lens	3.70mm
Axial length for emmetropia	24.09mm

Table 8.5. Optical specification of the Mark I model eye.

Corneal lens			
r_1	+ 8.75mm	F_1	+49.71D
r_2	+17.00mm	F_2	-6.00D
Axial thickness (t_1)	0.51mm		
Equivalent power		F_C	+43.82D
Crystalline Lens			
r_3	+13.08mm	F_3	+7.80D
r_4	-7.70mm	F_4	+13.25D
Axial thickness (t_2)	3.70mm		
Equivalent power		F_L	+20.78D

Conventional contact lens manufacturing techniques were used to make the cornea and lens. In this model, all the surfaces were of spherical form. To represent the fundus, a spherical surface of radius 11.5mm was used. It was attached to a micrometer head to enable the vitreous depth to be controlled, but was easily removable so that simulated fundus features or test objects could be mounted in contact with it (see figure 8.4).
The elements are housed in a box composed of panels made from a black Perspex sheet with a matt finish, the material also used for the corneal and lens mounts. The corneal mount forms the front end of the box, and the lens mount is removable. *Araldite* was used to glue the panels together, giving a water-tight seal.

The Mark II model

Tests with the Mark I model revealed that a number of modifications were needed. The most serious defect was that the process of mounting the corneal lens had distorted its surfaces and changed their central curvature. It was therefore decided to increase the axial thickness to 1.5mm so as to give the lens greater stability. Also, retinoscopy showed the refractive power of the model eye to increase significantly towards the periphery. To offset this effect the front surface of the new corneal lens was made with an arbitrary degree of asphericity. Provision was made for the insertion as required of any one of a range of pupillary diaphragms, and four holes were drilled in the crystalline lens mount to aid the water flow between the two chambers.

Measurement of optical dimensions

Optical dimensions of the Mark II eye were carefully checked by the following procedures.

Lenses

Radii of curvature were measured both before and after mounting by means of a Topcon DRA-1 radiuscope. Diameters were measured with a micrometer, taking care not to compress the lens. Centre thicknesses were measured with a Nissel thickness gauge MK2 (3" dial).

Axial separations

To solve the problem of obtaining reliable measurements of axial separations, the method illustrated in figure 8.5 was devised. X, Y, and Z are metric blocks of thicknesses x, y, and z respectively. Block X was chosen to give a snug fit between the corneal and lens mounts, and the fundus unit was moved inwards until blocks Y and Z were held tightly in

position. This arrangement avoided compression of the lens. The micrometer reading was then recorded, thus providing a known basis for subsequent calibration. In figure 8.5,

a = thickness of corneal lens mount

b = thickness of crystalline lens mount

c = axial distance to front vertex of corneal lens from front plane of its mount

d = axial distance to front vertex of lens from front plane of its mount

e = sagitta of spherical surface representing the fundus

It is then evident that

$$\text{anterior chamber depth} = a\text{-}c\text{-}t_1\text{+}x\text{+}d$$

where t_1 is the axial thickness of the corneal lens, and also that the micrometer reading in this setting refers to a vitreous depth of

$$(b+y+z+e) - (d+t_2)$$

where t_2 is the axial thickness of the model's crystalline lens. The vertex depths c and d were measured with a flat-ended depth micrometer fitted with a ratchet to prevent undue pressure. During this process the lens surfaces were protected by a paper tissue, the thickness of which was taken into account. The sagitta e was measured with a depth micrometer having a round-ended plunger.

Five separate readings were taken of each dimension. The mean results are shown in table 8.6. Conversions from radii to surface powers were based on mean refractive indices of 1.435 for the lens material and 1.333 for distilled water.

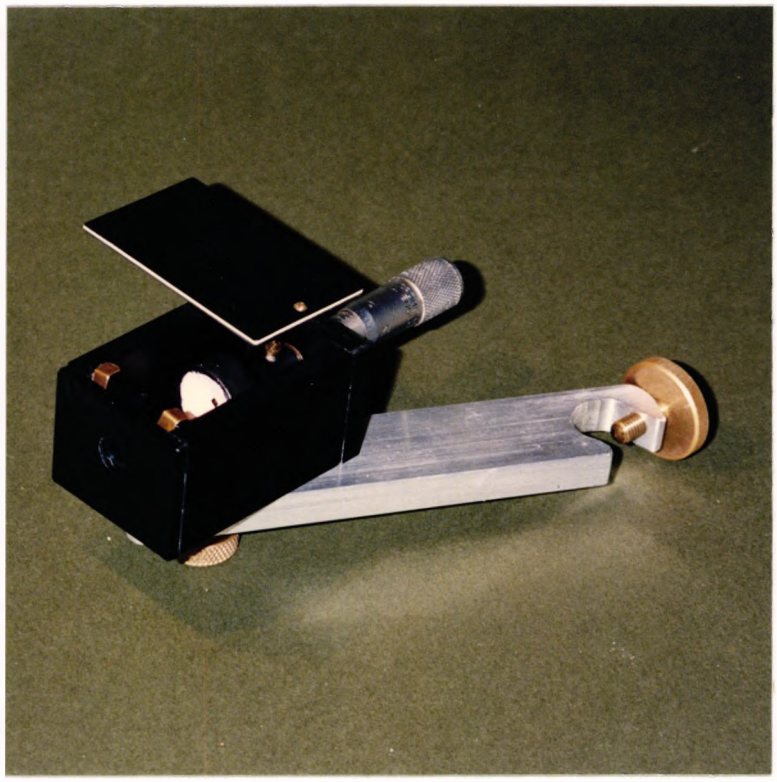

Figure 8.4. Photograph of the model eye with its support arm.

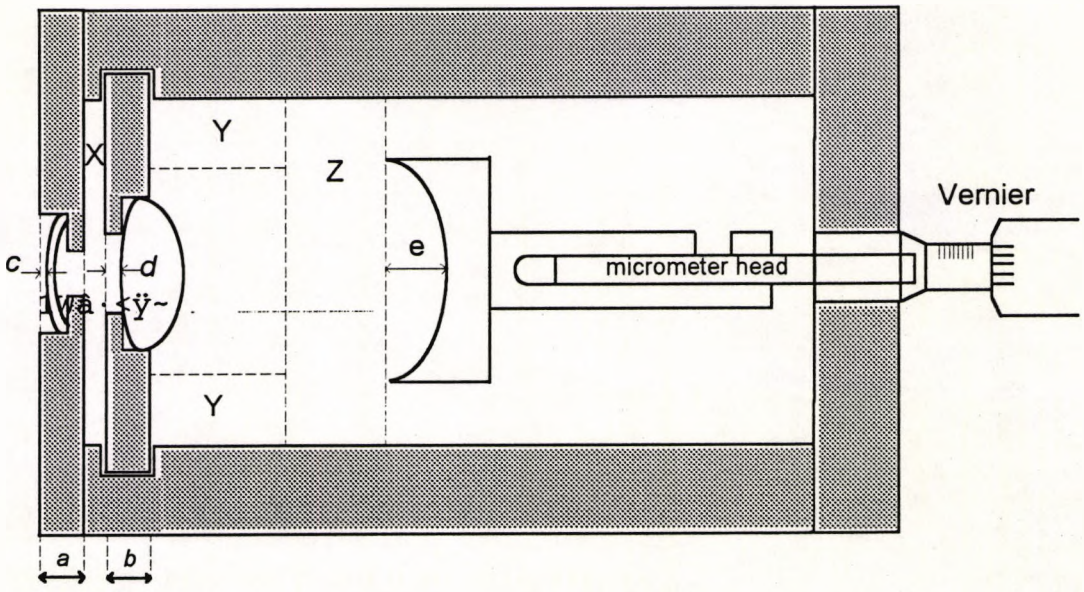

Figure 8.5. Cross section of the model eye showing metric blocks X, Y and Z used to measure the separations between the various components of the model.

Table 8.6. Measured dimensions and calculated optical constants of the Mark II model eye

Corneal lens		
Front radius	r_1	+ 8.765
Back radius	r_2	+16.85
Axial thickness	t_1	1.55
Diameter		8.30
Front surface power	F_1	+49.63
Back surface power	F_2	-6.05
Crystalline lens		
Front radius	r_3	+13.05
Back radius	r_4	-7.69
Axial thickness	t_2	3.72
Diameter		9.30
Front surface power	F_3	+7.82
Back surface power	F_4	+13.26
Other dimensions (see Figure 8.5)		
a = thickness of corneal lens mount		3.04
b = thickness of crystalline lens mount		3.05
c = vertex depth from front plane of corneal lens mount		0.66
d = vertex depth from front plane of crystalline lens mount		0.45
e = sagitta of fundus surface at effective aperture 15.07mm		2.81
x = thickness of spacer block X		2.30
y = thickness of spacer block Y		8.97
z = thickness of spacer block Z		8.99
Anterior chamber depth = $a-c-t_1+x+d$		3.58
Vitreous depth at reference vernier setting		
$= (b+y+z+e) - (d+t_2)$		19.65
Calculated values		
Equivalent power of cornea		+43.90
Equivalent power of lens		+20.81
Equivalent power of eye		+59.63
Axial length for emmetropia		24.45
Distances of principal points from corneal vertex		
First (A_1P)		1.79
Second (A_1P')		2.10

All linear distances in millimetres, powers in dioptres

8.3.3 Testing with an autorefractor

The Topcon Eye-Refractometer RM-A6500, which is based on the Scheiner disc principle, was used to assess the optical performance of the Mark II model eye. Readings of the spectacle refraction (at 12mm vertex distance) were taken by this instrument with the model eye adjusted for phakic ocular refraction from +11.00D to -14.00D. In this context, the term ocular refraction (K) is used in its strict sense to denote the reciprocal of the distance in metres from the eye's first principal point to its far point. For comparison, the Topcon readings were converted into ocular refraction defined as the reciprocal of the distance in metres from the eye's first principal point to its far point. A second set of readings was obtained at the same session to assess repeatability, and the same procedure was followed on a separate occasion to assess reproducibility.

The relationship between the means of the converted Topcon readings of ocular refraction (Kauto) and the corresponding values for which the model eye was adjusted (Kmod) is shown in figure 8.6. From this it will be seen that the difference between them can be considered constant over the whole range examined. Analysis of the complete set of results shows the 95% confidence intervals for both repeatability and reproducibility to have the same separate values of ±0.25D. The model eye setting minus the autorefractor value for ocular refraction emerges as 1.51 ±0.06D.

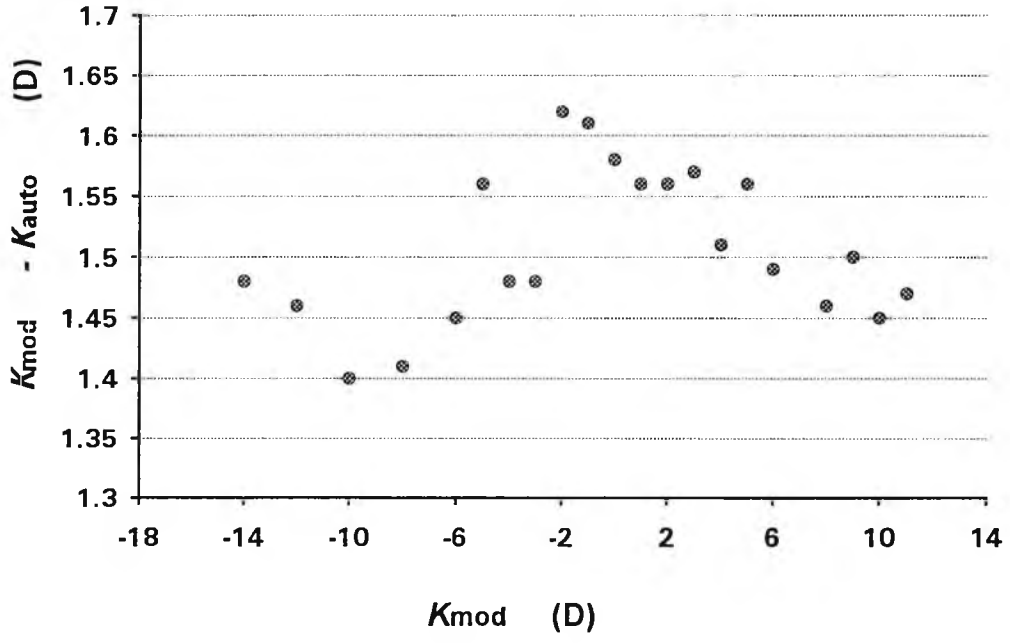

Figure 8.6. The model eye setting (Kmod) minus the autorefractor value for ocular refraction (Kauto), plotted against the former. The mean difference over the entire range is 1.51 ± 0.06D.

It seems unlikely that any single cause is responsible for the 1.5D discrepancy. An

accumulation of contributing factors is more probable. These are as follows, beginning with those pertaining to the model eye itself.

Spherical aberration

The sign of the discrepancy implies that the model eye is effectively more myopic, and therefore of greater positive power, than it is supposed to be. Uncorrected spherical aberration would operate in this direction.

Owing to the peripheral flattening of the anterior corneal and crystalline lens surfaces, the spherical aberration of the human eye rarely exceeds one dioptre. Conversely, the typical schematic or model eye with its spherical surfaces exhibits considerable aberration, about 0.4D at 1mm semi-aperture, 1.6D at 2mm and over 4D at 3mm. It was for this reason that in our Mark II model the front corneal surface was aspherised. Unfortunately, the exact equation to the aspherical profile is not known and we have no means at our disposal for determining it experimentally. Quite possibly, the spherical aberration is still under-corrected, even within the restricted area of about 4mm diameter in which autorefractors operate.

Zero setting error

The theoretical zero setting as recorded by the micrometer is the calculated second principal focus of the lens system. This setting represents emmetropia. If it is incorrect, the eye is actually ametropic. To check the zero setting experimentally a collimated beam from a point source was passed through the eye and recordings made of the vitreous chamber depth giving the sharpest fundus image. Five measurements gave a mean of 15.58mm (SD 0.07). This is close to the theoretical zero setting, which corresponds to a vitreous depth of 15.60mm. To demonstrate the effect of a zero setting error on the resulting ametropia, let us suppose that the vitreous depth assumed for emmetropia actually represents -0.50D of myopia. Because the ratio $\Delta k'/\Delta K'$ increases from myopia to hypermetropia, the resultant error is not a constant -0.50D but would vary from -0.29D to -0.68D between -14 and +10D.

Equivalent power of the eye

Another partial explanation for the apparent myopia of the model when in its zero setting is that its equivalent power is greater than the calculated value of +59.63D. This could arise from several causes including refractive index variations and dimensional errors in radii of curvature, lens thicknesses and axial separations. Practical difficulties thwarted attempts to determine F_e experimentally by various optical methods. However, the

method used to investigate the zero setting error yields a mean value for F_e of +59.69D (SD 0.16), which is within 0.06D of the calculated value. Assuming the zero setting to be correct but the equivalent power in excess, a change in k' produces a greater change in K' than predicted. Therefore K' is underestimated and the error increases outwards in both directions from zero at emmetropia. This is completely at variance with the pattern of the autorefractor results.

Combination of zero setting and equivalent power errors

Although neither error alone remains constant as ametropia changes, a particular combination of these errors could reduce the rate of change with varying ametropia. The resulting pattern of error would then be more in line with the relatively constant discrepancy found with the autorefractor.

Refractive indices of Boston RXD and distilled water

Corneal and crystalline lens radii were calculated for the manufacturer's stated value of 1.435 for the mean refractive index of Boston RXD. Contact lens buttons of this material were measured with an Abbe refractometer, the refractive index was found to confirm the manufacturer's figure. Nevertheless, a variation of as little as 0.001 would change the equivalent power of the eye by approximately 0.25D. Similarly, although the assumed value of 1.333 for the refractive index of the distilled water used in the model eye was confirmed by the Abbe refractometer, this is subject to error. Furthermore, both refractive indices are temperature dependent and it is possible that differences between assumed and actual refractive indices could contribute to the +1.50D discrepancy.

Chromatic aberration

The constringence or Abbe number of the Boston RXD material is not known but is likely to exceed that of the ocular media. As a result, the model eye would exhibit greater longitudinal chromatic aberration than the human eye, perhaps making a small contribution to the total discrepancy. In addition to the above there are contributory factors pertaining to the autorefractor.

Correction factors incorporated in infrared autorefractors

Infrared autorefractors use radiation having a wavelength in the region of 850nm. By comparison with this, radiation within the visible spectrum is reflected from a different retinal layer. Also, the refractive power of the eye is lower with infrared than with visible radiation. Infrared autorefractors therefore incorporate built-in correction factors for

these differences. It would be surprising if these correction factors were appropriate to the model eye.

Autorefractor error

All measurements of refractive error were taken with the autorefractor set to measure to 0.12D. Consequently, rounding errors may have occurred. It is not unreasonable to suppose that autorefractors, in common with all similar instruments, have margins of error which may not be the same in all ranges of ametropia. Published studies have indicated that some instruments tend to overestimate high myopia. It would be of interest to know how manufacturers themselves check the calibration. For example, do they rely on human subjects whose refraction has been assessed by other means? Autorefractors should not be regarded as providing a basic standard for comparison, though it is not suggested that errors from this source could be other than minor.

8.3.4 Experimental use of the Mark II model

Littmann's equation explained in section 8.2.2.1 can be put in the more generalised form which does not restrict it to one specific instrument. For this purpose the factor 1.37 can be replaced by the symbol p denoting the corresponding factor for **any** fundus camera of telecentric construction.

$$t = pqs$$

it follows that $p = t/qs$ (16)

Littmann (1982) defines as $q = t/U°$

from equation (7) and figures 8.1 and 8.2 it follows

$$q = t/nU' \quad (17)$$

where n is the refractive index of the final medium

and $U' = t/k'$ radians

$U' = 57.296\ t/k'$ degrees

substituting into equation (17)

$$q = t/(n57.296\ t/k')$$

$$q = (k'/n)/57.296$$

$$q = 0.01745/K'$$

substituting for q into (16)

$$p = t/(0.01745K's)$$

the dimensions t, s and k' are usually measured in mm thus

$$p = (t/s)(57.296K'/1000) \qquad (18)$$
$$p = (t/s)(K'/17.453)$$

The numerical relationship between p and K' or k' can be determined experimentally for any given fundus camera by the following method, using a model eye.

- the fundus test object was a square of measured side length (t) 1.512 +/-0.013mm as determined with a travelling microscope. The same fundus object of size t is used throughout.
- photographs were taken with the vitreous depth of the model eye set at values corresponding to a range of ocular refractions (K) from +11.00D to -17.00D. The term ocular refraction is used here in its strict (Gaussian) sense to denote the reciprocal of the distance in metres from the eye's first principal point to its far point
- the image size s on the camera film was then measured. To improve the accuracy of measurement of the corresponding image size (s), the camera film was projected under a fixed magnification of 17.5x and measured with a calibrated graticule.

If p is found to remain constant for all values of k', it can be concluded that the fundus camera is indeed of telecentric construction. The following numerical example illustrates the calculating procedure, given that the mean image size s was found to be 4.117mm when the vitreous depth of the model eye had been set for K = +5.00D.

From the basic expression $K' = K + F_e$,

K' = +5.00 + 59.63 = 64.63D

t/s = 1.512/4.117 = 0.3673'

p = 64.63 x 0.3673/17.453 = 1.360

8.3.5 Results

The p value for the Carl Zeiss Jena Retinophot camera (figure 8.7) increases as the ocular refraction is varied from -17.00D to +11.00D, demonstrating that this camera is not telecentric. The equation of the regression line in figure 8.7 is

$$p = 0.006K + 1.149$$

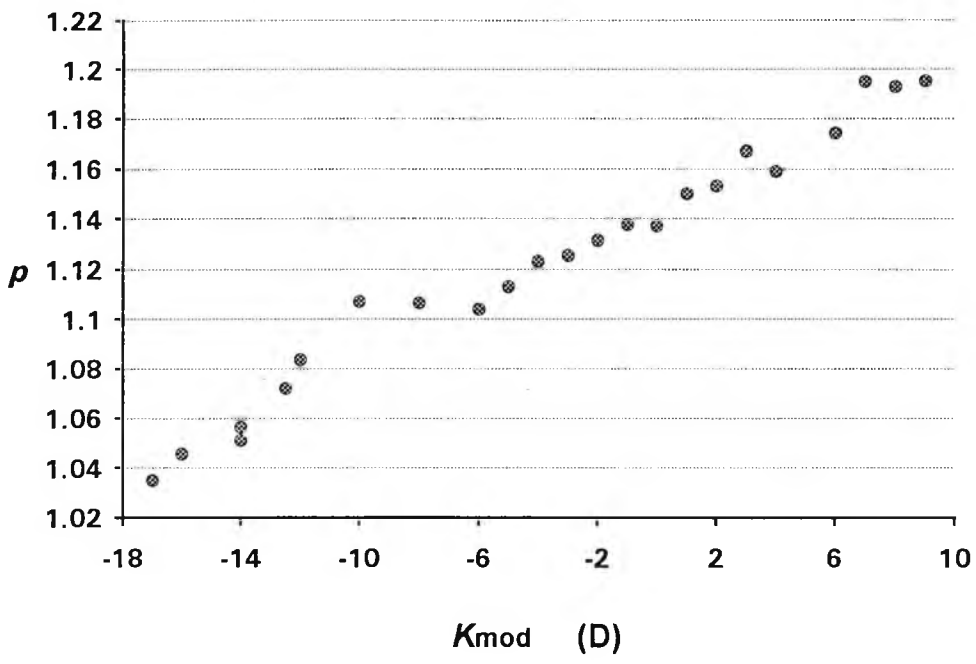

Figure 8.7. The calculated value of p for a Zeiss (Jena) fundus camera plotted against the model eye setting (Kmod).

Photographs were taken with a Zeiss Oberkochen fundus camera using two of the four interchangeable lenses or lens systems incorporated into the design of the camera to enable focusing over a wide range of ametropia. Two different values for p, 1.272 (SD 0.015) and 1.356 (SD 0.010), were obtained (figure 8.8). As the variations in p remain very slight over the entire range of ametropia studied, the telecentric design of the camera is confirmed.

Errors associated with the measurement of the image size s were assessed. For each photograph the side length of the square target was measured. This process was repeated on another occasion giving two separate values of s for each photograph. Differences between the two values were expressed as a percentage of their mean. Percentages were used because the image size on the film varies considerably with ocular refraction. From the mean and standard deviation of these percentage differences a confidence interval can be constructed. For the Carl Zeiss Jena camera the 95% confidence interval is +1.57/-1.87% and for the Zeiss Oberkochen fundus camera +1.64/-1.21%.

If a given fundus feature is photographed using the same camera but at a different session, variability of the image size on the film may occur. Photographs were taken over a range of ocular refractions from +11D to -17D. This procedure was repeated for the same camera at a separate session and the differences calculated as above. For the Carl

Zeiss Jena camera the 95% confidence interval is +2.92/-3.00% and for the Zeiss Oberkochen fundus camera +2.22/-2.19%.

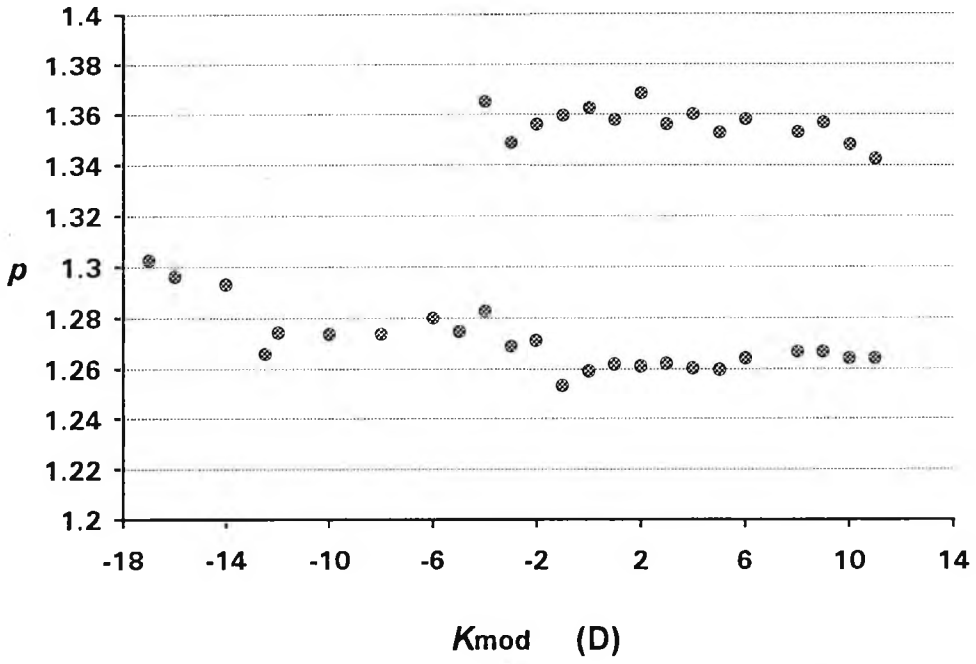

Figure 8.8. The calculated value of p for a Zeiss (Oberkochen) fundus camera plotted against the model eye setting (Kmod). The two separate sets of results relate to the use of different camera lens systems described in the text.

8.3.6 Discussion

The results indicate that accurately adjustable model eyes such as the Mark II design have an important role to play in the field of ocular dioptrics. Using the model eye the magnification properties of fundus cameras can be investigated. This information is essential prior to any study attempting to determine the size of fundus features, for example optic disc or neuroretinal rim areas. The incorporation of alternative lenses into the optical systems of fundus cameras to extend their focusing range may alter the value of p, as illustrated by the Zeiss Oberkochen camera.

It is evident that the telecentric principle does not apply to all fundus cameras. However, the relationship between p and ametropia may be linear, as for the Carl Zeiss Jena camera. For such cameras the value of p can be predicted from the equation of the regression line as shown above. This value can then be substituted into the appropriate

equations to find the true size of a fundus feature.

Axial ametropia can be easily varied on the Mark II model eye. Refractive ametropia has not been incorporated into the design of this model, apart from the special case when the lens is removed to render the eye aphakic.

8.4 INVESTIGATION OF THE AREA OF THE OPTIC NERVE HEAD, OPTIC CUP, NEURORETINAL RIM AND PERIPAPILLARY CRESCENTS IN MYOPIA

8.4.1 Introduction

In clinical research, features of the optic nerve head of quantitative interest are optic disc area, neuroretinal rim area, cup area and cup volume. Optic disc area is described as the entire retinal aspect of the optic nerve as delineated by the inner aspect of the scleral ring of Elschnig (Teal *et al* 1972; Britton *et al* 1987a; Jonas *et al* 1988b), which appears as a pale zone around the optic disc. This paler area can circumscribe the disc, in which case it is called a halo, or exist in part, and the dividing line between the edge of the optic disc and this pale zone may be pigmented (Hitchings *et al* 1983). The cup margin, and hence its area, is defined by a change in the slope along the inner edge of the neuroretinal rim, and not by a pallor change. Therefore, the neuroretinal rim area (NRA) is outlined by the margins of the optic disc and optic cup. This topographic definition of the intrapapillary disc structures has been widely used and is generally accepted (Betz *et al* 1982; Airaksinen *et al* 1985a and b; Drance *et al* 1986; Britton *et al* 1987a), and has been adopted for this study. One of the major problems in outlining these structures is the indistinct borders between them, which can be obscured by blood vessels. Even superimposing a grid onto fundus photographs is of little value (Hitchings *et al* 1983). Great intersubject variations in the optic disc parameters have been reported (Teal *et al* 1972; Bengtsson 1976; Jonas *et al* 1988a and b).

8.4.1.1 Optic disc

Disc area has been found to vary considerably between subjects, for example Bengtsson (1976) quoted a four fold variation and Jonas *et al* (1988a and b) a range from 0.68 to 5.39mm^2 (approximately x8 variation). Interestingly, Pach *et al* (1989) using the Zeiss Oberkochen fundus camera did not find any significant differences in optic disc diameter, measured directly from the slide, in adults with a range of refractive errors (-13.25 to +13.36D). They concluded that no correction factor was required for refractive ametropia when measuring optic disc size from fundus photographs, and that linear magnification of 2% in horizontal disc diameter occurred for every dioptre of axial myopia above 3D. It has already been shown in this chapter that the influence of the fundus camera and human eye must be taken into consideration for image size evaluations.

Jonas *et al* (1988a), measured the size of the scleral canal of the optic nerve in a sample of enucleated eyes and the optic disc size (area and diameters) in a group of eyes measured intravitally using Littmann's method, and the two measurements did not differ

significantly. They concluded that the form of the optic nerve head is governed by the scleral canal of the optic nerve.

According to Britton *et al* (1987a), Caprioli and Miller (1987) and Jonas *et al* (1988e) there is no significant difference in disc area between the sexes, but Quigley *et al* (1990) and Mansour (1991) found females to have significantly smaller horizontal disc diameters and disc areas (Mansour 1991) than males. Optic disc diameter does not appear to change with age (Drance and Balazsi 1984; Jonas *et al* 1988e; Quigley and Brown 1989; Quigley *et al* 1990; Mansour 1991), nor does disc area with age (Britton *et al* 1987a; Jonas *et al* 1988e). However, Heijl and Molder (1993) stated a trend for disc diameter to increase with age.

A strong correlation has been found between disc area and NRA (Britton *et al* 1987a; Caprioli and Miller 1987; Bottoni *et al* 1989; Quigley *et al* 1991), however no correlation was found between linear neuroretinal rim width and linear disc diameter (Britton *et al* 1987a; Bengtsson 1976). Some studies have found no correlation between disc area and axial length, nor between disc area and spherical equivalent refraction, (Britton *et al* 1987a; Jonas *et al* 1988b; Mansour 1991; Heijl and Molder 1993). Others have reported weak correlations between disc area and axial length ($r = +0.59$, Bottoni *et al* 1989; $r = +0.53$, Kim *et al* 1990), and vertical disc diameter and axial length ($r = +0.47$, Jaeger *et al* 1987). Jaeger *et al* (1983) observed hyperopic eyes generally to have smaller optic discs than myopic eyes. According to Jonas *et al* (1988d) the area of the optic disc increases by about $0.77mm^2$ for every dioptre increase in myopia ($r = -0.53$). In their group of subjects with refractive errors from -8.00D to -28.8D (mean -15.49 ± 5.76D) the mean disc area was $6.87mm^2$, which is far greater than that usually reported in normal subjects (see table 8.7). Also the interindividual variation increased with increasing myopia and the optic nerve head form became more oval.

Vertical disc diameters (Quigley and Brown 1989), and disc area (Chi *et al* 1988; Varma *et al* 1993), have been found to be larger in Blacks than Whites. In addition, Blacks have more oval optic discs than Whites (Quigley *et al* 1991). Mansour (1991) found the horizontal disc diameter and disc area to be smaller in Whites and Hispanics than in Blacks, Orientals and non-American Indians.

8.4.1.2 Optic cup

Cup-disc area ratio has been shown to be related to axial length and to intraocular pressure by Tomlinson and Phillips (1969). They felt the higher cup-disc area ratio observed in longer eyes to be a reflection of an association between optic disc area and axial length with a constant volume of nerve fibres. However, Jonas *et al* (1988b) did not

find cup area to be related to the axial length or refraction. Cup area has been shown to be heavily dependent upon disc area/size, larger normal discs have larger cups and also higher cup/disc ratios (Teal *et al* 1972; Bengtsson 1976; Caprioli and Miller 1987; Britton *et al* 1987a; Bottoni *et al* 1989; Heijl and Molder 1993). Cups which are larger in size tend to be deeper, while smaller cups tend to be shallower (Johnson *et al* 1979). Jonas *et al* (1988e) reported larger optic cups in discs with steep punched-out cups, as compared to discs whose cups have flat slopes temporally, but this may be an artefact from the process of identifying the borders of the optic cup. No correlation was found between the optic cup size and NRA (Teal *et al* 1972; Britton *et al* 1987a). This supports the contention that an apparently large cup does not necessarily represent any loss of viable nerve tissue. Cup/disc ratio has been shown to be statistically significantly larger in Black than in White normal individuals (Beck *et al* 1985a; Chi *et al* 1988; Katz *et al* 1990). Blacks have been shown to have larger cup areas than Whites (Varma *et al* 1993).

8.4.1.3 Neuroretinal rim

The neuroretinal rim area (NRA) is a representation within the disc margins of the retinal nerve fibres. Neuroretinal rim width in normals has been shown to be broadest at the inferior pole of the optic disc, followed by the superior and nasal pole, and narrowest temporally (Jonas *et al* 1988c and f). NRA increases significantly with increasing optic disc area (Britton *et al* 1987a; Caprioli and Miller 1987; Mikelberg *et al* 1986b; Jonas *et al* 1988e and f) and it is independent of sex, age, refraction (Britton *et al* 1987a; Jonas *et al* 1988e; Paczka *et al* 1992) and axial length (Jonas *et al* 1988b). High interindividual variations have been shown for the NRA, which are independent of age, sex, and refractive error (Britton *et al* 1987a; Caprioli and Miller 1987; Jonas *et al* 1988e). No correlation between rim area and cup area was found by Teal *et al* (1972) and Britton *et al* (1987a). As mentioned above larger discs tend to have larger cups which can complicate the diagnosis of optic cup enlargement in glaucoma. Bottoni *et al* (1989) recommended expressing the NRA as a percentage of the total disc area to try and alleviate this problem.

The positive relationship between disc area and NRA prompted the question of whether larger optic discs contain more nerve fibres, or more non-neuronal tissue. Caprioli and Miller (1987) have suggested that larger discs may contain more supporting tissue or a greater volume of non-neural elements within the region of the neuroretinal rim, and concluded that the rim area can not be assumed to reflect the number of retinal ganglion cells as believed by others (Radius and Pederson 1984; Airaksinen *et al* 1985 a and b). According to Jonas *et al* (1992b) nerve fibre count is positively correlated with increasing size of the inner aperture of the optic nerve scleral canal ($r = 0.82$), and

concluded that larger discs contain more nerve fibres. This is contrary to Mikelberg *et al* (1991) who found NRA to be unrelated to scleral canal area. In the former study larger optic discs showed greater nerve fibre spacing. Quigley *et al* (1990) in a sample of donor eyes demonstrated larger optic discs to contain more optic nerve fibres, however, this has not been shown by others (Mikelberg *et al* 1991; Balazsi *et al* 1984a; Jonas *et al* 1990a). Radius and Pederson (1984) found a strong relationship between the amount of rim tissue and the number of axons present in the optic nerves of primate eyes with experimentally induced glaucoma, as did Mikelberg *et al* (1991) in 16 donor human eyes. As pointed out by Mikelberg *et al* (1991), since total axon count is usually calculated as the product of neural area and axon density, a strong correlation between NRA and axon count is inevitable. The number of nerve fibres was found to increase linearly with disc area in monkeys (Quigley *et al* 1991). Normal human eyes exhibit a substantial variation in the number of nerve fibres (Balazsi *et al* 1984a; Quigley *et al* 1982; Repka and Quigley 1989) which may be partially responsible for the conflicting results between studies, especially if sample sizes are small.

Table 8.7. Published values for optic nerve head measurements in normal subjects. Mean values ± SD and range are given if available.

Investigators	No of subjects	Mean age or range (years)	Fundus camera system	Magnification equation	Mean disc area±SD (mm^2)	Mean NRA ±SD (mm^2)	Mean cup area± SD (mm^2)	Vertical disc diameter (mm)	Horizontal disc diameter (mm)
Teal *et al* 1972	64	not stated	Zeiss	None	4.37 ± 0.7	3.7 ± 0.5	0.67 ± 0.4		
Balazsi *et al* 1984b	12	52.0 ± 20.9	Zeiss (Stereo)	Littmann		1.75 ± 0.40 0.92-2.38			
Airaksinen *et al* 1985a	33	58.9 ± 13.0	stereophotos	Littmann		1.40 ± 0.19			
Britton *et al* 1987a	113	51.1 ± 16.8	stereophotos	Littmann	2.10 ± 0.5	1.65 ± 0.3		1.57	1.66
Caprioli & Miller 1987	38	36 ± 12	Rodenstock Analyzer	Littmann	1.70 ± 0.37	1.13 ± 0.37	0.57 ± 0.31		
Jonas *et al* 1988a	107	20-80	enucleated eyes		2.59 ± 0.72 0.68-4.42			1.76	1.92
Jonas *et al* 1988b	60	3-80	Zeiss stereophotos	Littmann	2.89 ± 0.76 0.86-5.39	2.26 ± 0.58 0.86-3.84	0.63 ± 0.64 0-3.1	1.97 ± 0.29 1.08-2.76	1.79 ± 0.27 0.91-2.42
Jonas *et al* 1988c	253	45.2 ± 22.5 3-80	Zeiss	Littmann	2.64 ± 0.80	2.01 ± 0.51	0.65 ± 0.72	1.90 ± 0.27	1.75 ± 0.31
Jonas *et al* 1988d	33	63.0 ± 12.1 27-87	Zeiss stereophotos	Littmann	6.87 ± 3.99 1.98-19.54			3.28 ± 1.00	2.90 ± 0.67
Jonas *et al* 1988e	319	42.7 ± 19.6	Zeiss stereophotos	Littmann	2.69 ± 0.70 0.8-5.54	1.97± 0.50 0.8-4.66	0.72 ± 0.70 0-3.41	1.92 ± 0.29 0.916-2.91	1.76 ± 0.31 0.91-2.61

Table 8.7 continued

Jonas *et al* 1988f		40.9 ± 23.4 3-80	Zeiss	Littmann		2.09 ± 0.60 0.8-3.80			
Bottoni *et al* 1989	30	43 ± 14 17-69	Topcon TRC stereophotos	Littmann	2.20 ± 0.58	1.83 ± 0.37	0.36 ± 0.29		
Quigley & Brown 1989	55	66 25-100		intravital				1.9 ± 0.2 1.5-2.3	
Miglior *et al* 1989	198	not stated	Topcon TRC stereophotos	Littmann	2.20 ± 0.58	1.83 ± 0.29	0.36 ± 0.29		
Pach *et al* 1989	40	not stated	Zeiss FF-3	none					4.28 ± 0.43
Quigley *et al* 1990	60	66.5 ± 13.9	enucleated eyes					1.88	1.77
Mansour 1990	68		Zeiss	Littmann 1					1.88 ± 0.21
				Littmann 2					1.81 ± 0.21
				BK					1.86 ± 0.20
Mansour 1991	125	21-54	Zeiss	Littmann	1.50-4.76				
von der Lippe *et al* 1992	32	not given	Zeiss	Littmann	2.52 ± 0.63	1.64 ± 0.30	0.89 ± 0.50		
Varma *et al* 1993	3234	at least 40	Topcon stereophotos	Littmann	2.86 ± 0.60	1.98 ± 0.46			
Heijl & Molder 1993	89	20-79	Zeiss	BK				1.59 ± 0.15	

Littmann 1 and 2 refer to the two methods suggested by Littmann (section 8.2.2) and BK refers to the Bengtsson-Krakau formula (Bengtsson and Krakau 1977).

8.4.2 Materials and methods

The subject population has already been described in the previous chapter. From the biometric measurements performed on each subject a personalised schematic eye was constructed for each individual as explained in section 8.2.2.3 and Appendix A2.1. This allowed calculation of the constant q for the human eye, and U_1 was taken as 15°, which approximates to the angle of eccentricity of the optic nerve head. In section 8.3.4 the magnification of the Carl Zeiss Jena fundus camera (p) was determined. This camera was used to photograph the subject's posterior pole using Kodak Ektachrome colour slide film. The optic nerve head and peripapillary crescents were centred within the camera field. Significant magnification may result from decentration of the object in the Zeiss fundus camera (Behrendt and Doyle 1965; Pach *et al* 1989).

From equation (1A) the true area of a retinal feature, t^2, can be determined

$$t^2 = (1{\cdot}37q)^2 s^2 \qquad (1A)$$

where s^2, represents the area of retinal feature of interest measured directly from the photographic slide. The diagram below illustrates the computer set-up used to measure the features of interest directly from the slide.

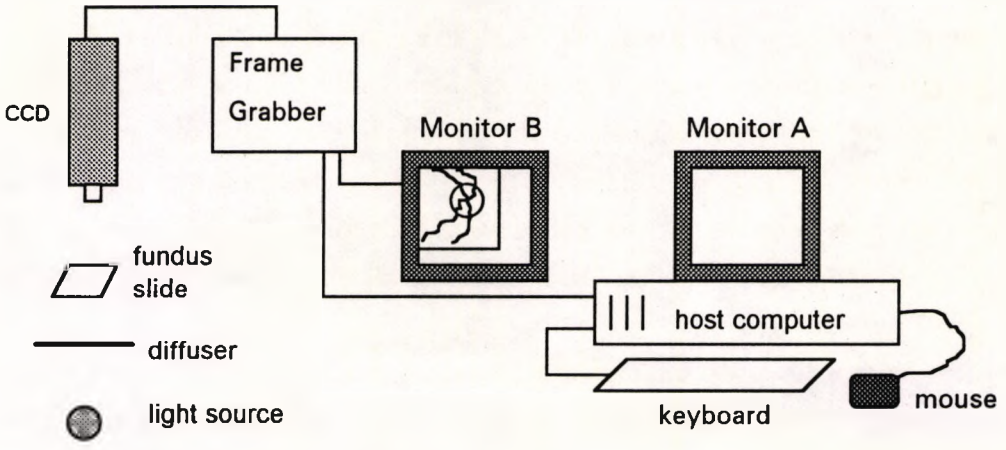

Figure 8.9. Instrumentation provided by the Institute of Ophthalmology courtesy of Dr F. Fitzke, and the Optics Laboratory of City University courtesy of Professor J. Barbur, used to digitise and measure the photographic slide. CCD= charge coupled device.

After developing the photographs from the Carl Zeiss Jena camera, the film was cut and the diapositives placed in glass mounts to ensure the film was kept perfectly flat. The slide was illuminated from below with a diffuse light source, and a charged coupled device, which is a black and white closed circuit video camera, was used to view the slide. Both the magnification, aperture and focus of the CCD camera need to be adjusted to obtain optimal image viewing conditions. The magnification was maximised so that the optic disc and peripapillary crescents fill the field of view. A video signal from this CCD camera was fed into a frame grabber. The frame grabber contains a video-digitising board which is controlled by an IBM PC/AT compatible computer which converts the video signal into an array of numbers which the computer can subsequently process.

This array of numbers divides the image up into 256 rows by 256 columns. Each point (pixel) in this array contains a number that represent the brightness of the image at that point. Values range from 0 representing black up to 255 for white. To maximise the contrast of the computer image the aperture of the CCD camera was adjusted so that the brightest points in an image were at the maximum brightness level of 255. Image processing is undertaken by the host computer and a black and white image is produced on monitor B. Digitised images can be stored on the computer hard drive or floppy discs and measured at any time. A mouse was used to click around the borders of retinal features to be measured. To complement this system a slide projector with a front screen was used to simultaneously view the same slide as that displayed on monitor B. In some cases the black and white image provided better distinction between tissue boundaries, whilst in others the colour offered by direct slide projection aided identification of tissue borders.

Once the magnification and focus of the CCD camera has been set for the object plane, a slide containing a grid with a 5mm spacing was captured and stored. Before any fundus slides were measured, this calibration slide was measured by the host computer. The real area of this grid is known and so calibrates the image processing system. For subsequent fundus slides the settings of the CCD camera were not altered. Monitor A displays the program menu and any calculations performed.

Optic disc, optic cup, and neuroretinal rim margins were delineated as described in section 8.4.1, and their areas calculated. Myopic peripapillary crescents were also outlined if present, and their areas calculated.

Statistical analysis

Subjects were divided into four groups as in Chapter 7 according to their ocular refraction and relative size of a myopic crescent if present

group 1-hypermetropes, emmetropes, and myopes with less than 1D of myopia without peripapillary crescents
group 2-myopes with more than 1D of myopia without peripapillary crescents
group 3-myopic eyes with relatively smaller peripapillary crescents
group 4-myopic eyes with relatively larger peripapillary crescents

For each group the mean values were calculated for optic disc area, optic cup area and NRA, and these shall be called collectively optic disc parameters. A one way ANOVA together with the least significant difference multiple comparison procedure was used to identify any significant differences between groups' mean optic disc parameters.

The dependence of the optic disc parameters on axial length and ocular refraction was investigated.

The racial characteristics will be given for each group, but racial comparisons shall not be made as numbers in the race categories are uneven, and in some cases very small.

Mean area of any peripapillary crescent was also calculated and a sample mean determined. The area of the peripapillary crescent in relation to the optic disc area, axial length and ocular refraction was investigated.

8.4.3 Results

8.4.3.1 Optic disc parameters

Means ±SD and ranges for the optic disc parameters in the four groups are given in table 8.8. A one way ANOVA yielded the following,

- groups 1, 2 and 3 did not differ from each other for any optic disc parameter ($p>0.05$)
- group 4 differed from groups 1 and 2 for disc area and NRA ($p<0.01$), and from group 3 for disc area ($p<0.05$)
- cup area did not differ significantly between the groups

The racial composition of each group is as follows

group 1 - 20 Caucasian, 10 Indian
group 2 - 22 Caucasian, 7 Indian, 1 Chinese
group 3 - 16 Caucasian, 10 Indian, 1 Hispanic, 3 Black
group 4 - 18 Caucasian, 5 Indian, 1 Chinese, 7 Black

A graphical example is given for optic disc area plotted against axial length (figure 8.10). It appears that the rate of increase of disc area with axial length is increasing as the axial length increases beyond approximately 26-28mm. The same applies to the NRA plotted against axial length, but not for cup area (figure 8.11). Visually similar plots were obtained when optic disc parameters were plotted against ocular refraction. A correlation analysis followed by linear regression analysis using a least squares method of the optic disc parameters against axial length and ocular refraction for each group gave the following results,

- groups 1 and 2 did not show any significant linear correlation between any of the optic disc parameters with either axial length or ocular refraction.
- groups 3 and 4 showed a significant linear correlation between disc area and both axial length and ocular refraction and between NRA and axial length and ocular refraction. In all cases $p<<0.01$. Both disc area and NRA increase with increasing axial length and with increasing myopia. In group 3 the R^2 values are very low and these results should be interpreted cautiously (see table 8.9).

However, the goodness of fit of the linear regression model was questionable in most cases because the residual plots did not show any even scatter of points at all x values.

A log transformation was performed on the optic disc parameters and the relationship with axial length and ocular refraction re-assessed.

The log of optic disc area plotted against axial length (figure 8.12) yielded a remarkably linear graph. Log transformation of NRA produced a similar picture when plotted against axial length (figure 8.14). Graphs of log(optic disc area) and log(NRA) plotted against ocular refraction are shown in figures 8.13 and 8.15. For log(cup area) there was no visible evidence of a linear relationship with either axial length nor ocular refraction.

Table 8.8. Mean ± SD and range in parenthesis are given for the optic disc parameters in the four groups

Group	Optic disc area (mm^2)	Cup area (mm^2)	NRA (mm^2)
1	2.00 ± 0.41 (1.36-2.88)	0.29 ± 0.37 (0.00-1.17)	1.71 ± 0.38 (0.99-2.56)
2	1.93 ± 0.38 (1.30-2.79)	0.28 ± 0.28 (0.00-1.12)	1.65 ± 0.29 (1.08-2.18)
3	2.36 ± 0.77 (1.50-5.04)	0.36 ±0.45 (0.00-1.56)	2.01 ± 0.62 (1.16-3.75)
4	3.01 ±1.75 (1.21-9.22)	0.29 ± 0.41 (0.00-1.46)	2.73 ± 1.86 (0.84-9.22)

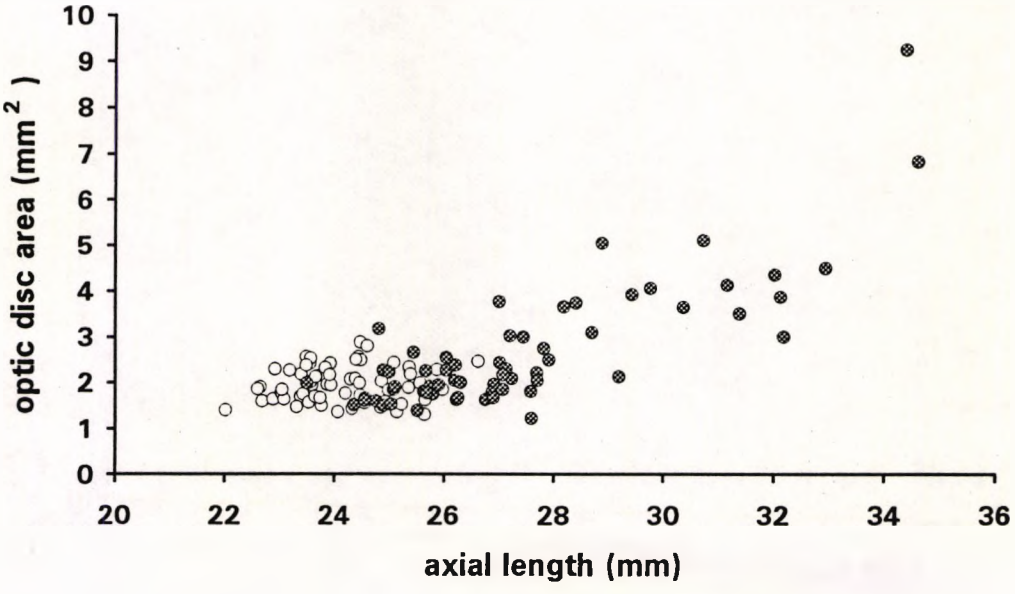

Figure 8.10. Disc area plotted against axial length for the entire sample. Open circles are subjects without peripapillary crescents, and grey circles are subjects with peripapillary crescents.

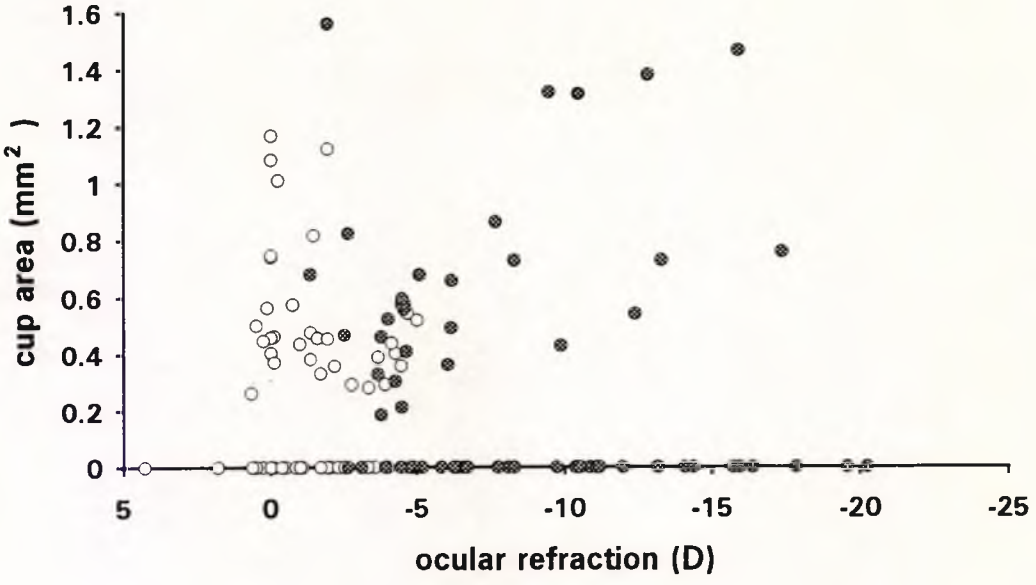

Figure 8.11. Cup area plotted against ocular refraction for the entire sample. Open circles are subjects without peripapillary crescents, and grey circles are subjects with peripapillary crescents.

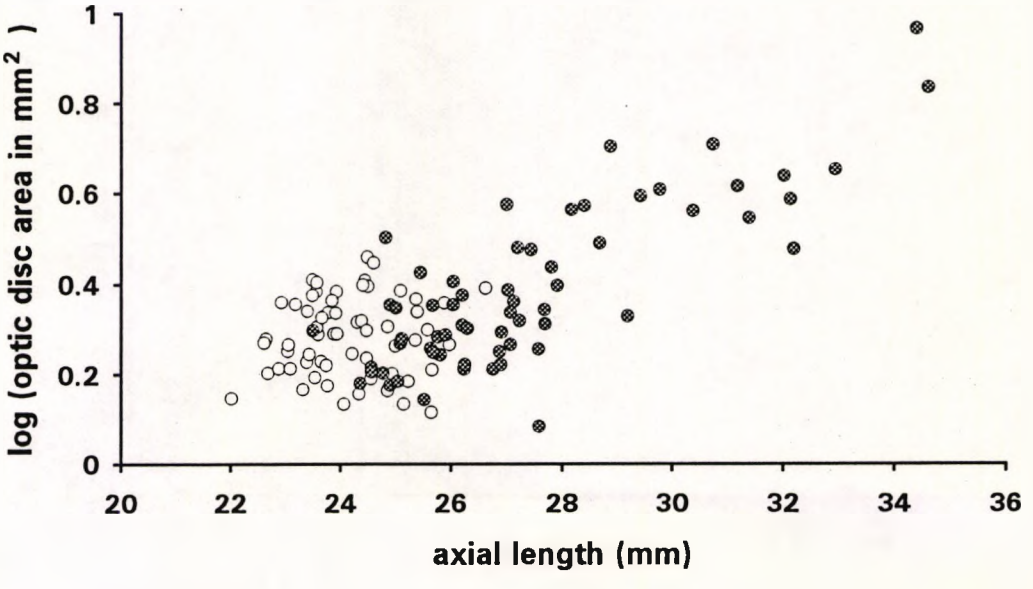

Figure 8.12. Log of optic disc area plotted against axial length for the entire sample. Open circles are subjects without peripapillary crescents, and grey circles are subjects with peripapillary crescents.

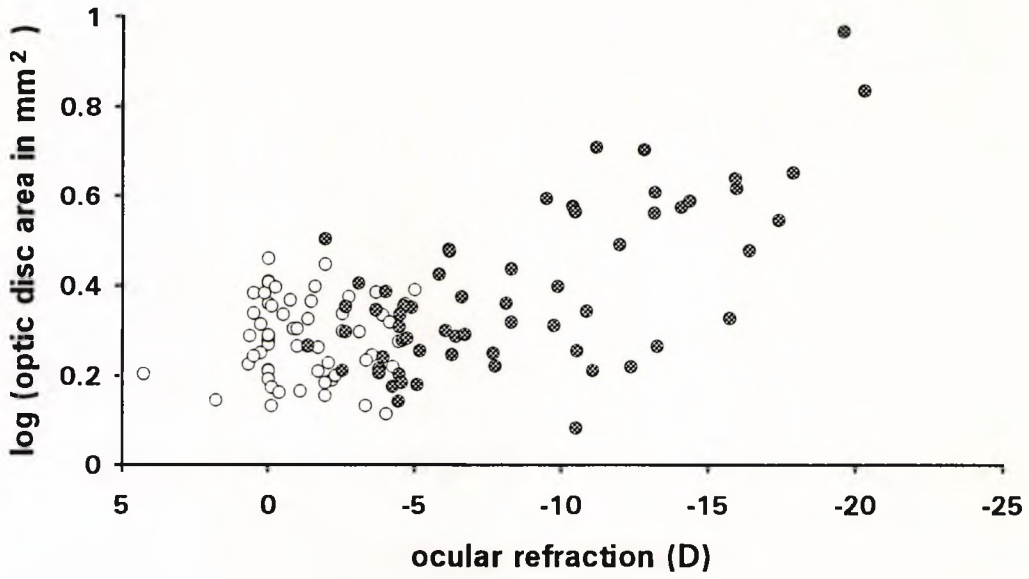

Figure 8.13. Log optic disc area plotted against ocular refraction for the entire sample. Open circles are subjects without peripapillary crescents, and grey circles are subjects with peripapillary crescents.

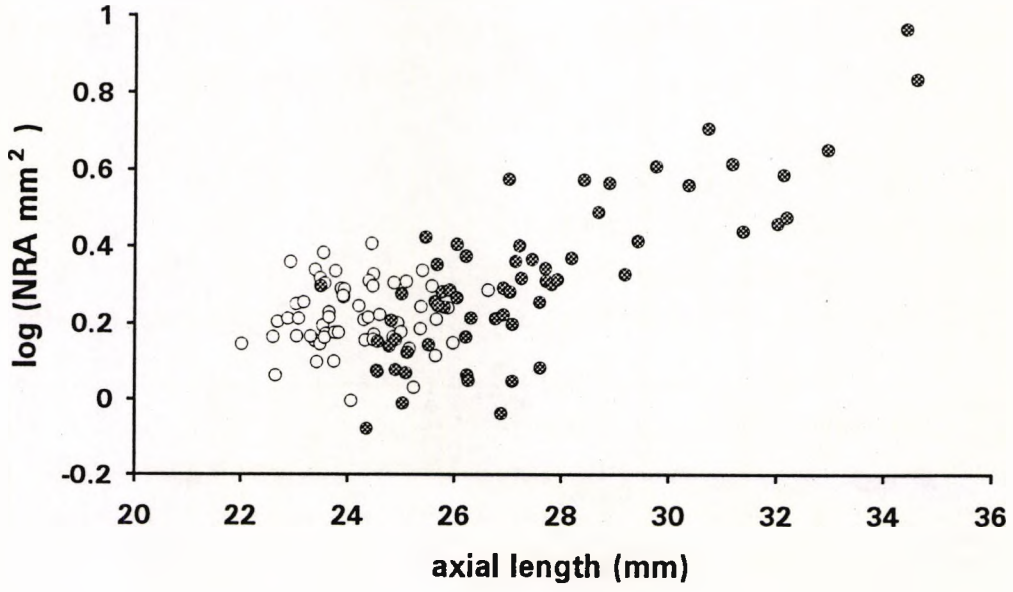

Figure 8.14. Log NRA plotted against axial length for the entire sample. Open circles are subjects without peripapillary crescents, and grey circles are subjects with peripapillary crescents.

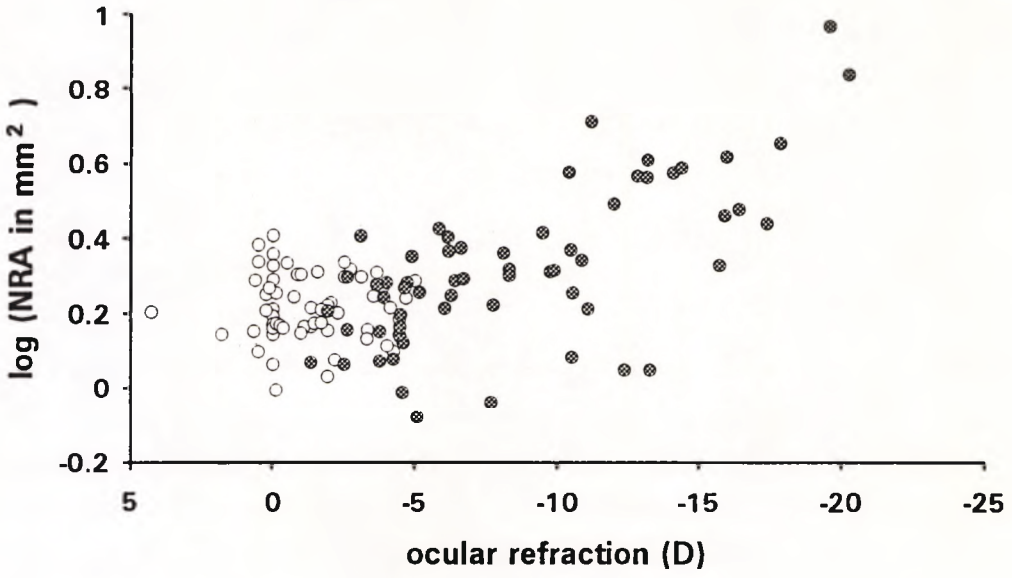

Figure 8.15. Log NRA plotted against ocular refraction for the entire sample. Open circles are subjects without peripapillary crescents, and grey circles are subjects with peripapillary crescents.

A linear regression analysis by the least squares method of log(optic disc area) and log(NRA) against axial length and ocular refraction for the entire sample is given in table 8. 9, in all cases $p << 0.01$. For cup area no significant linear relationship was found with either axial length or ocular refraction ($p>>0.05$).

Table 8.9. Summary of the results of correlation and linear regression analysis for optic disc area and NRA in mm² for groups 3 and 4, and log(optic disc area) and log(NRA) for the entire sample, against axial length and ocular refraction. In all cases $p << 0.01$.

	axial length		**ocular refraction**	
optic disc parameter	**R^2**	**gradient**	**R^2**	**gradient**
group 3 disc area mm²	0.36	0.34	0.26	-0.13
group 3 NRA mm²	0.38	0.28	0.45	-0.14
group 4 disc area mm²	0.70	0.49	0.51	-0.24
group 4 NRA mm²	0.69	0.52	0.50	-0.26
log (optic disc area mm²)	0.64	+0.06	0.44	-0.02
log (NRA mm²)	0.66	+0.07	0.47	-0.03

The goodness of fit of the linear regression model was very good. In all cases the residual plots showed an even scatter of points at all x values. Both disc area and NRA increase with increasing axial length and with increasing myopia. It is noteworthy that only regression against axial length gives values for R^2 above 0.6.

Intercorrelations of the optic disc parameters

Correlation analysis did not reveal any significant linear relationship for cup area with either disc area or NRA, if all subjects were included. However, if only subjects with optic cups were analysed then cup area was significantly positively correlated with both disc area ($R^2 = 0.55$) and NRA ($R^2 = 0.15$), in both cases $p<0.01$. The latter case must be interpreted cautiously as the coefficient of determination is very low. Analysing the entire sample NRA is significantly correlated with disc area ($R^2 = 0.88$) and the regression gradient by the least squares method is +0.95 ($p<0.01$). Graphical examples are given in figures 8.16 and 8.17.

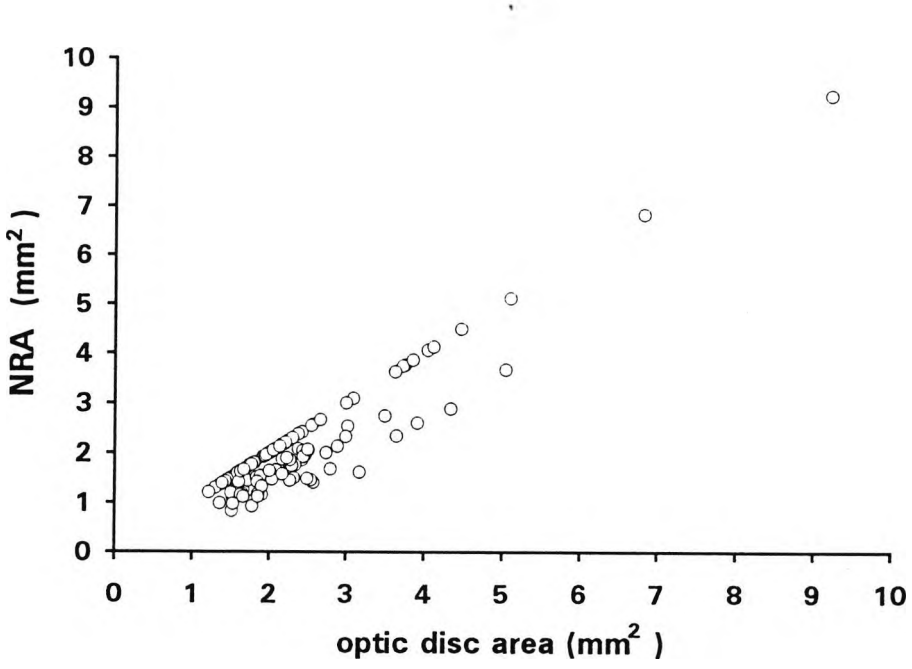

Figure 8.16. Neuroretinal rim area (NRA) plotted against optic disc area for the sample.

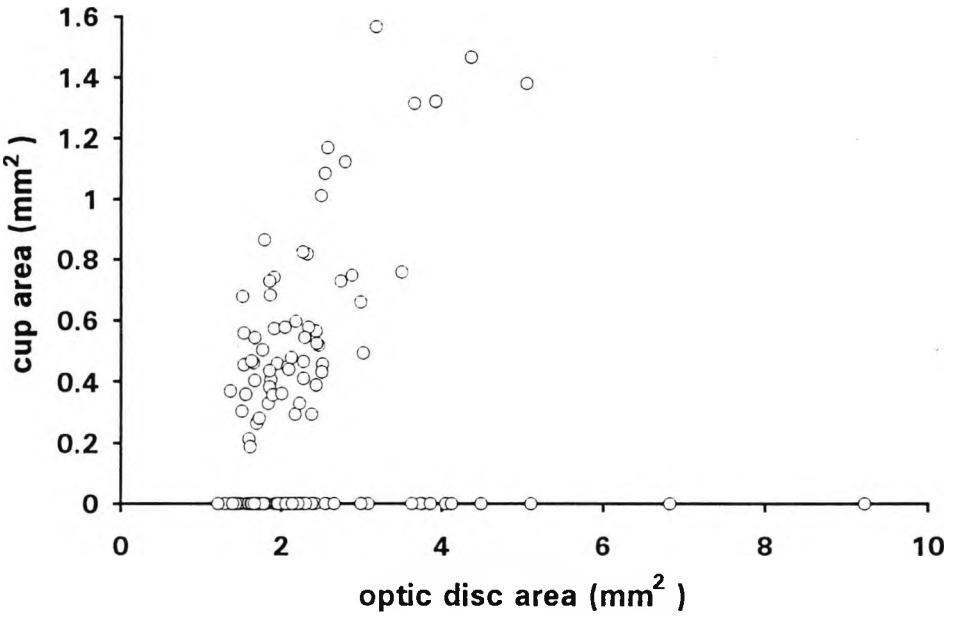

Figure 8.17. Cup area plotted against optic disc area for the entire sample.

8.4.3.2 Peripapillary crescents

Results in this section refer to groups 3 and 4, as only these two groups only contained subjects with myopic peripapillary crescents. They have been combined and treated as one group. Groups 1 and 2 showed variable amounts of pigmentation around the optic disc in only 10 subjects. These pigmented areas differ from the peripapillary crescents associated with myopia and shall not be considered further.

Some individuals had scleral crescents only, some choroidal crescents only and others had both. In some subjects at the border of the myopic crescent, distal to the disc, an area of hyperpigmentation was visible. However, a clear delineation between these three types of tissue boundaries was not possible in most cases. Tissue boundaries were indistinct and frequently there appeared to be a blurry transition from one type of crescent to another. It was thus decided to measure the area of the total peripapillary crescent including the scleral, choroidal and pigmented components. The mean peripapillary crescent area ±SD for this sample is 2.46 ± 4.96mm² with a minimum of 0.11mm² and a maximum of 35.09mm². There is considerable variation of the peripapillary crescent area in this sample. Photographic examples are given in the Appendix A1.2.

Plots of crescent area against either axial length (figure 8.18), ocular refraction and optic

disc area were very similar in appearance. It appears that the rate of increase of crescent area is increasing as the axial length increases beyond 28mm. A correlation analysis of crescent area with optic disc area, axial length and ocular refraction was performed followed by linear regression analysis using the least squares method. In all cases $p<<0.01$, but the R^2 values are quite low (see table 8.10). The goodness of fit of the linear regression model was questionable because the residual plots did not show an even scatter of points at all x values.

A log transformation of the peripapillary crescent area was performed and its relationship with axial length, ocular refraction and optic disc area re-assessed. A linear trend was evident in each case (figures 8.19, 8.20, 8.21). Correlation analysis of log(peripapillary crescent area) with optic disc area, axial length and ocular refraction was performed followed by linear regression using the least squares method. In all cases $p<<0.01$. Plots of the residuals showed an even scatter at all x values supporting the goodness of fit of this linear regression model.

Table 8.10. Summary of the results of correlation and linear regression analysis of peripapillary crescent area in mm^2, and log(peripapillary crescent area) against optic disc area, axial length, and ocular refraction. In all cases $p<<0.01$.

	optic disc area		**axial length**		**ocular refraction**	
	R^2	**gradient**	**R^2**	**gradient**	**R^2**	**gradient**
peripapillary crescent area (mm^2)	0.41	+2.92	0.47	+1.34	0.37	-0.62
log (peripapillary crescent area mm^2)	0.45	+0.23	0.64	+0.15	0.58	-0.07

It is noteworthy that only regression against axial length gives a value of R^2 above 0.6.

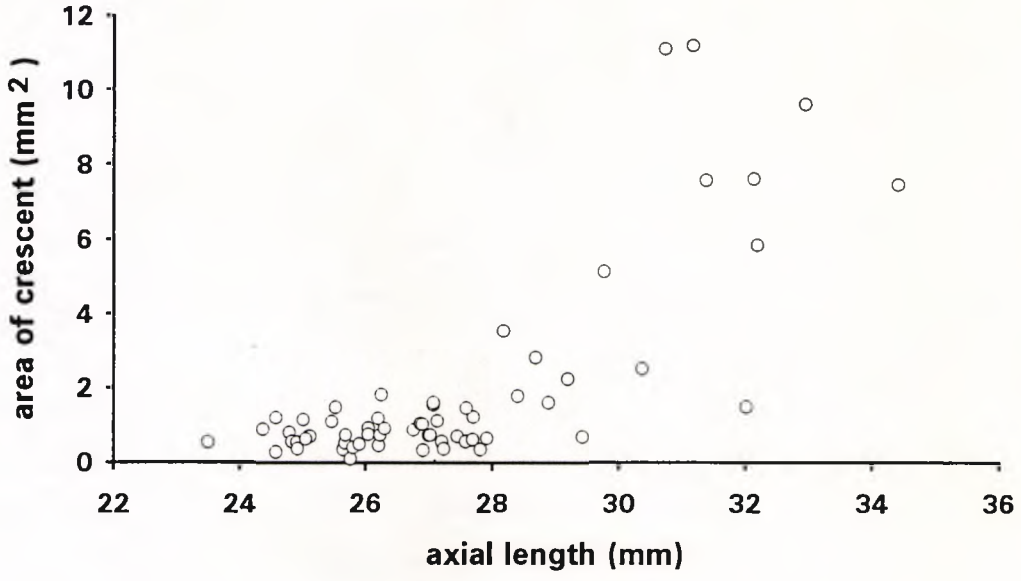

Figure 8.18. Area of the peripapillary crescent plotted against axial length.

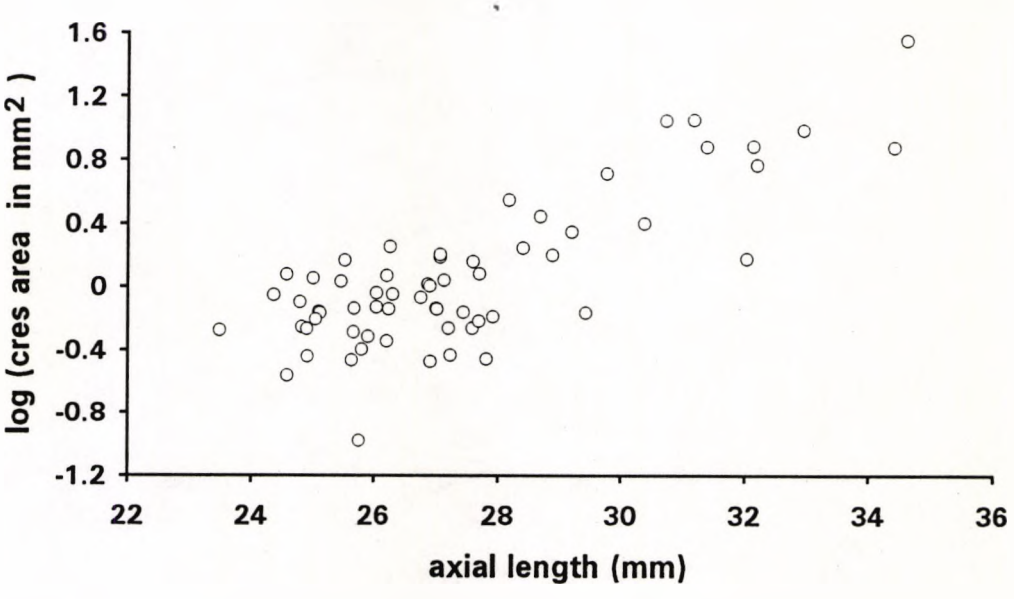

Figure 8.19. Log of the peripapillary crescent area plotted against axial length.

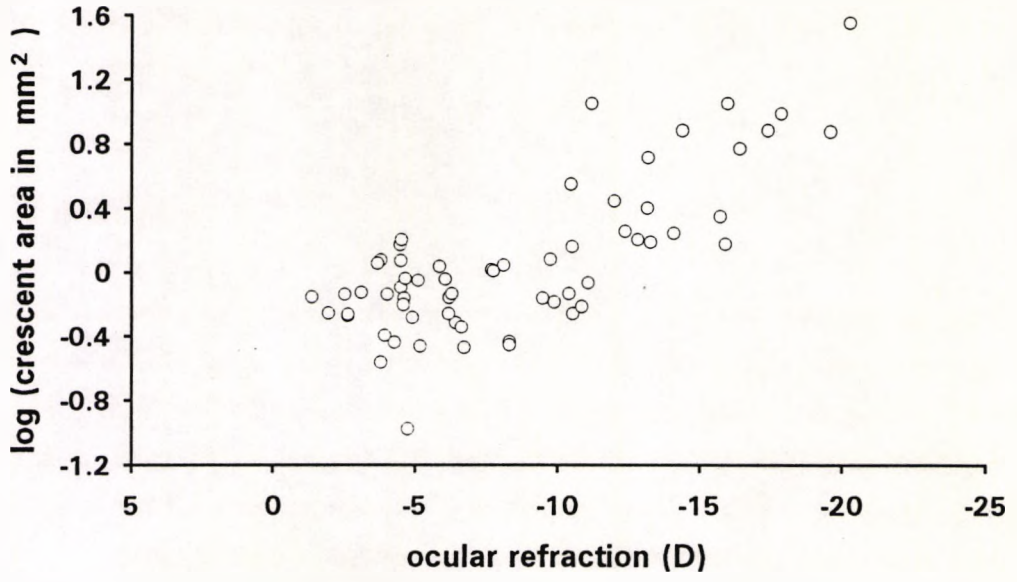

Figure 8.20. Log of the peripapillary crescent area plotted against ocular refraction.

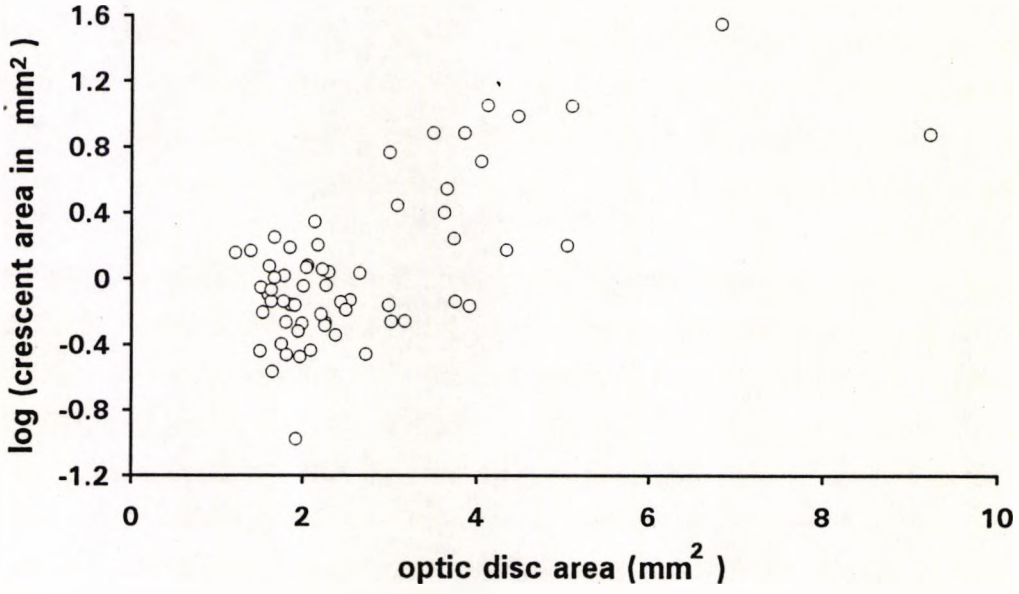

Figure 8.21. Log of the peripapillary crescent area plotted against optic disc area.

8.4.3.3 Repeatability of measurement

Repeated tracings of the same photo were performed in 35 subjects selected randomly. Differences between the two tracings were expressed as a percentage of their mean. Percentages were used because of the variation in the size of the features measured. A 95% confidence interval was constructed from the mean and SD of these differences. For

disc area the 95% confidence interval is +2.52/-2.17%, for cup area +6.63/-6.21%, for NRA +5.01/-5.31% and for peripapillary crescent area +8.13/-9.64%. In each case there were at least 15 subjects.

8.4.4 Discussion

The values obtained for disc area in groups 1 and 2 are in very good agreement with Britton *et al* (1987a), Caprioli and Miller (1987), Bottoni *et al* (1989), and Miglior *et al* (1989) and those from group 3 agree well with Mansour (1991). In table 8.7 Jonas *et al* (1988a, b, c, e), von der Lippe (1992), and Varma *et al* (1993) give the largest mean optic disc areas with a variation of approximately x8. Their results agree better with those from groups 3 and 4. In the study of Jonas *et al* (1988d) which included subjects with myopia from -8D to -28D, the maximum value for optic disc area was enormous (19.54mm^2), with considerable intersubject variation in this sample (~10 fold). In the current study, group 4 shows approximately a 7.5 fold variation in disc area. For groups 1 and 2 this variation is about x2 and in group 3 approximately x3.5. A one way ANOVA showed group 4 to be exhibit significantly larger disc areas than groups 1, 2 and 3 (p<0.05 at least). Group 4 subjects have relatively larger myopic crescents, and also tend to have longer axial lengths and more myopia. As myopia increases, disc area and intersubject variability for disc area increases, this agrees with Jonas *et al* (1988d).

Although a significant linear correlation was found between disc area and both axial length and refraction in groups 3 and 4, plots of the residuals question the validity of this model. A significant positive linear correlation was found between the log(optic disc area) and axial length. A negative linear correlation was found between log(disc area) and the former, indicating that the rate of increase in disc area increases with increasing myopia. Some investigators have reported a correlation between disc area and axial length, and disc area and ocular refraction (Bottoni *et al* 1987a; Kim *et al* 1990), and others have not (Britton *et al* 1987a; Mansour 1991). Jonas *et al* (1988d) found a correlation between disc area and refraction in a group of myopes between -8 to -28D, but not in a group of subjects with less than 8D of myopia (Jonas *et al* 1988b). In the former study they found disc area to increase with myopia by 0.77mm^2/D, this value is higher than that found in the current study (table 8.9). However, it appears that their sample contained many more higher myopes than this study which may account for the difference. None of these studies evaluated the log of optic disc area. A greater proportion of the variation in log(disc area) is explained by variations in axial length (64%) than variations in ocular refraction (44%) (table 8.9).

It has been shown by Jonas *et al* (1988a) that the size of the optic disc in 107 freshly

enucleated eyes is governed by the size of the scleral canal. It is very likely that the size of the scleral canal increases as the globe becomes stretched with axial extension in myopia. This increase in scleral canal area is accompanied by an increase in optic disc area.

Optic disc size has been thought to indicate the susceptibility of an optic nerve head to glaucomatous damage (Armaly 1970; Anderson 1987; Chi *et al* 1989). Ocular hypertensives have been found to have larger optic discs (Carassa and Schwartz 1991). Heijl and Molder (1993) demonstrated that in subjective evaluations of fundus photographs larger discs were more often classified as glaucomatous, whether they were glaucomatous or not, while smaller discs were more likely to be classified as normal. This compares well with Jonas *et al* (1990b) who noted glaucomatous eyes with small optic nerve heads to have misleadingly low cup/disc ratios. Burk *et al* (1992) found optic disc areas in eyes with normal tension glaucoma to be larger than those from eyes with ocular hypertension or high pressure glaucoma. Also, normotensive eyes (including normals, normotensive glaucoma suspects and normotensive glaucoma patients) exhibited larger cup areas, although this may be due an association between disc area and cup area (Bengtsson 1976). It has been suggested by Burk *et al* (1992) that larger discs may be more susceptible to glaucomatous field loss at statistically normal intraocular pressures. However, they did not find disc area to differ between a group of eyes classified as having normal visual fields (including normal, ocular hypertensive, normotensive glaucoma suspects, and ocular hypertensive glaucoma suspects patients) and a group of eyes with glaucomatous field defects (including high-pressure glaucoma and normal-tension glaucoma patients). Burk *et al* (1992) hypothesised that the '*laminar and prelaminar region of larger discs may be damaged more easily by localised hypoperfusion, probably because of longer diffusion distances. Small vessel disease could be one etiological factor. In addition, the lamina cribrosa of these large discs might be more susceptible to mechanical forces such as statistically normal intraocular pressure*'. Using a mathematical model Chi *et al* (1989) demonstrated that in larger discs the lamina cribrosa underwent greater displacement in the presence of an elevated intraocular pressure, and concluded that the absolute size of an optic disc may be a risk factor in developing glaucomatous field loss at any pressure. This poses a difficulty with myopic discs which have been shown to be larger in eyes without glaucoma. Whether myopic optic discs are more susceptible to glaucomatous damage because of their size is a matter for further research. There is evidence in the literature for myopia being a risk factor in developing glaucoma, as has been discussed in Chapters 1 and 7.

Mean cup area values agree well with Miglior *et al* (1989) and Bottoni *et al* (1989) (table 8.7). Cup area did not vary significantly between the four groups. Graphical

inspection did not reveal any visible linear relationship between cup area and axial length, nor cup area and ocular refraction. This was confirmed by correlation analysis which was not significant in either case, and agrees with Jonas *et al* (1988b) but not with Tomlinson and Phillips (1969). Cup area was found to be independent of disc area, and NRA if the entire sample was analysed. However, if only those subjects with optic cups were analysed, significant positive linear relationships were found with disc area, as in other studies (Teal *et al* 1972; Bengtsson 1976; Caprioli and Miller 1987; Britton *et al* 1987a; Bottoni *et al* 1989), and with NRA, which is at variance with others (Britton *et al* 1987a; Teal *et al* 1972), but R^2 was only 0.15, and this result must be regarded conservatively. A general observation in the present study was that subjects with higher myopia tended not to have an optic cup, whereas in subjects with moderate/low myopia it was observed more frequently. As mentioned before the position of the lamina cribrosa is more anterior in myopic eyes than in non-myopic-eyes (Donders 1864; Kolker and Hetherington 1976; Curtin 1985), which gives the cup a shallow appearance and limits the amount of excavation of the optic disc associated with for example glaucomatous damage. These factors should be borne in mind in the evaluation of myopic discs.

Mean values for NRA in groups 1, 2, and 3 (table 8.8) are in good agreement with published values given in table 8.7. Group 4 has the highest mean NRA with a larger range of NRA values. The mean value for NRA in group 4 (2.73mm^2) is higher than all published values (apart from Teal *et al* 1972) and is significantly larger ($p<<0.01$) than for emmetropes (group 1, 1.71mm^2) and lower degrees of myopia without peripapillary crescents (group 2, 1.65mm^2). Therefore in a high myope with a peripapillary crescent having a value for NRA similar to that of a normal emmetropic individual may represent loss of viable neural tissue. Although division of the myopes into these four groups was based upon an arbitrary division of crescent area, it does nevertheless show that myopes with larger crescents who tend to be more myopic have larger optic discs, and also tend to have larger NRA values. The implications of this are that a single absolute value or range of values for NRA can not be used as a diagnostic tool to distinguish between normal optic discs and those suffering loss of the neuroretinal rim from ocular disease.

Although a significant linear correlation was found between NRA and both axial length and refraction in groups 3 and 4, plots of the residuals showed several outliers, and question the validity of this linear model. As with log(disc area), there is a significant linear relationship between log(NRA) and both axial length and ocular refraction ($p<0.01$), and the goodness of fit of this model was confirmed by plots of the residuals. 66% of the variation in log(NRA) is explained by variation in the axial length, and from regression against ocular refraction 47% of the variation in log(NRA) is explained. Previous researchers did not elicit a relationship between NRA and axial length or ocular

refraction (Britton *et al* 1987a; Jonas *et al* 1988b and f; Paczka *et al* 1992). However, these studies did not encompass as wide a range of refractions or axial lengths as in this study.

NRA was found to be strongly correlated with optic disc area as in other studies (Britton *et al* 1987a; Caprioli and Miller 1987; Jonas *et al* 1988e). This is not surprising as NRA is governed by the margins of the optic disc. Scleral canal area was shown by Jonas *et al* (1988a) to govern the size of the optic disc. From the above one might expect NRA also to correlate with the scleral canal area. However, this was not confirmed by Mikelberg *et al* (1991) in their sample of 16 donor eyes.

It is evident from the literature that there is some controversy with regard to the possible association of optic disc parameters with each other and with other ocular dimensions. In addition to the various combinations of ocular dimensions possible in ametropia (section 1.1), considerable variation in the number nerve fibres in normal eyes has been reported (Balazsi *et al* 1984a; Quigley *et al* 1982; Repka and Quigley 1989). It is possible therefore, that a small sample may have a very different composition to another with respect to these ocular parameters. Different combinations of these parameters within a particular sample may account for the disagreements between investigators.

The mean area of the peripapillary crescent in this sample of myopes is lower than that reported by Jonas *et al* (1988d) in myopes ($33.05 \pm 23.84 mm^2$). The likely cause for this discrepancy is that Jonas and co-workers examined more subjects with higher degrees of myopia than this study. It is known that the area of the crescent increases with axial length and ocular refraction (Stenstrom 1946; Otsuka 1967; Huang *et al* 1987). Fulk *et al* (1992) found crescent size to increase with myopia but not axial length. However, it appears that their data contained a preponderance of low myopes, which may have been insufficient to elicit a relationship between crescent size and axial length.

From figure 8.18 an increase in the area of the peripapillary crescent with axial length is evident particularly beyond an axial length of 28mm. A similar observation was made in myopes with more than 10D of myopia and disc areas larger than approximately $3mm^2$. In all cases there is considerable inter-subject variation. The increase in log(crescent area) appeared reasonably linear when plotted against axial length, ocular refraction and disc area. Significant linear correlations were found in all cases. The highest R^2 value was obtained for regression against axial length (0.64). This is to be expected because an increase in the crescent area is believed to be a direct result of scleral expansion associated with axial elongation in myopia (Fantes and Anderson 1989; Curtin 1985). Crescents can also enlarge with age, or as part of retinal disease, or in glaucoma (Rockwood and Anderson 1988).

Jonas *et al* (1988d) found crescent area in a group of high myopes to be correlated with optic disc area (R^2=0.64) and refraction (R^2=0.35), but no comment was made about any association with axial length. The presence of this crescent poses problems in identifying glaucomatous disc changes in myopia. Peripapillary crescents have been described in association with glaucoma (Hayreh 1969; Wilensky and Kolker 1976; Anderson 1983; Buus and Anderson 1989). A higher prevalence of peripapillary atrophy has been reported in myopes with POAG compared with non-myopic POAG (Chihara and Sawada 1990), and in normal tension glaucoma compared with ocular hypertension (Anderson 1983), with a larger area of atrophy in the former (Buus and Anderson 1989). Caprioli and Spaeth (1985) do not support these findings. Anderson (1987) suggested that patients with POAG and peripapillary crescents are more likely to develop glaucomatous field damage than those without crescents.

Balazsi *et al* (1984b) found the accuracy of tracing the same photo to be within 1%, and from those taken consecutively to be within 6%. Airaksinen *et al* (1985a) measured 10 photos 10 times and the error between measurements was 1.6% for disc area and 2.9% for NRA. Coefficients of variation have been calculated to be 2.1% for disc area and 3.3% for NRA (Caprioli *et al* 1986) and 4.7% for cup area/disc area (Takamoto and Schwartz 1985). McNellis *et al* (1991) found the coefficients of variation to be 1.8% for disc area, 4.1% for NRA and 5.3% for peripapillary crescents. All the above studies used stereophotography. In the current study simultaneous stereophotography was not available with the Zeiss Jena camera, thus it is not surprising that the repeatability was slightly worse. It is generally accepted that simultaneous stereophotography is superior to mono- or sequential stereophotography (Rosenthal *et al* 1977).

8.4.5 Conclusions

Normal values for the optic disc parameters have been measured over a wide range of ametropia, and correlations of the optic disc parameters with axial length and ocular refraction have also been elicited. Knowledge of typical dimensional values for myopic optic nerve heads and their variation with axial length and increasing myopia will help in establishing criteria for abnormality, particularly in identifying glaucomatous changes in myopic discs. This is important because glaucoma is more prevalent in myopic than in emmetropic eyes, and myopia is found more often in glaucomatous patients than in the general population (see Chapter 1 section 1.5.1).

From the analysis performed here possible changes of the optic disc parameters in myopic eyes, in comparison with non-myopic eyes, can be estimated from the gradients of the linear regression lines. Taking log values for the optic disc parameters resulted in a

linear relationship, for the entire sample, with both axial length and ocular refraction. The goodness of fit of this model was confirmed by the residual plots showing an even scatter of points at all x values. The convenience and simplicity of this relationship is that it applies to the entire sample and does not require an arbitrary division of the subjects into groups by axial length or ocular refraction. Estimates from the regression would yield values in log units which can be converted back into regular units of measure.

Prospective evaluations of optic disc area, cup area and NRA over time in myopia would be informative. If the degree of myopia is stationary, as determined by refraction and axial length measurements, it seems reasonable to assume that the optic disc parameters would remain unchanged in the absence of other pathology. This may help in assessing progression of a disease process affecting the optic nerve head. It is possible that any increase in NRA with axial elongation may be masked by ocular disease causing a decline in NRA. .

Cup size, disc size and the presence of peripapillary atrophy are thought to indicate increased vulnerability of an optic nerve head to glaucomatous damage (Anderson 1987; Armaly 1970; Chi *et al* 1988). As shown above, myopic eyes in the absence of glaucoma have larger optic discs and peripapillary crescents. The latter may appear similar to peripapillary atrophy observed in glaucoma. Fantes and Anderson (1989) pointed out that with fundus photography or flourescein angiography it is impossible to distinguish between all the possible misalignments of the retina, RPE and choroid at the disc margin, nor between physiological and atrophic peripapillary changes. In addition to myopia progression, peripapillary crescents can enlarge as part of the ageing process or from retinal disease or glaucoma (Rockwood and Anderson 1988). The presence or enlargement of a peripapillary crescent in myopic eyes may not be a predisposing factor to developing glaucoma. From the linear regression analysis performed the area of the peripapillary crescent in a myope with a particular disc size, refraction or axial length, can be estimated. However, the R^2 values are low, and these results may be specific to this sample. The subjects in this study were not randomly selected and may not be a true representation of the population. Also errors may have occurred with measurements made from mono- as opposed to stereoscopic slides, which have invariably been reported to be superior. The subjects were mainly Caucasian individuals, racial influences have not been investigated.

CHAPTER 9

Topographical investigation of the blind spot

9.1 INVESTIGATION OF THE NORMAL BLIND SPOT BY MANUAL PERIMETRY

Topographical investigation of the blind spot (BS) was performed in this study to compare the size and position of the BS in emmetropes and myopes. Enlargement of the BS has been reported in myopia (Reed and Drance 1972; Harrington 1981; Nakase 1987a; Masukagami *et al* 1987; Jonas *et al* 1991), but this is an inconsistent finding, and this may be due to the variable presence and extent of peripapillary crescents associated with myopia. Differential light sensitivity was shown to be reduced beyond the visible borders of the optic disc in both normal and myopic individuals (Masukagami *et al* 1987). Analysis of the coecal and pericoecal area may provide information that may be of diagnostic and prognostic importance. Jonas *et al* (1991) demonstrated BS enlargement in POAG patients, and pericoecal sensitivity was shown to be markedly depressed in patients with ocular hypertension and early POAG (Brusini *et al* 1986).

The exact location and size of the normal BS is markedly dependent upon the stimulus size and background luminance employed. Traquair (1957) plotted the BS using a 2/2000mm white stimulus on the Bjerrum screen, and the average location of the BS was 15.5° temporally and 1.5° below the horizontal meridian, with a width of 5.5° and height 7.5°. Its position has been stated to be closer to the fixation point in myopes as compared with hypermetropes (Reed and Drance 1972). Discrepant values between experimenters, instruments (Schoessler 1976) and poor reproducibility of measurements of the BS led Armaly (1969) to conclude that manual investigation of the BS does not provide information of much diagnostic value. He described the absolute scotoma of the BS to be surrounded by a relative scotoma wider than 1°. This is supported by the values for the height and width of the BS obtained using different stimuli on the tangent screen and Goldmann perimeter. The mean BS height and width for the tangent screen using a 1/1000 white stimulus (0.06° angular subtense), were 10.4° and 7.4°, and for the Goldmann I2e stimulus (0.11° angular subtense), 14.1° and 9.6° respectively. The range of x and y values over which the BS lay was between 9.8° to 20.3° and 6.7° to -7.7° respectively (Armaly 1969). Jonas *et al* (1991) found the normal BS area with the Goldmann kinetic perimeter to be 59.9 ± 17.0 mm^2 for the I4e stimulus, and 39.2 ± 11.9 mm^2 for the III4e stimulus.

Physiological factors will affect the differential light sensitivity of the BS, and these have already been discussed in Chapter 3. Aulhorn and Harms (1969) showed that small fixation movements have a very strong effect upon threshold values along steep or

abrupt gradients. A fixation shift of one or two degrees can cause a change of 2 to 3 log units in the threshold at the BS borders. Marked interindividual variation exists in the configuration of the BS of normal subjects, and a reduction in light sensitivity of 0.6-0.8 log units in the pericoecal area can be expected with a size I stimulus, particularly at the upper and lower poles of the BS (Zingirian *et al* 1981). It is likely that angioscotomas are one reason for these irregularities in the contrast sensitivity profile. Drance *et al* (1967) found the size of the BS to increase with age.

9.2 INVESTIGATION OF THE BLIND SPOT BY AUTOMATED PERIMETRY

9.2.1 Introduction

Superior definition and reproducibility of the blind spot is available with automated perimetry as compared with manual kinetic perimetry (Gramer *et al* 1979; Faschinger 1984). A few studies have been devoted to the evaluation of the normal blind spot using automated perimetry (Fankhauser and Häberlin 1980; Häberlin *et al* 1980; Funkhouser *et al* 1988a and b; Haefliger and Flammer 1989). It has been suggested that the increase in SF observed with measurements performed at the border of the BS in normal subjects may be related to thresholds taken with any static perimeter at the borders of a depression in the field (Haefliger and Flammer 1989). They also found that larger values for SF were not restricted to points with low sensitivity values. The relationship between SF and sensitivity has already been discussed in Chapter 3. At the borders of the BS, where the slope of the scotoma is steep and the determination of the light sensitivity is not precise, small changes in fixation can markedly affect sensitivity levels at the BS margin (Häberlin *et al* 1980).

Fankhauser and Häberlin (1980) demonstrated that light spreads beyond the geometrical boundaries of the stimulus. This stray light would influence the contrast sensitivity profile of any scotoma, particularly with the high intensity stimuli used to plot the BS. This entoptic phenomenon was perceived as a large diffuse flash when a size III stimulus with maximum luminance was projected at the optic disc. The flash was never observed with a size I or II stimulus but was easily evoked using sizes IV and V. It is clear that by increasing stimulus luminance, stray light effects increase, and will reduce the apparent size of the BS (Fankhauser and Häberlin 1980; Funkhouser *et al* 1988a). Stray light may also result from scattering/reflection by the ocular media, the optic disc, and any regions of higher reflectance at the disc border, such as might be expected from a scleral crescent for example.

Bek and Lund-Anderson (1989) illustrated that with a small stimulus size, such as a

Goldmann I or II, the BS could be delimited as an absolute scotoma with sharp borders. However, with larger stimulus sizes (III to V) a relative scotoma zone gradually developed, extending centrally from the borders of the BS. The central absolute scotoma component of the BS totally disappeared for the larger stimuli (sizes IV and V). This agrees with Fankhauser and Häberlin (1980). Light scattering effects were considered responsible for this apparent disappearance of the BS, because the stimuli were small enough to be projected totally within the margins of the optic nerve head.

Optimal stimulus size to minimise the effects of stray light, and accurately identify the BS, was suggested by Häberlin *et al* (1980) to be the standard Goldmann size II, which gives a sharp sensitivity profile, and a grid separation of 3° is sufficient for detection purposes. A grid separation of 6° or even 4.2°, commonly used in automated perimetry, may not expose the BS (Wild *et al* 1986; King *et al* 1986; Stepanik 1986). High resolution programs are required for reliable assessment of the BS. Various grid constants have been proposed, 1.4° by Bek and Lund-Anderson (1989), 1° by Häberlin *et al* (1980), and 0.6° by Zulauf (1988).

Accurate delineation of the BS is complicated by angioscotomata. Zulauf (1988) demonstrated angioscotomata defects of up to 8dB in depth with a size III stimulus. Using a standard size I stimulus, Häberlin *et al* (1983) found them to be of the order of 10dB in depth and 0.6° wide.

Investigators have employed different cut-off sensitivity levels to avoid BS measurements being contaminated by angioscotomata. Safran *et al* (1989 and 1991) adopted a single-level strategy for a size III stimulus on the HFA. Intensity of light stimuli was set at 12dB below the normal age-corrected values of thresholds in locations surrounding the BS area. Test points not seen were regarded as belonging to the BS. This strategy, together with a grid separation of 1° horizontally and 1.5° vertically, identified an average of 17.5 test locations as lying within the BS. This gave the normal BS an average diameter between 3.31° and 5.95°. Others have used a single threshold level of 12dB (Funkhouser *et al* 1988a) and 18dB (Funkhouser *et al* 1988b), for a size III stimulus, or 15dB for a size II stimulus (Häberlin *et al* 1980), on the Octopus perimeter. Test locations with thresholds below these levels were considered to fall within the BS. Despite differences in methodology to ascertain the borders of the BS, the mean BS area for normal subjects does not vary significantly between investigators using a size III stimulus. According to Safran *et al* (1991) the BS area is 25.57 ± 5.67 degrees^2, and Funkhouser *et al* (1988b) measured it to be 28.29 ± 6.35 degrees^2. BS area as determined with a size II stimulus was approximately 20 degrees^2 by Häberlin *et al* (1980). Similar agreement exists for mean BS diameter, being 4.63 ± 0.53° in the study of Safran *et al* (1991), while Häberlin *et al* (1980) found the mean diameter to be

horizontally 4.58 ± 0.46° and vertically 5.77± 0.50°

Field test size may influence the size and depth of the BS,

- selective as opposed to global retesting of the central visual field has been shown to reduce the number of points with defective thresholds, particularly in pathological fields (Rutishauser and Flammer 1988)
- as field test size is reduced, the mean sensitivity, calculated from the same locations each time, improved and short-term fluctuation increased (Fujimoto and Adachi-Usami 1991). This may be caused by differences in the total number of stimulus presentations and hence, test duration (Fujimoto and Adachi-Usami 1992).

These factors could reduce the size and extent of the BS measurements.

Using the Octopus automated perimeter, Britton *et al* (1987b) plotted the BS with a stimulus subtending 10' of arc and 1000 apostilbs of background luminance, and found a correlation (r = 0.7) between the size of the BS and the size of the optic disc in a group of normal subjects. Jonas *et al* (1991), found the size of the BS measured with a size I4e and III4e stimuli on the Goldmann perimeter, to correlate with the size of the optic disc, with r values of 0.38 and 0.46 respectively. They concluded that the scleral crescent constituted part of the absolute scotoma, and any irregular pigmentation beyond the scleral crescent produced a relative scotoma. The size of the BS has been found not to be related to age (Britton *et al* 1987b).

9.2.2 Aims

The aim is to calculate the size of the BS over a wide range of ametropia, and to compare it with the true size of the optic nerve head and any peripapillary crescent.

9.2.3 Materials and methods

9.2.3.1 Grid configuration and stimulus size

Taking into consideration previous findings regarding stimulus size and grid resolution for investigating the BS, a size II stimulus was chosen to minimise stray light effects and give sharp definition of the BS. The highest grid resolution available on the HFA was employed. Two customised grid patterns with a spatial resolution of 2° were created on the HFA. In combination the two grids yielded a spatial resolution of 1.4°, taken as the diagonal distance between locations. The co-ordinates of the grid are given below (table 9.1) and considered adequate to encompass the BS.

Table 9.1. Essential features of the two customised BS programs devised on the HFA

Stimulus size	II ~ 0.22°
Strategy	full threshold
Grid A	
x	9° to 21°
y	6° to -8°
Number of stimuli	56
Grid B	
x	8° to 20°
y	7° to -7°
Number of stimuli	56
Total number of stimuli (A+B)	112
Resolution of combined grids (A +B)	1.4°

9.2.3.2 Subject sample and testing procedure

Ninety six out of the total of 122 subjects described in Chapter 7 returned to complete the two blind spot programs. Each subject performed both blind spot programs at one visit, with a rest period of at least 15 minutes between programs, using the same eye as before for the central visual field examination. The order of the two blind spot programs was randomised.

9.2.4 Results

Subjects were divided into the same four groups as in the previous chapters. Mean values for age, refraction, axial length and the number of subjects in each group are given in table 9.2.

Table 9.2. Number of subjects in each group, together with the means for age, ocular refraction and axial length. Values in parenthesis indicate the range.

Group	number of subjects	mean age (years)	mean ocular refraction (D)	mean axial length (mm)
1	27	22.56 (19.1-26.8)	+0.21 (4.3 to -0.9)	22.66 (22-25.4)
2	20	22.43 (19.5-32.8)	-2.57 (-1 to -5)	24.82 (23.5-26.6)
3	23	23.09 (18.5-35.4)	-6.62 (-1.4 to -12.8)	26.70 (23.5-29.4)
4	26	25.13 (18.9-35.2)	-11.37 (-4 to -20.3)	28.76 (24.57-34.6)

In group 4 the crescent area, expressed as fraction of the optic disc area, was at least 40% of the optic disc area, with a maximum of 6x disc area. In group 3 the area of the crescent ranged from 5% to 35% of the optic disc area.

From the above review of the literature it is clear that there is no standard definition for the sensitivity level constituting the relative scotoma around the blind spot with a size II stimulus on the HFA, nor is there any data relating to the age-corrected normal values for this stimulus size.

Sensitivity values from the BS programs were initially visually evaluated with the two programs combined. Data from the BS program were imported into an IMB compatible computer. A program was available which allowed the BS plot to be viewed with the sensitivity values colour coded every 5dB, starting at 0dB. In all cases an area with locations having sensitivities less than zero decibels (absolute scotoma for these testing conditions) was surrounded by a relative scotoma region of varying area and depth.

The pattern of distribution of sensitivity levels was viewed in conjunction with the corresponding fundus photograph. It became apparent that sensitivity values between 16

and 20dB appeared in most cases to follow the course of blood vessels. On this basis it was decided that sensitivity values in the range 16-20dB constituted angioscotomata, and values below 16dB were taken as forming part of the BS. In addition the BS programs were repeated in 5 emmetropic subjects testing the **nasal** field. Mean sensitivity of the nasal field for these subjects was 25.99 ± 5.42 dB, therefore it seemed reasonable to assume that values below 16dB constituted the BS.

Values of zero decibels or less were interpreted as the absolute scotoma of the BS. Values from 1 to 15dB were divided into three bands, 1 to 5dB, 6 to 10dB, and 11 to 15dB. The number of locations in each band was determined. Thus the results can be interpreted as a central absolute scotoma surrounded by three relative scotoma zones.

From knowledge of the number of stimulus locations and their separation, the BS area was determined for each sensitivity band. In any calculation of this nature assumptions must be made as to the sensitivity between neighbouring points, and the sensitivity profile at the edge of the region of interest. The diagram below helps explain the principles behind the method utilised here. Figure 9.1 illustrates some of the test locations from the blind spot programs. The black circles are the stimulus locations of one program and the grey circles are from the other program. The vertical or horizontal separation between a black and a grey circle is one degree. Therefore the separation between a black and an adjacent grey circle is $\sqrt{2}°$ which is 1.4°.

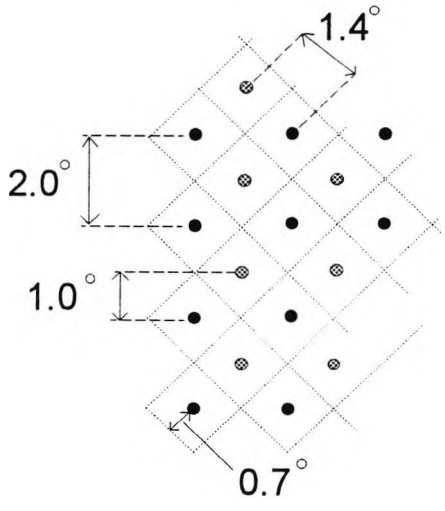

Figure 9.1. A section from the combined blind spot programs. The black circles are from one program and the grey circles from the other. The distance between a black circle and an adjacent grey circle is 1.4°.

The sensitivity at each stimulus location is assumed to apply over a square with a side length of 1.4°, as indicated by the dotted lines in figure 9.1, thus the area of this square is 1.96 degrees^2. If the total number of locations within a given sensitivity band is n, then the total area for this sensitivity band is $1.96n$ degrees^2.

This value can be converted into millimetres. Let the diameter of this square be a mm. The radius of the HFA hemispherical screen is 330mm, it follows that

$$\tan 1.4° = a/330$$
$$a = 330.\tan 1.4° \text{ mm}$$
$$a = 8.065 \text{ mm}$$

If each location is assumed to represent an area of a^2 mm^2, then the area of the BS within a particular sensitivity band is determined by counting the number of stimulus locations (n) within this sensitivity band and multiplying by a^2, to give the area of the BS in mm^2,

$$\text{BS area} = a^2n$$
$$a^2 = 65.045 \text{ mm}^2$$
$$\text{BS area} = 65.045n \text{ mm}^2$$

In order to compare directly the size of the optic disc with that of the BS, the size of the projection of the optic disc onto the HFA screen needs to be calculated. The method is described below with the aid of figure 9.2, which shows a ray trace from the retinal plane to the HFA screen for a retinal feature of diameter d. P and P' are the principal planes of the human eye, or of the combined optical set-up of the human eye with the optical correction utilised during BS perimetry (spectacle or contact lens). The position of the principal planes in these conditions needs to be determined. Calculation of the position of the principal planes of the human eye is described in Chapter 8, section 8.2.2.3 and Appendix A2. In subjects using a spectacle lens or contact lens during testing, the position of the principal planes is recalculated accordingly. Thus, the distance from the retinal plane to the second principal point, l, can be ascertained. It is assumed that the distance from HFA screen to the front of the eye is 33cm. From this and knowledge of the position of the principal planes, the distance from the HFA screen to the first principal point, x, can be established.

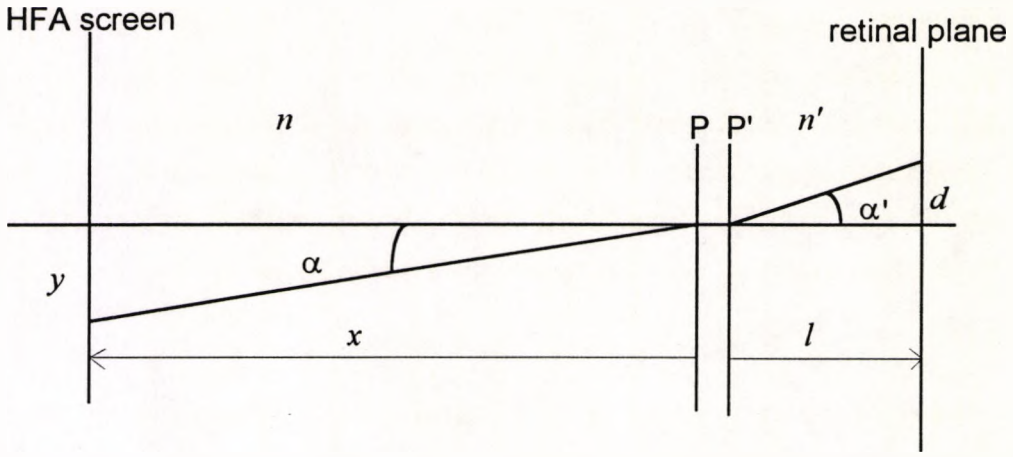

Figure 9.2. Schematic diagram of the projection of a retinal feature of diameter *d*, onto the HFA screen. The projected image diameter is *y*. P and P' are the first and second principal planes for the human eye, or the human eye and optical correction combined.

From paraxial theory and assuming small angles,

$$n\alpha = n'\alpha'$$
$$n(y/x) \approx n'(d/l)$$
$$y = dn'x/ln \qquad 9.1$$

$n = 1$
$n' = 1.336$
d = diameter of the retinal feature
x = distance from the HFA screen to the first principal point
l = distance from the second principal point to the retina
y = diameter of image of the retinal feature projected onto the HFA screen

Equation 9.1 becomes

$$y = 1.336xd/l$$

If d^2 represents the area of the retinal feature, the corresponding area projected onto the HFA screen, y^2, is calculated from

$$y^2 = (1.336xd/l)^2$$

In the previous chapter the areas of the optic discs and any associated peripapillary crescents were calculated. Thus the areas of these retinal features projected onto the HFA screen can be directly compared with the values for the BS areas (table 9.3).

The projected optic disc area does not vary significantly between the groups (one way ANOVA with least significant difference multiple comparison procedure). This may seem surprising considering optic disc area was shown in the previous chapter to increase with both increasing axial length and myopia. However, its projected area in visual space is reduced by two factors, a diminished angular subtense in longer eyes and the use of a negative correction.

It is clear that taking all values below 16dB as belonging to the BS results in a larger total BS area than the area of the projected optic disc, especially in group 4 where the BS area is considerably larger than the projected disc plus crescent areas. The absolute scotoma is surrounded by a relative scotoma, the area of which is approximately 0.6x the area of the absolute scotoma in groups 1, 2 and 3, and 0.8x in group 4. From table 9.3 it is evident that the BS area is larger in group 3 compared with groups 1 and 2, and group 4 compared with group 3.

The mean area of the absolute component of the BS is smaller than the mean projected optic disc area in groups 1, 2 and 3. This applies to each subject in group 1. The area of the absolute BS was larger than the projected optic disc area in 10 subjects in group 2, and 6 subjects in group 3. In group 4 the absolute scotoma of the BS extended beyond the borders of the projected optic disc area in all but 3 subjects, and these three subjects had choroidal crescents only. It has been suggested that scleral crescents contribute to the absolute scotoma of the BS (Jonas *et al* 1991). However, this is inconsistent with the current findings on three counts. Firstly, group 2 does not contain subjects with peripapillary crescents. Secondly, 5 of the subjects in group 3 exhibiting an enlarged absolute scotoma relative to the disc area, had choroidal crescents only. Thirdly 10 subjects in group 4 without scleral crescents displayed an enlarged absolute scotoma relative to the projected disc area. Also, the standard deviation of the group means for BS areas are particularly large in group 4, implying a larger inter-subject variability.

Table 9.3. Mean areas (±SD) of the optic disc, and any peripapillary crescent projected to 330mm on to the HFA screen, and the mean areas (±SD) of the BS for different sensitivity bands.

Group	Number of subjects	Mean projected disc area (mm^2)	Mean projected disc area + crescent area (mm^2)	Mean BS area (mm^2)				Mean BS area ($degrees^2$)			
				0dB	0-5dB	0-10dB	0-15dB	0dB	0-5dB	0-10dB	0-15dB
1	27	818.37 ± 159.32	-	638.40 ± 176.79	768.49 ± 195.16	920.26 ± 196.54	1040.71 ± 214.97	19.24 ± 5.33	23.16 ± 5.88	27.73 ± 5.92	31.36 ± 6.48
2	20	744.20 ± 161.32	-	663.45 ± 129.40	787.04 ± 129.92	933.39 ± 159.71	1050.47 ±185.51	19.99 ± 3.90	23.72 ± 3.92	28.13 ± 4.81	31.65 ± 5.59
3	23	801.19 ±235.08	1013.18 ±306.76	735.29 ± 249.95	865.38 ± 271.34	1029.40 ± 298.49	1190.60 ± 313.44	22.16 ± 7.53	26.08 ± 8.18	31.02 ± 8.99	35.88 ± 9.45
4	26	778.81 ±279.69	1764.52 ±1374.92	1183.31 ± 741.17	1418.47 ± 813.45	1646.13 ± 928.43	2126.46 ± 1397.44	35.66 ± 22.33	42.74 ± 24.51	49.60 ± 27.98	64.08 ± 42.11

A one way ANOVA together with the least significant difference multiple comparison procedure was used to identify any significant differences between groups' BS area for each sensitivity band. No significant differences were found between group 1, 2 and 3. Group 4 was significantly different from the other three groups in all cases ($p<0.01$). These results need to interpreted cautiously because of the increased variance in group 4.

It is interesting that in Chapter 7 both groups 3 and 4 showed significant differences from groups 1 and 2, for the sensitivity of the central 30° field. Analysis of BS areas reveals however, only group 4 to be significantly different from groups 1 and 2. Group 4 contains subjects with relatively larger peripapillary crescents, who tend to have longer axial lengths and more myopia. This suggests that enlargement of the BS in myopia is not a significant contributor to the central field changes observed in group 3 myopes and described in Chapter 7. This is supported by the impression of an enlarged BS in the gray scale printouts of the central field of group 4 subjects.

9.2.5 Discussion

If values below 16dB with the size II stimulus are considered to form the BS, reduction of the differential light sensitivity associated with the physiological BS extends beyond the anatomical margins of the optic disc or peripapillary crescent. This sensitivity cut-off seems reasonable, as the mean sensitivity using the same test programs in the nasal field was found to be 25.99 ± 5.42 dB. Masukagami *et al* (1987) has shown using fundus perimetry that the reduction in sensitivity associated with the BS spreads beyond the margins of the optic disc in normal and myopic eyes. No mention was made to peripapillary crescents.

A significant enlargement of the BS was observed in group 4 subjects, who have relatively larger peripapillary crescents, and tend to have longer axial lengths and more myopia. Enlargement of the BS in myopia agrees with previous studies using manual (Takizawa 1983) and automated perimetry (Nakase 1987a; Martin-Boglind; Masukagami *et al* 1987; Jonas *et al* 1991). In the study of Jonas *et al* (1991), it was believed that the increase in the BS size was due to the increase in optic disc area in myopia, however, it has been shown above that the optic disc area projected on to the HFA screen does not vary significantly in this sample. In addition to myopic peripapillary changes, enlargement of the BS can occur with pathology of the optic disc or optic nerve and has been described in glaucoma (Gramer *et al* 1982; Jonas *et al* 1991), although this is not a consistent finding.

Jonas *et al* (1991) using Goldmann kinetic perimetry concluded that peripapillary

crescents exposing the underlying sclera contributed to the absolute scotoma, and peripapillary atrophy with irregular pigmentation contributed to the relative scotoma of the BS. This conclusion is not supported by this study. Subjects without scleral crescents demonstrated the absolute scotoma of the BS to be larger than the projected optic disc area.

Values for the BS area in this study are somewhat larger, for all groups, than previously recorded with automated perimetry by Safran *et al* (1991), Funkhouser *et al* (1988b) and Haberlin *et al* (1980). However in the former two studies a larger stimulus size was used which may account for the differences. In the latter study a size II stimulus was used on the Octopus perimeter but a different testing strategy was utilised. Stimuli were presented at 15dB and those not seen were re-tested at 0dB. Additional locations were added to the starting grid when locations were missed at 0dB. Values not seen at 15dB were considered to fall within the normal BS. Different types of spatially adaptive strategies were utilised, and the mean BS area was approximately 20 degrees^2 in a normal subject. In this study the full threshold strategy was employed, which is more time consuming. Fatigue effects may have caused a reduction in light sensitivity, sufficient to increase the number of locations considered as constituting the BS.

Measurement of the area of the BS will be influenced by the negative prescription worn during testing by myopic subjects. Minification of the test stimulus by the negative spectacle lens may have caused a reduction in the light sensitivity which could cause enlargement of the BS. This phenomenon would be less pronounced with contact lenses.

CHAPTER 10

General Discussion

10.1 SUMMARY OF RESULTS

In Chapter 5 repeatability and reproducibility of the Allergan Humphrey Ultrasonic 820 Biometer was assessed, and found to be within acceptable limits for both an experienced and inexperienced experimenter. Optimal investigation strategy was in agreement with the manufacturers guidelines, which state that the gain of the instrument should be set initially to 60%, and adjusted accordingly to obtain clean, sharp echo spikes of equal amplitude from the corneal, crystalline lens and retinal surfaces.

Psychophysical learning associated with sequential visual field testing using the HFA was demonstrated over the first two tests performed (Chapter 6). It was concluded that the first two tests performed on each individual would be excluded to account for learning. However, this was only evident when the data was analysed using a novel 'proportion index'. Analysis of the sample means for the global indices did not yield any evidence of a learning effect. This discrepancy between the two methods of analysis may be due to the considerable intersubject variations in the learning process, which can have a marked influence on the values of sample means of global indices. The proportion index used in this study is influenced less by intersubject differences and extreme values.

It is clear that the sensitivity of the visual field declines as the degree of myopia increases. This decline is most pronounced in those subjects with larger peripapillary crescents, who also tend to have longer axial lengths and more myopia. A generalised depression of sensitivity is observed, with localised involvement as the field deteriorates further. In some cases the upper-temporal quadrant seems preferentially affected. Careful examination of the myopic fundus is necessary, as the field depression may be related to ectasia/thinning of the retina. Possible causes for field loss have already been discussed in Chapter 7.

Correlation analysis showed a relationship between the sensitivity of the visual field, taken as either the global indices or regional mean sensitivities, and both axial length and ocular refraction, in subjects with peripapillary crescents. In all cases the correlation was stronger with axial length (R^2 above 0.6). Results from a linear regression analysis can be utilised clinically to obtain an estimate of a global index or regional mean sensitivity if either the axial length or degree of myopia are known (Chapter 7 and Appendix A1). Those subjects with more than 5D of myopia or axial lengths above 26mm may show

deficits in their visual field sensitivity, while if the myopia is more than 10D or the axial length above 28mm reduction in field sensitivity is very likely. It can be seen from the HFA single field analysis printouts that the total and pattern probability plots are more useful than the corresponding numerical plots. Locations exhibiting depressed thresholds were scattered throughout the central field, and there was no evidence of typical glaucomatous type defects. In some myopes with peripapillary crescents the sensitivity loss was clearly associated with an enlarged BS. In Chapter 9, it was shown that the sensitivity loss associated with the BS extended beyond the anatomical borders of the optic nerve head, and that the peripapillary crescents contributed to both the absolute and relative components of the BS.

Knowledge of the likely field defects to be encountered in myopia will assist practitioners in their task of distinguishing between physiological and pathological fields in myopes. It is hoped to bring the clinical implication of this research to a wider audience through a series of publications based on this thesis.

In Chapter 8 methods for determining the true area of a retinal feature from its photographic image were presented, and compared with a commonly used method proposed by Littmann (1982 and 1988). A ray tracing method for estimating the equivalent power and optical configuration of a human eye from dimensions which can be measured easily was devised (see also appendix A2). This provided very interesting data concerning the optical components of human eyes in this sample. A more detailed evaluation of these data is to be undertaken. In addition a method is described whereby the magnification characteristics of any fundus camera can be investigated using a model eye. This is required if the absolute dimensions of a retinal feature are to be determined.

There is considerable intersubject variation in the areas of the optic disc parameters. All of which, including crescent size, increase with both increasing axial length and ocular refraction. A logarithmic transformation of the data demonstrated a linear relationship between these posterior pole structures and axial length and ocular refraction for the entire sample. In all cases correlation analysis gave values of R^2 above 0.6 for axial length only. Intercorrelation between the optic disc parameters was of a considerable degree between disc area and NRA only. Results also demonstrate the difficulty in using absolute values for the optic disc parameters as an indicator of pathology of the optic disc, and monitoring individual changes over time is probably more useful.

10.2 FUTURE WORK

As an extension of the work in Chapter 6, the use of different types of filters to remove

the inherent variability in visual field data is currently being investigated further. It may be useful to compare the pointwise differences between unfiltered and filtered visual field data of both normal and pathological visual fields. This may give more information about the variability at different locations within the field, and perhaps give an alternative measure of variability.

A more complex form of analysis (multivariate analysis) should be undertaken to ascertain which ocular factor (axial length, crescent size and/or ocular refraction) is most important in predicting field depression.

From the current study the trend of progressive field loss as myopia increases in an individual can not be ascertained. A longitudinal study of the visual field in myopes would be most useful in this regard. This type of study could in addition give information about changes in the optic disc parameters with the progression of myopia.

To confirm the results from Chapter 9 it would be very interesting to perform some kind of fundus perimetry. If the area of the retina being stimulated could be visualised, it would be possible to directly identify those structures giving rise to relative and absolute scotomas in the BS region in both non-myopic and myopic subjects.

Other fundus imaging devices are at present being investigated with the model eye. This will provide clinicians and researchers using these instruments with invaluable information, which is otherwise unavailable, regarding their magnification properties.

APPENDICES

APPENDIX A1

A1.1 VISUAL FIELD ANALYSIS

Supplementary results for the field regions from Chapter 7. Summary from the one way ANOVA for the axial length and ocular refraction categories.

axial length groups

- groups i and ii did not differ for any field region
- subjects in groups iv, v and vi were significantly different from groups i, ii and iii for all field regions ($p<0.01$)
- comparison of group iii with groups i and ii gave significant differences for the majority of field regions ($p<0.01$)
- differences between groups iv, v and vi were varied and not significant in most cases, but comparisons will be affected by the small number of subjects in these groups.

ocular refraction groups

- groups A and B did not differ for any field region
- subjects in groups D and E were significantly different from the other three groups for all field regions ($p<0.01$)
- comparison of group C with groups A and B gave significant differences for the majority of field regions ($p<0.05$)
- groups, D and E differed significantly in all cases ($p<0.01$), except for the outer annulus.

Correlation and linear regression analysis for subjects with axial lengths above 26mm and more than 5D of myopia are given in table A1.1.

Table A1.1 Summary of the results of correlation and linear regression for global indices and regional mean sensitivities against axial length and ocular refraction. In all cases p <<0.01.

	Subjects with axial length greater than 26mm		Subjects with ocular refraction above 5D of myopia	
Global indices	**R^2**	**gradient dB/mm**	**R^2**	**gradient dB/D**
MS	0.61	-0.89	0.66	+0.51
MD	0.65	-0.90	0.64	+0.48
PSD	0.41	+0.22	0.40	-0.12
CPSD	0.40	+0.25	0.37	-0.14
Field regions				
fovea	0.30	-0.51	0.25	0.28
Annuli				
inner	0.71	-0.94	0.61	+0.47
middle	0.66	-0.88	0.68	+0.50
outer	0.27	-1.00	0.31	+0.60
Quadrants				
upper-temporal	0.49	-0.97	0.53	+0.55
upper-nasal	0.50	-0.85	0.59	+0.51
lower-temporal	0.68	-1.04	0.64	+0.57
lower-nasal	0.57	-0.80	0.65	+0.47
Sectors				
superior	0.36	-0.81	0.47	+0.51
inferior	0.57	-0.79	0.64	+0.47
nasal	0.53	-0.89	0.59	0.52
temporal	0.52	-1.07	0.54	0.61

A1.2 EXAMPLES OF FUNDUS PHOTOGRAPHS AND CORRESPONDING VISUAL FIELD PLOTS.

The following examples illustrate the 30-2 program, and on the facing page a merged printout of the 30-1 and 30-2 programs together with the corresponding fundus photograph.

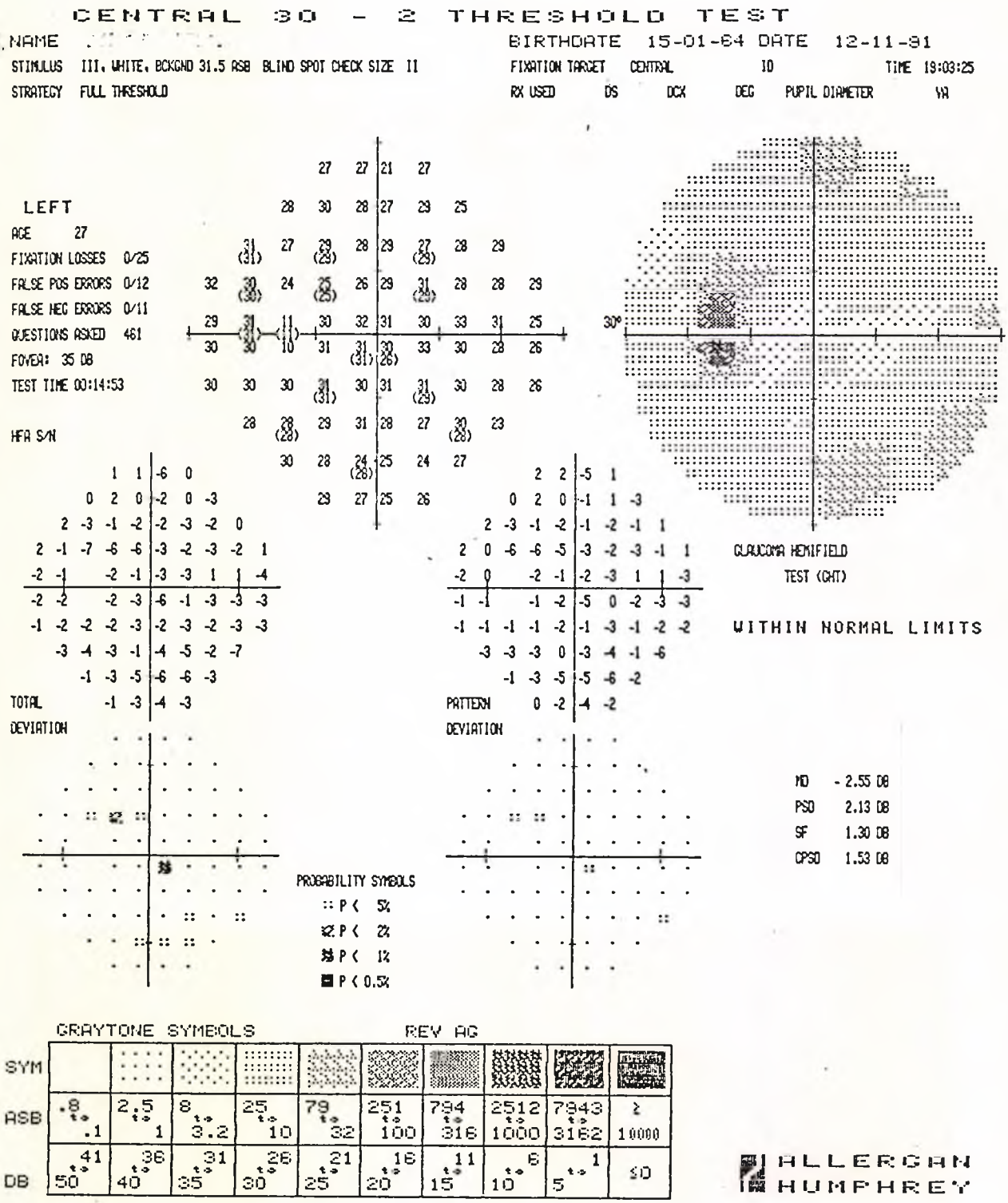

SUBJECT 1: Axial length = 27.07mm; Ocular refraction = -4.57D

MRG-C30-2,C30-1 THRESHOLD TEST

STIMULUS III, WHITE, BCKGND 31.5 ASB NAME
BLIND SPOT CHECK SIZE II ID BIRTHDATE 15-01-64
FIXATION TARGET CENTRAL
STRATEGY FULL THRESHOLD

REFERENCE DATES

C30-1, 12-11-91
C30-2, 12-11-91

FOVEA: 35 DB

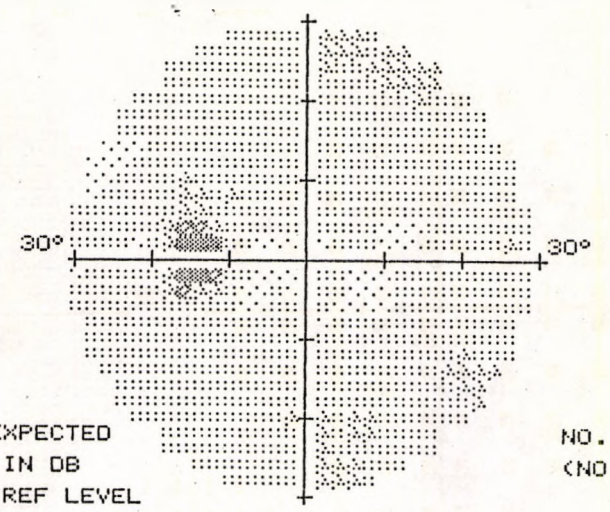

° = WITHIN 4 DB OF EXPECTED
NO. = DEFECT DEPTH IN DB
36 DB = CENTRAL REF LEVEL

NO. = THRESHOLD IN DB
(NO.) = 2ND TIME

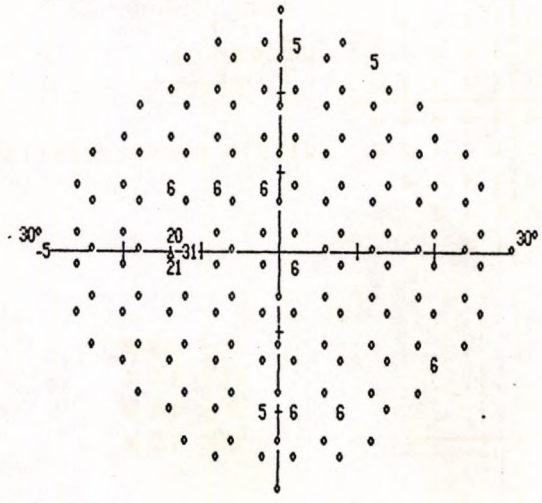

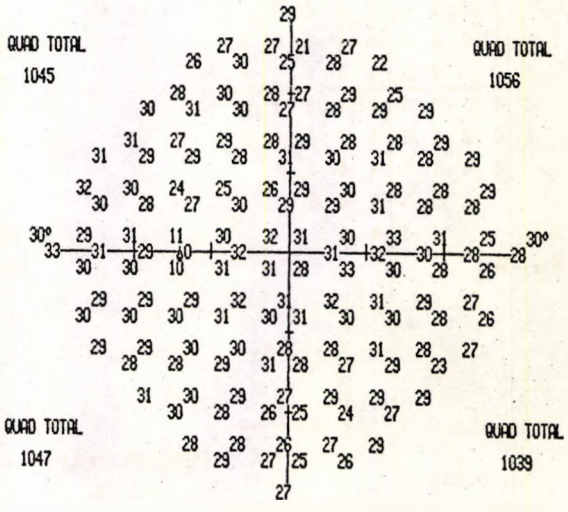

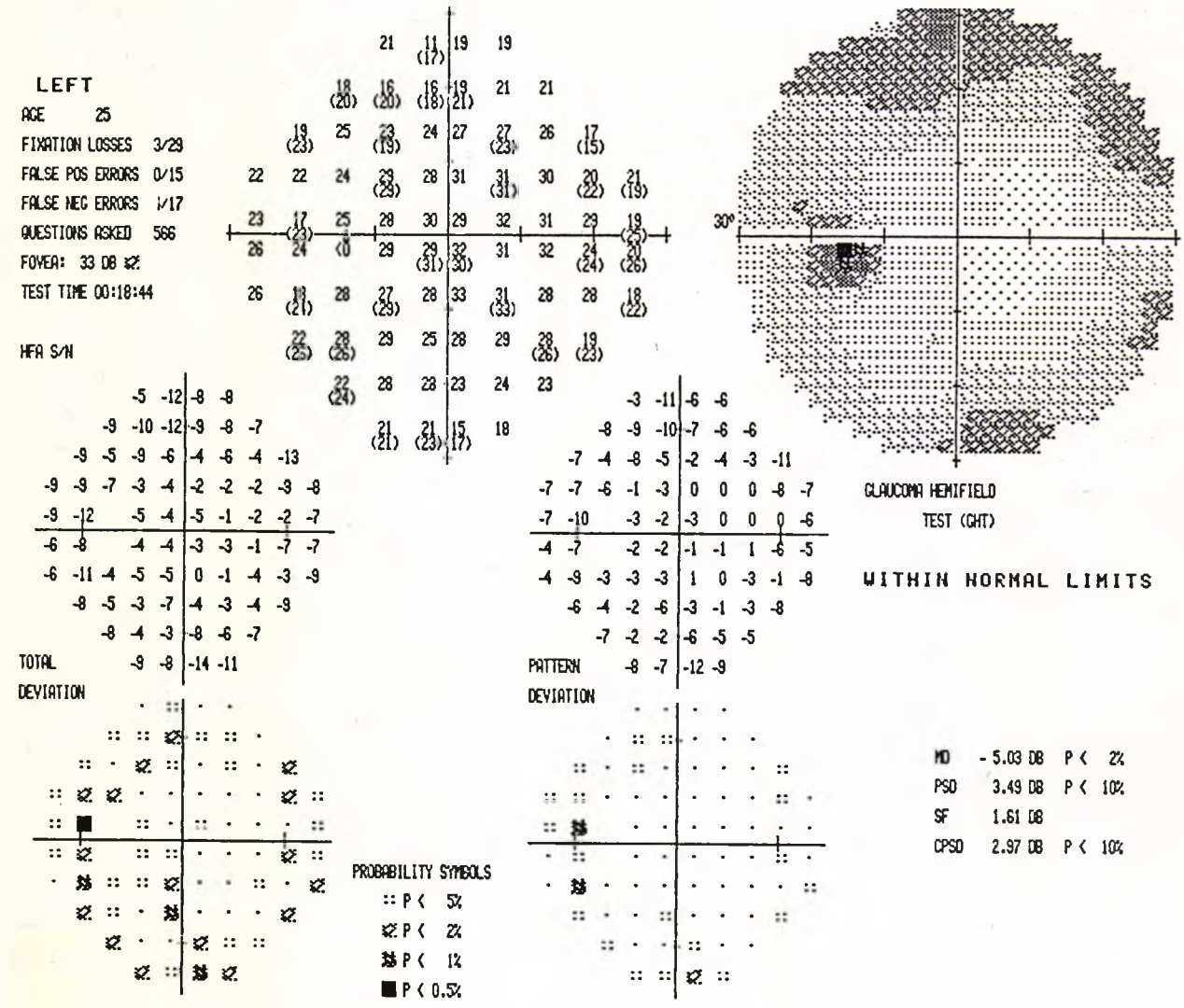

SUBJECT 2: Axial length = 29.42mm; Ocular refraction = -9.46D

MRG-C30-2, C30-1 THRESHOLD TEST

2 STIMULUS III, WHITE, BCKGND 31.5 ASB NAME
BLIND SPOT CHECK SIZE II ID BIRTHDATE 18-07-66
FIXATION TARGET CENTRAL
STRATEGY FULL THRESHOLD

REFERENCE DATES

C30-1, 13-12-91
C30-2, 13-12-91

FOVEA: 34 DB

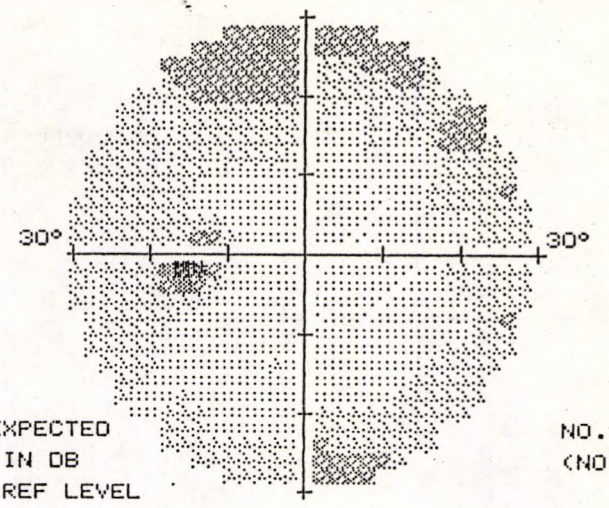

LEFT

° = WITHIN 4 DB OF EXPECTED
NO. = DEFECT DEPTH IN DB
35 DB = CENTRAL REF LEVEL

NO. = THRESHOLD IN DB
(NO.) = 2ND TIME

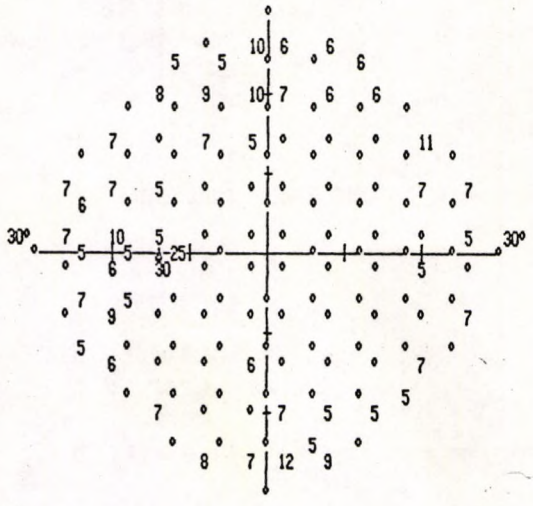

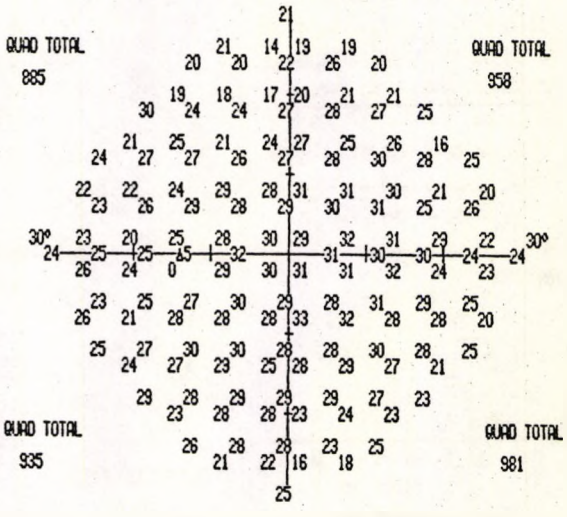

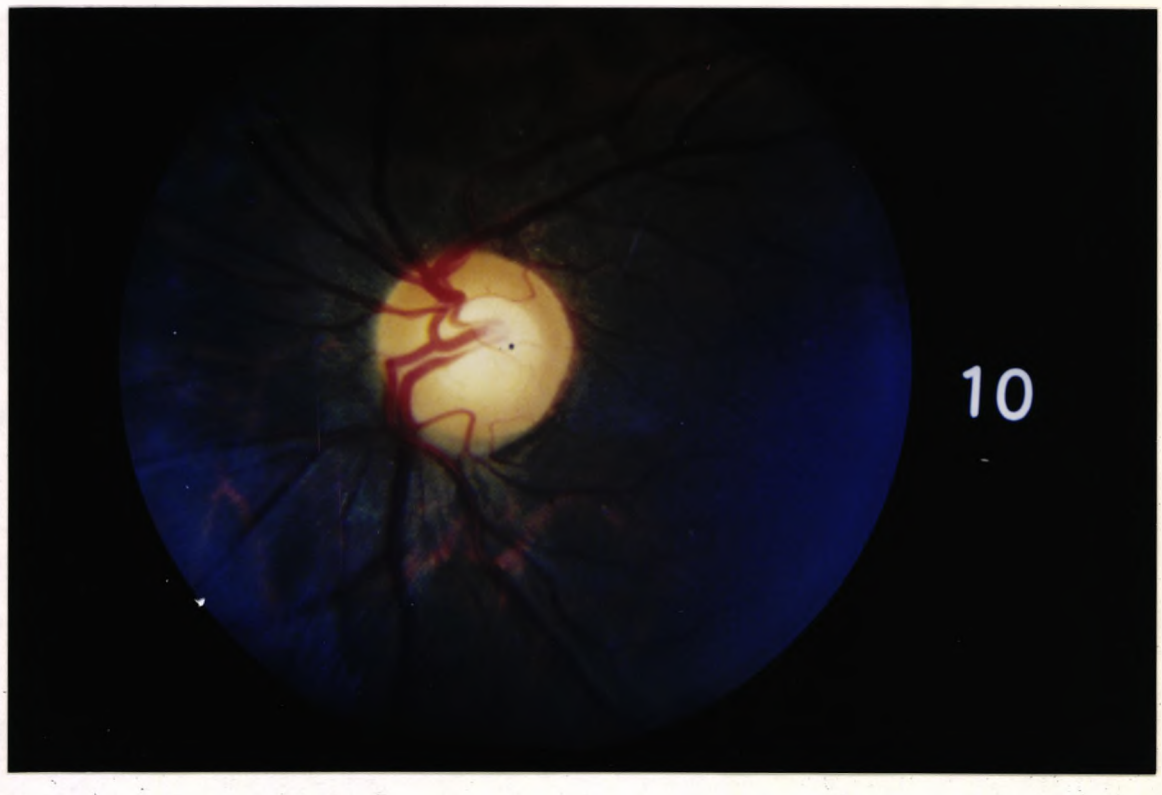

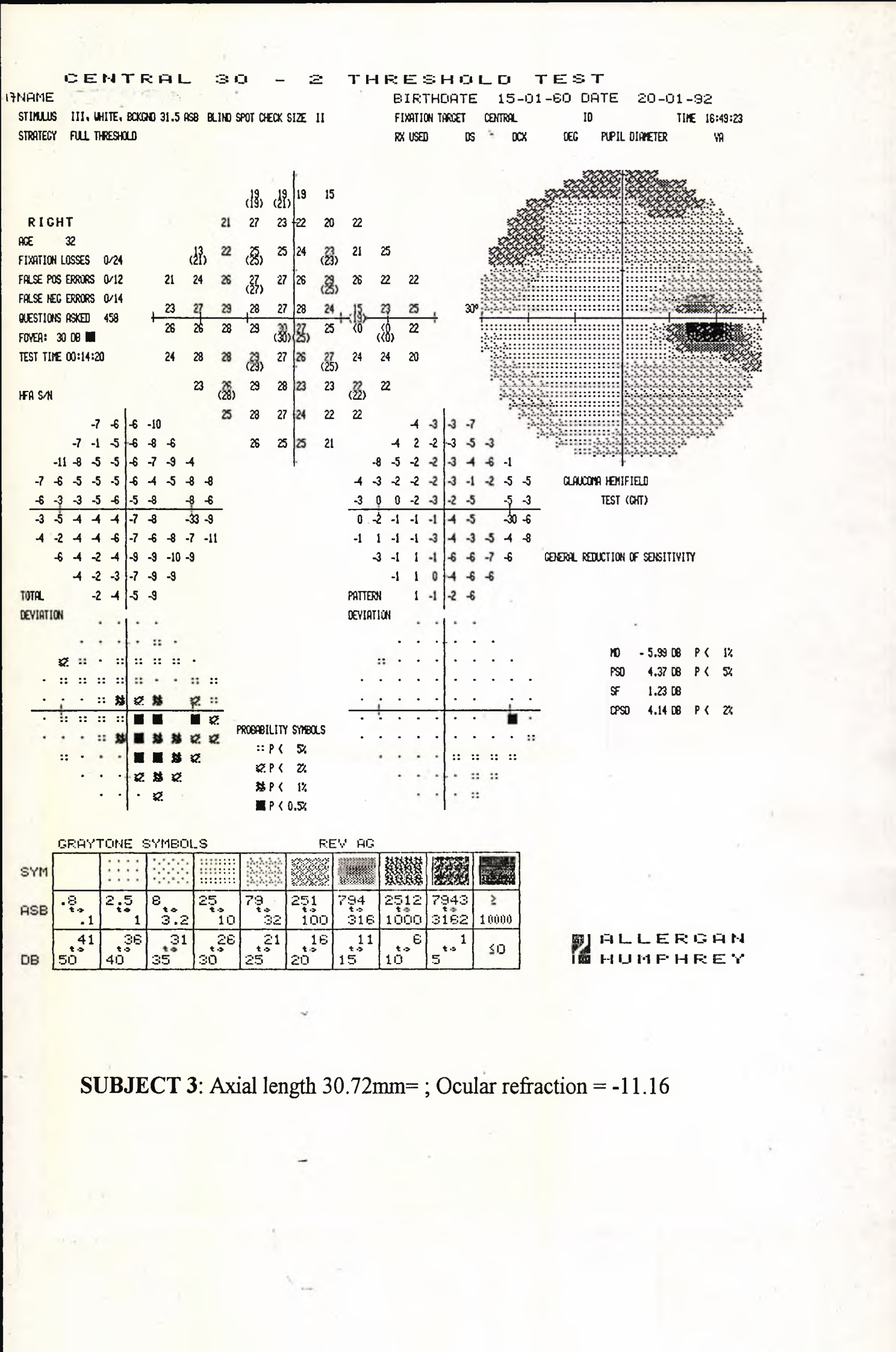

SUBJECT 3: Axial length 30.72mm= ; Ocular refraction = -11.16

ARG-C30-2,C30-1 THRESHOLD TEST

STIMULUS III, WHITE, BCKGND 31.5 ASB NAME
BLIND SPOT CHECK SIZE II ID BIRTHDATE 15-01-60
FIXATION TARGET CENTRAL
STRATEGY FULL THRESHOLD

REFERENCE DATES
C30-1, 20-01-92
C30-2, 20-01-92

RIGHT

FOVEA: 30 DB

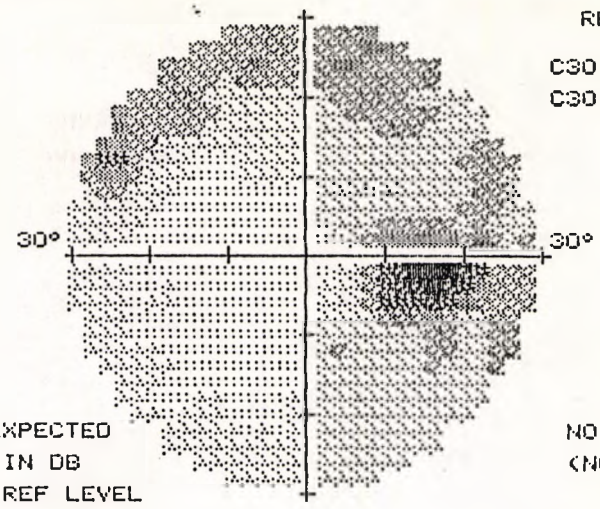

° = WITHIN 4 DB OF EXPECTED
NO. = DEFECT DEPTH IN DB
33 DB = CENTRAL REF LEVEL

NO. = THRESHOLD IN DB
(NO.) = 2ND TIME

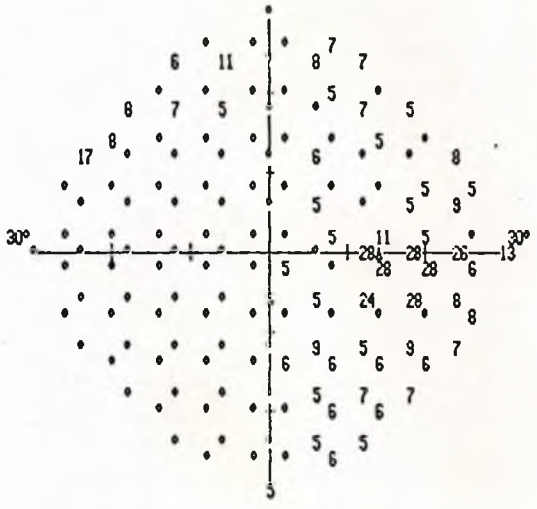

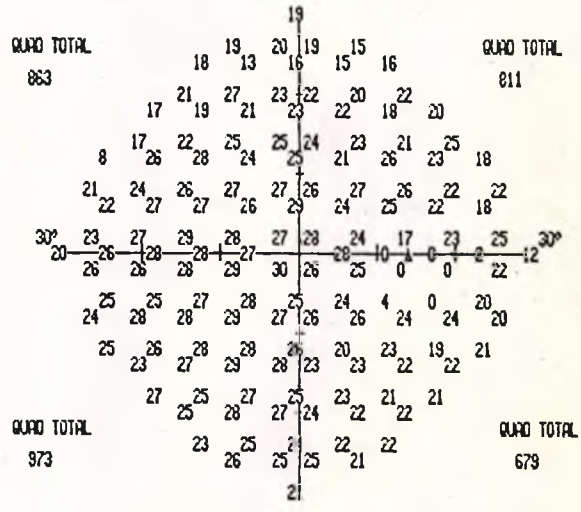

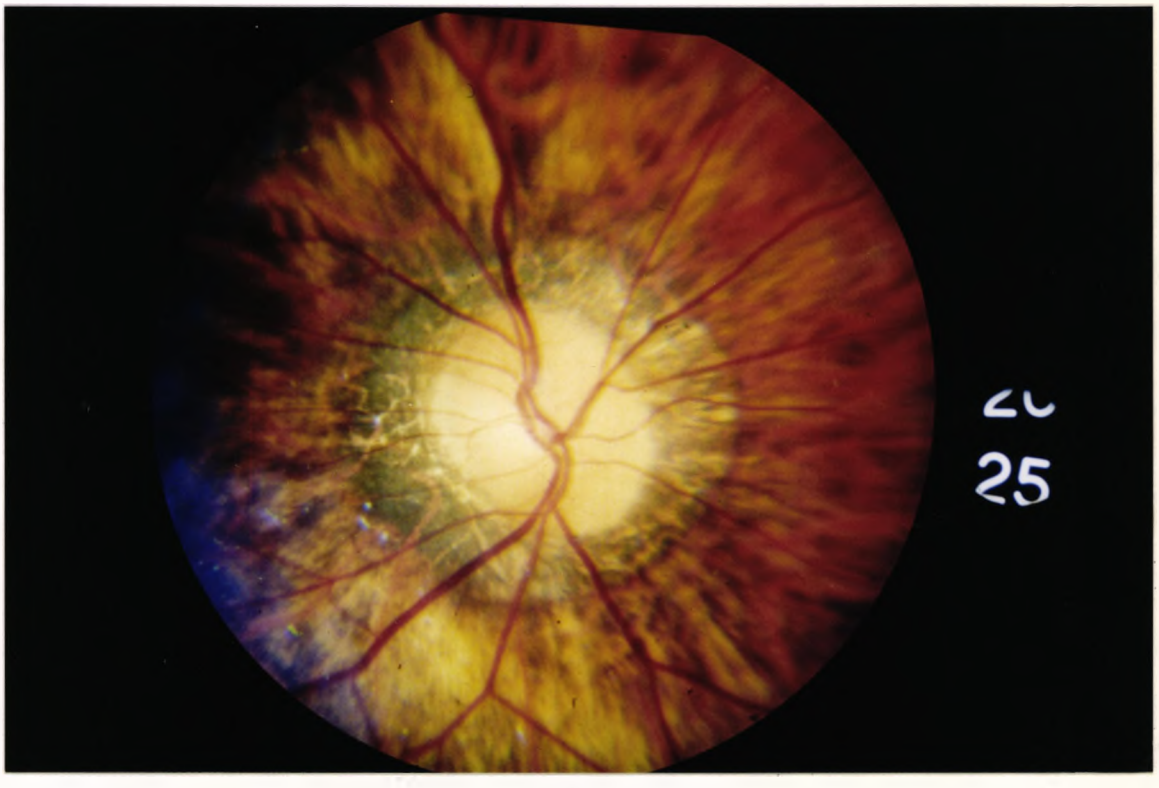

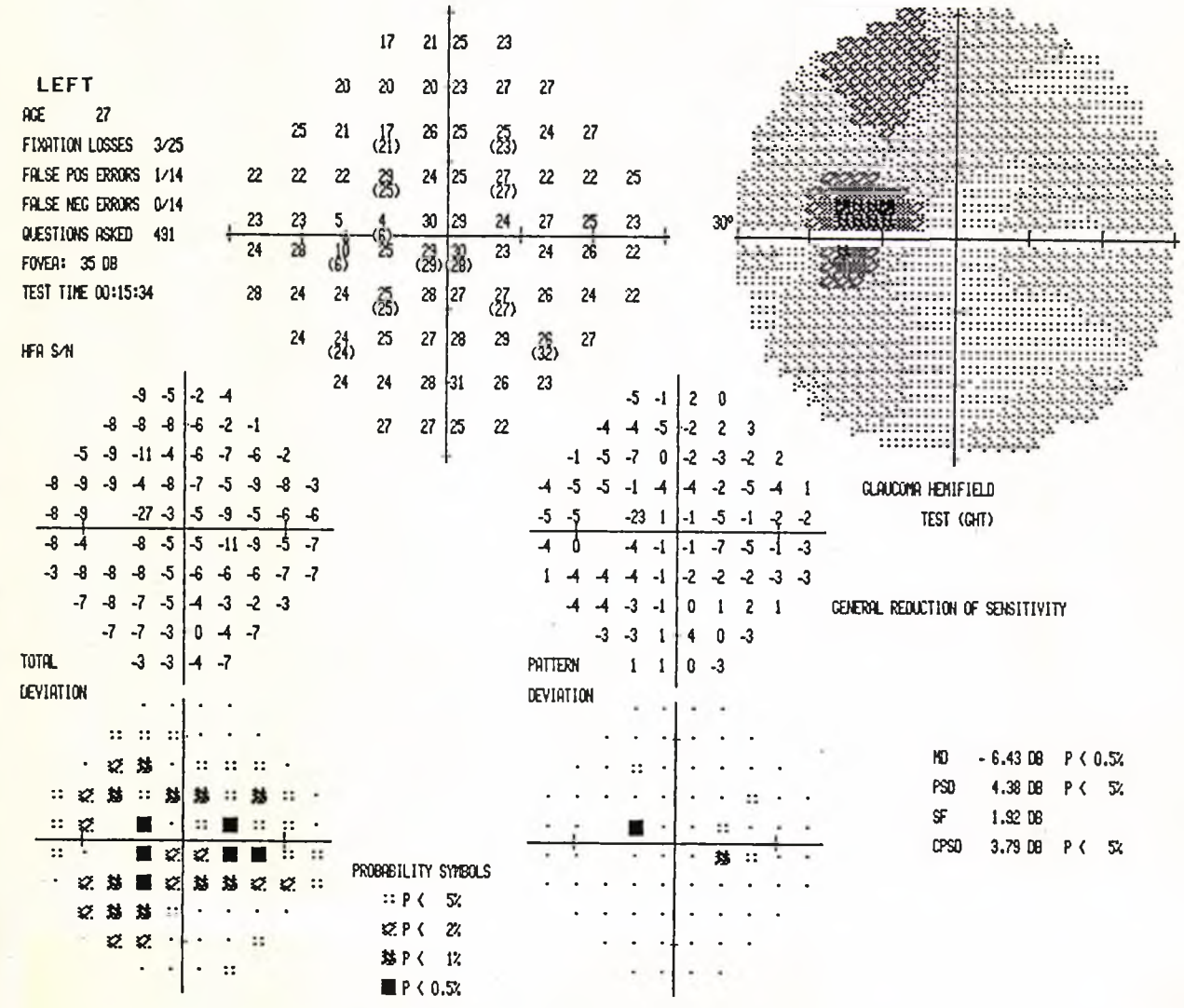

GRAYTONE SYMBOLS REV AG

SYM										
ASB	.8 to .1	2.5 to 1	8 to 3.2	25 to 10	79 to 32	251 to 100	794 to 316	2512 to 1000	7943 to 3162	≥ 10000
DB	41 to 50	36 to 40	31 to 35	26 to 30	21 to 25	16 to 20	11 to 15	6 to 10	1 to 5	≤0

ALLERGAN HUMPHREY

SUBJECT 4: Axial length = 31.37mm; Ocular refraction = -17.36.

MRG-C30-2,C30-1 THRESHOLD TEST

.4STIMULUS III, WHITE, BCKGND 31.5 ASB NAME
BLIND SPOT CHECK SIZE II ID BIRTHDATE 12-01-65
FIXATION TARGET CENTRAL
STRATEGY FULL THRESHOLD

REFERENCE DATES

C30-1, 27-03-92
C30-2, 27-03-92

LEFT

FOVEA: 34 DB

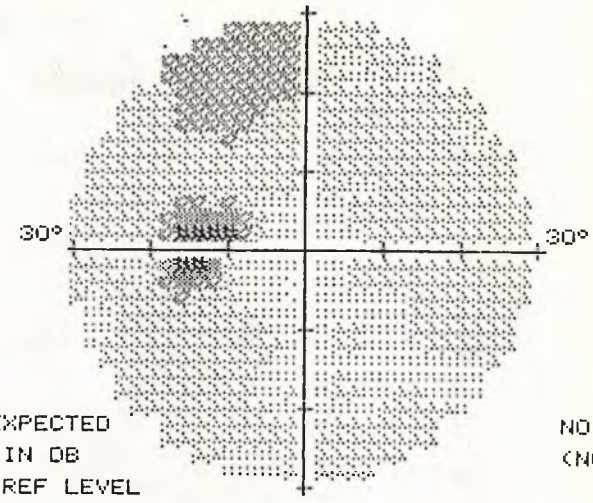

° = WITHIN 4 DB OF EXPECTED
NO. = DEFECT DEPTH IN DB
31 DB = CENTRAL REF LEVEL

NO. = THRESHOLD IN DB
(NO.) = 2ND TIME

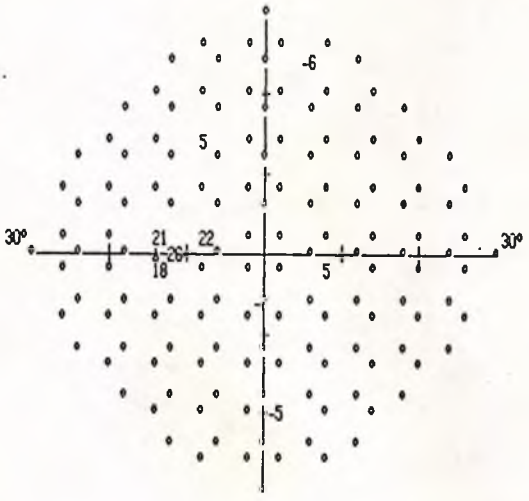

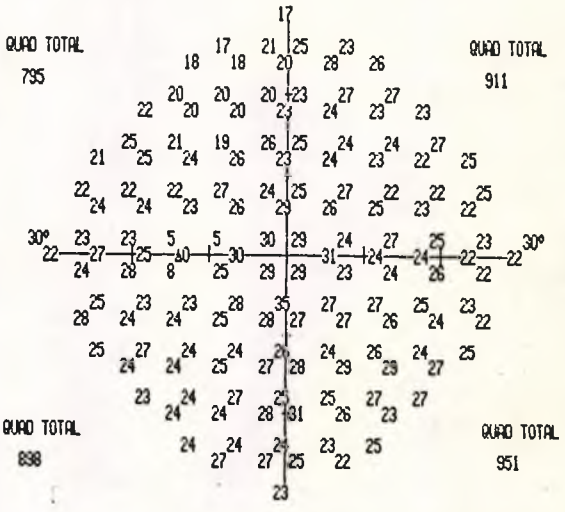

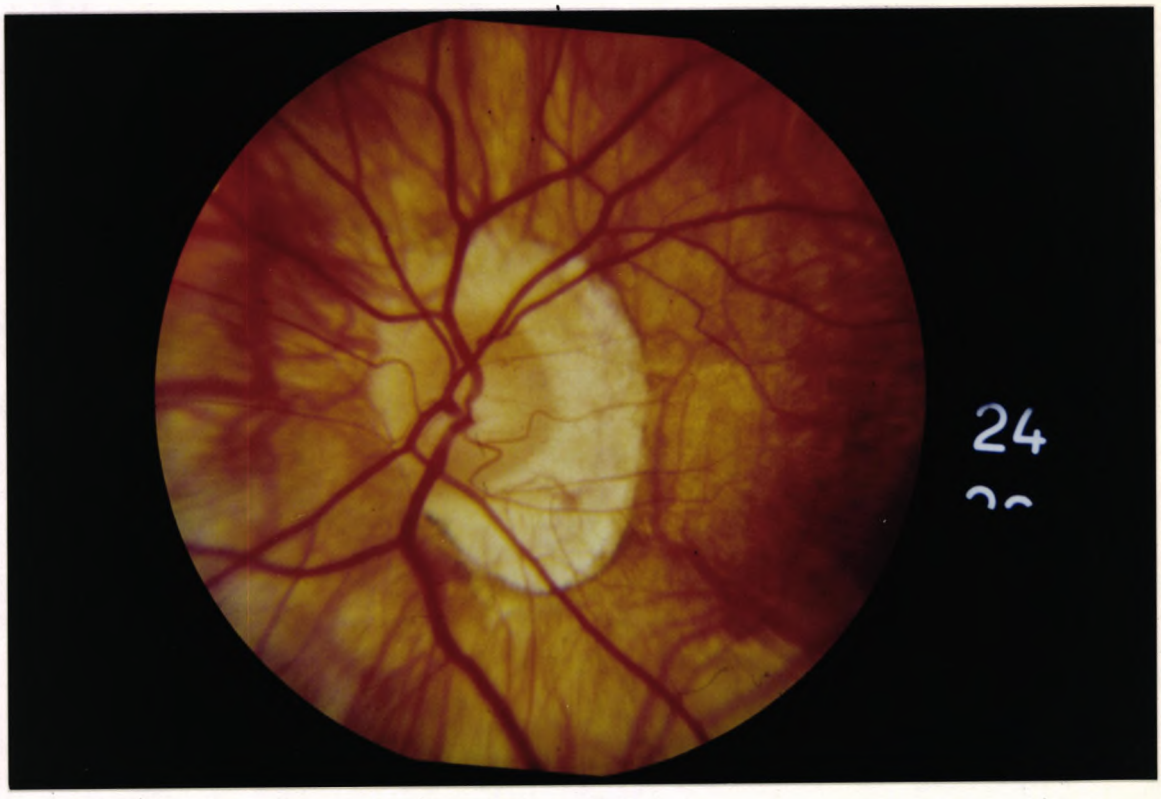

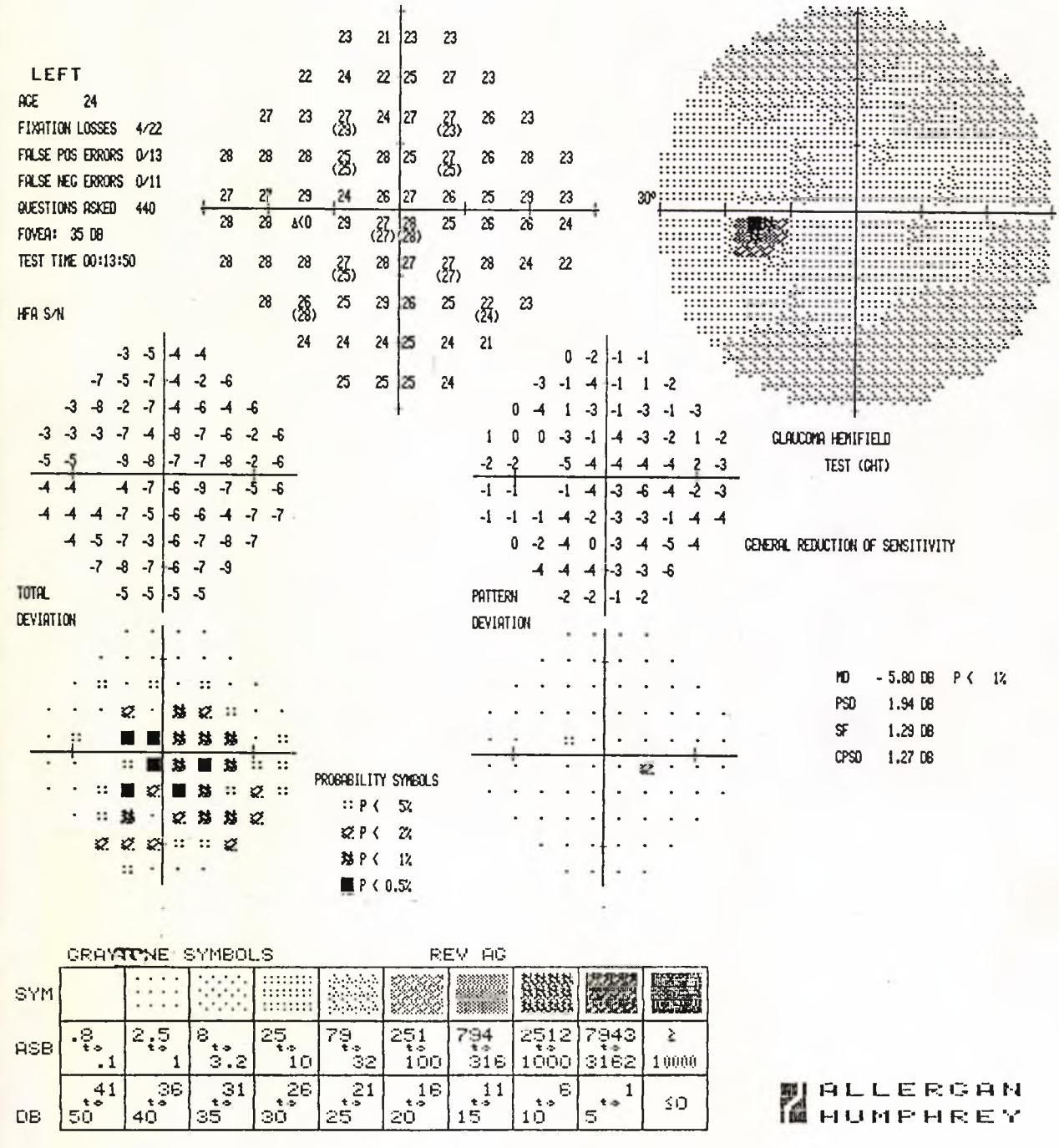

SUBJECT 5: Axial length 32.01mm= ; Ocular refraction = -15.88D.

MRG-C30-2,C30-1 THRESHOLD TEST

5 STIMULUS III, WHITE, BCKGND 31.5 ASB NAME
BLIND SPOT CHECK SIZE II ID BIRTHDATE 01-05-87
FIXATION TARGET CENTRAL
STRATEGY FULL THRESHOLD

REFERENCE DATES

C30-1, 12-11-91
C30-2, 12-11-91

FOVEA: 34 DB

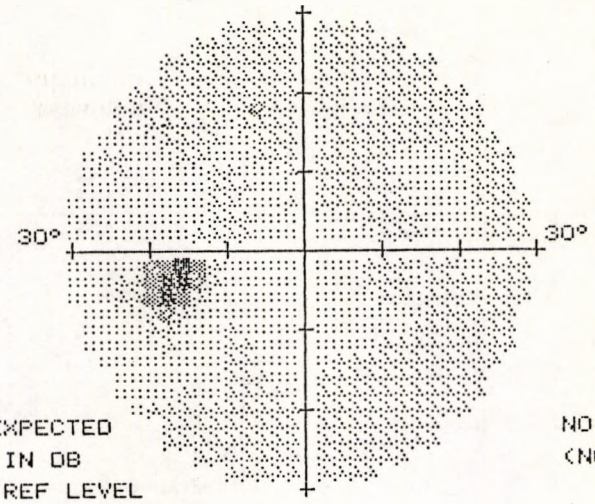

LEFT

° = WITHIN 4 DB OF EXPECTED
NO. = DEFECT DEPTH IN DB
32 DB = CENTRAL REF LEVEL

NO. = THRESHOLD IN DB
(NO.) = 2ND TIME

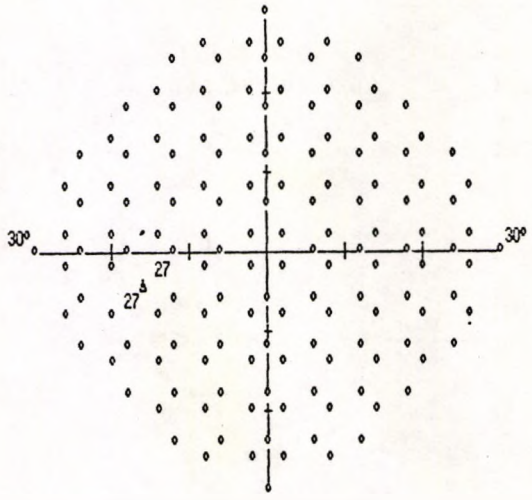

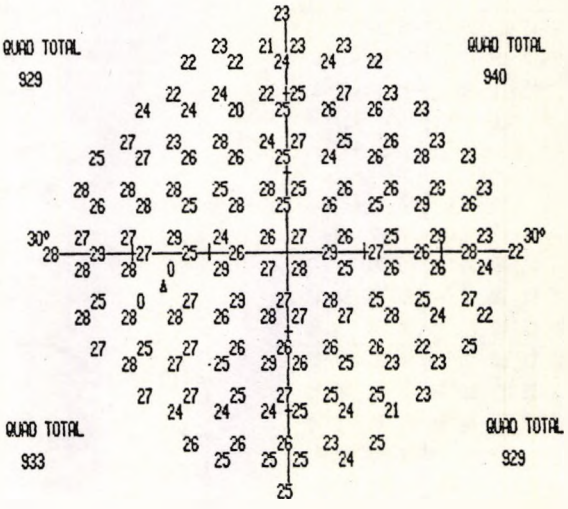

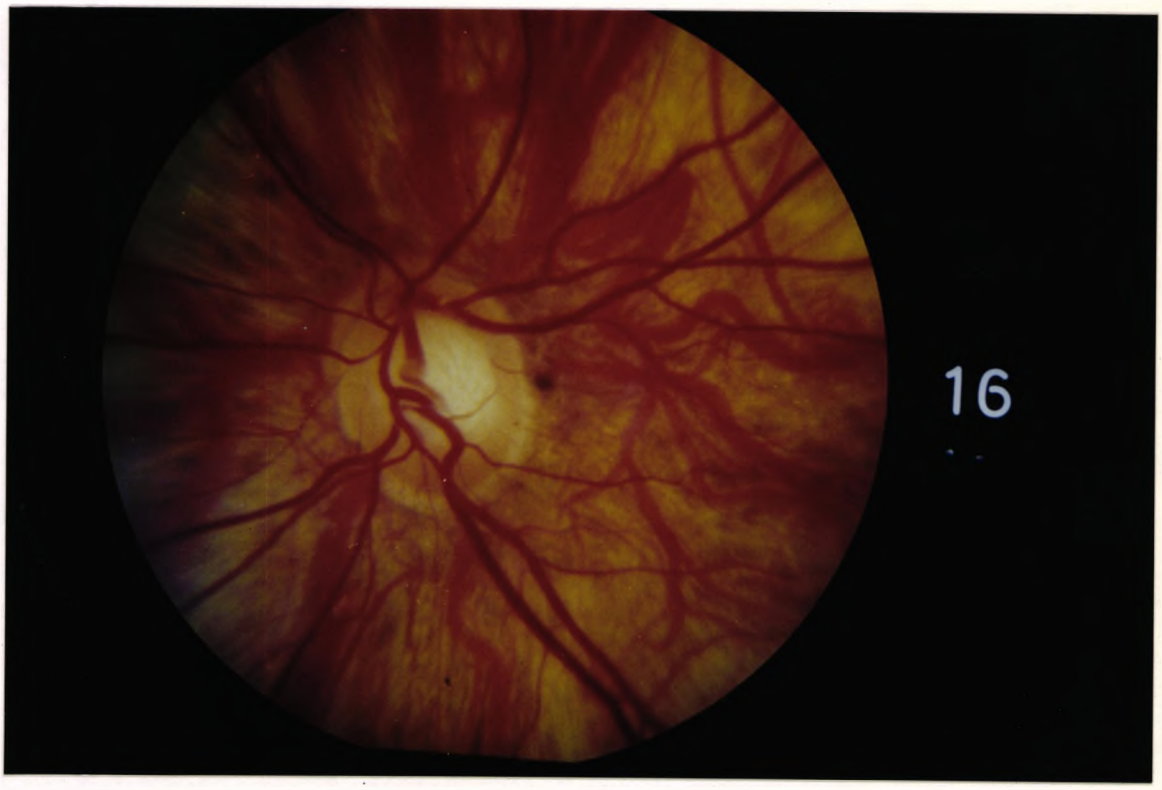

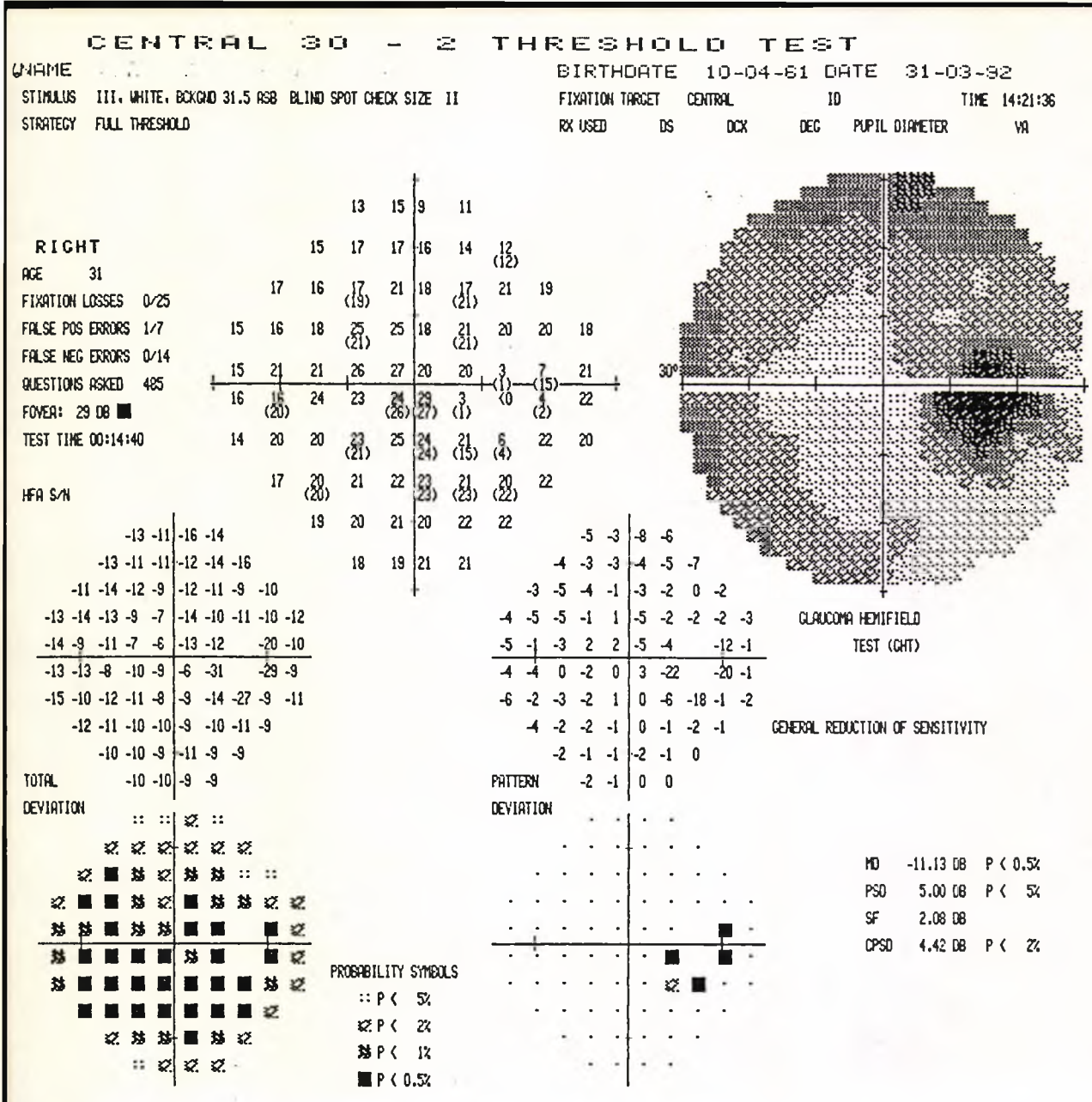

SUBJECT 6: Axial length = 34.60mm; Ocular refraction = -20.25.

MRG-C30-1,C30-2 THRESHOLD TEST

6 STIMULUS III, WHITE, BCKGND 31.5 ASB NAME
BLIND SPOT CHECK SIZE II ID BIRTHDATE 10-04-61
FIXATION TARGET CENTRAL
STRATEGY FULL THRESHOLD

RIGHT

REFERENCE DATES
C30-2, 31-03-92
C30-1, 31-03-92

FOVEA: 30 DB

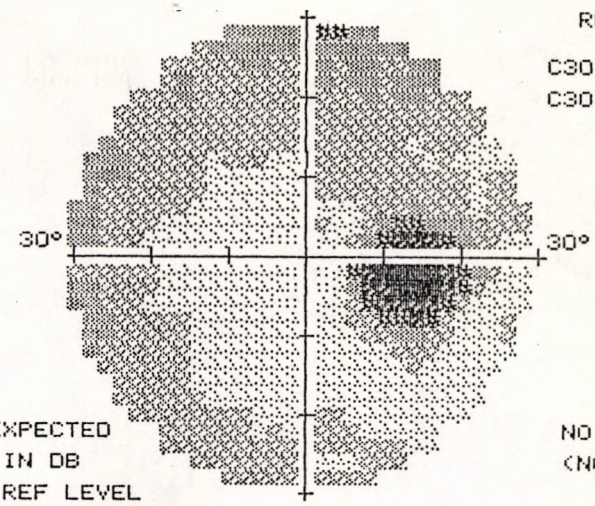

° = WITHIN 4 DB OF EXPECTED
NO. = DEFECT DEPTH IN DB
28 DB xx = CENTRAL REF LEVEL

NO. = THRESHOLD IN DB
(NO.) = 2ND TIME

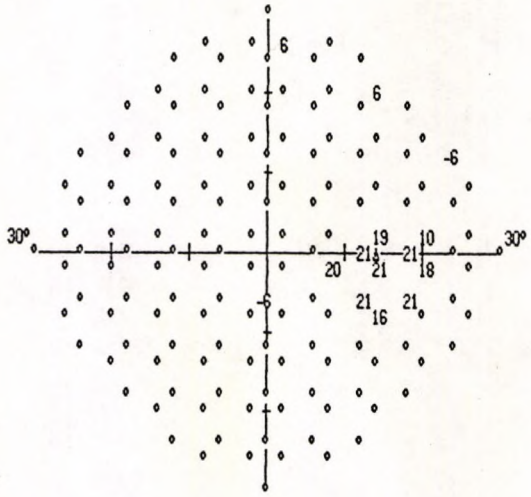

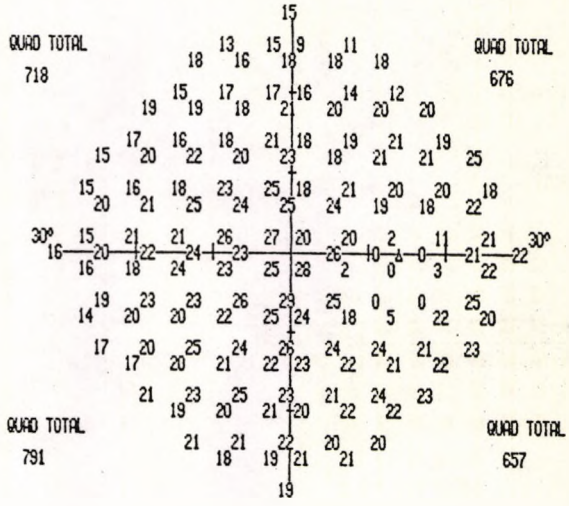

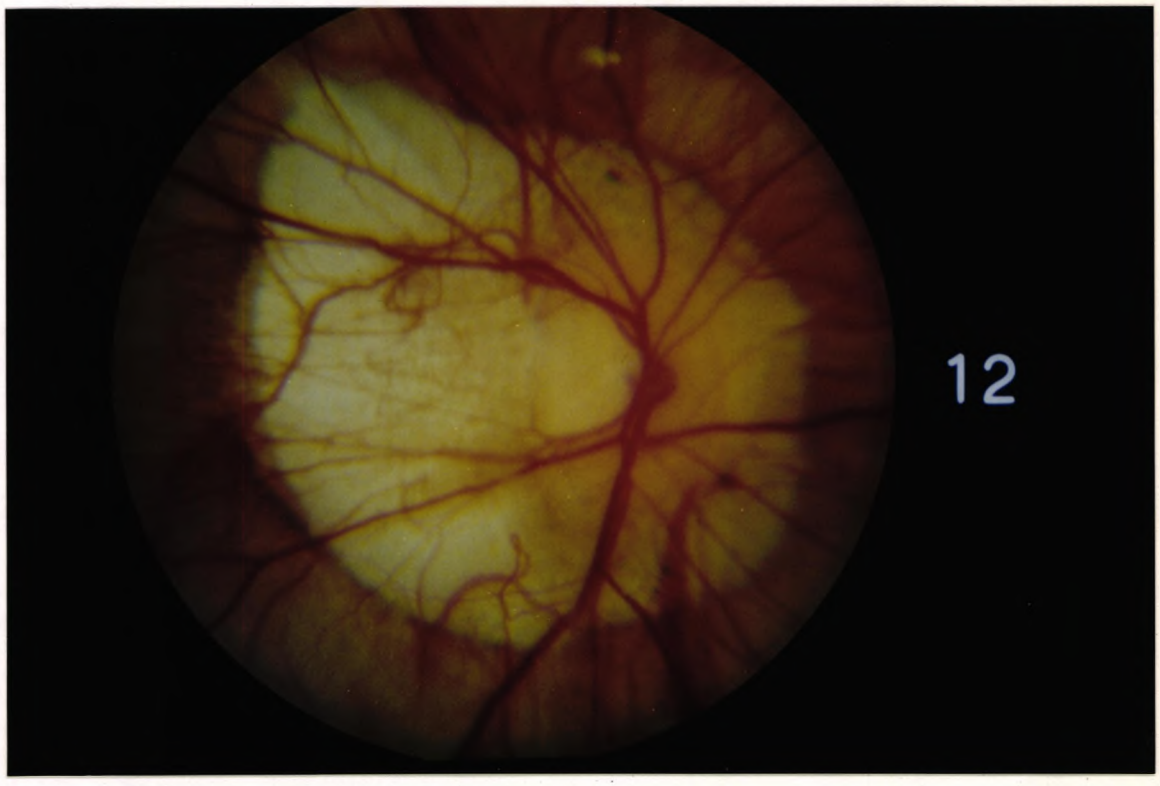

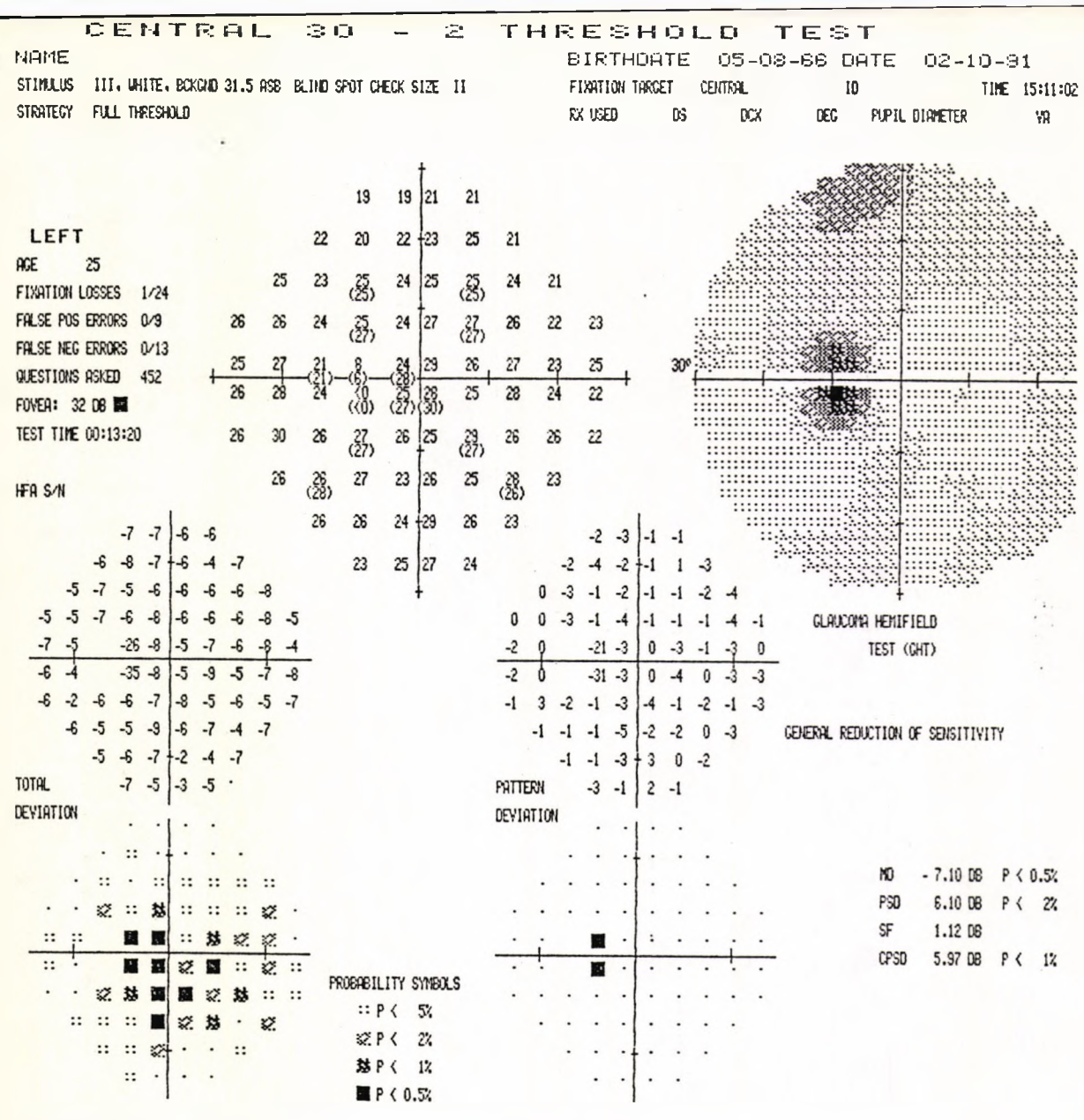

SUBJECT 7: Axial length 32.12mm; Ocular refraction -14.36D

+ ARG-C30-2,C30-1 THRESHOLD TEST

STIMULUS III, WHITE, BCKGND 31.5 ASB NAME
BLIND SPOT CHECK SIZE II ID BIRTHDATE 05-08-66
FIXATION TARGET CENTRAL
STRATEGY FULL THRESHOLD

REFERENCE DATES

C30-1, 02-10-91
C30-2, 02-10-91

FOVEA: 32 DB

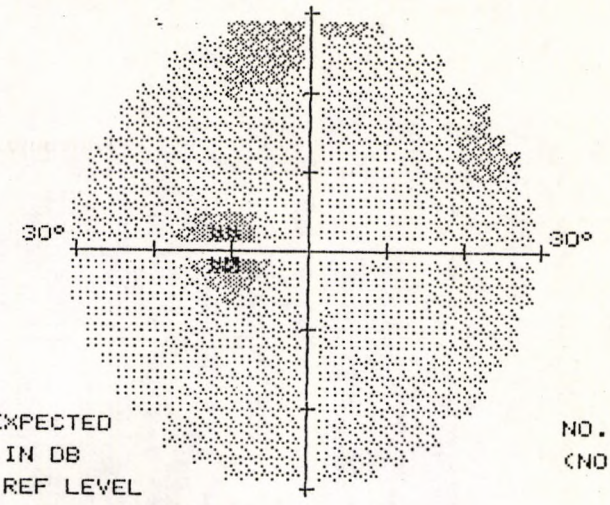

LEFT

° = WITHIN 4 DB OF EXPECTED
NO. = DEFECT DEPTH IN DB
33 DB = CENTRAL REF LEVEL

NO. = THRESHOLD IN DB
(NO.) = 2ND TIME

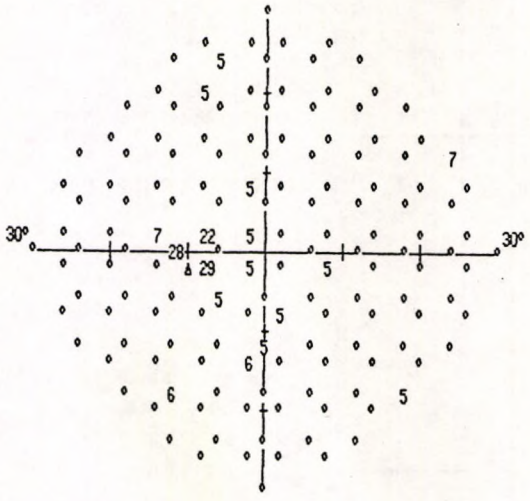

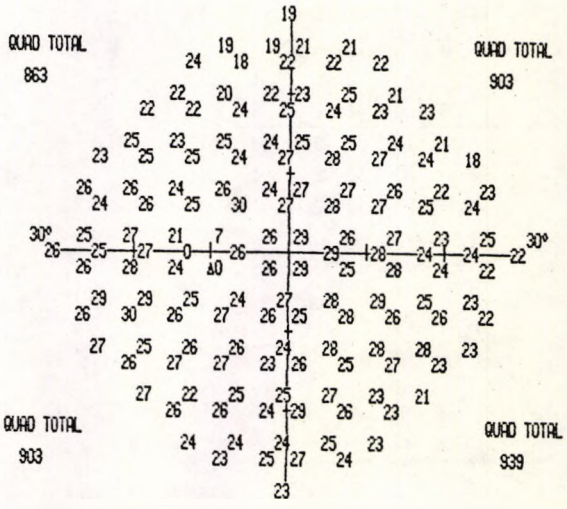

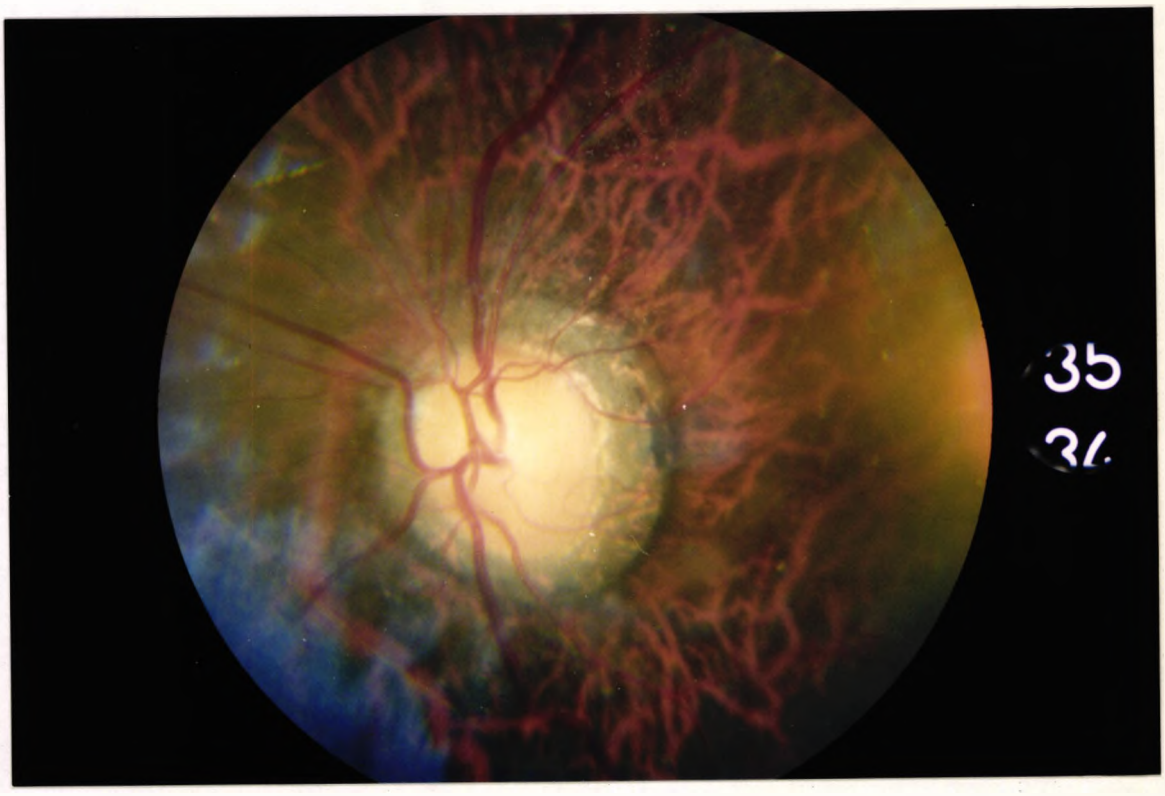

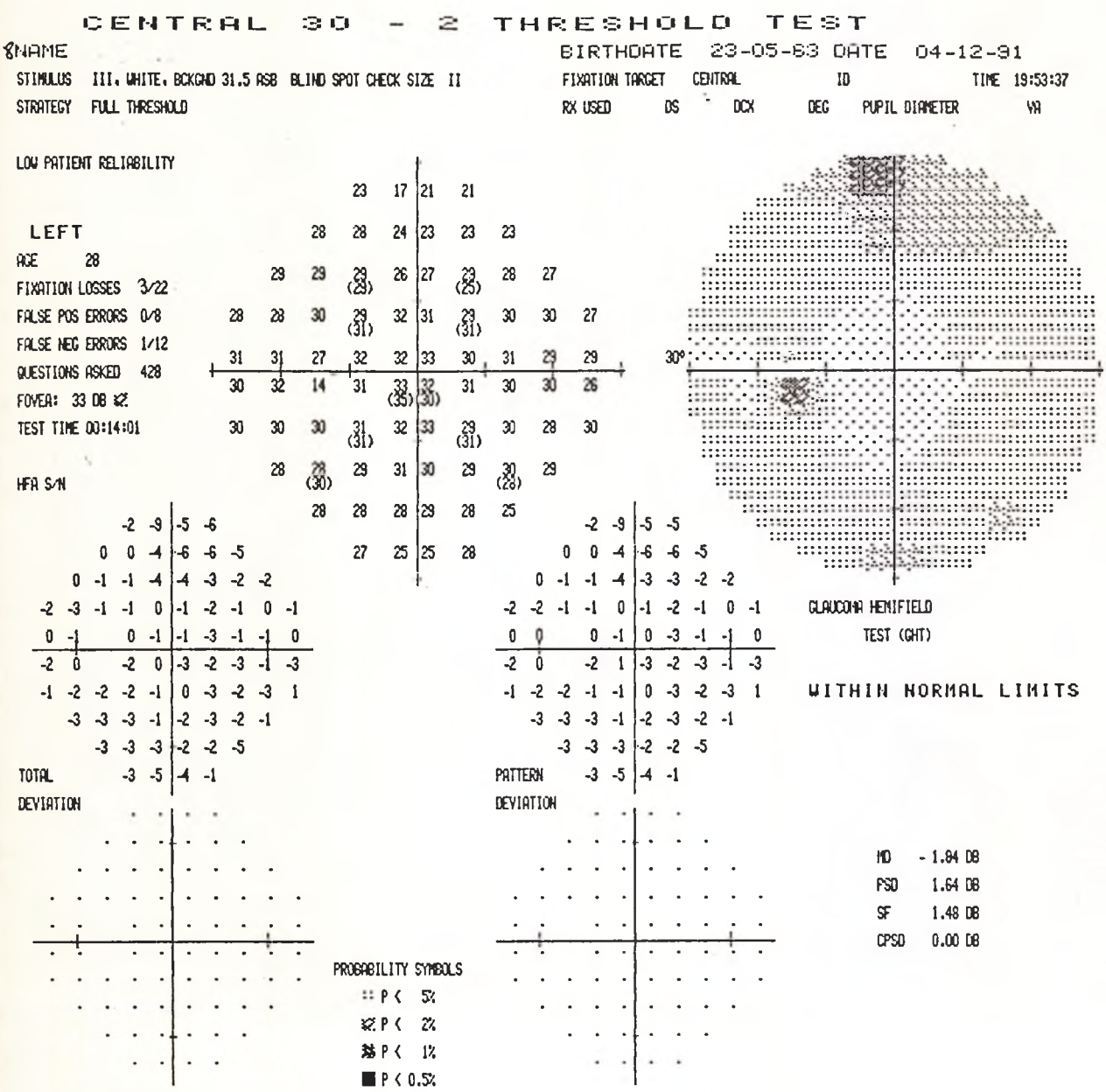

SUBJECT 8: Axial length = 26.25mm; Ocular refraction = -12.37D.

MRG-C30-2, C30-1 THRESHOLD TEST

STIMULUS III, WHITE, BCKGND 31.5 ASB NAME
BLIND SPOT CHECK SIZE II ID BIRTHDATE 23-05-63
FIXATION TARGET CENTRAL
STRATEGY FULL THRESHOLD

REFERENCE DATES

C30-1, 04-12-91
C30-2, 04-12-91

FOVEA: 34 DB

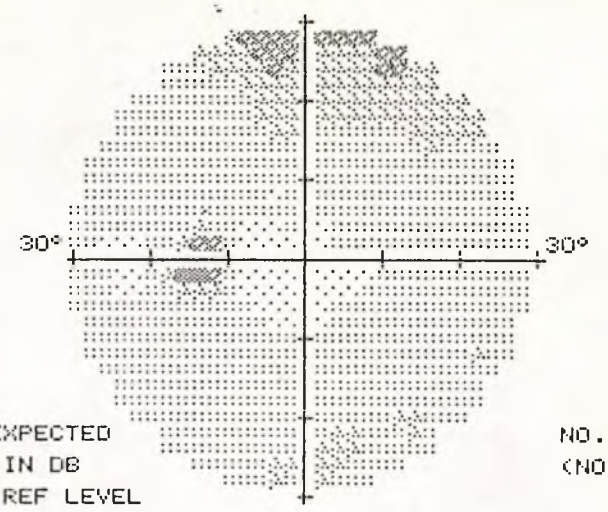

LEFT

° = WITHIN 4 DB OF EXPECTED
NO. = DEFECT DEPTH IN DB
34 DB = CENTRAL REF LEVEL

NO. = THRESHOLD IN DB
(NO.) = 2ND TIME

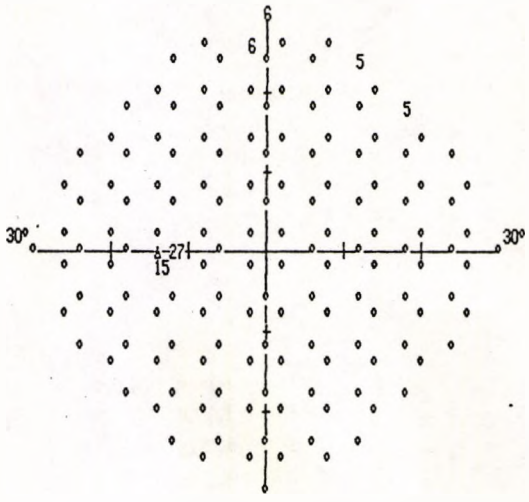

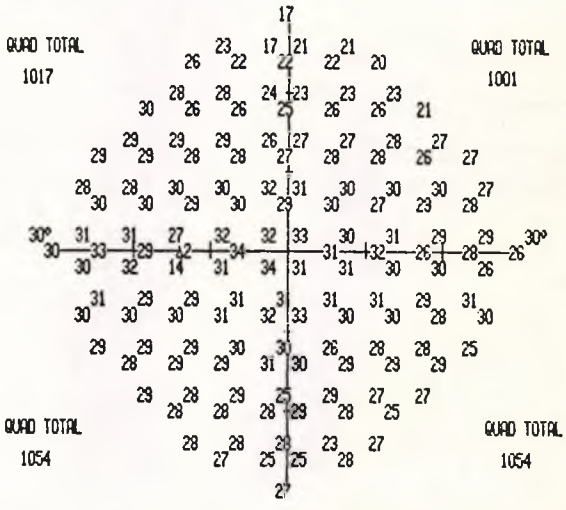

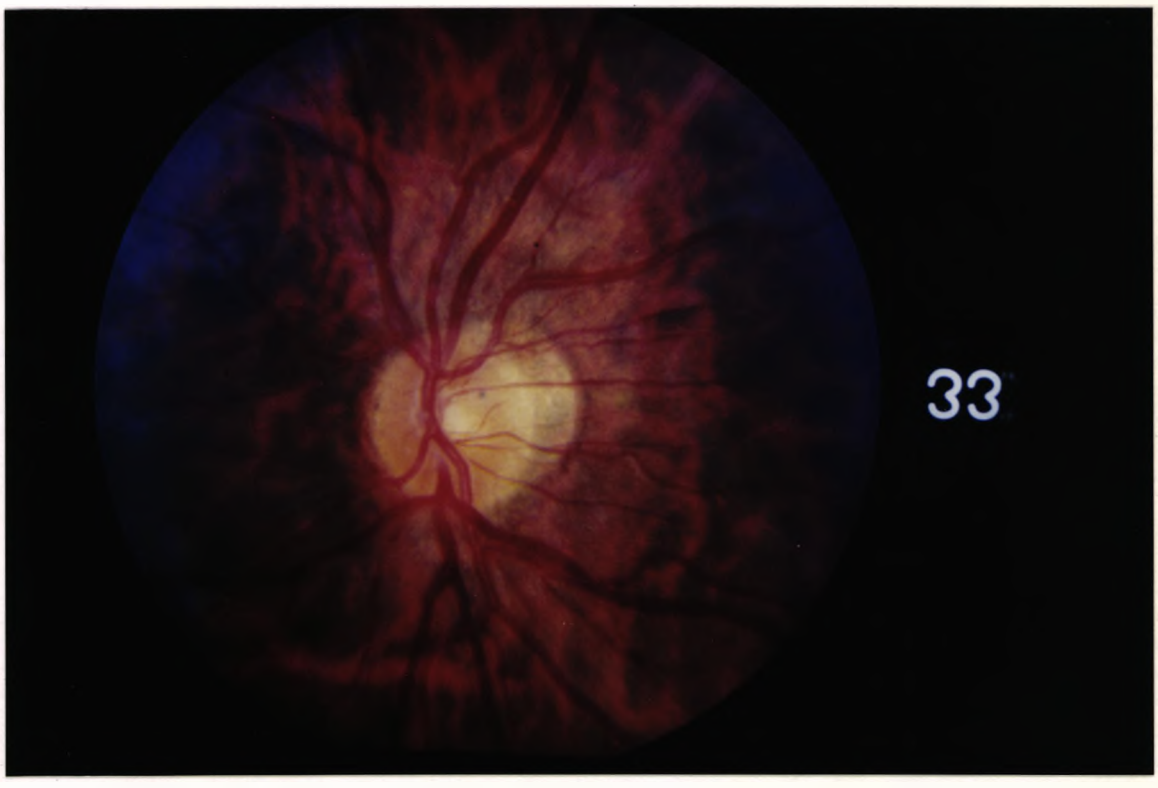

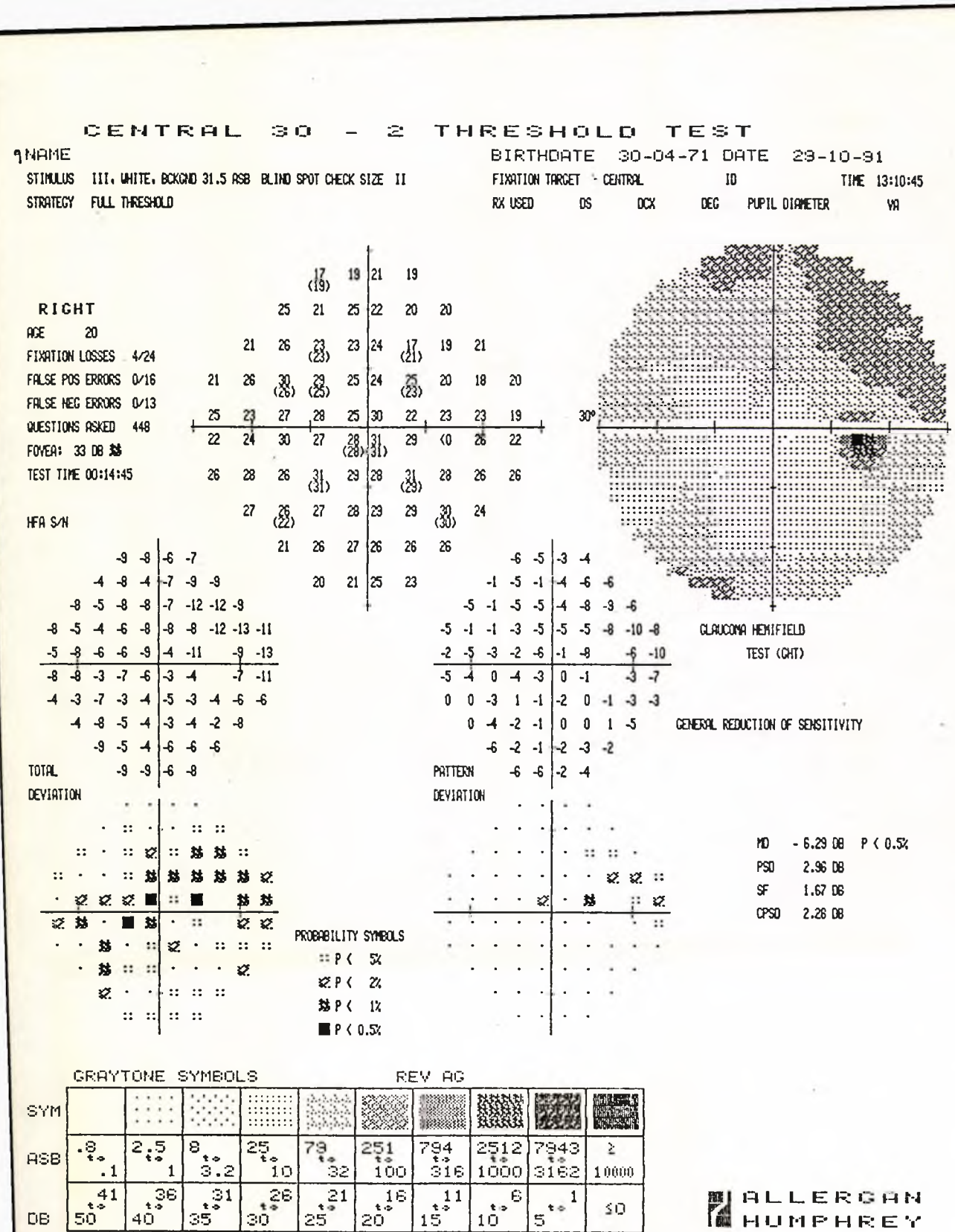

SUBJECT 9: Axial length = 27.01mm; Ocular refraction = -4.02D.

MRG-C30-2,C30-1 THRESHOLD TEST

¶STIMULUS III, WHITE, BCKGND 31.5 ASB NAME
BLIND SPOT CHECK SIZE II ID BIRTHDATE 30-04-71
FIXATION TARGET CENTRAL
STRATEGY FULL THRESHOLD

REFERENCE DATES
C30-1, 29-10-91
C30-2, 29-10-91

RIGHT

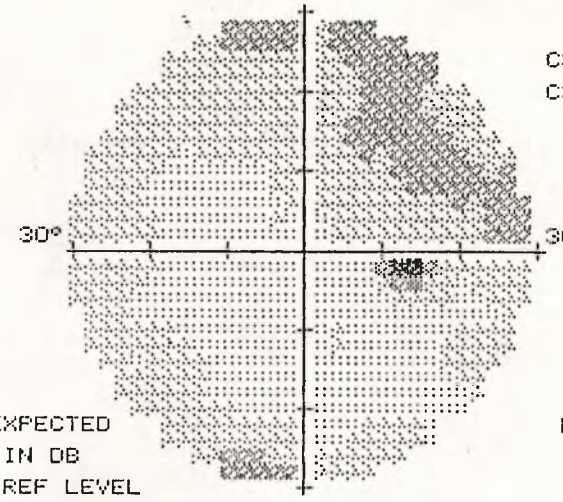

FOVEA: 33 DB

° = WITHIN 4 DB OF EXPECTED
NO. = DEFECT DEPTH IN DB
34 DB = CENTRAL REF LEVEL

NO. = THRESHOLD IN DB
(NO.) = 2ND TIME

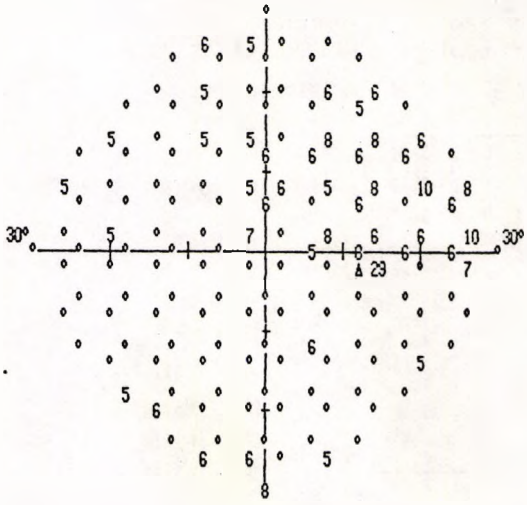

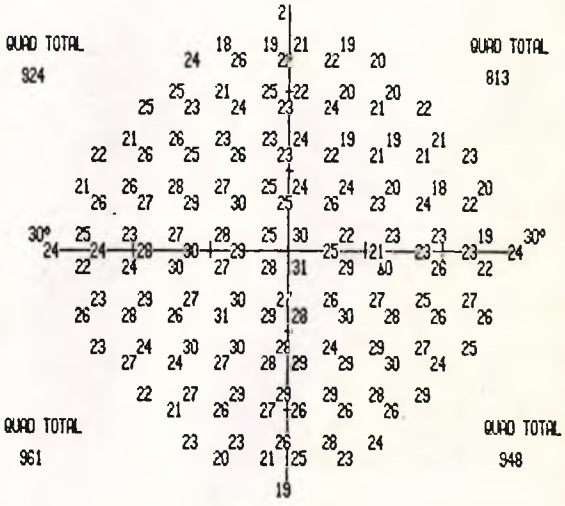

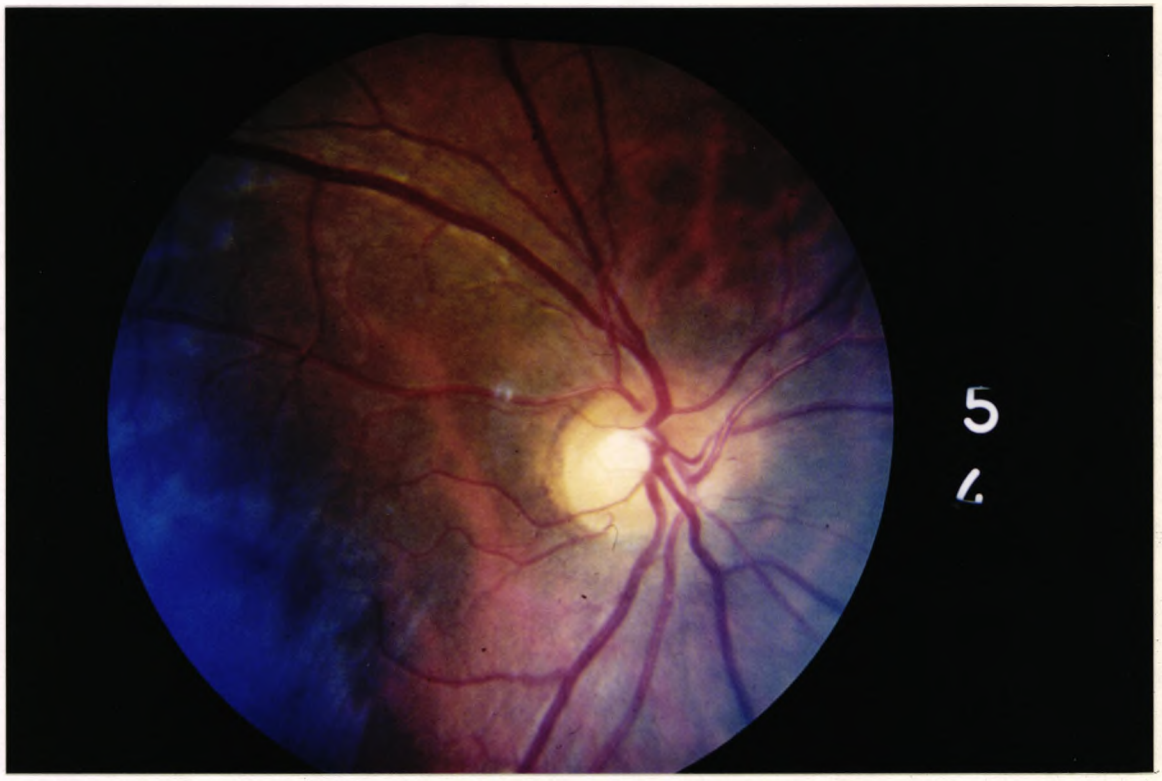

CENTRAL 30 - 2 THRESHOLD TEST

ID NAME BIRTHDATE 07-02-67 DATE 29-10-91

STIMULUS III, WHITE, BCKGND 31.5 ASB BLIND SPOT CHECK SIZE II FIXATION TARGET CENTRAL ID TIME 13:50:53

STRATEGY FULL THRESHOLD RX USED DS DCX DEG PUPIL DIAMETER VA

LEFT

AGE 24

FIXATION LOSSES 0/23

FALSE POS ERRORS 0/11

FALSE NEG ERRORS 0/11

QUESTIONS ASKED 438

FOVEA: 36 DB

TEST TIME 00:14:29

HFA S/N 630-3910

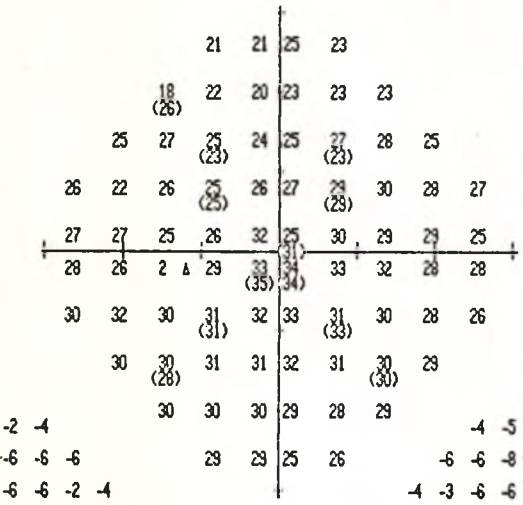

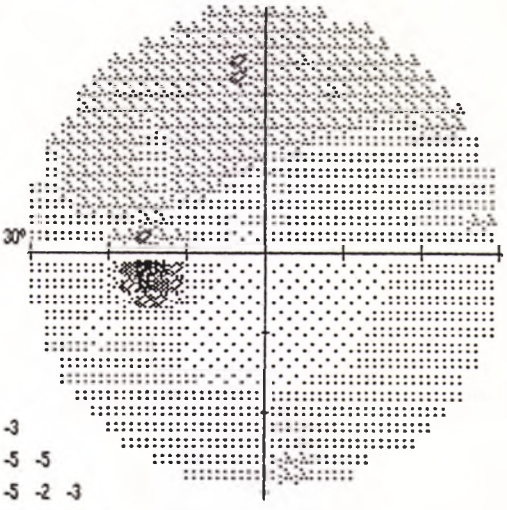

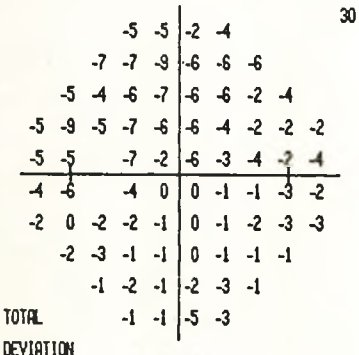

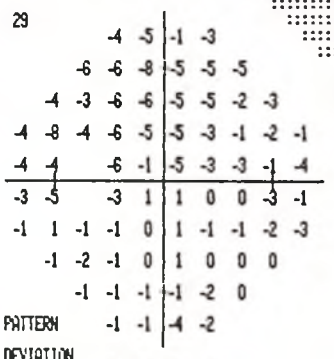

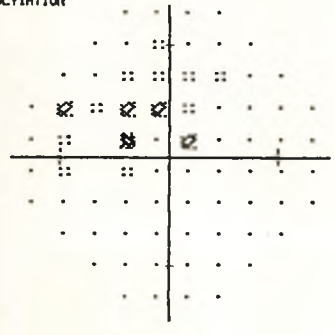

PROBABILITY SYMBOLS

:: P < 5%

P < 2%

P < 1%

■ P < 0.5%

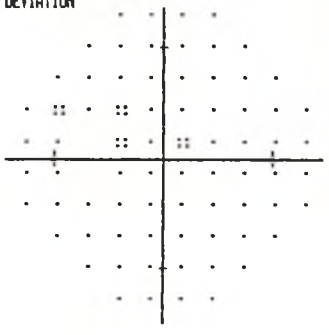

GLAUCOMA HEMIFIELD TEST (GHT)

WITHIN NORMAL LIMITS

MD	-2.87 DB	P < 10%
PSD	2.52 DB	
SF	1.21 DB	
CPSD	2.11 DB	

GRAYTONE SYMBOLS REV AG

SYM										
ASB	.8 to .1	2.5 to 1	8 to 3.2	25 to 10	79 to 32	251 to 100	794 to 318	2512 to 1000	7943 to 3162	≥ 10000
DB	41 to 50	36 to 40	31 to 35	26 to 30	21 to 25	16 to 20	11 to 15	6 to 10	1 to 5	≤0

ALLERGAN HUMPHREY

SUBJECT 10: Axial length = 26.30mm; Ocular refraction = -6.04D.

MRC-C30-1,C30-2 THRESHOLD TEST

\@STIMULUS III, WHITE, BCKGND 31.5 ASB NAME
BLIND SPOT CHECK SIZE II ID BIRTHDATE 07-02-67
FIXATION TARGET CENTRAL
STRATEGY FULL THRESHOLD

REFERENCE DATES

C30-2, 29-10-91
C30-1, 29-10-91

FOVEA: 36 DB

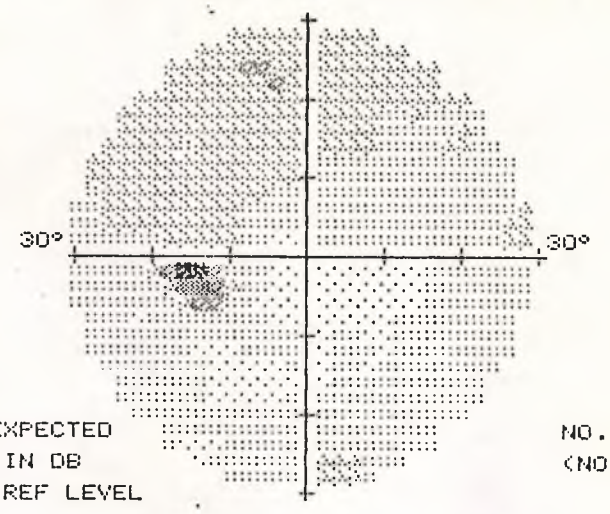

LEFT

° = WITHIN 4 DB OF EXPECTED
NO. = DEFECT DEPTH IN DB
35 DB = CENTRAL REF LEVEL

NO. = THRESHOLD IN DB
(NO.) = 2ND TIME

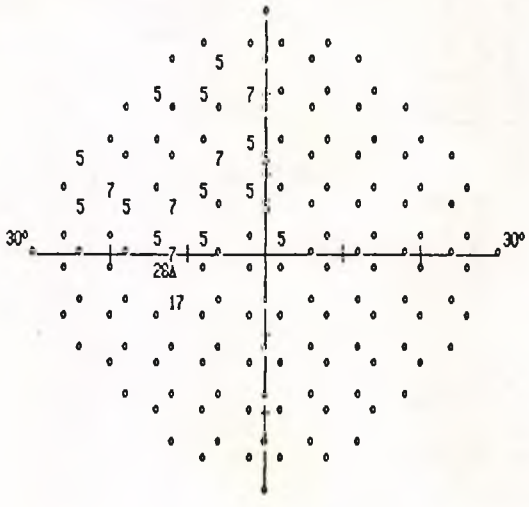

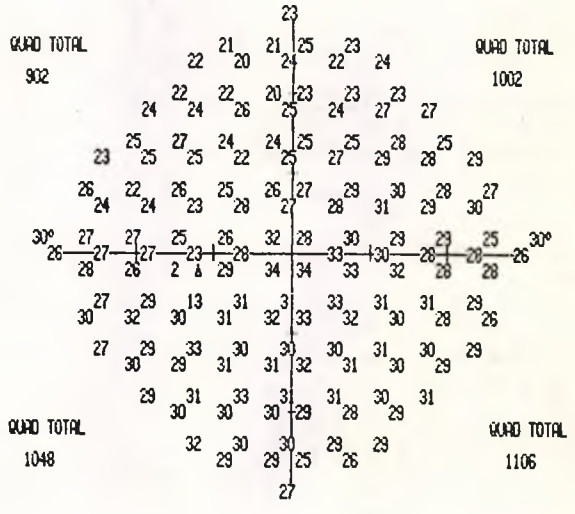

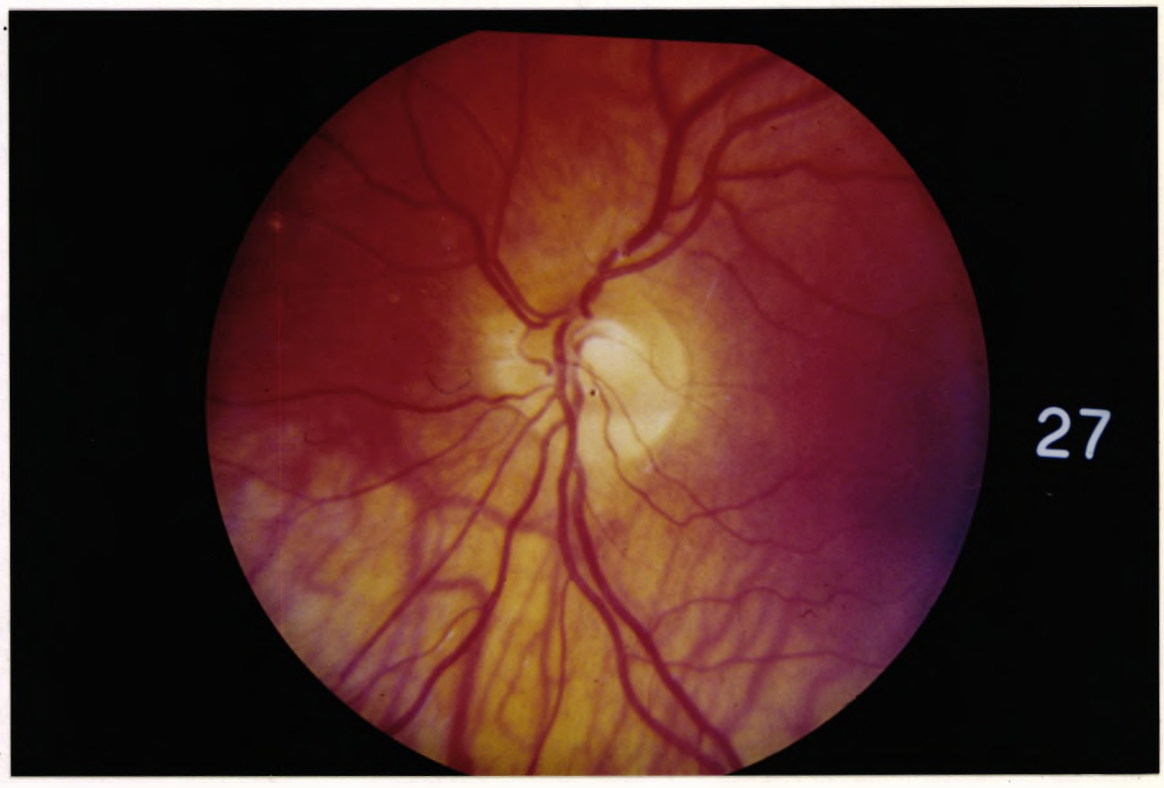

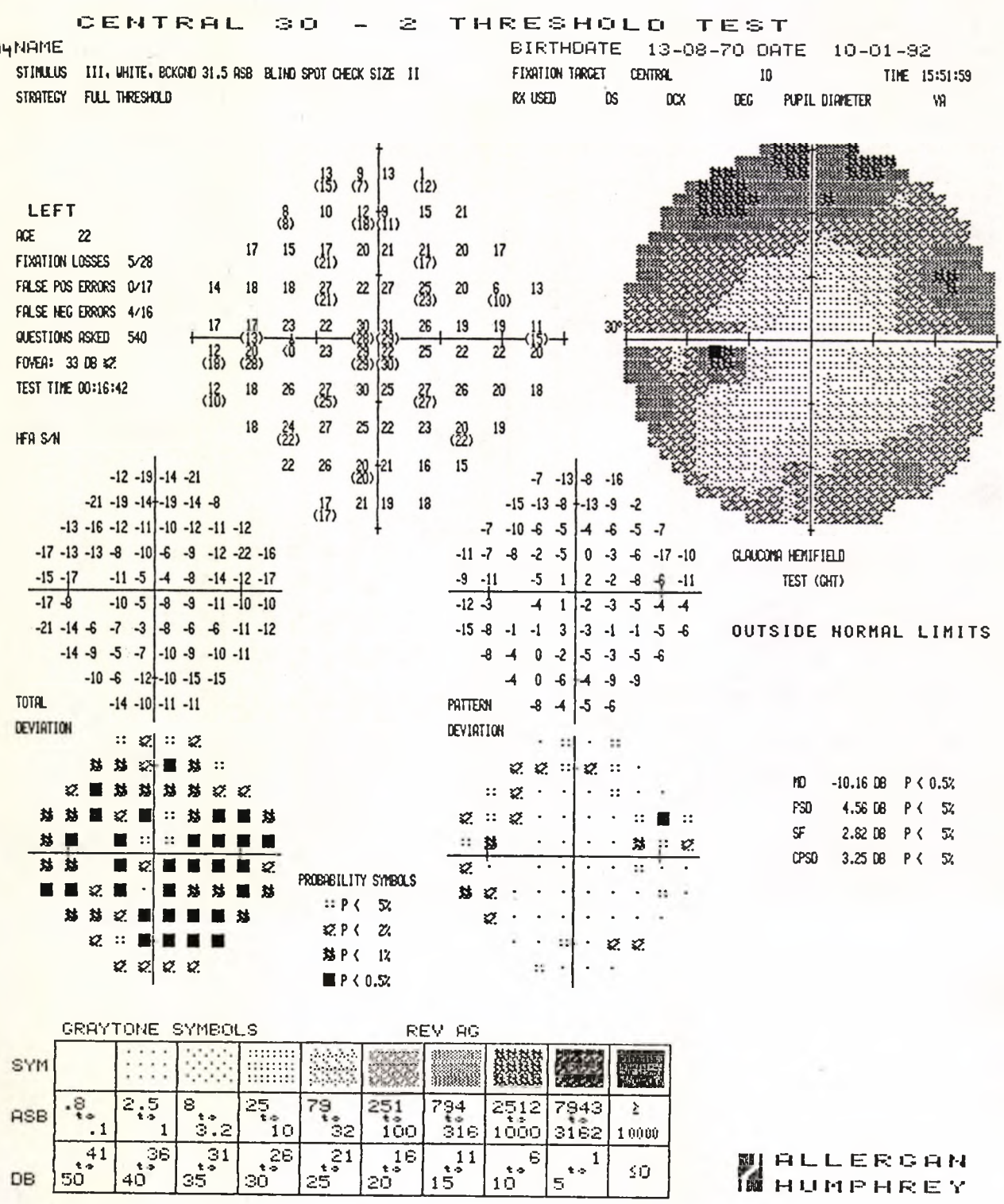

SUBJECT 11: Axial length = 29.19mm; Ocular refraction = -15.70D.

MRG-C30-1,C30-2 THRESHOLD TEST

STIMULUS III, WHITE, BCKGND 31.5 ASB NAME
BLIND SPOT CHECK SIZE II ID BIRTHDATE 13-08-70
FIXATION TARGET CENTRAL
STRATEGY FULL THRESHOLD

REFERENCE DATES

C30-2, 10-01-92
C30-1, 10-01-92

FOVEA: 33 DB

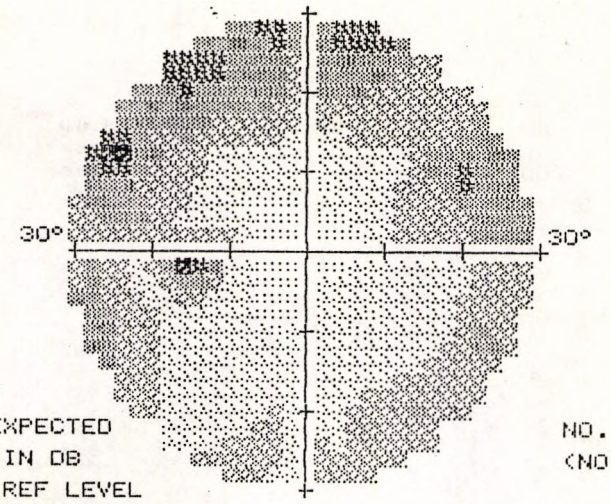

LEFT

° = WITHIN 4 DB OF EXPECTED
NO. = DEFECT DEPTH IN DB
30 DB = CENTRAL REF LEVEL

NO. = THRESHOLD IN DB
(NO.) = 2ND TIME

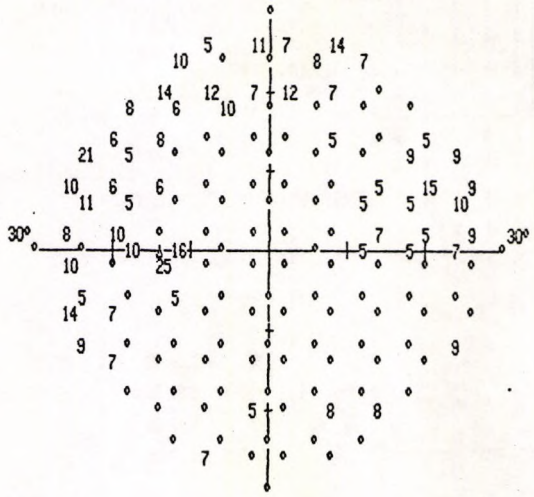

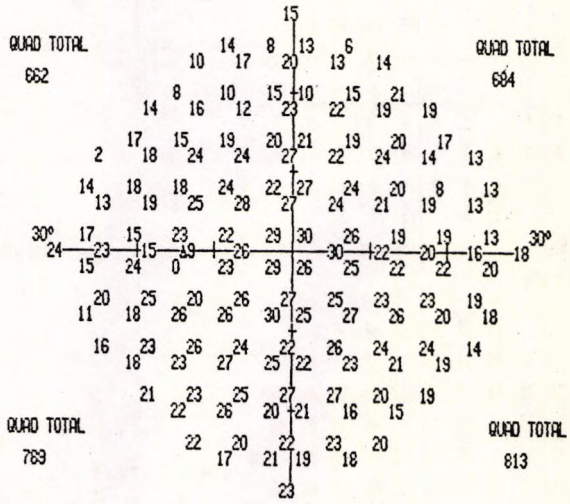

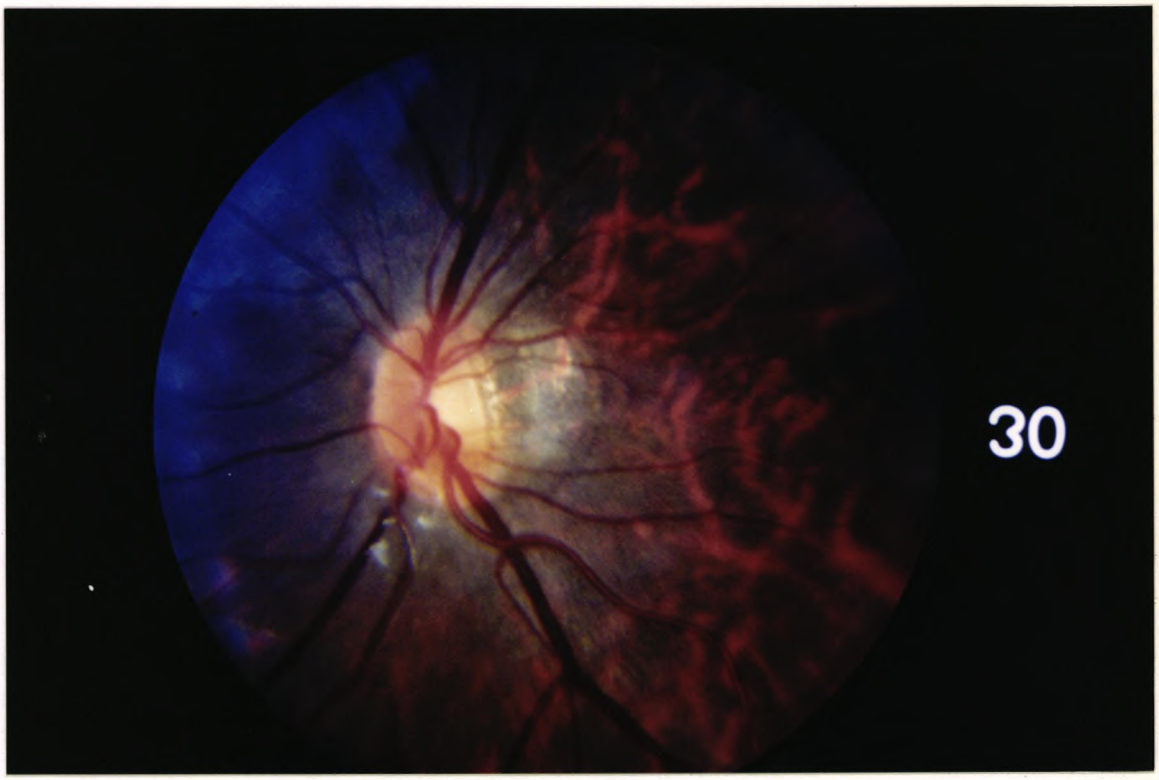

CENTRAL 30 - 2 THRESHOLD TEST

15 NAME BIRTHDATE 27-09-56 DATE 28-02-92

STIMULUS III, WHITE, BCKGND 31.5 ASB BLIND SPOT CHECK SIZE II FIXATION TARGET CENTRAL ID TIME 14:15:12

STRATEGY FULL THRESHOLD RX USED DS DCX DEG PUPIL DIAMETER MM

RIGHT
AGE 36
FIXATION LOSSES 0/24
FALSE POS ERRORS 0/15
FALSE NEG ERRORS 0/14
QUESTIONS ASKED 445
FOVEA: 32 DB
TEST TIME 00:14:01

HFA S/N

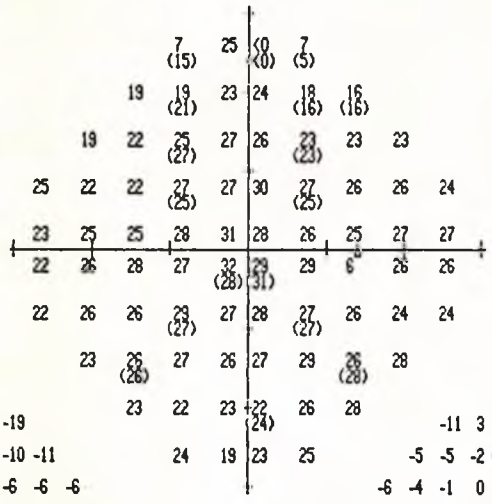

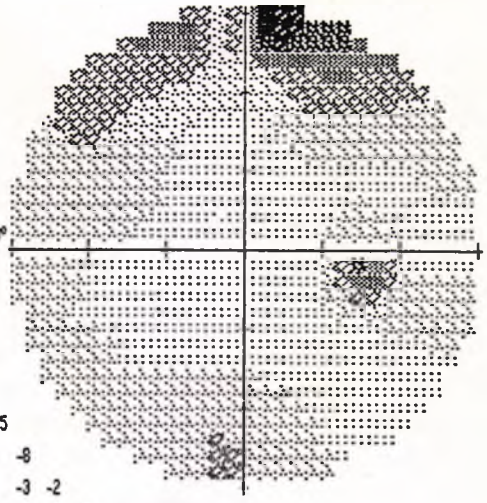

GLAUCOMA HEMIFIELD TEST (GHT)

GENERAL REDUCTION OF SENSITIVITY

TOTAL DEVIATION

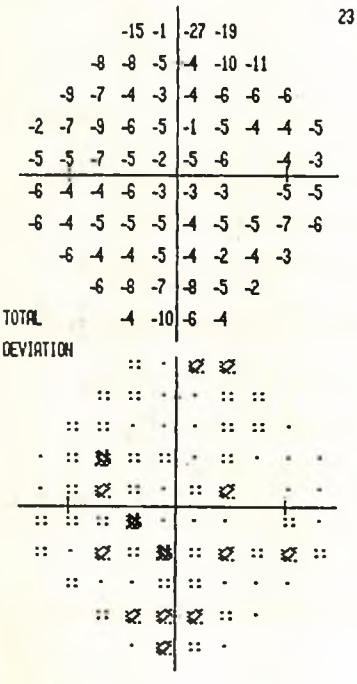

PATTERN DEVIATION

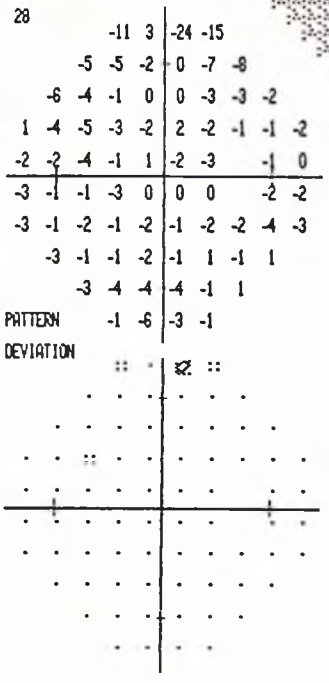

PROBABILITY SYMBOLS
:: P < 5%
P < 2%
P < 1%
■ P < 0.5%

MD	-5.04 DB P < 2%
PSD	2.82 DB
SF	1.47 DB
CPSD	2.27 DB

GRAYTONE SYMBOLS REV AG

SYM										
ASB	.8 to .1	2.5 to 1	8 to 3.2	25 to 10	79 to 32	251 to 100	794 to 316	2512 to 1000	7943 to 3162	≥ 10000
DB	41 to 50	36 to 40	31 to 35	26 to 30	21 to 25	16 to 20	11 to 15	6 to 10	1 to 5	≤0

ALLERGAN HUMPHREY

SUBJECT 12: Axial length 27.91mm= ; Ocular refraction = -9.87D

MRC-C30-2,C30-1 THRESHOLD TEST

STIMULUS III, WHITE, BCKGND 31.5 ASB NAME
BLIND SPOT CHECK SIZE II ID BIRTHDATE 27-09-56
FIXATION TARGET CENTRAL
STRATEGY FULL THRESHOLD

RIGHT

REFERENCE DATES
C30-1, 28-02-92
C30-2, 28-02-92

FOVEA: 32 DB

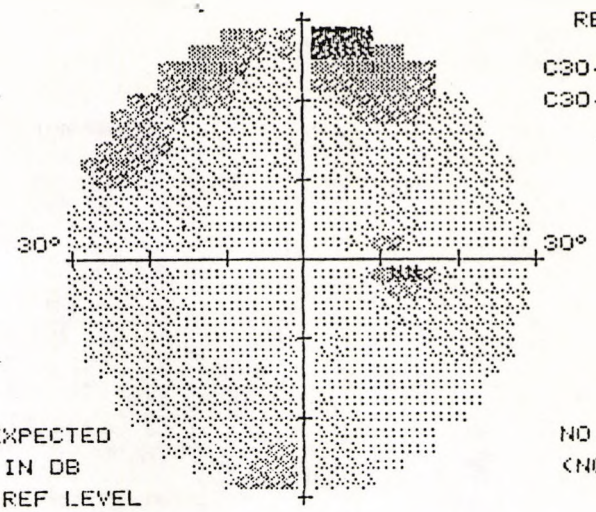

° = WITHIN 4 DB OF EXPECTED
NO. = DEFECT DEPTH IN DB
32 DB = CENTRAL REF LEVEL

NO. = THRESHOLD IN DB
<NO.> = 2ND TIME

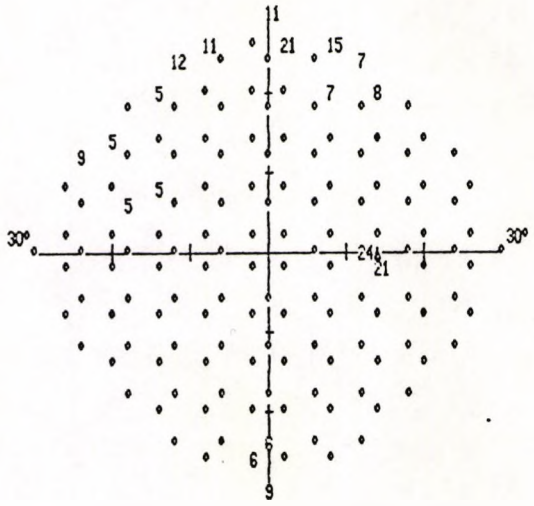

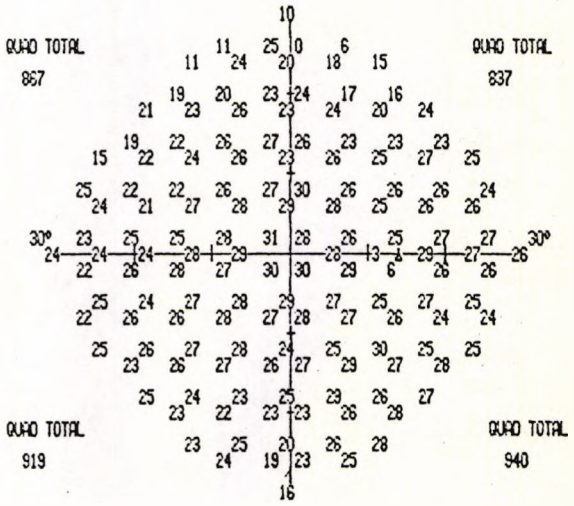

APPENDIX A2

A2.1 RAY-TRACING PROGRAM COMPUTATIONS

A2.1.1 Determination of personalised schematic eye

The calculation of the personalised schematic eye is illustrated for one example to calculate the paraxial value q_p.

Table A2.1. Patient data

Refraction		
sphere	S	+4.00
cylinder	C	0
axis	θ	0
vertex distance	ν	15
Keratometry		
longer principal radius	r_L	7.98
meridian containing r_L	ϕ	0
shorter principal radius	r_S	7.98
Ultrasonography		
depth of anterior chamber	d_1	3.32
axial lens thickness	d_2	3.47
depth of vitreous chamber	d_3	15.89

All distances are in mm and powers in dioptres

Computation

Primarily the quantities e_L, $'e_L$, w, and the equivalent power of the eye (F_E) and the power of the crystalline lens (F_L) need to be determined. Figure A2.1 represents a Gaussian construction of the eye as a single-surface cornea with both its principal points at the vertex A_1, combined with a biconvex lens with its principal points P_L and P'_L at distances e_L and e'_L from A_2 and A_3 respectively.

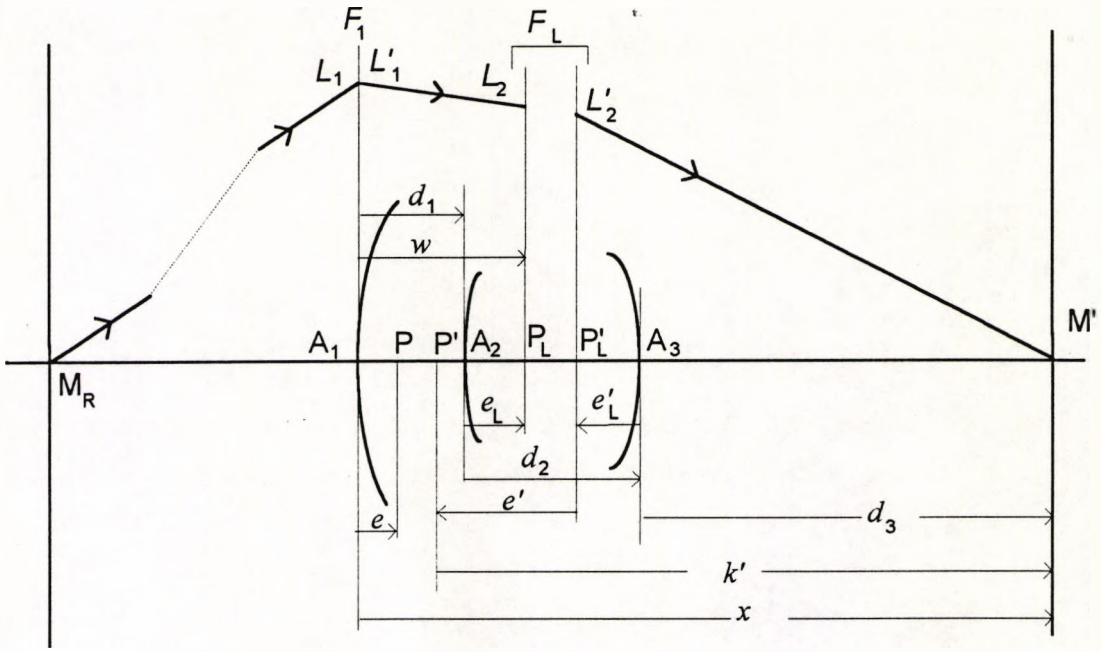

Figure A2.1 Axial ray trace through a schematic eye with principal points at P and P'. Corneal vertex is at A_1, and the front and back vertices of the crystalline lens are at A_2 and A_3 respectively. P_L and P'_L are the principal points of the crystalline lens. M_R is the eye's far point plane and M' represents the retinal plane.

The following assumptions apply

- refractive index of the aqueous and vitreous humours was taken as 1.336, and 1.422 for the crystalline lens as in the Bennett-Rabbetts schematic eye (Bennett and Rabbetts 1989).
- both surfaces of the crystalline lens are assumed to be spherical.
- the values for e_L and e'_L are taken as constant fractions of the lens thickness (d_2). Calculation of these fractions is demonstrated in Bennett (1988) but they have been adjusted according to the new constants of the Bennett-Rabbetts schematic eye (Bennett and Rabbetts 1989).
- the ratio between the front surface power and equivalent power of the crystalline lens was assumed to be a constant value. This was proposed by Bennett (1988), and this ratio has been recalculated as 0.3754 according to the updated Bennett-Rabbetts schematic eye constants.

Ocular astigmatism creates complications, especially if the principal meridians do not coincide with those of corneal astigmatism. The horizontal meridian was chosen as the reference meridian, to determine the notional powers of the correcting lens and cornea The power of the correcting lens is expressed as S sphere combined with C cylinder at axis θ°, at a vertex distance v from the cornea. The effective power or vergence L at the

corneal vertex was calculated for both principal meridians (L_A and L_B). The notional power of the vergence L_1 was then calculated in the horizontal meridian.

$L_A = S/(1-\nu S)$	along axis meridian θ
$L_B = (S + C)\{1-\nu(S + C)\}$	perpendicular to axis meridian
$L_1 = L_A + (L_B - L_A)\sin^2\theta$	

For the cornea let r_L be the radius of curvature of the longer principal meridian, and r_S the shorter radius. The corresponding surface powers are F_W (weaker) and F_S (stronger). If $\phi°$ is the direction of the r_L , then the notional power F_1 of the cornea in the horizontal meridian is

$$F_1 = F_w + (F_S - F_W)\sin^2\phi$$

Ray trace to calculate paraxial value q_p is as follows

$L_A = S/(1-0.001S\nu)$	4.255
$L_B = (S + C)\{1-0.001(S + C)\nu\}$	4.255
$L_1 = L_A + (L_B - L_A)\sin^2\theta$	4.255
$F_w = 336/r_L$	42.105
$F_S = 336/r_S$	42.105
$F_1 = F_w + (F_S - F_W)\sin^2\phi$	42.105
$L'_1 = L_1 + F_1$	46.360
$e_L = 0.599d_2$	2.079
$e'_L = -0.353d_2$	-1.225
$w = d_1 + e_L$	5.399
$L_2 = L'_1/\{1 - (w/1336)L'_1\}$	57.048
$l'_2 = -e'_L + d_3$	17.115
$L'_2 = 1336/l'_2$	78.060
$F_L = L'_2 - L_2$	21.012
$M = wF_1F_L/1336$	3.575
$N = F_1 + F_L$	63.117
$F_E = N - M$	59.542
$F_2 = 0.3754F_L$	7.888
$r_2 = 86/F_2$	10.903
$F_3 = (F_L - F_2)/\{1 - (d_2/1422)F_2\}$	13.382
$r_3 = -86/F_3$	-6.427
$e = A_1P = w(F_L/F_E)/1.336$	1.426
$e' = P'_LP' = -w(F_1/F_E)$	-3.818
$k' = -e' - e'_L + d_3$	20.933

$q_p = 0.013064k'$	0.273
notional $r_1 = 366/F_1$	7.98
axial length A'M' = $d_1 + d_2 + d_3$	22.68

A2.1.2 Determination of q for oblique rays

The ray paths for refraction at the first and second surfaces are illustrated below (figures A2.2 and A2.3). At each surface the angle of incidence with the optical axis is U and g is the perpendicular distance from the vertex of the surface to the ray. The real or virtual point B at which the ray intercepts the axis is defined by its distance b from the vertex of the surface. For the refracted ray the equivalent quantities are U', g', B' and b'. The perpendicular from the point of incidence E, to the optical axis is denoted by y. In the case of a ray directed towards the principal point of an optical system, the finally refracted ray should appear to originate from the second principal point P'. Thus, point B' obtained after refraction by the last surface should coincide with P'. After refraction U' becomes U for the next surface, while g' is used to calculate the next g. Subscript numerals refer to the surface number in order, the cornea is number 1, 2 and 3 are the front and back surfaces of the crystalline lens respectively, and 4 is the retina. Refractive index of the aqueous and vitreous humours, denoted by n, is taken as 1.336, and that for the crystalline lens, n', as 1.422.

An example is illustrated below (table A2.2) of an oblique ray trace for determination of $q_{y,}$ for $U_1 = -8°$. The same subject data as in table A2.1 is used. Figures A2.2, A2.3 and A2.4 illustrate the ray trace.

Table A2.2. Oblique ray trace for U_1 = -8°.

	Refracting surface			
	1	2	3	4
$g_1 = A_1 P \sin U_1$	-0.19846	0.16809	0.52523	2.18146
$I_1 = \arcsin(g/r - \sin U)$	6.563	7.235	1.212	-5.056
$I' = \arcsin\{\sin I(n/n')\}$	4.908	6.795	1.290	
$\Delta = I - I'$	1.655	0.440	-0.078	
$U' = U + \Delta$ (= next U)	-6.345	-5.905	-5.983	
$g' = g\left(\frac{\cos I' + \cos U'}{\cos I + \cos U}\right)$*	-0.19882	0.16824	0.52519	
$\{g' - d\sin U'\}$ = next g	0.16809	0.52523	2.18146	
$y = r\sin(U+I)$	-0.200	-0.169	0.525	2.171
$q_y = y_4/U_1°$				
$b' = g'/\sin U'$			-5.03860	0.271
$s = r_4 - \sqrt{(r_4^2 - y_4^2)}$				0.2098
$B'_3M' = -b_3 + d_3$				20.929

* this relationship was proven many years ago by Arthur Bennett, a photocopy of his original work is enclosed below.

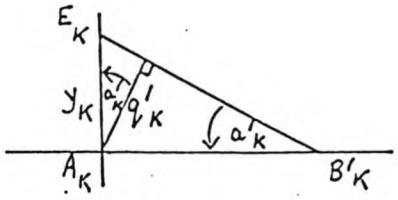

If $R_K = 0$,

$q'_K / y_K = \cos a'_K$

where $y_K = \dfrac{q'_K}{\cos a'_K}$

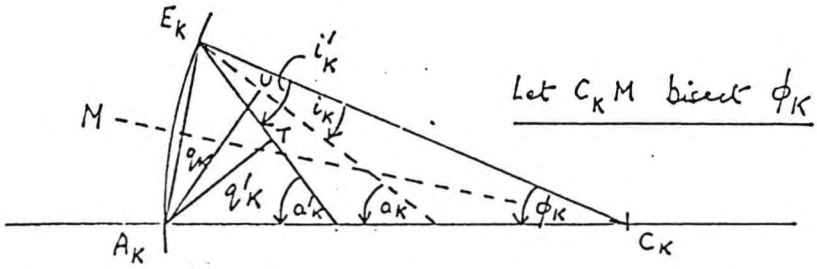

Let $C_K M$ bisect ϕ_K.

Let $x = \dfrac{\cos i_K + \cos a_K}{\cos i'_K + \cos a'_K} = \dfrac{2\cos\left(\frac{i_K + a_K}{2}\right)\cos\left(\frac{i_K - a_K}{2}\right)}{2\cos\left(\frac{i'_K + a'_K}{2}\right)\cos\left(\frac{i'_K - a'_K}{2}\right)}$

But $(i_K + a_K) = (i'_K + a'_K) = \phi_K$

$\therefore x = \dfrac{\cos\left(\frac{i_K}{2} - \frac{a_K}{2}\right)}{\cos\left(\frac{i'_K}{2} - \frac{a'_K}{2}\right)} = \dfrac{\cos\left(\frac{\phi_K}{2} - a_K\right)}{\cos\left(\frac{\phi_K}{2} - a'_K\right)}$

$E_K \hat{A}_K U = E_K \hat{A}_K C_K - U \hat{A}_K C_K = \left(90 - \frac{\phi_K}{2}\right) - (90 - a_K) = a_K - \frac{\phi_K}{2}$

Similarly, $E_K \hat{A}_K T = a'_K - \frac{\phi_K}{2}$

$\therefore x = \dfrac{\cos E_K \hat{A}_K U}{\cos E_K A_K T} = \dfrac{q_K}{q'_K}$

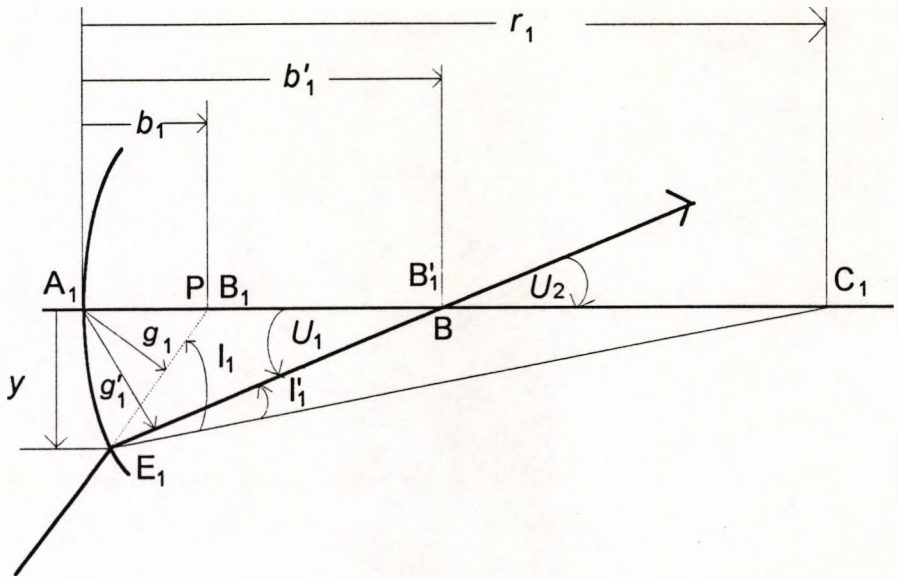

Figure A2.2. Refraction at the first surface

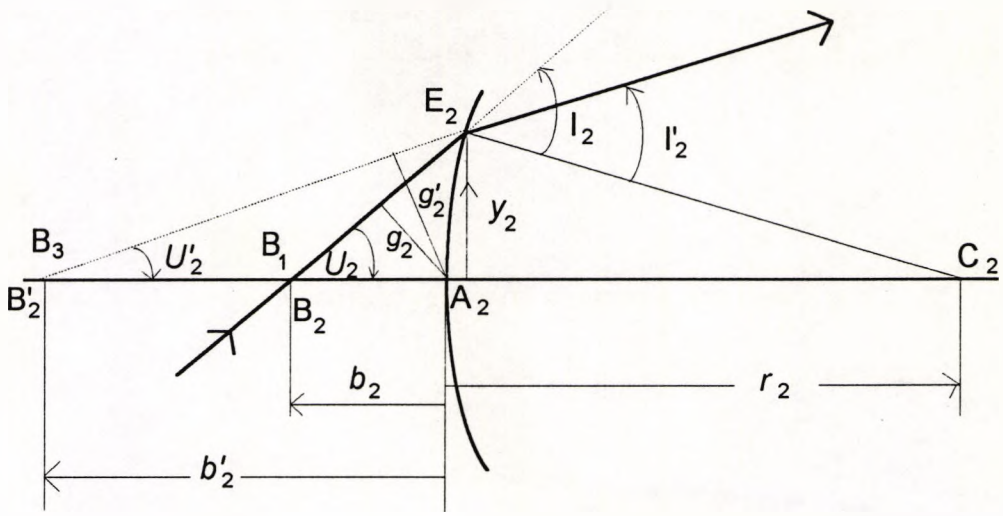

Figure A2.3. Refraction at the second surface.

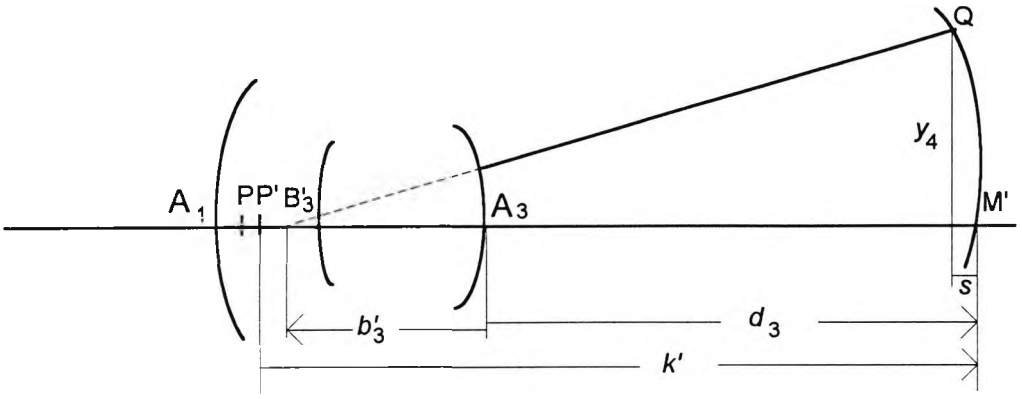

Figure A2.4. Refraction at the third surface.

Calculation of peripheral values of *q* from two oblique rays

In some cases it may be better to perform two oblique traces which would straddle the retinal feature of interest to determine *q*. Figure A2.5 shows two oblique traces incident on the retina at Q_G and Q_L. The distance *t* between them which is calculated as follows

$$t = \sqrt{(y_G - y_L)^2 + (s_G - s_L)^2}$$

All these quantities emerge from the individual oblique ray traces, and this value of *t* is then used to calculate *q* using the equation below introduced in Chapter 8 section 8.2.2.3,

$$q = t/\Delta U°$$

where ΔU is the difference between the two incident rays in degrees.

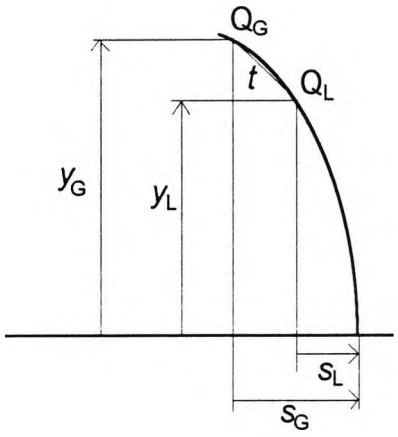

Figure A2.5. Two oblique traces incidents on the retina at Q_G and Q_L, and t is the diagonal distance between them

A2.2 Computation of Littmann's axial length method to determine q

Littmann's second nomogram was intended to be used if the axial length is known. The first nomogram is used as before to determine q. From the other nomogram the value of the axial length is found. If it agrees with the known measured value then the value for q already determined is confirmed. If it does not agree the axial length nomogram is used again to find the adjusted notional value of r_1 (corneal radius) given by the true value of axial length and A (ametropia at the corneal vertex). Finally an improved value for q is obtained from the original nomogram, using the notional r_1 and A. Littmann (1988) presented tables enabling values of q and axial length to be obtained by calculation from knowledge of r_1 and A using the formula

$$x = dA^2 - eA + f \qquad \text{(A1)}$$

where x is the theoretical axial length on the assumption that the ametropia is purely axial. The requisite values of d, e, and f, all varying with r_1, could be obtained from a table provided. Values of r_1 ranged from 6·0 to 10·0mm at intervals of 0·2mm, in general requiring interpolation at intermediate values of r_1. To facilitate explanation, four lines from the middle of Littmann's table 2 in his 1988 paper of the co-efficients d, e, and f are here reproduced.

Table A2.1. Extract from Littmann's own table 2 (Littmann 1988).

r_1 (mm)	d	e	f
7.6	0.0063	0.3988	24.16
7.8	0.0067	0.4137	24.59
8.0	0.0070	0.4287	25.02
8.2	0.0074	0.4437	25.44

Inspection of the complete table shows that the three co-efficients all increase with r_1 at different rates. Nevertheless, in each one of them taken separately, the increments are nearly constant, especially when r_1 falls within the range 7·0 to 9·0 mm, which covers the great majority of eyes. It is possible to express d, e, and f as simple functions of r_1 as follows

$$d = 0.0070 + 0.0018(r_1 - 8) = 0.0018r_1 - 0.0074 \quad \text{(A2)}$$

$$e = 0.4287 + 0.0748(r_1 - 8) = 0.0748r_1 - 0.1697 \quad \text{(A3)}$$

$$f = 25.02 + 2.12(r_1 - 8) = 2.12r_1 + 8.06 \quad \text{(A4)}$$

Example:
A = -10.60D, r_1 = 7.75mm and the measured axial length is 27.59mm.
It follows that d = 0.0066, e = 0.410and f = 24.49. From equation A1 x becomes

$$x = 0.007(-10.60)^2 - 0.410(-10.60) + 24.49 = 29.57 \text{ mm}$$

This does not agree with the measured value. Therefore a notional r_1 is determined by resolving equations A1, A2, A3, and A4 using the values for the measured axial length and the ametropia. This notional r_1 value is used as in the original calculations described in Chapter 8 section 8.2.2.1, to obtain a refined value for q.

A3. SUPPORTING PUBLICATIONS

REFEREED PAPERS

Rudnicka, A.R., Steele, C.F., Crabb, D.P., Edgar, D.F. (1992). Repeatability, reproducibility and intersession variability of Allergan Humphrey ultrasonic biometer. *Acta Ophthalmol* **70**: 327-344.

Rudnicka, A.R., Bennett, A.G., Edgar, D.F. (1992). Construction of a model eye and its applications. *Ophthalmic Physiol Opt* **12**: 485-490.

Rudnicka, A.R., Crabb, D.P., Edgar, D.F., Fitzke, F.W. (1993). Pointwise analysis of serial visual fields in normal subjects. **In**: *Perimetry Update 1992/1993*, ed. by A. Heijl and RP Mills, (Amsterdam: Kugler Publications), pp 41-48.

Guttridge, N.M., Allen, P.M., Rudnicka, A.R., Edgar, D.F., Renshaw, A.E. (1991). Influence of learning on the peripheral field as assessed by automated perimetry. **In**: *Perimetry Update 1990/1991*, ed. by RP Mills and A Heijl, (Amstelveen: Kugler and Ghedini)pp 567-575.

Bennett, A.G., Rudnicka, A.R., Edgar, D.F. (1994). Improvements on Littmann's method of determining the size of retinal features by fundus photography. *Graefes Arch Clin Exp Ophthalmol.* **232**: 361-367

REFEREED CONFERENCE ABSTRACTS

Rudnicka, A.R., Steele, C.F., Crabb, D.P., Edgar, D.F. (1991). Clinical evaluation of Allergan Humphrey ultrasonic biometer. *Invest Ophthalmol Vis Sci (suppl)* **32**: 1155.

Rudnicka, A.R., Bennett, A.G., Edgar, D.F. (1991). Construction of a model eye and its applications. *Ophthalmic Physiol Opt* **11**: 394 . - also presented at ARVO 1992, the European Glaucoma Society Congress 1992, and The Rank Prize Funds mini-symposium on ophthalmological image processing June 1992.

Rudnicka, A.R., Burk, R.O.W., Fitzke, F.W., Edgar, D.F. (1993). Magnification characteristics of fundus imaging systems. *Invest Ophthalmol Vis Sci* (suppl) **34**: 1169. - also presented at the Fourth Scanning Laser Ophthalmoscopy, Tomography and Microscopy meeting in Heidelberg, May 1993.

Rudnicka, A.R., Crabb, D.P., Edgar, D.F., Fitzke, F.W. (1993). Pointwise analysis of

serial visual fields in normal subjects. *Ophthalmic Physiol Opt* **13**: 103.

Rudnicka, A.R., Edgar, D.F. (1994). Central visual field by automated perimetry in myopes with peripapillary crescents. *Invest Ophthalmol Vis Sci (suppl)* **35**: 1510.

PAPERS IN PRESS

Edgar, D.F., Stewart-Jones, J.H., Crabb, D.P., Rudnicka, A.R., Lawrenson, J.G., Guttridge, N.M., O'Brien, C. (1994). Effects of pilocarpine and propine on pupil diameter, automated perimetry and logmar acuity. *Ophthalmology*

REFERENCES

Adelson, A.J., Werner, E.B., Krupin, T. (1988). Learning effects in automated perimetry in ocular hypertensive and early glaucoma patients. *Invest Ophthalmol Vis Sci (suppl)* **29**: 356.

Aetisov, E.S., Savitskaya, N.F. (1977). Some features of ocular microcirculation in myopia. *Ann Ophthalmol* **9**: 1261-1264.

Airaksinen, P.J., Drance, S.M., Schulzer, M. (1985a). Neuroretinal rim area in early glaucoma. *Am J Ophthalmol* **99**: 1-4.

Airaksinen, P.J., Drance, S.M., Douglas, G.R., Schulzer, M. (1985b). Neuroretinal rim areas and visual field indices in glaucoma. *Am J Ophthalmol* **99**: 107-110.

Airaksinen, P.J., Drance, S.M., Douglas, G.R., Schulzer, M., Wisjman, K. (1985c). Visual field and retinal nerve fibre layer comparisons in glaucoma. *Arch Ophthalmol* **103**: 205-207.

Airy, G.B. Letter to Dr. Dionysius Lardner, April 25, 1828. (Original in Wellcome Historical Medical Library, reproduced in Levene 1966).

Altman, D.G., Bland, J.M. (1983). Measurement in medicine: the analysis of method comparison studies. *Statistician* **32**: 307-317.

Altman, D.G. (1991). Practical Statistics for Medical Research. (London: Chapman and Hall), pp 210-212.

Amalric, P., Bessou, P., Aubry, J.P. (1966). Quelques resultats de retinographie par la fluoresceine. *Bull Soc Ophtal Franc* **66**: 290-302.

Anderson, D.R. (1983). Correlation of the peripapillary anatomy with the disc damage and field abnormalities in glaucoma. *Doc Ophthamol Proc Ser* **35**: 1-10.

Anderson, D.R. (1987). Relationship of peripapillary haloes and crescents to glaucomatous cupping. **In**: *Glaucoma Update III*, ed by G.K. Kreigelstein (Springer-Verlag: Berlin, Heidelberg), pp 103-105.

Anderson, D.R. (1983). Correlation of the peripapillary anatomy with the disc damage and field abnormalities in glaucoma. *Doc Ophthalmol Proc Ser* **35**: 1-10.

Arell, A., Kolari, S. (1978). Experiments on a model eye. *Am J Physics* **46**: 613-614.

Armaly, M.F. (1969). The size and location of the normal blind spot. *Arch Ophthalmol*

81: 192-201.

Armaly, M. (1970). Optic cup in normal and glaucomatous eyes. *Invest Ophthalmol Vis Sci* **9**: 425-429.

Artaria, L.G. (1986). Messung der Bulbuslange mit ver- schiedenen Ultraschall-Geraten. *Monatbl Augenheilkd* **188**: 492-494.

Asman, P., Heijl, A. (1992). Glaucoma hemifield test. Automated visual field evaluation. *Arch Ophthalmol* **110**: 812-819.

Aulhorn, E., Harms, H. (1969). Glaukom-Gesichtsfeld. *Ophthalmologica* **158**: 469-487.

Aulhorn, E., Harms, H. (1972). Visual perimetry. **In**: *Handbook of Sensory Physiology* vol. VII/4, ed. by D. Jameson and L.M. Hurvich. (Berlin, Heildelberg: Springer-Verlag), pp 102-145.

Autzen, T., Work, F. (1990). The effect of learning and age on short-term fluctuation and mean sensitivity of automated static perimetry. *Acta Ophthalmol* **68**: 327-330.

Balazsi, A.G., Rootman, J., Drance, S.M., Schulzer, M., Douglas, G.R. (1984a). The effect of age on the nerve fibre population of the human optic nerve. *Am J Ophthalmol* **97**: 760-766.

Balazsi, A.G., Drance, S.M., Schulzer, M., Douglas, G.R.(1984b). Neuroretinal rim area in suspected glaucoma and early chronic open-angle glaucoma: Correlation with parameters of visual function. *Arch Ophthalmol* **102**: 1011-1014.

Baum, G. (1956). The effect of ultrasonic radiation upon the eye and ocular adnexa. *Am J Ophthalmol* **42**: 696-706.

Baum, T.D., Schwartz, B. (1992). Trends of change of visual fields of normal subjects on long-term serial automated perimetry. *Invest Ophthalmol Vis Sci* **33**: 1388.

Bear, J.C., Richler, A., Burke, G. (1981). Near work and familial resemblances in ocular refraction: a population study in Newfoundland. *Clin Genet* **19**: 462-472.

Bebie, H., Fankhauser, F., Spahr, J. (1976a). Static perimetry: strategies. *Acta Ophthalmol* **54**: 325-338.

Bebie, H., Fankhauser, F., Spahr, J. (1976b). Static perimetry: accuracy and fluctuations. *Acta Ophthalmol* **54**: 339-348.

Bebie, H., Fankhauser, F. (1982). DELTA manual. Interzeag AG, CH-8952 Schieren,

Switzerland.

Bebie, H. (1985). Computerised techniques of visual field comparisons. **In**: *Automated perimetry in glaucoma: a practical guide*, ed by S.M. Drance and D.R. Anderson, (London: Grune and Stratton), pp 147-160.

Beck, R.W., Messner, D.K., Musch, D.C., Martonyi, C.L., Lichter, P.R. (1985a). Is there a racial difference in physiological cup size. *Ophthalmology* **92**: 873-876.

Beck, R.W., Bergstrom, T.J., Lichter, P.R. (1985b). A clinical comparison of visual field testing with a new automated perimeter, the Humphrey Field Analyzer, and the Goldmann perimeter. *Ophthalmology* **92**: 77-82.

Bedwell, C. H., Davies, S.A. (1977). The effect of pupil size on multiple static quantitative visual field threshold. *Doc Ophthalmol Proc Ser* **14**: 363-366.

Behrendt, T., Doyle, K.E. (1965). Reliability of size measurements in the new Zeiss fundus camera. *Am J Ophthalmol* **59**: 896-899.

Bek, T., Lund-Anderson, H. (1989). The influence of stimulus size on the perimetric detection of scotomata. *Graefes Arch Clin Exp Ophthalmol* **227**: 531-534.

Benedetto, M.D., Cyrlin, M.N. (1985). The effect of blur upon static perimetric thresholds. *Doc Ophthalmol Proc Ser* **42**: 563-567.

Bengtsson, B. (1976). The variation and covariation of cup and disc diameters. *Acta Ophthalmol* **54**: 804-818.

Bengtsson, B., Krakau, C.E.T. (1977). Some essential features of the Zeiss fundus camera. *Acta Ophthalmol* **55**: 123-131.

Bengtsson, B., Krakau, C.E.T. (1992). Correction of optic disc measurements on fundus photographs. *Graefes Arch Clin Exp Ophthalmol* **230**: 24-28.

Bennett, A.G. (1988) A method of determining the equivalent powers of the eye and its crystalline lens without resort to phakometry. *Ophthalmic Physiol Opt* **8**: 53-59.

Bennett, A.G., Rabbetts, R.B. (1989). Clinical Visual Optics. 2nd edn. (London: Butterworths).

Bennett, G.R., Werner, E.B., Seraydarian, L. (1991). Correlation of reliability indices and test-retest reproducibility in normal subjects undergoing automated perimetry on the Humphrey Visual Field Analyzer. **In**: *Perimetry Update 1990/1991*, ed by R.P. Mills and A. Heijl, (Amstelveen: Kugler and Ghedini), pp 211-215.

Berry, H. (1963). Bitemporal depression of the visual fields due to an ocular disease. *Br J Ophthalmol* **47**: 441-444.

Betz, P., Camps, F., Collignon-Brach, J. (1982). Biometric study of the disc cup in open-angle glaucoma. *Graefes Arch Clin Exp Ophthalmol* **218**: 70-74.

Bickler-Bluth, M., Trick, G.L., Kolker, A.E., Cooper, D.G. (1989). Assessing the utility of reliability indices for automated visual fields. *Ophthalmology* **96**: 616-619.

Binkhorst, R.D. (1981). The accuracy of ultrasonic measurement of the axial length of the eye. *Ophthalmic Surg* **12**: 363-365.

Bland, J.M., Altman, D.G. (1986). Statistical methods for assessing agreement between two methods of clinical measurement. *Lancet* **8**: 307-310.

Boeglin, R.J., Caprioli, J., Zulauf, M. (1992). Long-term fluctuation of the visual field in glaucoma. *Am J Ophthalmol* **113**: 393-400.

Bottoni, F.G., Gonnella, P.M., Porta, A.S., Consalez, G.G. (1989). Neuroretinal rim area in normal eyes: A study on a randomised group of 30 subjects. *Ophthalmologica* **198**: 40-45.

Brazitikos, P.D., Safran, A.B., Simona, F., Zulauf, M. (1990). Threshold perimetry in tilted disc syndrome. *Arch Ophthalmol* **108**: 1698-1700.

Brenton, R.S., Phelps, C.D. (1986). The normal visual field on the Humphrey Field Analyzer. *Ophthalmologica* **193**: 56-74.

Brenton, R.S., Phelps, C.D., Rojas, P., Woolson, R.F. (1986). Interocular differences of the visual field in normal subjects. *Invest Ophthalmol Vis Sci* **27**: 799-805.

Brenton, R.S., Argus, W.A. (1987). Fluctuations on the Humphrey and Octopus perimeters. *Invest Ophthalmol Vis Sci* **28**: 767-771.

British Standards Institution (1979). Precision of test methods, part 1: guide for the determination of repeatability and reproducibility for a standard test method. BS 5497, Part 1, London.

Britton, R.J., Drance, S.M., Schulzer, M., Douglas, G.R., Mawson, D.K. (1987a). The area of the neuroretinal rim of the optic nerve in normal eyes. *Am J Ophthalmol* **103**: 497-504.

Britton, R.J., Drance, G.R., Douglas, G.R., Schulzer, M. (1987b) The correlation of the physiological blind spot and the disc area. *Doc Ophthalmol Proc Ser* **49**: 663-666.

Brown, G., Tasman, W. (1983). Congenital anomalies of the optic disc. (New York: Grune and Stratton), pp 172-177, 261-263.

Brusini, P., Tosoni, C. (1985). Two years experience with the perimetron automatic perimeter in glaucomatous patients. *Doc Ophthalmol Proc Ser* **42**: 167-172.

Brusini, P., Della Mea, G., Tosoni, C. (1986). Pericoecal light sensitivity in suspected glaucoma and in early primary open-angle glaucoma. *New Trends Ophthalmol* **1**: 235.

Bullimore, M.A., Gilmartin, B. (1987). Tonic accommodation, cognitive demand and ciliary muscle innervation. *Am J Optom Physiol Opt* **64**: 45-50.

Burk, R.O.W., Rohrschneider, K., Noack, H., Völcker, H.E. (1992). Are large optic nerve heads susceptible to glaucomatous damage at normal intraocular pressure? *Graefes Arch Clin Exp Ophthalmol* **230**: 552-560.

Buus, D.R., Anderson, D.R. (1989). Peripapillary crescents and haloes in normal-tension glaucoma and ocular hypertension. *Ophthalmology* **96**: 16-19.

Caccamise, W. (1954). Situs inversus of the optic disc. *Am J Ophthalmol* **38**: 854-865.

Campbell, F.W., Gubisch, C. (1966). Optical quality of the human eye. *J Physiol* **186**: 558-578.

Caprioli, J., Spaeth, G.L. (1985). Comparison of the optic nerve head in high and low-tension glaucoma. *Arch Ophthamol* **103**: 1145-1149.

Caprioli, J., Klingbeil, U., Sears, M., Pope, B. (1986). Reproducibility of optic disc measurements with computerised analysis of stereoscopic video images. *Arch Ophthalmol* **104**: 1035-1039.

Caprioli, J., Miller, J.M. (1987). Optic disc rim area is related to disc size in normal subjects. *Arch Ophthalmol* **105**: 1683-1685.

Caprioli, J., Miller, J.M., Sears, M. (1987). Quantitative evaluation of the optic nerve head in patients with unilateral visual field loss from primary open angle glaucoma. *Ophthalmology* **94**: 1484-1487.

Carassa, R.G., Schwartz, B. (1991). Optic disc areas and their asymmetrical differences between right and left eyes in normals and ocular hypertensives. *Invest Ophthalmol Vis Sci (suppl)* **32**: 717.

Cascairo, M.A., Stewart, W.C., Sutherland, S.E. (1991). Influence of missed catch trials on the visual field in normal subjects. *Graefes Arch Clin Exp Ophthalmol* **229**: 437-441.

Casson, E., Shapiro, L., Johnson, C. (1990). Short-term fluctuation and estimate of variability in visual field data. *Invest Ophthalmol Vis Sci* **31**: 2459-2463.

Chalmers, S.D., Ryland, H.S. (1906). British Patent No.4386. An artificial or model eye for demonstration and practice purposes.

Chauhan, B.C., Henson, D.B., Hobley, A.J. (1989). Cluster analysis in suprathreshold perimetry. **In**: *Perimetry Update 1988/1989*, ed. by A. Heijl, (Amsterdam: Kugler and Ghedini), pp 217-221.

Chauhan, B.C., Le Blanc, R.P., Wijsman, K., Cruz, A.M. (1991). Effect of the number of threshold determinations on short-term fluctuation in automated perimetry. *Ophthalmology* **98**: 1420-1424.

Chi, T., Ritch, R., Tsai, C. (1988). Racial differences in optic nerve head parameters. *Invest Ophthalmol Vis Sci (suppl)* **29**: 274.

Chi, T., Ritch, R., Stickler, D., Pitman, B., Tsai, C., Hsieh, F.Y. (1989). Racial differences in optic nerve head parameters. *Arch Ophthalmol* **107**: 836-839.

Chihara, E., Sawada, A. (1990). Atypical nerve fibre layer defects in high myopia with high-tension glaucoma. *Arch Ophthalmol* **108**: 228-232.

Collin, H.B., Han, C., Khor, P.C. (1988). Age changes in the visual field using the Humphrey Visual Field Analyzer. *Clin Exp Optom* **71**: 174-178.

Collin, H.B., Banks, R., Dimitratos, M. (1993). The effect of refractive error on perimetric thresholds using the Humphrey Field Analyser. *Clin Exp Optom* **76**: 162-171.

Coman, L., Flanagan, J.G., Wild, J.M. (1994). Quantification of perimetric fatigue and its reduction using strategies to improve vigilance. *Invest Ophthalmol Vis Sci (suppl)* **35**: 2188.

Cook, R.C., Glassock, R.E. (1951). Refractive and ocular findings in the newborn. *Am J Ophthalmol* **34**: 1407-1413.

Cornsweet, T.N. (1962). The staircase method in psychophysics. *Am J Psychol* **75**: 485-491.

Crosswell, H.H., Stewart, W.C., Cascairo, M.A., Hunt, H.H. (1991). The effect of background intensity on the components of fluctuation as determined by threshold-related automated perimetry. *Graefes Arch Clin Exp Ophthalmol* **229**: 119-122.

Curtin, B.J. (1963). The pathogenesis of congenital myopia. *Arch Ophthalmol* **69**: 166-

173.

Curtin, B.J. (1970). Myopia. A review of its aetiology, pathogenesis, and treatment. *Surv Ophthalmol* **1**: 1-17.

Curtin, B.J., Karlin, D.B. (1971). Axial length measurements and fundus changes of the myopic eye. *Am J Ophthalmol* **71**: 42-53.

Curtin, B.J. (1985). The Myopias. Basic science and clinical management. (London: Harper and Row).

Curtin, B.J. (1988). Pathological myopia. *Acta Ophthalmol (suppl)* **185**:105-106.

Daubs, J.G., Crick, R.P. (1981). Effect of refractive error on the risk of ocular hypertension and open angle glaucoma. *Trans Ophthalmol Soc UK* **101**: 121-126.

David, R., Zangwill, L.M., Tessler, Z., Yassur, Y. (1985). The correlation between intraocular pressure and refractive status. *Arch Ophthalmol* **103**: 1812-1815.

Donders, F.C. (1864). On the anomalies of accommodation and refraction of the eye. Translated by W.D. Moore. London, New Sydenham Society.

Drance, S.M., Berry, V., Hughes, A. (1967). Studies of the effects of age on the central and peripheral isopters of the visual field in normal subjects. *Am J Ophthalmol* **63**: 1667-1672.

Drance, S.M., Sweeney, V.P., Morgan, R.W., Feldmann, F. (1973). Studies of factors involved in the production of low tension glaucoma. *Arch Ophthamol* **89**: 457-465.

Drance, S.M., Balazsi, G. (1984). Die neuroretinale Randzone beim fruhen Glaukom *Klin Mbl Augenheilk* **184**: 271-273.

Drance, S.M., Airaksinen, P.J., Price, M., Schulzer, M., Douglas, G.R., Tansley, B.W. (1986). The correlation of functional and structural measurements in glaucoma patients and normal subjects. *Am J Ophthalmol* **102**: 612-616.

Duke-Elder, S. (1970). System of Ophthalmology. Vol. V. ed. by S. Duke-Elder and D. Abraham. (London: Henry Kimpton).

Dunn, O.J., Clark, V.A. (1974). Applied Statistics. (New York: Wiley), pp 343- 345.

Ebenholtz, S.M. (1983). Accommodative hysteresis: a precursor for induced myopia? *Invest Ophthalmol Vis Sci* **24**: 513-515.

Elenius, V., Sopanen, V. (1963). Power of the correcting lens of the aphakic eye as

calculated from the keratometric measurement of the corneal radius and the ultrasonically measured axial length of the eye. *Acta Ophthalmol* **41**:71-74.

Fankhauser, F., Enoch, J.M. (1962). The effects of blur upon perimetric thresholds. *Arch Ophthalmol* **68**: 240-251.

Fankhauser, F. (1969). Kinetische Perimetrie. *Ophthalmologica* **185**: 406-418.

Fankhauser, F., Koch, P., Roulier, A. (1972). On automation of perimetry. *Graefes Arch Clin Exp Ophthalmol* **184**: 126-150.

Fankhauser, F. (1979). Problems related to the design of automatic perimeters. *Doc Ophthalmologica* **47**: 89-139.

Fankhauser, F., Bebie, H. (1979). Threshold fluctuations, interpolations and spatial resolution in perimetry. *Doc Ophthalmol Proc Ser* **19**: 295-309.

Fankhauser, F., Häberlin, H. (1980). Dynamic range and stray light. An estimate of falsifying effects of stray light in perimetry. *Doc Ophthalmol* **50**: 143-167.

Fantes, F.E., Anderson, D.R. (1989). Clinical histologic correlation of human peripapillary anatomy. *Ophthalmology* **96**: 20-25.

Faschinger, C. (1984). Definition of the blind spot by computer perimetry. *Klin Mbl Augenheilk* **185**: 465-467.

Fincham, W.H.A. (1959). The practice eye. *Optician* **137**: 247-249.

Fitzke, F.W., Kemp, C.M. (1989). Probing visual function with psychophysics and photochemistry. *Eye* **3**: 84-89.

Flammer, J., Drance, S.M., Schulzer, M. (1983). The estimation and testing of the components of long-term fluctuation of the differential light threshold. *Doc Ophthalmol Proc Ser* **35**: 383-389.

Flammer, J., Drance, S.M., Zulauf, M. (1984a). Differential light threshold. Short- and long-term fluctuations in patients with glaucoma, normal controls and patients with suspected glaucoma. *Arch Ophthalmol* **102**: 704-706.

Flammer, J., Drance, S.M., Fankhauser, F., Augustiny, L. (1984b). Differential light threshold in automatic threshold perimetry: factors influencing the short-term fluctuation. *Arch Ophthalmol* **102**: 876-879.

Flammer, J., Drance, S.M., Schulzer, M. (1984c). Covariates of the long-term

fluctuations of the differential light threshold. *Arch Ophthalmol* **102**: 880-882.

Flammer, J., Drance, S.M., Augustiny, L., Funkhouser, A. (1985). Quantification of glaucomatous visual field defects with automated perimetry. *Invest Ophthalmol Vis Sci* **26**: 176-181.

Flammer, J., Zulauf, M. (1985). The frequency distribution of the deviations in static perimetry. *Doc Ophthalmol Proc Ser* **42**: 17-23.

Flanagan, J.G., Wild, J.M., Hovis, J.K. (1991). The differential light threshold as a function of retinal adaptation - the Weber-Fechner/Rose-de-Vries controversy revisited. **In**: *Perimetry Update 1990/1991*, ed. by R.P. Mills and A.Heijl, (Amstelveen: Kugler and Ghedini), pp 551-554.

Flanagan, J.G., Moss, I.D., Wild, J.M., Hudson, C., Prokopich, L., Whittaker, D., O'Neill, E.C. (1993a). Evaluation of FASTPAC: a new strategy for threshold estimation with the Humphrey Field Analyser. *Graefes Archiv Clin Exp Ophthalmol* **231**: 465-469.

Flanagan, J.G., Wild, J.M., Trope, G.E. (1993b). The visual field indices in primary open angle glaucoma. *Invest Ophthalmol Vis Sci* **34**: 2266-2274.

Fledelius, H.C. (1981). Accommodation and juvenile myopia. *Doc Ophthalmol Proc Ser* **21**: 103-108.

Fujimoto, N., Adach-Usami, E. (1991). Effect of test field size on the results of automated perimetry in normal subjects and patients with optic neuritis. *Acta Ophthalmol* **69**: 367-370.

Fujimoto, N., Adach-Usami, E. (1992). Effect of number of test points in automated perimetry. *Am J Ophthalmol* **113**: 317-320.

Fulk, G.W., Goss, D.A., Christensen, M.T., Cline, K.B., Herrin-Lawson, G.A. (1992). Optic nerve crescents and refractive error. *Optom Vis Sci* **69**: 208-213.

Funkhouser, A.T., Kwasniewska, S., Fankhauser, F. (1988a). Clinical interest and problems related to the measurement of the blind spot and the pericoecal region by means of the programs SAPRO, SAPPAR, and BSPOT. *Ophthalmic Surg* **19**: 485-500.

Funkhouser, A.T., Kwasniewska, S., Fankhauser, F. (1988b). BSPOT: A blind spot data evaluation program for SAPRO examinations. *Ophthalmic Surg* **19**: 590-601.

Garner, L.F., Yap, M., Scott, R. (1992). Crystalline lens power in myopia. *Optom. Vis Sci* **69**: 863-865.

Geijssen, H.C., Greve, E.L. (1992). Myopic normal pressure glaucoma and visual field progression. *Invest Ophthalmol Vis Sci (suppl)* **33**: 1278.

Gilmartin, B., Bullimore, M.A. (1987). Sustained near-vision augments inhibitory sympathetic innervation of the ciliary muscle. *Clin Vis Sci* **1**: 197-208.

Gliddon, G.H. (1929). An optical replica of the human eye for the study of the retinal image. *Arch Ophthalmol* **2**: 138-163.

Gloor, B., Schmied, U., Fassler, A. (1980). Changes of glaucomatous field defects: degree of accuracy of measurements with the automatic perimeter Octopus. *Int Ophthalmol* **1**: 5-10.

Gloor, B., Schmied, U., Fassler, A. (1981). Changes of glaucomatous field defects-analysis of Octopus fields with programme Delta. *Doc Ophthalmol Proc Ser* **26**: 11-15.

Gloor, B., Stürmer, J., Vökt, B. (1984). Was hat die automatisierte perimetrie mit dem Octopus für neue kenntnisse über glaukomatöse gesichtsfeldveränderungen gebracht? *Klin Mbl Augenheilk* **184**: 249-253.

Gloor, B., Vokt, B. (1985). Long-term fluctuations versus actual field loss in glaucoma patients. *Dev Ophthalmol* **12**: 48-69.

Goldschmidt, E. (1968). On the etiology of myopia: An epidemiological study. *Acta Ophthalmologica (kbh) 46 (suppl)* **98**: 1-172.

Goldschmidt, E. (1969). Refraction in the newborn. *Acta Ophthalmol (Kbh)* **47**: 570-578.

Goldstick, B.J., Weinreb, R.N. (1987). The effect of refractive error on automated global analysis program G1. *Am J Ophthalmol* **104**: 229-232.

Goldwyn, R., Waltman, S.R., Becker, B. (1970). Primary open angle glaucoma in adolescents and young adults. *Arch Ophthalmol* **84**: 579-582.

Goss, D., Cox, V.D., Herrin-Lawson, G.A., Nielsen E.D., Dolton, W.A. (1990). Refractive error, axial length, and height as a function of age in young myopes. *Optom Vis Sci* **67**: 332-338.

Graham, M.V., Wakefield, G.J. (1973). Bitemporal visual field defects associated with anomalies of the optic disc. *Br J Ophthalmol* **57**: 307-314.

Gramer, E., Proll, M., Kreigelstein, G.K. (1979). The perimetry of the blind spot. A comparison of kinetic and static computerised strategies. *Ophthalmologica* **179**: 201-

208.

Gramer, E., Gerlach, R., Kreigelstein, G.K., Lydhecker, W. (1982). Zur Topographie früher glaukomatöser Gesichtsausfälle bei der Computerperimetrie. *Klin Mbl Augenheilkd* **180**: 515-523.

Grammer, E., De Natale, R., Leydhecker, W. (1986). Training effect and fluctuation in long-term follow-up of glaucomatous visual field defects calculated with program Delta of the Octopus perimeter 201. *New Trends Ophthalmol* **1**: 219-228

Greene, P.R. (1980). Mechanical considerations in myopia: relative effects of accommodation, convergence, intraocular pressure, and the extraocular muscles. *Am J Optom Physiol Opt* **57**: 902-914.

Greve, E.L. (1973). Single and multiple stimulus static perimetry in glaucoma; the two phases of the visual field examination. *Doc Ophthalmol* **36**: 1-355.

Greve, E.L. (1975). Static perimetry. *Ophthalmologica* **171**: 26-38.

Greve, E.L., Groothuyse, M.T., Verduin, W.M. (1976). Automation of perimetry. *Doc Ophthalmologica* **40**: 342-254.

Greve, E.L., Furuno, F. (1980). Myopia and glaucoma. *Graefes Arch Clin Exp Ophthalmol* **213**: 33-41.

Greve, E.L., (1982). Performance of computer assisted perimeters. *Doc Ophthalmologica* **53**: 343-380.

Grosvenor, T. (1987). A review and a suggested classification system for myopia on the basis of age-related prevalence and age of onset. *Am J Optom Physiol Opt* **64**: 545-554.

Gundersen, K.G., Heijl, A., Asman, P. (1993). Stimulus size and normal inter-individual variability in static perimetry. *Invest Ophthalmol Vis Sci (suppl)* **34**: 1262.

Guttridge, N.M., Allen, P.M., Rudnicka, A.R., Edgar, D.F., Renshaw, A.E. (1990). Influence of learning on the peripheral field as assessed by automated perimetry. **In**: *Perimetry Update 1990/1991*, ed. by R.P. Mills and A. Heijl, (Amstelveen: Kugler and Ghedini), pp 567-575.

Guttridge, N.M. (1993). Personal communication.

Haas, A., Flammer, J., Scheinder, U. (1986). Influence of age on the visual fields of normal subjects. *Am J Ophthalmol* **101**: 199-203.

Häberlin, H., Jenni, A., Fankhauser, F. (1980). Researches on adaptive high resolution programming for automatic perimeter. *Int Ophthalmol* **2**: 1-9.

Häberlin, H., Funkhouser, A.T., Fankhauser, F. (1983). Angioscotomata: Preliminary results using the new spatially adaptive program SAPRO. *Doc Ophthalmol Proc Ser* **35**: 337-344.

Haefliger, I.O., Flammer, F. (1989). Increase of the short-term fluctuation of the differential light threshold around a physiological scotoma. *Am J Ophthalmol* **107**: 417-420.

Haider, M., Dixon, N.F. (1961). Influences of training and fatigue on the continuous recording of a visual differential threshold. *Br J Psychol* **52**: 227-237.

Haley, M.J., Patells, V.M., Wong, M.M. (1986). Statpac user's guide. Allergan Humphrey Inc., San Leandro, California.

Haley, M.J. (1987). ed. The Field Analyzer Primer. 2nd edition. Allergan-Humphrey Inc., San Leandro, California.

Harrington, D.O. (1981). The visual field: a textbook and atlas of clinical perimetry. 5th edn. (London: The CV Mosby Co).

Hauff, W. (1983). Biometry - a precise method for measuring axial length of the eye. *Wein Klin Wochenschr* **95**: 271-274.

Hayreh, S.S. (1969). Blood supply of the optic nerve head and its role in optic atrophy, glaucoma, and oedema of the optic disc. *Br J Ophthalmol* **53**: 721-747.

Heijl, A., Krakau, C.E.T. (1975a). An automatic perimeter, design and pilot study. *Acta Ophthalmol* **53**: 293-310.

Heijl, A., Krakau, C.E.T. (1975b). An automatic perimeter for glaucoma visual field screening and control. Construction and cases. *Graefes Arch Klin Exp Ophthalmol* **197**: 13-23.

Heijl, A. (1977a). Time changes of contrast thresholds during automated perimetry. *Acta Ophthalmol* **55**: 696-708.

Heijl, A. (1977b). Computer test logics for automatic perimetry. *Acta Ophthalmol* **55**: 837-853.

Heijl, A., Krakau, C.E.T. (1977). A note on fixation during perimetry. *Acta Ophthalmol* **55**: 854-861.

Heijl, A., Drance, S.M. (1983a). Deterioration of thresholds in glaucomatous patients during perimetry. *Doc Ophthalmol Proc Ser* **35**: 129-136.

Heijl, A., Drance, S.M. (1983b). Changes in differential light threshold in patients with glaucoma during prolonged perimetry. *Br J Ophthalmol* **67**: 512-516.

Heijl, A. (1984). Computerised perimetry. *Trans Ophthalmol Soc UK* **104**: 76-87.

Heijl, A. (1985a). A simple routine for demonstrating increased threshold scatter by comparing stored computer fields. *Doc Ophthalmol Proc Ser* **42**: 35-38.

Heijl, A. (1985b). The Humphrey Field Analyzer, construction and concepts. *Doc Ophthalmol Proc Ser* **42**: 77-84.

Heijl, A., Samander, C. (1985). Peripapillary atrophy and glaucomatous visual field defects. *Doc Ophthalmol Proc Ser* **42**: 403-407.

Heijl, A. (1987). The implications of the results of computerised perimetry in normals for the statistical evaluation of glaucomatous visual fields. **In**: *Glaucoma Update III*, ed. by G.K. Kriegelstein (Berlin, Heidelberg: Springer-Verlag), pp 115-122.

Heijl, A., Lindgren, G., Olsson, J. (1987a). Variability of computerised threshold measurements across the central visual field in a normal population. *Doc Ophthalmol Proc Ser* **49**: 91.

Heijl, A., Lindgren, G., Olsson, J. (1987b). A package for the statistical analysis of visual fields. *Doc Ophthalmol Proc Ser* **49**: 153-168.

Heijl, A., Lindgren, G., Olsson, J. (1987c). Reliability parameters in computerised perimetry. *Doc Ophthalmol Proc Ser* **49**: 593-600.

Heijl, A., Lindgren, G., Olsson, J. (1987d). Normal variability of static perimetric threshold values across the central visual field. *Arch Ophthalmol* **105**: 1544-1549.

Heijl, A. (1989). Test point density and early detection of glaucomatous visual field loss. *Invest Ophthalmol Vis Sci (suppl)* **30**: 55.

Heijl, A., Asman, P. (1989a). A clinical study of perimetric probability maps. *Arch Ophthalmol* **107**: 199-203.

Heijl, A., Asman, P. (1989b). Clustering of depressed points in the normal visual field. **In**: *Perimetry Update 1988/1989*, ed. by A. Heijl (Amsterdam: Kugler & Ghedini), pp 185-189.

Heijl, A., Lindgren, G., Olsson, J. (1989a). The effect of perimetric experience in normal subjects. *Arch Ophthalmol* **107**: 81-86.

Heijl, A., Lindgren, G., Olsson, J., Asman, P. (1989b). Visual field interpretation with empirical probability maps. *Arch Ophthalmol* **107**: 204-208.

Heijl, A., Lindgren, A., Lindgren, G. (1989c). Test-retest variability in glaucomatous visual fields. *Am J Ophthamol* **108**:130-135.

Heijl, A., Molder, H. (1993). Optic disc diameter influences the ability to detect glaucomatous disc damage. *Acta Ophthalmol* **71**: 122-129.

Henson, D.B., Dix, S.M., Obourne, A.C. (1984). Evaluation of the Friedmann Analyzer Mark II: results from a normal population. *Br J Ophthalmol* **68**: 458-462.

Herse, P. (1992). Factors influencing normal perimetric thresholds obtained using the Humphrey Field Analyzer. *Invest Ophthalmol Vis Sci* **33**: 611-617.

Heuer, D.K., Anderson, D.R., Feuer, W.J., Gressel, M.G. (1987). The influence of refraction accuracy on automated perimetric threshold measurements. *Ophthalmology* **94**: 1550-1553.

Heuer, D.K., Anderson, D.R., Feuer, W.J., Gressel, M.G. (1989). The influence of retinal illumination on automated perimetric threshold measurements. *Ophthalmology* **108**: 643-650.

Hirsch, J. (1985). Statistical analysis in computerised perimetry. **In**: *Computerised visual fields*. ed. by W.R. Whalen and G.L. Spaeth, (Thorofare, NJ: Slack Inc), pp 309-344.

Hirsch, M.J. (1950). An analysis of inhomogeneity of myopia in adults. *Am J Optom Arch Am Acad Optom* **27**: 562-571.

Hitchings, R.A., Genio, C., Anderton, S., Clark, P. (1983). An optic disc grid: its evaluation in reproducibility studies on the cup/disc ratio. *Br J Ophthalmol* **67**: 356-361.

Hodapp, E. (1985). Computerised perimetry in glaucoma. **In**: *Computerised Visual Fields*. ed. by W.R. Whalen and G.L. Spaeth, (Thorofare, NJ: Slack Inc), pp 195-238.

Holden, A.L., Hodos, W., Hayes, B.P., Fitzke, F.W. (1988). Myopia: induced, normal and clinical. *Eye* **2**: 242-256.

Holmin, C., Krakau, C.E.T. (1979). Variability of glaucomatous visual field defects in computerised perimetry. *Graefes Arch Clin Exp Ophthalmol* **210**: 235-250.

Holmin, C., Krakau, C.E.T. (1982). Regression analysis of the central visual field in chronic glaucoma cases. *Acta Ophthalmol* **60**: 267-274.

Hoskins, H.D., Migliazzo, C. (1985). Development of a visual field screening test using a Humphrey Visual Field Analyzer. *Doc Ophthalmol Proc Ser* **42**: 85-90.

Hoskins, H.D., Magee, S.D., Drake, M.V., Kidd, M.N. (1987). A system for the analysis of visual fields using the Humphrey Visual Field Analyzer. *Doc Ophthalmol Proc Ser* **49**:145-151.

Hoskins, H.D., Magee, S.D., Drake, M.V., Kidd, M.N. (1988). Confidence intervals for change in automated visual fields. *Br J Ophthalmol* **72**: 591-597.

Huang, W.L., Sheu, M.M., Chen, C.E.T. (1987). Quantitative study of the conus/optic disc ratio among myopes with a planimeter. **In**: *Proceedings of the XXVth International Congress of Ophthalmology, 1986.* (Amsterdam: Kugler and Ghedini), pp 833-839.

Huang, S.J., Tokoro, T. (1990). Early change of visual field in high myopia. **In**: *Proceedings of Fourth International Conference on Myopia, Singapore 1990*, (New York: Myopia International Research Foundation Inc), pp 109-118.

Huang, L., Zhou, W. (1990). The relationship of structure in vivo of low tension glaucoma and myopia. *Yen Ko Hsueh Pao Eye Science* **6**: 58-9. (abstract only).

Huang, S.J. (1993). Early change of visual function in high myopia measured and analysed by Octopus automated perimetry. *Nippon Ganka Gakkai Zashi* **97**: 881 (abstract only).

Hudson, C., Wild, J.M., Searle, A.E.T., O'Neill, E.C. (1992). Fatigue effects during a single session of automated perimetry in normals and ocular hypertensives. *Invest Ophthalmol Vis Sci (suppl)* **33**: 1382.

Iwase, A., Kitazawa, Y., Ohno, Y. (1988). On age-related norms of the visual field. *Jpn J Ophthalmol* **32**: 429-437.

Iwase, A., Shirai, H., Ido, T., Shimizu, U., Kitazawa, Y., Patella, V.M. (1989). The analysis of normal fields with the Humphrey Statpac. **In**: *Perimetry Update 1988/1989*, ed. by A. Heijl (Amsterdam: Kugler and Ghedini), pp 239-244.

Jaeger, W. (1983). Ermittlung der wahren Papillengrösse an patienten (Beitrag zur Diagnose der Mikropapille). *Fortschr Ophthalmol* **80**: 527-532.

Jaeger, M.J., Quigley, H.A., Green, W.R. (1987) Optic nerve head and axial length of human eyes: a morphometrical and morphological analysis. *Invest Ophthalmol Vis Sci*

(*suppl*) **28**: 61.

Jaffe, G.J., Alvarado, J.A., Juster, R.P. (1986). Age related changes of the normal visual field *Arch Ophthalmol* **104**: 1021-1025.

Jansson, F., Kock, E. (1962). Determination of the velocity of ultrasound in the human lens and vitreous. *Acta Ophthalmol* **40**: 420-433.

Jansson, F. (1963). Measurement of intraocular distances by ultrasound and comparison between optical and ultrasonic determinations of the depth of the anterior chamber. *Acta Ophthalmologica* **41**: 25-61.

Jansson, F., Sundmark, E, (1961). Determination of the velocity of ultrasound in ocular tissues at different temperatures. *Acta Ophthalmol* **39**:899-910.

Jensen, H. (1992). Myopia progression in young school children and intraocular pressure. *Doc Ophthalmol* **82**: 249-255.

Johns, E.G. (1979). Clinical evaluation of the DBR A-scan unit. *Am Intra-ocular Implant Soc J* **5**: 213-216.

Johnson, C.A., Keltner, J.L., Balaestray, F. (1978). Effects of target size and eccentricity on visual detection and resolution. *Vis Res* **18**: 1217-1222.

Johnson, C.A., Keltner, J.L., Krohn, M.A., Portney, G.L. (1979). Photogrammetry of the optic disc in glaucoma and ocular hypertension with simultaneous stereo photography. *Invest Ophthalmol Vis Sci* **18**: 1252-1263.

Johnson, C.A., Adams, C.W., Lewis, R.A. (1988). Fatigue effects in automated perimetry. *Applied Optics* **27**: 1030-1037.

Johnson, C.A., Nelson-Quigg, J.M. (1993). A prospective three-year study of response properties of normal subjects and patients during automated perimetry. *Ophthalmology* **100**: 269-274.

Jonas, J.B., Handel, A., Naumann, G.O.H. (1987) Tatsachliche Maße der vitalen papilla nervi optici des menschen. *Fortschr Ophthamol* **84**: 356-357.

Jonas, J.B., Gusek, G.C., Guggenmous-Holzmann, I., Naumann, G.O.H. (1988a). Size of the optic nerve scleral canal and comparison with intravital determination of optic disc dimensions. *Graefes Arch Clin Exp Ophthalmol* **226**: 213-215.

Jonas, J.B., Gusek, G.C., Guggenmous-Holzmann, I., Naumann, G.O.H. (1988b). Variability of the real dimensions of normal human optic discs. *Graefes Arch Clin Exp*

Ophthalmol **226**: 332-336.

Jonas, J.B., Gusek, G.C., Naumann, G.O.H. (1988c). Optic disc morphometry in chronic primary open-angle glaucoma I. Morphometric intrapapillary characteristics. *Graefes Arch Clin Exp Ophthalmol* **226**: 522-530.

Jonas, J.B., Gusek, G.C., Naumann, G.O.H. (1988d). Optic disc morphometry in high myopia. *Graefes Arch Clin Exp Ophthalmol* **226**: 587-590.

Jonas, J.B., Gusek, G.C., Naumann, G.O.H. (1988e) Optic disc, cup and neuroretinal rim size, configuration and correlations in normal eyes. *Invest Ophthalmol Vis Sci* **29**: 1151-1158.

Jonas, J.B., Gusek, G.C., Guggenmous-Holzmann, I., Naumann, G.O.H. (1988f). Correlations of the neuroretinal rim area with ocular and general parameters in normal eyes. *Ophthalmic Res* **20**: 298-303.

Jonas, J.B., Müller-Bergh, J.A., Scholtzer-Schrehardt, U.M., Douglas, G.R. (1990a). Histomorphometry of the human optic nerve. *Invest Ophthamol Vis Sci* **31**: 736-744.

Jonas, J.B., Fernandez, M.C., Naumann, G.O.H. (1990b). Glaucomatous optic nerve atrophy in small discs with low cup-disc ratios. *Ophthalmology* **97**: 1211-1215.

Jonas, J.B., Gusek, G.C., Fernandez, M.C. (1991). Correlation of the blind spot size to the area of the optic disc and parapapillary atrophy. *Am J Ophthalmol* **111**: 559-565.

Jonas, J.B., Fernandez, M.C., Naumann, G.O.H. (1992a). Glaucomatous parapapillary atrophy. *Arch Ophthalmol* **110**: 214-222.

Jonas, J.B., Schmidt, A.M., Müller-Bergh, J.A., Schöltzer-Schrehardt, U.M., Naumann, G.O.H. (1992b). Human optic nerve fibre count and optic disc size. *Invest Ophthalmol Vis Sci* **33**: 2012-2018.

Katz, J., Tielsch, K.S., Sommer, A. (1990). Racial variations in optic disc characteristics: the Baltimore eye survey. *Invest Ophthalmol Vis Sci (suppl)* **31**: 431.

Katz, J., Sommer, A. (1986). Asymmetry and variation in the normal hill of vision. *Arch Ophthalmol* **104**: 65-68.

Katz, J., Sommer, A. (1987). A longitudinal study of the age-adjusted variability of automated visual fields. *Arch Ophthalmol* **105**: 1083-1086.

Katz, J., Sommer, A. (1988). Reliability indexes of automated perimetric tests. *Arch Ophthalmol* **106**: 1252-1254.

Katz, J., Sommer, A. (1990). Screening for glaucomatous visual field loss. The effect of patient reliability. *Ophthalmology* **97**: 1032-1037.

Katz, J., Sommer, A., Witt, K. (1991). Reliability of visual field results over repeated testing. *Ophthalmology* **98**: 70-75.

Keltner, J., Johnson, C.A., Lewis, R. (1985). Quantitative office perimetry. *Ophthalmology* **92**: 862-872.

Kennedy, S.J., Schwartz, B., Takamoto, T., Eu, J.K.T. (1983). Interference fringe scale for absolute ocular fundus measurement. *Invest Ophthalmol Vis Sci* **24**: 169-174.

Kim, C., Juzych, M.S., Shin, D.H., Tsai, C.S., McCarty, B.D., Lee, S.Y. (1990). Correlation of axial length and optic disc area. *Invest Ophthalmol Vis Sci (suppl)* **31**: 459.

King, D., Drance, S.M., Douglas, G.R., Wijsman, K. (1986). The detection of paracentral scotomas with varying grids in computed perimetry. *Arch Ophthalmol* **104**: 524-525.

Klein, R.M., Curtin, B.J. (1975). Lacquer cracks in pathologic myopia. *Am J Ophthalmol* **79**:386-392.

Klewin, R.M., Radius, R.L. (1986). Background illumination and automated perimetry. *Arch Ophthalmol* **104**: 395-397.

Koerner, F., Fankhauser, F., Bebie, H., Spahr, J. (1977). Threshold noise and variability of visual field defects in determinations by manual and automatic perimetry. *Doc Ophthalmol Proc Ser* **14**: 53-59.

Kolker, A.E., Hetherington, J. (1976). Diagnosis and therapy of the glaucomas. (St Louis: CV Mosby), pp 131-149.

Kosoko, O., Sommer, A., Auer, C. (1986). Duration of automated suprathreshold vs quantitative threshold field examination. Impact of age and ocular status. *Arch Ophthalmol* **104**: 398-401.

Krakau, C.E.T. (1978). Aspects on the design of an automatic perimeter. *Acta Ophthalmol* **56**: 389-405.

Langerhorst, C., van den Berg, T.J.T.P., van Spronsen, N.R., Greve, E.L. (1985). Results of a fluctuation analysis and defect volume program for automated static threshold perimetry with the Scoperimeter. *Doc Ophthalmol Proc Ser* **42**: 1-6.

Langerhorst, C., van den Berg, T.J.T.P., Boersma, H., Greve, E. (1987a). Short-term

and long-term fluctuation of thresholds in automated perimetry in normals, ocular hypertension and glaucoma. *Doc Ophthalmol Proc Ser* **49**: 71-76.

Langerhorst, C.,van den Berg, T.J.T.P., Veldman, E., Greve, E.L. (1987b). Population study of global and local fatigue with prolonged threshold testing in automated perimetry. *Doc Ophthalmol Proc Ser* **49**: 657- 662.

Langerhorst, C.T., Lambron, G., Temporelli, F., van den Berg, T.J.T.P. (1991). Accurate estimation of local defects in glaucoma. **In**: *Perimetry Update 1990/1991*, ed. by R.P. Mills and A. Heijl, (Amstelveen: Kugler and Ghedini), pp 225-227.

Le Blanc, R.P. (1985). Abnormal values in computerised perimetry. **In**: *Computerised visual fields*. ed. by W.R. Whalen and G.L. Spaeth, (Thorofare, NJ: Slack Inc), pp 165-193.

Le Grand, Y. (1968). Light, Colour and Vision. 2nd edition. (London: Chapman and Hall), pp 85-88.

Leighton, D.A., Tomlinson, A. (1973). Ocular tension and axial length of the eyeball in open-angle glaucoma and low tension glaucoma. *Br J Ophthalmol* **57**: 499-502.

Levene, J.R. (1966). G.B.Airy's model eye. *Med Hist* (England) **10**: 198-200 and plate.

Lewis, R.A., Johnson, C.A., Keltner, J.L., Labermeier, P.K. (1986). Variability of quantitative automated perimetry in normal observers. *Ophthalmology* **93**: 878-881.

Lindenmuth, K.A., Skuta, G.L., Rabbani, R., Musch, D.C. (1989). Effects of pupillary constriction on automated perimetry in normal eyes. *Ophthalmology* **96**: 1298-1301.

Lindenmuth, K.A., Skuta, G.L., Rabbani, R., Musch, D.C., Bergstrom, T.J. (1990). Effects of pupillary dilation on automated perimetry in normal patients. *Ophthalmology* **97**: 367-370.

Littmann, H. (1982). Zur Bestimmung der wahren Größe eines Objektes auf dem Hintergrund des lebenden Auges. *Klin Mbl Augenheilk* **180**: 286-289.

Littmann, H. (1988) Zur Bestimmung der wahren Größe eines Objektes auf dem Hintergrund eines lebenden Auges. *Klin Mbl Augenheilk* **192**: 66-67.

Lotufo, D., Ritch, R., Szmyd, L., Burris, J.E. (1989). Juvenile glaucoma, race, and refraction. *JAMA* **261**: 249-252.

Lovasik, J.V. (1983) A simple continuously recording infrared optometer. *Am J Optom* **60**: 80-87.

Low, F. (1946). Some characteristics of peripheral visual performance. *Am J Physiol* **146**: 573-584.

Magee, S.D., Hoskins, H.D., Kidd, M.N. (1987). Long-term fluctuation in glaucomatous fields: point by point analysis. *Invest Ophthalmol Vis Sci* **28**: 269.

Manor, R.S. (1974). Temporal field defects due to nasal tilting of discs. *Ophthalmologica* **168**: 269-281.

Mansour, A.M. (1990). Measuring fundus landmarks. *Invest Ophthalmol Vis Sci* **31**: 41-42.

Mansour, A.M. (1991). Racial variation of optic disc size. *Ophthalmic Res* **23**: 67-72.

Martin-Boglind, L. (1991). High-pass resolution perimetry in uncomplicated myopia. *Acta Ophthalmol* **69**: 516-520.

Mastropasqua, L., Lobefalo, L., Mancini, A., Ciancaglini, M., Palma, S. (1992). Prevalence of myopia in open angle glaucoma. *European J Ophthalmol* **2**: 33-35.

Masukagami, H., Furuno, F., Matsuo, H. (1987). Blind spots of normal and high myopic eyes measured by fundus photo-perimetry. *Doc Ophthalmol Proc Ser* **49**: 489-493.

Matsumoto, C., Uyama, K., Okuyama, S., Nakao, Y., Otori, T. (1991). Study of the influence of target size on the pericentral visual field. **In**: *Perimetry Update 1990/1991*, ed. by R.P. Mills and A. Heijl, (Amstelveen: Kugler and Ghedini), pp 153-159.

Matsuno, C., Kurozumi, I., Kani, K. (1967). Cases of visual field defects due to myopia. *Folia Ophthalmol Jpn* **18**: 330-332.

Matthews, J.N.S., Altman, D.G., Campbell, M.J., Royston, J.P. (1990). Analysis of serial measurements in medical research. *Br Med J* **300**: 230-235.

McBrien, N.A., Millodot, M. (1987). A biometric investigation of late onset myopic eyes. *Acta Ophthalmologica* **65**: 461-468.

McCluskey, D.J., Douglas, J.P., O'Connor, P.S., Story, K., Ivy, L.M., Harvey, J.S. (1986). The effect of pilocarpine on the visual field in normals. *Ophthalmology* **93**: 843-846.

McMillan, T.A., Stewart, W.C., Hunt, H.H. (1992). Association of reliability with reproducibility of glaucomatous visual fields. *Acta Ophthalmol* **70**: 665-670.

McNellis, E.L., Caprioli, J., Zulauf, M., Boeglin, R.J. (1991). Reproducibility of a

method for quantitative stereoscopic measurement of the optic nerve head. *Invest Ophthalmol Vis Sci (suppl)* **32**: 1018.

Miglior, S., Bottoni, F., Gonnella, P., Bergamini, F., Orzalesi, N, (1989). Morphometric analysis of optic disc parameters in normal and glaucomatous eyes. *Invest Ophthalmol Vis Sci (suppl)* **30**: 174.

Mikelberg, F.S., Schulzer, M., Drance, S.M., Lau, W. (1986a). The rate of progression of scotomas in glaucoma. *Am J Ophthalmol* **101**: 1-6.

Mikelberg, F.S., Douglas, F.S., Schulzer, M., Airaksinen, P.J., Wijsman, K., Mawson, D. (1986b). The correlation between cup-disc ratio, neuroretinal rim area and optic disc area measured by the video-ophthalmograph (Rodenstock analyzer) and clinical measurement. *Am J Ophthalmol* **101**: 7-12.

Mikelberg, F.S., Drance, S.M., Schulzer, M., Wijsman, K. (1987). The effect of miosis on visual field indices. *Doc Ophthalmol Proc Ser* **49**: 645-649.

Mikelberg, F.S., Yidegiligne, H.M., White, V.A., Schulzer, M. (1991). Relation between optic nerve axon number and axon diameter to scleral canal area. *Ophthalmology* **98**: 60-63.

Mills, R.P., Hopp, R.H., Drance, S.M. (1986). Comparison of quantitative testing with the Octopus, Humphrey and Tubingen perimeters. *Am J Ophthalmol* **102**: 496-504.

Mills, R.P., Schulzer, M., Hopp, R.H., Drance, S.M. (1987). Estimates of variance in visual field data. *Doc Ophthalmol Proc Ser* **49**: 93-101.

Mills, R.P., Lau, W., Schulzer, M. (1991). Estimating short-term fluctuation without double determinations. **In** *Perimetry Upate 1990/1991*, ed. by R.P. Mills and A. Heijl, (Amstelveen: Kugler and Ghedini), pp 203-208.

Mundt, G.H., Hughes, W.F. (1956). Ultrasonics in ocular diagnostics. *Am J Ophthalmol* **41**: 488-498.

Nakase, Y. (1987a). Primary open angle glaucoma in high myopia. Report 1. Effect of high myopia on visual field defects. *Acta Soc Ophthalmol Jpn* **91**: 376-382. (abstract only)

Nakase, Y. (1987b). Primary open angle glaucoma in high myopia. Report 2. Effect of high myopia on glaucomatous cupping of the optic disc. *Acta Soc Ophthalmol Jpn* **91**: 442-447. (abstract only)

Naylor, E.J., Ardern, W. (1947) An instrument for the demonstration of the principles of

subjective refraction. *Br J Physiol Optics* **4**: 111-115.

Nelson-Quigg, J.M., Twelker, J.D., Johnson, C.A. (1989). Response properties of normal observers and patients during automated perimetry. *Arch Ophthalmol* **107**: 1612-1615.

Niles, C.R., Trope, G.E. (1988). The influence of experience on mean defect and reliability factors in automated perimetry. *Invest Ophthalmol Vis Sci (suppl)* **29**: 356.

Odland, M. (1967). Bitemporal defects of the visual field due to anomalies of the optic discs. *Acta Neurol Scandinav* **43**: 630-639.

Oksala, A., Varonen, E. (1964). Analysis of echoes from the rear eye wall with the aid of experimental research I. The sound beam directed to the rear wall past the lens. *Acta Ophthalmol* **42**: 616-628.

Olsen, T., Nielsen, P.J. (1989). Immersion versus contact technique in the measurement of axial length by ultrasound. *Acta Ophthalmol* **67**: 101-102.

Olsen, T. (1989). The accuracy of ultrasonic determination of axial length in pseudophakic eyes. *Acta Ophthalmol* **67**: 141-144.

Ossoining, K.C. (1983). How to obtain maximum measurement accuracies with standardised A-scan. *Doc Ophthalmol Proc Ser* **38**: 197-216.

Otsuka, J. (1967). Research on the etiology and treatment of myopia. *Acta Soc Ophthalmol Jpn (suppl)* **71**: 1-212.

Pach, J., Pennell, D.O., Romano, P.E. (1989). Optic disc photogrammetry: magnification factors for eye position, centration, and ametropias, refractive and axial; and their application in the diagnosis of optic nerve hypoplasia. *Ann Ophthalmol* **21**: 454-462.

Paczka, J.A., Corkid, G., Hernandez-Quintela, E., Wheelock-Arguello, J.T., Santos, A., Merikansky, A., Gil-Carrasco, F., Jimenez-Roman, J. (1992). Biomorphometric analysis of normal and glaucomatous discs in Hispanic subjects. *Invest Ophthalmol Vis Sci (suppl)* **33**: 881.

Parish, R.K., Schiffmann, J., Anderson, D.R. (1984). Static and kinetic visual field testing: reproducibility in normal volunteers. *Arch Ophthalmol* **102**: 1497-1502.

Parssinen, O. (1990). Intraocular pressure in school myopia. *Acta Ophthalmol* **68**: 559-563.

Pennebaker, G.E., Stewart, W.C., Stewart, J.A., Hunt, H.H. (1992). The effect of

stimulus duration upon the components of fluctuation in static automated perimetry. *Eye* **6**: 353-355.

Perkins, E.S. (1979). Morbidity from myopia. *Sight Saving Review*, Spring 1979, pp 11-19.

Perkins, E.S., Phelps, C.D. (1982). Open angle glaucoma, ocular hypertension, low-tension glaucoma and refraction. *Acta Ophthalmol* **100**: 1464-1467.

Phelps, C.D. (1982). Effect of myopia on prognosis in treated primary open-angle glaucoma. *Am J Ophthalmol* **93**: 622-628.

Pierro, L.M., Brancato, R., Avanza, P., Galli, L., Pece, A. (1993). Posterior fundus changes and axial myopia. *Invest Ophthalmol Vis Sci (suppl)* **34**: 1168.

Piltz, J.R., Starita, R.J., Fechtner, R.D., Twersky, Y.D. (1986). Fluctuations of serial automated visual fields in glaucomatous and normal eyes. *Invest Ophthalmol Vis Sci (suppl)* **27**: 159.

Podos, S.M., Becker, B., Morton, W.R. (1966). High myopia and primary open-angle glaucoma. *Am J Ophthalmol* **62**: 1039-1043.

Poinoosawmy, D., Wu, J.X., Hitchings, R., Fitzke F. (1994). Dominantly inferior hemifield defects are associated with myopia in glaucoma. *Invest Ophthalmol Vis Sci (suppl)* **35**: 2188.

Polyak, S.L. (1941) The Retina. (Illinois: University of Chicago Press), pp 136-139.

Primrose, J. (1971). Early signs of the glaucomatous disc. *Br J Ophthalmol* **55**: 820-825.

Pruett, R.C. (1988). Progressive myopia and intraocular pressure: what is the linkage? A literature review. *Acta Ophthalmol (Copenh suppl)* **185**: 117-127.

Quigley, H.A., Addicks, E.M., Green, W.R. (1982). Optic nerve damage in human glaucoma III. Quantitative correlation of nerve fibre loss and visual field defect in glaucoma, ischemic neuropathy, papilledema and toxic neuropathy. *Arch Ophthalmol* **100**: 135-146.

Quigley, H.A., Brown, A.E. (1989). Size and configuration of the normal optic disk. *Invest Ophthalmol Vis Sci (suppl)* **30**: 430.

Quigley, H.A., Brown, A.E., Morrison, J.D., Drance, S.M. (1990). The size and shape of the optic disc in normal human eyes. *Arch Ophthalmol* **108**: 51-57.

Quigley, H.A., Coleman, A.L., Dorman-Pease, M.E. (1991). Larger optic nerve heads have more nerve fibres in the normal monkey eyes. *Arch Ophthalmol* **109**: 1441-1443.

Rabie, E.P., Storey, J.K. (1984). The reliability of ultrasonic axial length measurement. *Trans First Int Congr BCO*, London, pp 51-57.

Rabineau, P.A., Gloor, B.P., Tobler, H.J. (1985). Fluctuations in threshold and effect of fatigue in automated static perimetry (with the Octopus 201). *Doc Ophthalmol Proc Ser* **42**: 25-33.

Radius, R.L. (1978). Perimetry in cataract patients. *Arch Ophthalmol* **96**: 1574-1579.

Radius, R.L., Pederson, J.E. (1984). Laser-induced primate glaucoma: II. Histopathology. *Arch Ophthalmol* **102**: 1693-1698.

Raviola, E., Wiesel, T.N. (1985). An animal model of myopia. *N Engl J Med* **312**: 1609-1615.

Rebolleda, G., Munoz, F.J., Victorio, J.M.F., Pellier, T., Munrube del Castillo, J. (1992). Effects of pupillary dilation on automated perimetry in glaucoma patients receiving pilocarpine. *Ophthalmology* **99**: 418-423.

Reed, H. (1960). The essentials of perimetry. (Oxford: Oxford University Press).

Reed, H., Drance, S.M. (1972). The essentials of perimetry. 2nd edn. (London: Oxford University Press).

Repka, M.X., Quigley, H.A. (1989). The effect of age on normal human optic nerve fibre number and diameter. *Ophthalmology* **96**: 26-32.

Riise, D. (1966). Visual field defects in optic disc malformation with ectasia of the fundus. *Acta Ophthalmol* **44**: 906-918.

Rockwood, E.J., Anderson, D.R. (1988). Acquired peripapillary changes and progression in glaucoma. *Graefes Arch Clin Exp Ophthalmol* **226**: 510-515.

Rosenthal, A.R., Kottler, M.S., Donaldson, D.D., Falconer, D.G. (1977). Comparative reproducibility of the digital photogrammetric procedure utilizing three methods of stereophotography. *Invest Ophthalmol Vis Sci* **16**: 54-60.

Rosenthal, A.R., Falconer, D.G., Barrett, D. (1980) Digital measurement of pallor-disc ratio. *Arch Ophthalmol* **98**: 2027-2031.

Rucker, C.W. (1946). Bitemporal defects in the visual field resulting from developmental

anomalies of the optic discs. *Arch Ophthalmol* **35**: 546-554.

Rutishauser, C., Flammer, J. (1988). Retests in static perimetry. *Graefes Arch Clin Exp Ophthalmol* **226**: 75-77.

Rutishauser, C., Flammer, J., Haas, A. (1989). The distribution of normal values in automated perimetry. *Graefes Arch Clin Exp Ophthalmol* **227**: 513-517.

Safran, A.B., Mermoud, C. (1989). A neuro-ophthalmological global analysis program (N1) developed with the Octopus measurement unit. **In**: *Perimetry Update 1988/1989*, ed. by A. Heijl. (Amsterdam: Kugler and Ghedini), pp 151-155.

Safran, A.B., Almeida, L., Mermoud, C., Desangles, D., de Weiss, C., Lang, R. (1991). Intraocular and interocular variability of blind spot surface measurements by means of automated perimetry. **In**: *Perimetry Update 1990/1991*, ed. by R.P. Mills and A. Heijl. (Amsterdam: Kugler and Ghedini), pp 409-412.

Safran, A.B., Bader, C., Brazitikos, P.D., de Weisse, C., Desangles, D. (1992). Increasing short-term fluctuation by increasing the intensity of the fixation aid during perimetry. *Am J Ophthalmol* **113**: 193-197.

Sato, Y., Yamashita, M., Hayashi, K., Tokoro,T. (1984). Abnormality of visual field in pathological myopia. *Acta Soc Ophthalmol Jpn* **88**: 977-982.

Scheffe H (1959).The Analysis of Variance, Chapter 10. (New York: Wiley).

Scheiner, C. (1619). *Oculus, hoc est: Fundamentum Opticum.* Daniel Agricola, Oenoponti (Innsbruck).

Schelenz, J., Kammann, T. (1989). Comparison of contact and immersion techniques for axial length measurement and implant power calculation. *J Cataract Refract Surg* **15**: 425-428.

Schmidt , T. (1955). Perimetric relativer skotome. *Ophthalmologica* **129**: 303-315.

Schoessler, J.P. (1976). The influence of visual field decay testing procedure on blind spot size. *J Am Optom Assoc* **47**: 898-902.

Schulzer, M., Mills, R.P., Hopp, R.H., Lau, W., Drance, S.M. (1990). Estimation of the short-term fluctuation from a single determination of the visual field. *Invest Ophthalmol Vis Sci* **31**: 730-735.

Schwartz, B., Nagin, P. (1985). Probability maps for evaluating automated visual fields. *Doc Ophthalmol Proc Ser* **42**: 39-48.

Scott, R., Grosvenor, T. (1993). Structural model for emmetropic and myopic eyes. *Ophthalmic Physiol Opt* **13**: 41-47.

Searle, A.E.T., Shaw, D.E., Wild, J.M., O'Neill, E.C. (1991a). Within and between test learning and fatigue effects in normal perimetric sensitivity. **In**: *Perimetry Update 1990/1991*, ed. by R.P. Mills and A. Heijl (Amstelveen: Kugler and Ghedini), pp 533-537.

Searle, A.E.T., Wild, J.M., Shaw, D.E., O'Neill, E.C. (1991b). Time-related variations in normal automated static perimetry. *Ophthalmology* **98**: 701-707.

Shammas, H.J. (1984). A comparison of immersion and contact techniques for axial length measurements. *Am Intra-ocul Lens Implant Soc J* **10**: 444-447.

Shammas, H.J., Milkie, C.F. (1989). Mature cataracts in eyes with unilateral axial myopia. *J Cataract Refract Surg* **15**: 308-311.

Sivak, J.G., Barrie, D.L., Weerheim, J.A. (1989). Bilateral experimental myopia in chicks. *Optom Vis Sci* **66**: 854-858.

Sloan, L.L. (1961). Area and luminance of test object as variables in examination of the visual field by projection perimetry. *Vision Res* **1**: 121-138.

Snead, M.P., Rubinstein, M.P., Hardman-Lea, S., Haworth, S.M. (1990). Calculated versus A-scan result for axial length using different types of probe tip. *Eye* **4**:718- 722.

Sommer, A., Quigley, H.A., Robin, A.L., Miller, N.R., Katz, J., Arkell, S. (1984). Evaluation of nerve fibre layer assessment. *Arch Ophthalmol* **102**: 1766-1771.

Sommer, A., Duggan, C., Auer, C., Abbey, H. (1985). Analytic approaches to the interpretation of automated threshold perimetric data for the diagnosis of early glaucoma. *Trans Am Ophthalmol Soc* **83**: 250-267.

Sorsby, A., O'Connor, A. (1945). Measurement of the diameters of the living eye by means of X-ray. *Nature* **156**: 779-780.

Sorsby, A., Benjamin, B., Davey, J.B., Sheridan, M., Tanner, J.M. (1957). Emmetropia and its aberrations. Special Report Series of The Medical Research Council, No.293. HMSO, London, UK.

Sorsby, A., Benjamin, B., Sheridan, M. (1961). Refraction and its components during growth of the eye from the age of three. Medical Research Council Report Series No.301. HMSO, London.

Sorsby, A., Leary, G.A. (1970). A longitudinal study of refraction and its components during growth. Medical Research Council Report Series No.309. HMSO, London.

Sorsby, A. (1973). Growth of the eye in relation to refraction. **In**: *Modern Trends in Ophthalmology 5*, (Glasgow: Butterworths), pp 100-108.

Sorsby, A., Benjamin, B. (1973). Modes of inheritance of errors of refraction. *J Med Genet* **10**: 161-164.

Spahr, J. (1975). Optimization of the presentation pattern in automated static perimetry. *Vis Res* **15**: 1275-1281.

Sperduto, R.D., Seigel, D., Roberts, J., Rowland, M. (1983). Prevalence of myopia in the United States. *Arch Ophthamol* **101**: 405-407.

Stürmer, J., Gloor, G., Tobler, H.J. (1985). The glaucomatous visual field in detail as revealed by the Octopus F-programs. *Doc Ophthalmol Proc Ser* **42**: 391-401.

Starita, K.J., Piltz, J., Lynn, J.R., Fellman, R.L. (1987a). Total variance of serial Octopus visual fields in glaucomatous eyes. *Doc Ophthalmol Proc Ser* **49**: 85-90.

Starita, K.J., Fellman, R.L., Lynn, J.R. (1987b). Static automated perimetry: background luminance and global visual field indices in the quantification of normal, suspect, and glaucomatous visual fields. *Invest Ophthalmol Vis Sci (suppl)* **28**: 269.

Steele, C.F., Crabb, D.P., Edgar, D.F. (1992). Effects of different ocular fixation conditions on A-scan ultrasound biometry measurements. *Ophthalmic Physiol Opt* **12**: 491-495.

Stenstrom, S. (1946). Investigation of the variation and the covariation of the optical elements of human eyes. Translated by D. Woolf. **In**: *Am J Optom Arch Am Acad Optom* **25**: (5), 218-232; (6), 286-299; (7), 340-350; (8), 388-397; (9), 438-449; (10), 496-504 (1948). Monograph 58.

Stepanik, J. (1986). The blind spot: A critical review of the interpretation of a well-known scotoma by automated perimetry. *Klin Mbl Augenheilk* **198**: 409-412.

Stiles, W.S., Crawford, B.H. (1934). The liminal brightness increment for white light for different conditions of the foveal and parafoveal retina. *Proc R Soc B* **116**: 55-102.

Storey, J.K. (1982). Measurement of the eye with ultrasound. *Ophthalmic Optn* **22**: 150-160.

Storey, J.K., Rabie, E.P. (1983). Ultrasound - a research tool in the study of

accommodation. *Ophthalmic Physiol Opt* **3**: 315-320.

Sunabrai, O., Feuer, W.J., Anderson, D.R. (1991). Pseudo-loss of fixation in automated perimetry. *Ophthalmology* **98**: 76-78.

Sveinsson, K. (1982). The refraction of Icelanders. *Acta Ophthalmol* **60**: 779-787.

Takamoto, T., Schwartz, B. (1985). Reproducibility of photogrammetric optic disc cup measurements. *Invest Ophthalmol Vis Sci* **26**: 814-817.

Takizawa, E. (1983). Retinal sensitivity in the papillomacular area in high myopia by fundus controlled perimetry. *Jpn J Clinicophthalmol* **37**: 495-501.

Tate, G.W., Lynn, J.R. (1977). Principles of quantitative perimetry testing and interpreting the visual field. (New York: Grune and Stratton), pp. 1-28.

Tate, G.W. (1985). The physiological basis for perimetry. **In**: *Automatic perimetry in glaucoma,* ed. by S.M. Drance and D. Anderson. (London: Grune and Stratton), pp 1-28.

Teal, P.K., Morin, J.D., McCulloch, C. (1972). Assessment of the normal disc. *Trans Am Ophthalmol Soc* **70**: 164-177.

Tokoro, T., Muto, M., Hayashi, K., Asahara, N. (1976). A study on the measurement of visual field in high myopia. *Folia Ophthalmol Jpn* **27**: 627-632.

Tomlinson, A., Phillips, C.I. (1969). Ratio of optic cup to optic disc in relation to axial length of the eyeball and refraction. *Br J Ophthalmol* **53**:765-768.

Tomlinson, A., Phillips, C.I. (1970). Applanation tension and axial length of the eyeball. *Br J Ophthamol* **54**: 548-553.

Traquair, H.M. (1957). Clinical Perimetry. 7th edn, ed. by G.I. Scott, (London: Kimpton).

Tron, E.J. (1940). The optical elements of the refractive power of the eye. **In**: *Modern Trends of Ophthalmology*, ed. by F. Ridley, A. Sorsby. (London: Butterworths), pp 245.

Ts'o, M.O., Friedman, E. (1968). The retinal pigment epithelium. *Arch Ophthalmol* **80**: 214-216.

Tscherning, M. (1924). Physiological Optics, 4th edn. (English translation by C. Weiland), (Philadelphia: Keystone Publishing Co), pp 262-263.

Van Alphen, W.G.H.M. (1961). On emmetropia and ametropia. *Ophthalmologica*

(suppl) **142**. (Basel and New York: S.Karger)

Varma, R., Hilton, S., Tielsch, J.M., Quigley, H.A. (1993). Image analysis of the normal optic disc: a population based study. *Invest Ophthalmol Vis Sci (suppl)* **34**: 895.

Vivell, P.M., Lachenmayr, B.J., Ostermaier, N. (1993). Normal visual field data for the Humphrey Field Analyzer. *Invest Ophthalmol Vis Sci (suppl)* **34**: 1261.

Von der Lippe, I., Jonas, J.B., Naumann, G.O.H. (1992). Follow-up of parapapillary chorioretinal atrophy in glaucomatous eyes. *Invest Ophthalmol Vis Sci (suppl)* **33**: 1092.

Von Rohr, M. (1920). Zür Wurdigung von Scheiners Augenstudien. *Arch Augenheilk* **86**: 247-263.

Voronova, T.B. (1967). Results of ophthalmoperipheroscopic, perimetric and scotometric exploration in myopes. *Vestn Oftal* **80**: 14-18.

Wall, M., Kardon, R., Moore, P. (1993). Large size stimuli of automated perimetry have lower variability. *Invest Ophthalmol Vis Sci (suppl)* **34**: 1262.

Wallman, J., Gottlieb M.D., Rajaram, V., Fugate-Wenztek, L.A. (1987). Local retinal regions control local eye growth and myopia. *Science* **237**: 73-77.

Weber, J., Dobek, K. (1986). What is the most suitable grid for computer perimetry in glaucoma patients? *Ophthalmologica* **192**: 88-96.

Weber, J. (1987). Computerised perimetry in neuro-ophthalmology: comparison of different test patterns by an information index. *Doc Ophthalmol Proc Ser* **49**: 621-628.

Weber, J., Geiger, R. (1989). Gray scale displays of perimetric results. The influence of different interpolation procedures. **In**: *Perimetry Update 1988/1989*, ed. by A. Heijl, (Amsterdam: Kugler and Ghedini), pp 447-454.

Weber, J., Rau, S. (1992). The properties of perimetric thresholds in normal and glaucomatous eyes. *German J Ophthalmol* **1**: 79-85.

Weinreb, R.N., Perlman, J.P. (1986). The effect of refractive correction on automated perimetric thresholds. *Am J Ophthalmol* **101**: 706-709.

Werner, E.B., Drance, S.M. (1977). Early visual field disturbances in glaucoma. *Arch Ophthalmol* **95**: 1173-1175.

Werner, E.B., Saheb, N., Thomas, D. (1982). Variability of static visual threshold responses in patients with elevated IOPs. *Arch Ophthalmol* **100**: 1627-1631.

Werner, E.B., Bishop, K.I., Davis, P., Krupin, T., Petrig, B., Sherman, C. (1987). Visual field variability in stable glaucoma patients. *Doc Ophthalmol Proc Ser* **49**: 77-83.

Werner, E.B., Bishop, K.I., Koelle, J., Douglas, G.R., Le Blanc, K.P., Mills, R.P., Schwartz, B., Whalen, W.R., Wilensky, J.T. (1988a). A comparison of experienced clinical observers and statistical tests in detection of progressive visual field loss in glaucoma using automated perimetry. *Arch Ophthalmol* **106**: 619-623.

Werner, E.B., Adelson, A., Krupin, T. (1988b). Effect of patient experience on the results of automated perimetry in clinically stable glaucoma patients. *Ophthalmology* **95**: 764-767.

Werner, E.B., Krupin, T., Adelson, A., Feitl, M.E. (1990). Effect of patient experience on the results of automated perimetry in glaucoma suspect patients. *Ophthalmology* **97**: 44-48.

Werner, E.B., Ganigan, G., Balazsi, A.G. (1991). Effect of test point location on the magnitude of threshold fluctuations in glaucoma patients undergoing automated perimetry. **In**: *Perimetry Update 1990/1991*, ed. by R.P. Mills and A. Heijl (Amstelveen: Kugler and Ghedini), pp 175-181.

Wild, J.M., Wood, J.M., Flanagan, J.G., Good, P.A., Crews, S.J. (1986). The interpretation of the differential light threshold in the central visual field. *Doc Ophthalmol* **62**: 191-202.

Wild, J.M., Wood, J.M., Flanagan, J.G. (1987). Spatial summation and the cortical magnification of perimetric profiles. *Ophthalmologica* **195**: 88-96.

Wild, J.M., Dengler-Harles, M., Searle, A.E.T., O'Neill, E.C., Crews, S.J. (1989). The influence of the learning effect on automated perimetry in patients with suspected glaucoma. *Acta Ophthalmol* **67**: 537-545.

Wild, J.M., Searle, A.E.T., Dengler-Harles, M., O'Neill, E.C. (1991). Long-term follow-up of baseline learning and fatigue effects in the automated perimetry of glaucoma and ocular hypertensive patients. *Acta Ophthalmol* **69**: 210-216.

Wildberger, H., Robert, Y. (1988). Visual fatigue during prolonged testing in optic neuropathies. *Neuro-Ophthalmology* **8**: 167-174.

Wilensky, J.T., Kolker, A.E. (1976). Peripapillary changes in glaucoma. *Am J Ophthalmol* **81**:341-345.

Wilensky, J., Joondeph, B. (1984). Variation in visual field measurements with an

automated perimeter. *Am J Ophthalmol* **97**: 328-331.

Wilson, M.R., Hertzmark, M.A., Walker, A.M., Childs-Shaw, K., Epstein, D.L. (1987). A case controlled study of risk factors in open-angle glaucoma and low tension glaucoma. *Arch Ophthalmol* **105**: 1066-1071.

Winer, B.J. (1972). Statistical Principles in Experimental Design. (New York: McGraw-Hill), pp 205-210, 514-539.

Wood, J.M., Wild, J.M., Drasdo, N., Crews, S.J. (1986). Perimetric profiles and cortical representation. *Ophthalmic Res* **18**: 301-308.

Wood, J.M., Wild, J.M., Hussey, M., Crews, S.J. (1987a). Serial examination of the normal visual field using Octopus projection perimetry: evidence of a learning effect. *Acta Ophthalmol* **65**: 326-333.

Wood, J.M., Wild, J.M., Smerdon, D.L., Crews, S.J. (1987b). The role of intraocular light scatter in the attenuation of the perimetric response. *Doc Ophthalmol Proc Ser* **49**: 51-59.

Wood, J.M., Wild, J.M., Crews, S.J. (1987c). Induced intraocular light scatter and the sensitivity gradient of the normal visual field. *Graefes Arch Clin Exp Ophthalmol* **225**: 366-373.

Wood, J.M., Wild, J.M., Bullimore, M.A., Gilmartin, B. (1988a). Factors affecting the normal perimetric profile derived by automated static threshold LED perimetry. I. pupil size. *Ophthalmic Physiol Opt* **8**: 26-31.

Wood, J.M., Bullimore, M.A., Wild, J.M., Gilmartin, B. (1988b). Factors affecting the normal perimetric profile derived by automated static threshold LED perimetry. II. Accommodative microfluctuations. *Ophthalmic Physiol Opt* **8**: 32-36.

Wu, D.C., Schwartz, B., Nagin, P. (1987). Trend analysis of automated visual fields. *Doc Ophthalmol Proc Ser* **49**: 175-189.

Young , F.A. (1961). The effect of restricted visual space on the primate eye. *Am J Ophthalmol* **52**: 799-806.

Young, F.A., Leary, G.A., Box, R.A., Baldwin, W.R., West, D.C., Harris, E., Johnson, C. (1969). The transmission of refractive errors within Eskimo families. *Am J Optom Arch Am Acad Optom* **46**: 676-685.

Young, F.A. (1975). The development and control of myopia in human and subhuman primates. *Contacto* **19**: 16-31.

Young, S., Watsh, I., Knox, D. (1976). The tilted disc syndrome. *Am J Ophthalmol* **82**: 16-23.

Zadnik, K., Mutti, O.D., Adams, A.J. (1992). The repeatability of measurements of the ocular components. *Invest Ophthalmol Vis Sci* **33**: 2325-2333.

Zingirian, M., Calabria, G., Gandolfo, E., Sandini, G. (1981). The normal pericoecal area - a static method for investigation. *Doc Ophthalmol Proc Ser* **26**: 393-403.

Ziylan, S., Quinn, G.E., Berlin, J.A., Young, T.L., Stone, R.A. (1993). An association of intraocular pressure and myopia in children. *Invest Ophthalmol Vis Sci (suppl)* **34**: 896.

Zulauf, M. (1988). Preliminary findings concerning angioscotometry: stimulus size and program recommendations. *Klin Mbl Augenheilk* **192**: 613-618.

Zulauf, M., Caprioli, J., Hoffmann, D.C., Tressler, C.S. (1991a). Fluctuation of the differential light sensitivity in clinically stable glaucoma patients. **In**: *Perimetry Update 1990/1991*, ed. by R.P. Mills and A. Heijl (Amstelveen: Kugler and Ghedini), pp 183-188.

Zulauf, M., Caprioli, J., Hoffmann, D. (1991b). Asymmetry of the visual field in a normal population. *Invest Ophthalmol Vis Sci (suppl)* **32**: 1192.

Zulauf, M., Caprioli, J. (1993). Stimulus sizes 3 and 5 in perimetry for glaucoma. *Invest Ophthalmol Vis Sci (suppl)* **34**: 1262.